1996

Cold Acclimation: A Complex Interaction Of Low Temperature, Light And The Redox State Of Photosystem Ii

Gordon R. Gray

COLD ACCLIMATION: A COMPLEX INTERACTION OF LOW TEMPERATURE, LIGHT AND THE REDOX STATE OF PHOTOSYSTEM II

by

Gordon R. Gray

Department of Plant Sciences

Submitted in partial fulfilment
of the requirements for the degree of
Doctor of Philosophy

Faculty of Graduate Studies
The University of Western Ontario
London, Ontario
August 1996

ISBN 0-612-15052-6

ABSTRACT

The process of cold acclimation refers to the physiological processes by which cold-tolerant plants such as cereals, when developed at low temperature, acquire freezing tolerance. Photosynthesis provides the energy required for these complex metabolic changes to take place. However, photosynthetic organisms must maintain a balance between energy input as a result of photochemical reactions and energy consumption through intersystem electron transport and the various biochemical reactions of cellular metabolism. Imbalances may be sensed by changes in the redox state of photosystem II (PSII), as this represents the rate-limiting step of photosynthetic electron transport. The redox state of PSII is sensitive to both temperature and irradiance. I demonstrate in this thesis that the photosynthetic adjustments which occur as a result of cold acclimation are responses to the redox state of PSII and not low temperature *per se*. In addition, plant growth habit and the mRNA accumulation of a nuclear gene associated with the acquisition of freezing tolerance (*Wcs19*) are also modulated by the redox state of PSII. Thus, changes in the environment which perturb the redox state of PSII, act to generate a chloroplastic redox signal, which may represent the first component in a sensing/signalling pathway which acts synergistically with other transduction pathways to elicit the appropriate responses to all environmental stresses.

Key words: cold acclimation, light, photosynthesis, redox poise, temperature.

"Science is to see what everyone else has seen

but to think what no one else has thought."

- Albert Szent-Györgyi

ACKNOWLEDGEMENTS

A document such as this does not evolve solely due to one person. The contents of this thesis are the result of the contributions of numerous individuals whom I wish to acknowledge at this time.

Norman P.A. Huner for always providing support and encouragement, while allowing me to peruse my own personal interests.

Marilyn Griffith for introducing me to plant physiology during my undergraduate years at the University of Waterloo.

Bruce M. Greenberg and *William G. Hopkins* who served on my advisory committee.

Alexander Ivanov for his diligence with the P_{700} measurements and his HPLC assistance.

Marianna Król for her assistance with the plastoquinone determinations.

Leonid Savitch for his expertise in dealing with the carbon metabolism analyses.

Antibodies for the immunological analyses were kindly donated by *Eva-Mari Aro*, *Kent Burkey*, *Stan Dunn*, *Stefan Jansson*, *Anastasios Melis* and *John Thompson*. Thanks also to *Mobashsher Khan* and *John P. Williams* at the University of Toronto for the lipid and fatty acid analyses.

In addition, I would like to thank *Fathey Sarhan* for welcoming me into his lab at the Université du Québec à Montréal. Special thanks to *Louis-Pierre Chauvin* for his assistance with all aspects of the *Wcs* work. Remember LP, its all in the delivery!

Also, thanks to;

Cheryl Ketola for providing friendship, gc d food and a place to stay.

Paul Slawek for your help with all those posters.

Indira L. Pillay for two great years of companionship. You made my time in London something to remember. Good luck in Chiropractic College.

Finally, thanks to my parents for their continuing support.

TABLE OF CONTENTS

CHAPTER 5 - PHOTOINHIBITORY RESPONSES IN RELATION TO PSII EXCITATION PRESSURE

CHAPTER 6 - COLD ACCLIMATORY PROCESSES IN RESPONSE TO LOW TEMPERATURE, LIGHT AND THE REDOX STATE OF PSII

LIST OF TABLES

LIST OF FIGURES

LIST OF ABBREVIATIONS

Abbreviation	Description
α-Car	alpha-carotene
β-Car	beta-carotene
μ	micro (10^{-6})
μL	microliter
μM	micromolar
Φ_{app}	apparent quantum yield
ΦO_2	quantum yield of oxygen evolution
Φ_{PSII}	effective quantum yield of PSII electron transport
$1\text{-}q_P$	photosystem II excitation pressure
16:0	palmitic acid
18:1	oleic acid
18:3	linolenic acid
18:2	linoleic acid
18:0	stearic acid
$^1O_2$	singlet oxygen
3-PGK	3-phosphoglucokinase
$^3O_2$	triplet oxygen
A	absorbance
A	ampere
Ax	antheraxanthin
A_0	primary electron acceptor of PSI
A_1	secondary electron acceptor of PSI
ADP	adenosine 5'-diphosphate
ATP	adenosine 5'-triphosphate
B	blue light (400-480 nm)
Bicine	*N,N'*-bis(2-hydroxyethylglycine)
BPB	bromophenol blue
BSA	bovine serum albumin
CABP	2-carboxyarabinatol 1,5-bisphosphate
CF_0	chloroplast coupling factor (membrane)
CF_1	chloroplast coupling factor (extrinsic)
Chl	chlorophyll
C_L	electrical conductivity of leachate
cm	centimeter
ΦCO_2	quantum yield of CO_2 exchange
CP	chlorophyll-binding protein
C_T	total electrical conductivity
Cyt	cytochrome

d	day
dATP	2'-deoxyadenosine-5'-triphosphate
DCMU	3-(3,4-dichlorophenyl)-1,1-dimethylurea
dCTP	2'-deoxycytidine-5'-triphosphate
dd	double distilled
DEPC	diethyl pyrocarbonate
DGDG	digalactosyldiacylglycerol
dGTP	2'-deoxyguanosine-5'-triphosphate
DHAP	dihydroxyacetonephosphate
DNA	deoxyribonucleic acid
DOC	deoxycholic acid
DTT	dithiothreitol
dTTP	thymidine-5'-triphosphate
DW	dry weight
E	extinction coefficient
e^-	electron
EDTA	ethylenediaminetetraacetate
EPS	epoxidation state of the xanthophyll pool
f	femto (10^{-15})
F_A	iron-sulfer cluster of PSI
FAME	fatty acid methyl esters
F_B	iron-sulfer cluster of PSI
FBPase	fructose-1,6-bisphosphatase
Fd	ferridoxin
F_M	maximum fluorescence in the dark-adapted state
F_M'	maximum fluorescence in the light-adapted state
FNR	ferridoxin-$NADP^+$-oxidoreductase
F_O	minimum fluorescence in the dark-adapted state
F_O'	minimum fluorescence in the light-adapted state
FR	far red light (725-735 nm)
Fru	fructose
Fru-1,6-bisP	fructose-1,6-bisphosphate
Fru-6-P	fructose-6-phosphate
F_S	steady-state level of fluorescence under actinic illumination
F_V	variable fluorescence in dark-adapted leaves
F_V / F_M	maximal photochemical yield of PSII in the dark-adapted state
F_V'	variable fluorescence in the light-adapted state
F_V' / F_M'	maximal photochemical yield of PSII in the light-adapted state
FW	fresh weight
F_X	iron-sulfer cluster of PSI
g	gravity

g	gram
GAP	glyceraldehyde-3-phosphate
GAPDH	glyceraldehyde-3-phosphate dehydrogenase
Glc	glucose
Glc-6-P	glucose-6-phosphate
Glc-6-PDH	glucose-6-phosphate dehydrogenase
Glyc	glycolate
h	hour
HEP	high PSII excitation pressure
Hepes	*N*-2-hydroxyethylpiperazine-*N*'-2-ethanesulfonic acid
H_{II}	hexagonal type-II phase
HPLC	high-performance liquid chromatography
Hz	hertz
IgG	immunoglobulin G
IR	infra-red
J_F	rate of electron transport from fluorescence measurements
k	kilo (10^3)
k_f	rate constant
kb	kilobase pair
kD	kilodalton
LED	light-emitting diode
LEP	low PSII excitation pressure
Lhca	chlorophyll *a/b*-binding proteins of PSI
Lhcb	chlorophyll *a/b*-binding proteins of PSII
LHCI	light-harvesting complex associated with PSI
LHCII	light-harvesting complex associated with PSII
ln	natural logarithm
LT_{50}	lethal temperature at which 50% death occurs
Lut	lutein
m	meter
M	molar (moles/liter)
mA	milliampere
mg	milligram
MGDG	monogalactosyldiacylglcerol
min	minute
mL	milliliter
mM	millimolar
mol	mole
Mops	3-(*N*-morpholino)propanesulfonic acid
mosmol	milliosmolal (milliosmoles/kilogram)
mRNA	messenger RNA
MT	multiple turnover
n	sample size

N	normal
NAD^+	nicotinamide adenine dinucleotide
NADH	nicotinamide adenine dinucleotide (reduced form)
$NADP^+$	nicotinamide adenine dinucleotide phosphate
NADPH	nicotinamide adenine dinucleotide phosphate (reduced form)
nd	none detected
Neo	neoxanthin
nm	nanometer
NPQ	non-photochemical quenching
$O_2^{\bullet -}$	superoxide
OEC	oxygen evolving complex
$OH^\bullet$	hydroxyl radical
OLB	oligo labelling buffer
p	plasmid
P_{680}	primary electron donor of PSII
P_{700}	primary electron donor of PSI
Pa	pascals
PAGE	polyacrylamide gel electrophoresis
PAM	pulse amplitude moduation
PAR	photosynthetically active radiation (400-700 nm)
PBS	phosphate-buffered saline
PBS-T	phosphate-buffered saline with Tween 20
PC	phosphatidylcholine
PCO	photosynthetic carbon oxidation
PCR	photosynthetic carbon reduction
PE	phosphatidylethanolamine
PG	phosphatidylglycerol
PGI	phosphoglucoisomerase
Pheo	pheophytin
Pi	inorganic phosphate
PMSF	phenylmethylsulfonyl fluoride
P_N	rate of CO_2 assimilation
PPFD	photosynthetic photon flux density
PQ	plastoquinone
PQA	plastoquinone A
PQH_2	plastoquinol
PSI	photosystem I
PSII	photosystem II
PSM	plant stress meter
PS_{max}	maximum light-saturated rate of photosynthesis
PVPP	polyvinylpolypyrrolidone
Q_A	primary quinone acceptor of PSII
Q_B	secondary quinone acceptor of PSII

q_N	coefficient of non-photochemical quenching
q_O	coefficient of F_O quenching
q_P	coefficient of photochemical quenching
R	red light (655-665 nm)
r^2	square of the product-moment correlation coefficient
rA	ribonucleotide adenine
rC	ribonucleotide cytosine
RC	relative conductance
R_D	rate of mitochondrial respiration
RET	relative electron transport
RNA	ribonucleic acid
Rubisco	ribulose-1,5-bisphosphate carboxylase/oxygenase
RuBP	ribulose-1,5-bisphosphate
s	seconds
S_0	ground state
S_1*	excited singlet state
SD	standard deviation
SDS	sodium dodecyl sulfate
SE	standard error
SLW	specific leaf weight
SOD	superoxide dismutase
SPS	sucrose phosphate synthase
SQDG	sulfoquinovosyldiacylglycerol
SSC	saline sodium citrate
ST	single turnover
Suc	sucrose
Suc-P	sucrose phosphate
TBS	Tris-buffered saline
TBS-T	Tris-buffered saline with Tween 20
TE	Tris-EDTA
TLC	thin layer chromatography
tr	trace amounts
trans-16:1	*trans*-Δ^3-hexadecenoic acid
Tricine	*N*-tris(hydroxymethyl)-methylglycine
Tris	tris(hydroxymethyl)-aminomethane
triose-P	triose-phosphate
tRNA	transfer RNA
Tween-20	polyoxyethylenesorbitan monolaurate
Tyr	tyrosine
UDP	uridine 5'-diphosphate
UDP-Glc	uridine 5'-diphosphoglucose
UTP	uridine 5'-triphosphate

UV	ultra-violet radiation
UV-A	ultra-violet-A radiation (320-400 nm)
UV-B	ultra-violet-B radiation (290-320 nm)
v/v	volume/volume (concentration)
V	volts
Vx	violaxanthin
v_C	rate of carboxylation
V_{max}	maximum velocity of a reaction
v_O	rate of oxygenation
w/w	weight/weight (concentration)
W	watt
Wcs	wheat cold stimulated (gene nomenclature)
WCS	wheat cold stimulated (polypeptide nomenclature)
Z	electron donor to P_{680}^+
Zx	zeaxanthin
°C	Celsius

CHAPTER 1

GENERAL INTRODUCTION

1.0 Photosynthesis

The conversion of solar radiant energy to chemical energy by photosynthetic organisms sustains all life on earth, providing a source of energy which can then be utilized by other forms of life. The components involved in light-harvesting, electron transport, proton translocation, and the enzymatic catalysis required for the production of energy (ATP) and reducing equivalents (NADPH) are all either bound within or closely associated with the thylakoid membranes of the cellular organelle known as the chloroplast (Andersson and Barber, 1994). The chloroplast consists of an envelope which is composed of two membranes separated by an intramembrane space. This envelope encloses a complex of continuous membranes known as thylakoids, with the space in between referred to as the chloroplast stroma. The stroma is an aqueous compartment which contains the enzymes responsible for the conversion of CO_2 to carbohydrate. In addition, the biosynthetic pathways of amino acid and lipid synthesis, sulfate reduction and nitrogen metabolism are also located in the chloroplast stroma (Greenberg, 1991).

1.1 The Thylakoid Membranes

The thylakoid membranes consist of a lipid bilayer, the matrix of which is composed of diacylglycerol lipids. The majority of these lipids are galactolipids

(MGDG and DGDG) which can represent up to 75% of the lipid composition of the thylakoid membranes, with the remainder composed of the polar lipids SQDG, PC, and PG. These lipids exhibit a lateral and transverse heterogeneity in their distribution. The fatty acids associated with these lipid classes are usually highly unsaturated with linolenic acid (18:3) dominating for the galactolipids (Quinn and Williams, 1985; Williams, 1994). The thylakoids exhibit a high degree of organizational complexity, forming a continuous membranous network of folded lamellae systems composed of stacked (granal) and non-stacked (stromal) regions enclosing a luminal space (Anderson, 1986). There are four major protein complexes contained within the thylakoid membrane which are PSII, Cyt b_6/f, PSI, and the ATP synthase complex. These complexes are distributed asymmetrically within the thylakoid and undergo electron transfer reactions with concominent proton transport across the bilayer from the stroma to the lumen (Andersson and Barber, 1994). There is also a heterogenous organization of these complexes along the plane of the membrane such that the structural differentiation between appressed and non-appressed regions is parallelled by function (Anderson, 1986). We know of nearly sixty polypeptides associated with these four complexes, of which almost all of the corresponding genes have been sequenced. Approximately 45% of these polypeptides are encoded by the chloroplast genome. The balance are encoded by the nuclear genome and therefore must be imported to the chloroplast (Keegstra et al., 1995). In addition, 70% of the polypeptides present in plant thylakoids are

integral membrane proteins, with the remainder being extrinsic, attached to the outer or inner thylakoid surface by electrostatic forces and/or hydrogen bonding (Andersson and Barber, 1994).

1.1.1 PSII

PSII is a multi-protein complex composed of at least twenty distinct sub-units, and is thought to exist as a dimeric structure *in vivo* (Boekema et al., 1995; Santini et al., 1994). These polypeptides perform a variety of catalytic, regulatory, and structural functions. The D1 protein is a rapidly synthesized in the light with a molecular mass of 32 kD and is a product of the chloroplastic *psbA* gene, while the D2 protein has a molecular mass of 31 kD and is a product of the chloroplastic *psbD* gene (Andersson and Styring, 1991; Andersson and Barber, 1994). The D1/D2 heterodimer binds all the redox components required for primary photochemistry and the Mn cluster which catalyzes photosynthetic water oxidation. These two polypeptides provide the binding environment for a special dimer of Chl *a* known as P_{680} and a Pheo. The heterodimer also binds two quinones (Q_A and Q_B) functioning in charge stabilization on the reducing side of PSII (Andréasson and Vänngård, 1988; Mattoo et al., 1989). A specific tyrosine residue (Tyr_{161}) of the D1 protein, known as TyrZ, functions in electron donation directly to P_{680} (Fig. 1) (Andersson and Styring, 1991; Andersson and Barber, 1994).

Cyt b_{559} is a polypeptide closely associated with the PSII heterodimer,

Figure 1. Organization of the thylakoid membrane in higher plants. Modified from Greenberg (1991). The four major thylakoid membrane complexes are shown; PSII, Cyt b_6/f, PSI and the ATP synthase. In addition, the mobile electron carriers plastocyanin and PQ are indicated.

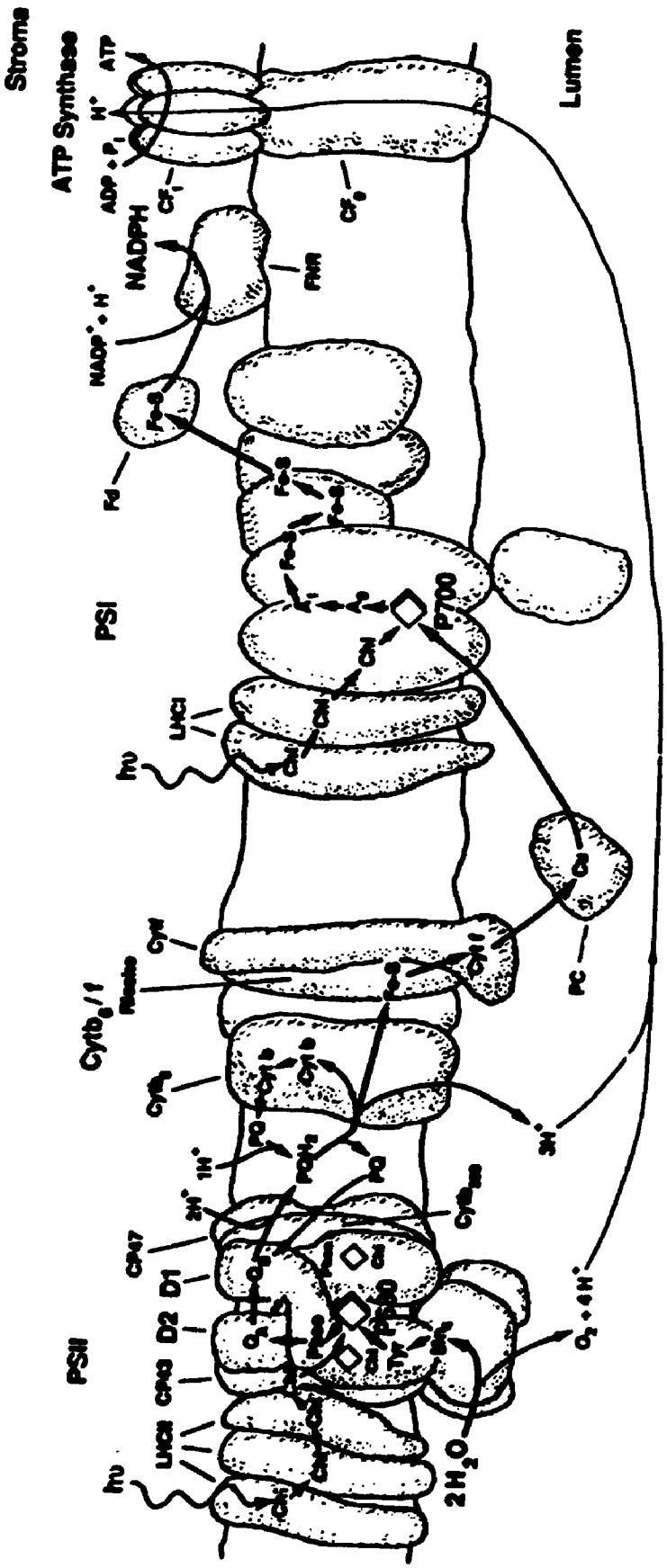
Stroma
Lumen
ATP Synthase
ATP
H+
ADP + Pi
NADPH
NADP+ + H+
FNR
Fd
PSI
P700
LHCI
hν
PC
Cyt f
Rieske
Cytb6
Cytb6
CP47
D1
D2
CP43
LHCII
PSII
2H2O
O2 + 4H+

composed of two sub-units (Fig. 1). This was one of the first proteins to be associated with PSII but its function remains elusive. It has been suggested that Cyt b_{559} may be involved in cyclic electron transfer around PSII (Andersson and Styring, 1991). Cyt b_{559} can attain a high potential or several low potential redox forms. The high potential form is thought to be the active form and perturbations in the water oxidizing system transform the Cyt to its low potential form. There are two Cyt b_{559} molecules on a PSII reaction center basis (Nanba and Satoh, 1987; Andersson and Barber, 1994).

Three proteins of molecular masses 33 kD, 23 kD, and 16 kD, comprise what is known as the OEC (Andersson and Styring, 1991). These proteins are extrinsic membrane proteins, present in equimolar amounts. The 33 kD protein is thought to be required for stabilization of the Mn cluster while the 23 and 16 kD sub-units are essential for the binding of Ca^{2+} and Cl^- ions which are required as cofactors for photosynthetic water oxidation (Andersson and Barber, 1994).

In addition, two Chl *a*-binding proteins also make up the PSII core referred to as CP47 and CP43 (Andersson and Styring, 1991). These polypeptides have molecular masses of 47 and 43 kD respectively and are regarded as core antenna, functioning in energy transfer to the PSII reaction center core. These proteins bind in total 50 Chl *a* and 5 β-Car (Bassi et al., 1990). The inner antenna is tightly bound to the reaction center core and recent findings suggest that CP47 plays a role in stabilization of the dimeric structure of PSII (Santini et al., 1994).

1.1.2 PSI

To date, approximately thirteen sub-units have been associated with the PSI core complex (Golbeck, 1992; Chitnis, 1996). The PSI reaction center is also a heterodimer composed of two polypeptides, PSI-A and PSI-B, each of which have an apparent molecular mass of 82 to 83 kD and are encoded by the chloroplastic *psaA* and *psaB* genes respectively. The PSI-A/PSI-B heterodimer ligates the primary electron donor, a special Chl *a* dimer referred to as P_{700}, in addition to the early electron acceptors A_0, a Chl *a* monomer, A_1, a phylloquinone and the iron-sulfer [4Fe-4S] cluster F_x (Andréasson and Vänngård, 1988). The extrinsic PSI-C protein is also functionally important as it binds the terminal electron acceptors of the complex, designated F_A and F_B, both [4Fe-4S] clusters. In addition, the heterodimer also binds approximately 100 Chl *a* per reaction center which act as inner antennae (Fig. 1) (Bassi et al., 1990).

1.1.3 Cyt b_6/f

The Cyt b_6/f complex consists of five sub-units which are all integral membrane proteins and mediates electron transfer from PSII to PSI. Cyt *f* is a 33 kD protein, while the apoprotein of Cyt b_6 (Cyt b_{563}) has an apparent molecular mass of 23 kD, Both of these polypeptides are plastid encoded. A nuclear gene encodes a 20 kD subunit which harbours a Rieske [2Fe-2S] iron-sulfer cluster. There are two Cyt b_6, one Cyt *f*, one Rieske iron-sulfer cluster, two non-heme irons and some bound quinone present per complex (Fig. 1)

(Andersson and Barber, 1994).

1.1.4 ATP Synthase

This complex, also known as the chloroplast coupling factor or ATPase, is composed of nine polypeptides which are arranged in two parts, an integral membrane component (CF_0) and an extrinsic portion exposed to the stroma (CF_1) (Fig. 1). This complex functions in proton translocation, capable of utilizing the *pmf* generated by the *trans*-thylakoid electrochemical proton gradient, thus catalyzing ATP synthesis (Dilley et al., 1987; Mitchell, 1961). CF_1 contains five subunits designated α (60 kD), β (56 kD), γ (39 kD), δ (19 kD) and ε (14 kD). Of these, the α, β and ε subunits are encoded by plastid genes, while the γ and δ subunits are encoded by nuclear genes. The β subunit carries the catalytic site of the enzyme, while the other subunits perform organizational and regulatory roles. CF_0 is comprised of four subunits, CF_0-I to CF_0-IV ranging from 8 to 19 kD. All with the exception of CF_0-II are encoded in the chloroplast (Andersson and Barber, 1994).

1.1.5 Additional Components

1.1.5.1 Fd, FNR and Plastocyanin

Two other important polypeptides are located on the external thylakoid surface and are involved in photosynthetic electron transfer. The first is Fd, a nuclear encoded protein with an approximate molecular mass of 11 kD bound to

PSI on the stromal side of the thylakoid surface (Fig. 1) (Andersson and Barber, 1994). Fd is a non-heme [2Fe-2S] protein which mediates electron transfer from the F_A and F_B centers on the acceptor side of PSI (Andréasson and Vänngård, 1988). The second protein is also nuclear encoded and is known as FNR with an apparent molecular mass of approximately 34 kD (Fig. 1). This enzyme catalyzes the final reduction of $NADP^+$ during photosynthetic electron transport and is associated with Fd on the stromal surface of PSI (Andersson and Barber, 1994).

Plastocyanin is a hydrophilic copper (Cu^{2+}) containing protein which is located on the lumenal side of the thylakoid membrane (Fig. 1). This nuclear encoded polypeptide has a molecular mass of 9 to13 kD and functions as a mobile electron carrier between the Cyt b_6/f complex and PSI (Andersson and Barber, 1994).

1.1.5.2 PQ/PQH_2

The PQ/PQH_2 pool serves to mediate electron flow between PSII and the Cyt b_6/f complex (Fig. 1) The acutal quinone species is PQA which is a hydrophobic molecule with two methyl groups attached to its quinone ring and a side chain of nine isoprenes (Andersson and Barber, 1994). PQ/PQH_2 is located evenly throughout the lipid bilayer and functions in electron transport as a two-electron gate. One electron is passed to PC while the other is recycled via Cyt b_6 back to the PQ pool, also known as the the Q-cycle (Mitchell, 1975). Since

PQ must diffuse through the membrane, it is thought to represent the rate-limiting step in linear electron flow (Andersson and Barber, 1994).

1.1.6 Photosynthetic Pigments

The principle photosynthetic pigment, Chl *a*, is a tetrapyrrol ring having a flat porphyrin 'head' with a magnesium atom coordinately bonded in the center. In addition, there is a non-polar phytol 'tail' which orients the Chl pigment-protein complex in the lipid bilayer of the thylakoid membrane. Higher plants also possess Chl *b* which differs from Chl *a* by the substitution of a formyl group (-CHO) for a methyl group ($-CH_3$) (Shipman, 1982). All Chl molecules exist *in vivo* non-covalently bound to specific proteins termed Chl *a/b*-binding proteins or pigment-protein complexes. The Chl *a/b*-binding proteins are all nuclear encoded and imported into the chloroplast via transit peptides (Keegstra et al., 1995). The nomenclature and organization of the Chl *a/b*-binding proteins described in this thesis is based on the model of Jansson (1994).

Carotenoids comprise a large group of accessory pigments composed of repeating isoprene units (Koyama, 1991). These pigments play a dual role in photosynthetic antenna complexes, augmenting the energy absorbed by Chl and thus increasing the spectrum of visible light that can be utilized by photosynthesis. They also perform a photoprotective role against the oxidative reactions caused by toxic singlet oxygen ($^1O_2$) and in the dissipation of excess excitation energy as heat (Young, 1991; Frank et al., 1994; McKersie and

Leshem, 1994). In higher plants, recent evidence suggests that their principle role is that of photoprotection via mediation of NPQ formation (Demmig-Adams and Adams, 1996; Demmig-Adams et al., 1996). The carotenoids may be divided into two groups, the first being the carotenes, comprised of α-Car and ß-Car. The second group is the xanthophylls, which include Lut, Neo, Vx, Ax and Zx. The later three xanthophylls are interconvertible upon a high *trans*-thylakoid ΔpH gradient and comprise what is known as the xanthophyll or violaxanthin cycle (Pfündel and Bilger, 1994; Demmig-Adams and Adams, 1996). The carotenoids are bound to polypeptides with the carotenes typically associated with the reaction center or core antennae complexes (CP43, CP47), while the xanthophylls are located with the minor Chl *a/b*-binding proteins (Demmig-Adams et al., 1996).

1.1.7 Photosynthetic Light-Harvesting

In all organisms capable of oxygenic photosynthesis, most photosynthetic pigments do not play a direct role in charge separation. Rather, they function to absorb photons of light and transfer the energy via other pigment molecules to the reaction centers to drive the essential reactions of photosynthesis.

1.1.7.1 PSII Light-Harvesting

The major Chl *a/b*-binding protein complex of PSII is presumed to be a

trimeric complex which is commonly referred to as LHCII or PSII outer antennae. The LHCII monomeric unit binds two specific lipids, PG and DGDG. The role of DGDG is thought to be that of structural integrity of the trimeric complex, while PG has been suggested to participate directly in trimer formation at the level of sub-unit interactions between the monomers (Kühlbrandt, 1994). LHCII is thought to be composed of the Lhcb1 and Lhcb2 polypeptides which range in apparent molecular mass from 25 to 28 kD. Recent electron crystallography data indicate 7 Chl *a* and 5 Chl *b* molecules bound per monomeric unit, while biochemical studies also point to trace xanthophylls (Jansson, 1994; Kühlbrandt, 1994; Kühlbrandt et al., 1994). Apart from their photoprotective function, the carotenoids associated with LHCII are thought to play a structural role, contributing to the rigidity of the complex which binds 60 to 70% of the Chl present in green plants (Bassi et al., 1990).

Lhcb3 is another Chl *a/b*-binding protein of apparent molecular mass 24 to 25 kD which is tightly bound to the PSII reaction center. The Chl content of Lhcb3 is similar to that of Lhcb1/Lhcb2. In addition, three minor Chl *a/b*-binding proteins also exist and are known as Lhcb4, Lhcb5 and Lhcb6 (Jansson, 1994). These polypeptides are referred to as PSII inner antennae and account for 10 to 15% of all the Chl associated with PSII and contain varying amounts of xanthophyll pigments. Estimations of bound pigment for Lhcb4 (29 to 31 kD) are 10 Chl *a* and 4 Chl *b* molecules per monomer (Jansson, 1994). Lhcb5 (26 to 29 kD) contains 9 Chl *a* and 5 Chl *b* molecules bound per polypeptide, while Lhcb6

(20 to 22 kD) contains 11 Chl *a* and 9 Chl *b* (Jansson, 1994).

1.1.7.2 PSI Light-Harvesting

There are four Chl *a/b*-binding proteins associated with PSI which are designated Lhca1(20 to 22 kD), Lhca2 (19 to 23 kD), Lhca3 (23 to 25 kD) and Lhca4 (18 to 21 kD) (Jansson, 1994). In addition, a variable number of Lhcb1/Lhcb2 trimers are associated with PSI which, when combined with the Lhca polypeptides, comprise what is referred to as LHCI or PSI inner antennae. Lhca1 and Lhca4 are thought to be associated together as a pigment-protein complex. Estimates of bound pigment indicate 40 Chl *b* per 100 Chl *a* molecules with associated carotenoids, primarily xanthophllys (Jansson, 1994). Lhca2 and Lhca3 are also thought to exist as a loosely associated pigment-protein complex with a Chl *a/b* ratio of 1.4 (Jansson, 1994).

1.1.8 Organization of the Antennae System

The recent model proposed by Jansson (1994) of higher plant light-harvesting antennae (Fig. 2) is one in which trimers of Lhcb1/Lhcb2, representing the outer antennae and are able to associate with either PSI or PSII. It is suggested that 2 Lhcb1/Lhcb2 trimers are associated with the PSI reaction center core and 4 Lhcb1/Lhcb2 trimers with the PSII reaction center core, although these numbers are variable (Jannson, 1994). The PSI inner antennae is composed of 2 of each of the Lhca polypeptides, that is, 2 Lhca1, 2

Figure 2. Model for the organization of LHCI and LHCII in higher plants. Modified from Jansson (1994). Indicated are the core antennae of PSII (CP43, CP47), inner antennae of PSII (Lhcb3 to Lhcb5 polypeptides) and the outer antennae of PSII (Lhcb1/Lhcb2 trimers). The Lhca polypeptides comprising the inner antennae of PSI are also shown.

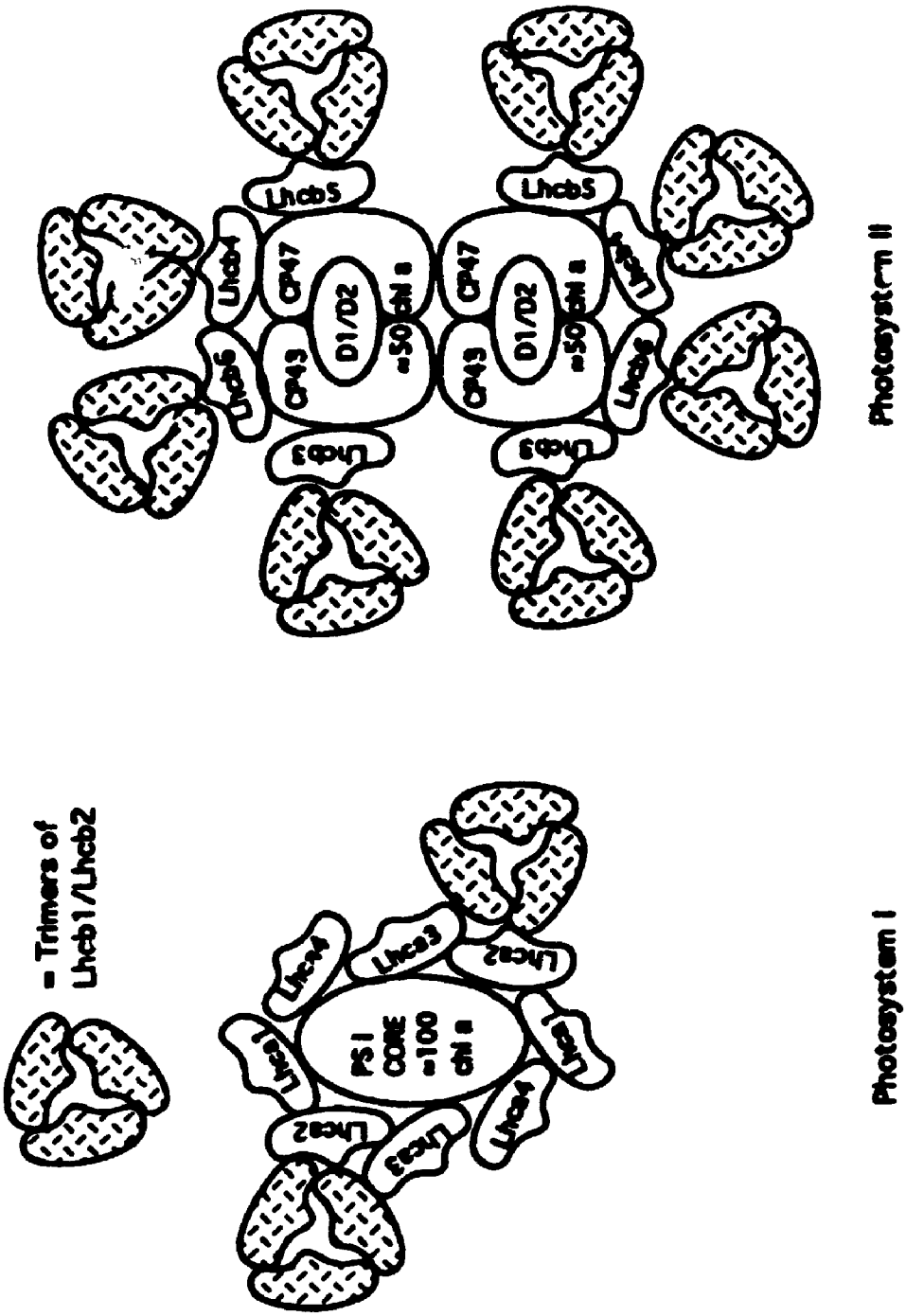
= Trimers of Lhcb1/Lhcb2
Photosystem I
PS I CORE =100 chl a
Lhca1
Lhca2
Lhca3
Lhca4
Photosystem II
Lhcb5
Lhcb4
Lhcb6
CP47
CP43
D1/D2 =50 chl a

Lhca2, 2 Lhca3, and 2 Lhca4. The corresponding PSII inner antennae consists of 1 Lhcb3, 1 Lhcb4, 1 Lhcb5 and 1 Lhcb6 associated with each PSII reaction center (Jansson, 1994). These inner antennae are thought to regulate the energy transfer from the outer antennae to the core antennae and function as linkers of the trimers (Boekema et al., 1995). The localization of the xanthophyll cycle to the inner antennae is thought to play a role in this regulation. This would result in an antennae size of ≈210 Chl molecules for PSI and ≈100 Chl molecules for PSII, without the Lhcb1/Lhcb2 trimers (Jansson, 1994).

1.1.9 Energy Transfer

The reactions of photochemistry depend upon the absorption of light by antennae pigment molecules and subsequent transfer of the absorbed energy to the reaction centers. A pigment molecule in its ground state (S_0) has no net spin of outer orbital electrons. When a photon of the proper wavelength and energy is absorbed, the molecule is raised to an excited singlet state (S_1^*). The favoured route of de-excitation for this excited molecule is energy transfer through photochemistry (Kühlbrandt, 1994). The highly conjugated ring structure of the porphyrin head provide many delocalized π electrons which can participate in light absorption. Photon capture by Chl molecules occurs when the energy of a photon of light causes a π electron to resonate and become excited. The orientation and distances between Chl molecules in LHCII are optimal for energy transfer from Chl *b* to Chl *a* in the order of 200 fs. Each Chl *b* molecule is in van

der Waals contact with a molecule of Chl *a*, which enables this ultra-fast energy transfer by a process known as delocalized exciton coupling (Kühlbrandt, 1994). This occurs by energy oscillation between donor and acceptor without localization to either molecule. Subsequent energy transfer from LHCI or LHCII to the reaction center cores is suggested to occur by a Förster mechanism between Chl *a* molecules. The transfer is a long range dipole-dipole interaction, resulting in an excited acceptor molecule while the donor molecule drops to ground state (Kühlbrandt, 1994). This allows the collected energy to be spread over a large distance in a short time period, dependent upon the packing of LHCII in the membrane. The Chls have absorption maxima in the violet-blue (400 to 480 nm) and orange-red (620 to 700 nm) regions of the visible light spectrum (Greenberg, 1991). The organization of the outer and inner light-harvesting antennae is such that absorption maxima for the pigments involved in excitation transfer are greater as one approaches the reaction center. Thus, excitation energy is funnelled directionally from the outer antennae to the inner antennae to the reaction centers (Kühlbrandt, 1994). The specialized Chl dimers present in the reaction centers, P_{680} and P_{700}, associated with PSII and PSI respectively, are then able to trap the energy released from the de-excitation of the singlet energy states of the surrounding pigments of the core antennae, which causes charge separation within the reaction centers and electron transfer to primary acceptors (Andréasson and Vänngård, 1988). This type of energy transfer forms the basis of the bipartite model of energy distribution and transfer

proposed by Butler and co-workers (Butler and Kitajima, 1975; Butler, 1978). According to this model, primary photochemistry is limited by the rate of energy migration from the antennae to the reaction center. Thus, the rate constant for energy transfer to the reaction center is greater than the rate constant of back transfer from the reaction center to the antennae and charge separation is essentially irreversible (Butler, 1978). Therefore, the reaction centers are designed to prevent charge recombination and thus promote electron transport in the forward direction by stabilizing charge separation. This describes the so-called 'funnel' model of the reaction center (Dau, 1994b). However, another type of model has recently been suggested which proposes energy transfer between the antennae and reaction center is so fast that it is effectively delocalized (Schatz et al., 1988). This is the reversible radical pair or 'shallow trap' model (Dau, 1994b). This model also differs from the classic Butler model in that charge separation is readily reversible.

1.1.10 Photochemical Redox Reactions

Oxygenic photosynthesis involves the cooperation of both photosystems, PSI and PSII with electron transport following what is commonly referred to as the Z-scheme (Hill and Bendall, 1960). Linear or non-cyclic electron transport involves the photooxidation of H_2O to O_2 and the reduction of $NADP^+$ to NADPH ($H_2O \rightarrow NADP^+$) as first proposed by Hill and Bendall (1960). However, this is not the only path available for electron transport. Pseudo-cyclic electron transfer

($H_2O \rightarrow O_2$) may occur which results in the production of the superoxide radical ($O_2^{\cdot-}$), also known as the Mehler reaction (Mehler, 1951). Superoxide is then converted to hydrogen peroxide by the action of SOD. Cyclic electron transfer around PSI may occur where electrons move from soluble Fd back to the PQ pool via Cyt b_6 (Fork and Herbert, 1993). Electrons may also cycle around PSII via Cyt b_{559} which competes with intersystem carriers for the electron equivalents of PQH_2. This has been proposed as a possible mechanism of protection against photoinhbition (Barber and De Las Rivas, 1993). In addition, it has been proposed that PSII can drive the complete non-cyclic electron transport ($H_2O \rightarrow$ Fd) without the collaboration of PSI (Arnon et al., 1981; Prince, 1996).

When P_{700} is excited it readily gives up an electron to the primary acceptor, A_0. On the acceptor side, the electron is rapidly transferred through the series of secondary acceptors, A_1, F_X, F_A and F_B and finally to soluble Fd which acts as a final acceptor (Andréasson and Vänngård, 1988). Reduced soluble Fd subsequently interacts with the flavoprotein, FNR which catalyzes the reduction of $NADP^+$ to NADPH. The oxidized form of P_{700} is usually reduced by plastocyanin (Andersson and Barber, 1994).

Charge separation is initiated at PSII with the excitation of P_{680} which acts as the primary electron donor. Pheo is the immediate electron acceptor which passes its electron to the bound PQ known as Q_A. The electron is then passed to the second bound PQ acceptor, Q_B, forming the semiquinone anion $PQ^{\cdot-}$. However, this second acceptor, which is the final acceptor in PSII, is a two-

electron acceptor and is not fully reduced until a second photochemical turnover occurs resulting in PQ^{2-} (Andréasson and Vänngård, 1988). When fully reduced, Q_B is pronated to form plastoquinol (PQH_2) and dissociates from PSII as a mobile redox component freely diffusing in the lipid matrix of the thylakoid membrane, leaving the Q_B site open for a new PQ to bind (Andersson and Barber, 1994). This is the rate limiting step of photosynthetic electron transport. On the donor side, P_{680}^+ is rapidly reduced from TyrZ on the D1 protein. The oxidized $TyrZ^+$ is then reduced by an electron derived from water. The PSII reaction center must absorb four photons to produce one molecule of O_2, concomitant with the release of four protons, since the complete oxidation of water is a four electron process. The ability to accumulate four oxidizing equivalents and coordinate the release of four electrons, four protons and one molecule of O_2 from water is accomplished by a cluster of four Mn atoms cycling through a series of sequential valency changes (Hansson and Wydrzynski, 1990; Ghanotakis and Yocum, 1990).

Reduced PQ is then used to reduce plastocyanin oxidized by PSI which is mediated by Cyt b_6/f complex. Oxidized plastocyanin extracts electrons from Cyt *f* while PQH_2 reduces the Rieske iron-sulfer center located on Cyt b_6/f. The flow of electrons is then from the Rieske iron-sulfer to Cyt f^+ (Andersson and Barber, 1994).

The protons associated with PQH_2 are released into the thylakoid lumen following its oxidation. Since this electron/proton transfer occurs vectorially

across the thylakoid membrane, protons are shuttled from the stromal to the lumenal side. The resulting electrochemical potential gradient provides the free energy or *pmf* required to drive the conversion of ADP to ATP, according to the chemiosmotic hypothesis of Mitchell (1961). This phosphorylation is catalyzed by the ATP synthase complex. The ATP and NADPH generated by photosynthetic electron transport are then utilized for the reduction of CO_2 to carbohydrate. However, nitrogen and sulfer metabolism, as well as amino acid and lipid synthesis also occur in the chloroplast and thus, also compete for these end products of photosynthetic electron transport (Greenberg, 1991).

1.1.11 Photosynthetic Carbon Metabolism

The process of carbon fixation occurs in the stroma of the chloroplast and is dependent upon the PCR or reductive pentose phosphate cycle also known as the Calvin-Benson-Bassham cycle. The principle reaction of the PCR cycle is the carboxylation of RuBP, catalyzed by Rubisco, leading to the formation of an unstable six carbon intermediate which dissociates into two molecules of PGA (Fig. 3) (Lorimer, 1981). PGA is converted to triose-P (DHAP or GAP) and exported to the cytoplasm via the phosphate translocator to be utilized in the Suc biosynthetic pathway. The production of starch, a major storage carbohydrate is also an alternative. Triose-P also stays within the chloroplast and is used to regenerate RuBP. The reactions of the PCR cycle require energy in the form of ATP and reducing equivalents in the form of NADPH which are supplied from

Figure 3. Photosynthetic carbon metabolism in the chloroplast and cytosol leading to starch and Suc synthesis. The photosynthetic carbon reduction (PCR) and oxidation (PCO) cycles are indicated. The ATP and NADPH utilized are products of photosynthetic electron tranport. Photosynthetic enzymes examined in this thesis are italicized.

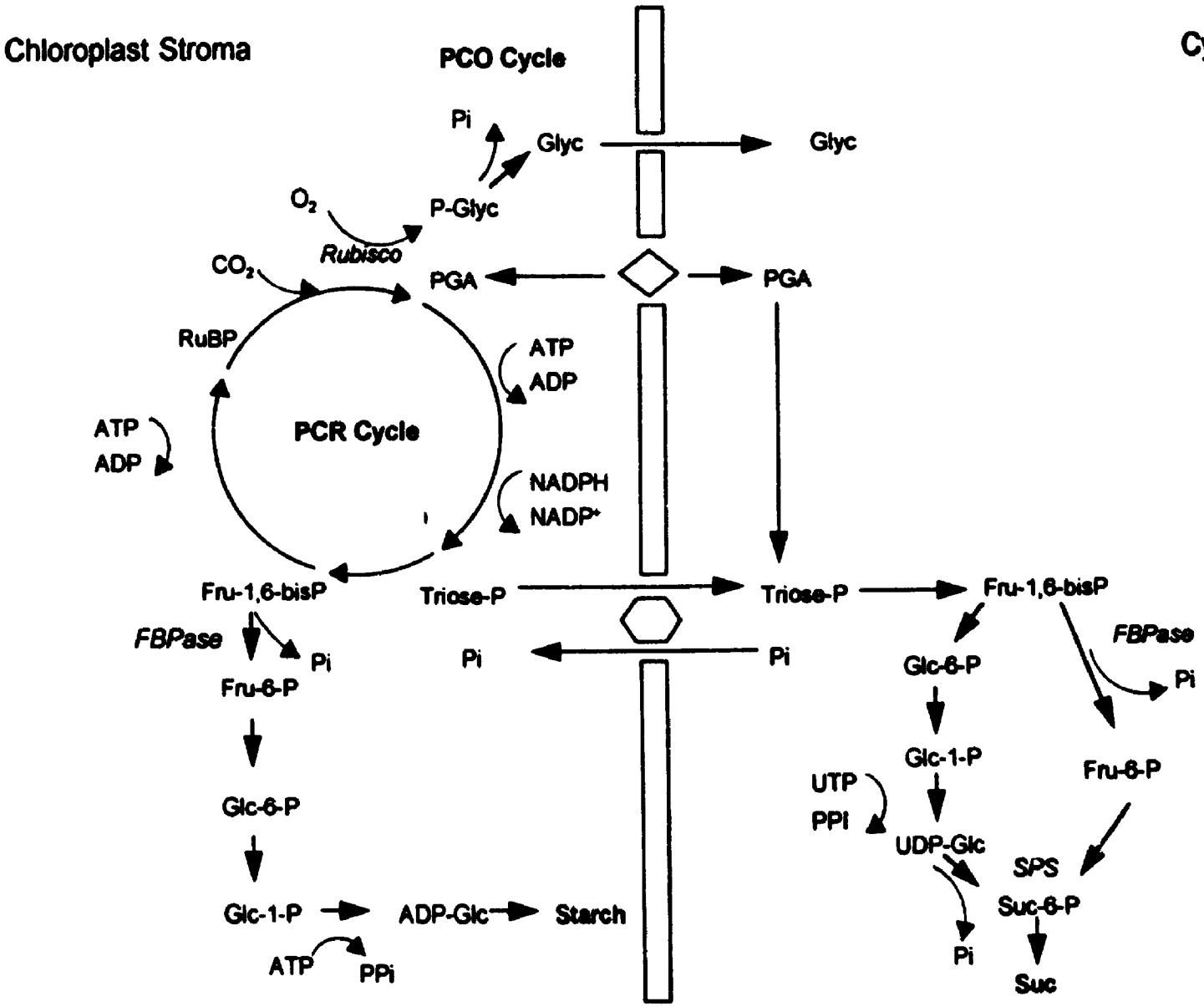
Chloroplast Stroma
PCO Cycle
Cytosol
Pi
Glyc
Glyc
O_2
P-Glyc
Rubisco
CO_2
PGA
PGA
RuBP
ATP
ADP
ATP
ADP
PCR Cycle
NADPH
$NADP^+$
Fru-1,6-bisP
Triose-P
Triose-P
Fru-1,6-bisP
FBPase
Pi
Pi
Pi
FBPase
Pi
Fru-6-P
Glc-6-P
Glc-1-P
UTP
PPi
Fru-6-P
Glc-6-P
UDP-Glc
SPS
Glc-1-P
ADP-Glc
Starch
Suc-6-P
ATP
PPi
Pi
Suc

photosynthetic electron transport. The PCR cycle requires two NADPH and three ATP molecules to fix one CO_2 molecule. For each NADPH generated, four photons must be absorbed to obtain the required two electrons, resulting in the pumping of four protons. One ATP molecule requires three protons, thus 1.33 ATP are produced for every $NADP^+$ reduced by linear electron transport (Heber and Walker, 1992). However, 1.5 ATP are required, the difference of which is provided by cyclic and pseudo-cyclic electron transport mechanisms.

Rubisco may also act as an oxygenase, which catalyzes the addition of O_2 to RuBP which forms one molecule of PGA and one molecule of P-Glyc in a process referred to as the PCO cycle (Fig. 3). This is the principle reaction in photorespiration (Ogren, 1984). If O_2 partial pressures ($p(O_2)$) in the chloroplast are high or CO_2 partial pressures ($p(CO_2)$) low, the PCO cycle will be stimulated and photorespiration will be favoured. Photorespiration consumes O_2 and ATP while liberating CO_2. Thus, photorespiration represents a major pathway for carbon loss in C_3 plants (Lorimer, 1981).

Under conditions of low light, it is light itself which limits photosynthesis through reduced electron transport, and hence a lack of ATP and NADPH for the PCR cycle (Leegood et al., 1985; Woodrow and Berry, 1988). In contrast, under light-saturating conditions, it is the capacity of the PCR cycle to regenerate RuBP which limits photosynthesis, as energy input exceeds demand and the capacity of the PCR cycle to fix CO_2 (Woodrow and Berry, 1988). Insufficient sink demands for photosynthate may also limit RuBP regeneration (Leegood et al.,

1985; Dujardyn and Foyer, 1989), although, external factors are most often responsible. These may include availability of CO_2 due to diffusional limitations, insufficient availability of Pi or reduced enzyme activity. These conditions all lead to limited CO_2 fixation as a result of the imbalance between the capacity for electron transport and the capacity of the PCR cycle to keep the electron transport chain oxidized. This imbalance results in an increase in the or *trans*-thylakoid ΔpH which effectively reduces the rate of electron transport at PSII (Foyer et al., 1990). Carbon metabolism is then able to regulate the rate of electron transport by the *trans*-thylakoid ΔpH gradient through a process known as photosynthetic control (Foyer et al., 1990). However, this is not an immediate response, as a large proportion of Q_A can stay in the oxidized state (q_P) under light levels much greater than those of saturation (Dietz et al., 1985). Instead, what occurs is a decline in the quantum yield of open PSII centers (F_V'/F_M') or a decrease in the ability to trap light and close PSII centers.

1.2 Photosynthetic Measurements

1.2.1 Photosynthetic Gas Exchange

The following equation indicates the relationship between carbon assimilation and O_2 evolution as a result of photosynthesis;

$$6CO_2 + 6H_2O \rightarrow light \rightarrow C_6H_{12}O_6 + 6O_2$$

The rate of O_2 evolved is directly related to PSII activity and electron transport

through the oxidation of water. CO_2 assimilation is a measure of the photosynthetic carbon gain by the plant. The ability of the plant to regulate the harvesting of radiant energy and the subsequent utilization of chemical energy in the PCR cycle can be assessed *in vivo* by measuring the rates of exchange of either CO_2 or O_2 (Foyer et al., 1990; Harbinson et al., 1990).

O_2 evolution measurements are made using a membrane covered electrode, utilizing a saturated potassium chloride (KCl) solution as an electrolyte to join a silver (Ag) anode and platinum (Pt) cathode. A polarographic measurement is made through the application of a small potential across the electrode. Dissolved O_2 diffuses through the membrane and is reduced at the cathode, resulting in a current flow proportional to the oxygen concentration (Dilieu and Walker, 1981).

When the rate of O_2 evolution is plotted as a function of PPFD, the slope of the linear portion of the curve is referred to as the apparent quantum yield (Φ_{app}) of O_2 evolution, which reflects the number of photons required to evolve one mole of O_2 (Walker, 1990). This is only an apparent measurement as it assumes that all incident light is captured and utilized photosynthetically by the plant, with no loss due to reflectance or transmittance. If the absorptance of the leaf is known, this value can be corrected and expressed as the actual quantum yield (Φ) of O_2 evolution (Öquist et al., 1992b). Since two photons of light must be absorbed to cause the net transfer of one electron along the electron transport chain from H_2O to $NADP^+$, the evolution of one molecule of O_2 requires

eight photons of light to transfer the four electrons released from the oxidation of two molecules of water. Therefore, the theoretical maximum quantum yield of oxygen evolution is 1/8 = 0.125 mol O_2 mol photons^{-1} (Walker, 1990). Under CO_2 -saturating conditions, for every molecule of CO_2 fixed, one mole of O_2 is liberated in a 1:1 ratio. In addition, 6 molecules of CO_2 must be fixed to generate 1 molecule of hexose sugar in a 6:1 ratio. Thus, measurements of O_2 evolution can be utilized to examine overall photosynthetic capacity under these conditions. However, the relationship between O_2 evolved and CO_2 consumed is not necessarily a 1:1 ratio. It is possible to evolve more O_2 than CO_2 that is being fixed due to competing metabolic processes for ATP and NADPH. This increases the number of photons required to fix one mole of CO_2 (Walker, 1990).

1.2.2 Chl *a* Fluorescence

1.2.2.1 Fluorescence Relations

Fluorescence refers to the non-destructive release of a photon of a longer wavelength than that absorbed. Chl *a in vivo* displays large changes in fluorescence yield upon illumination, and at room temperature, almost all Chl *a* fluorescence originates exclusively from PSII. The low fluorescence yield of PSI at room temperature is due to the stability of P_{700}, which in the oxidized state (P_{700}^+) can still act as a trap for excitons, thus representing a quencher of fluorescence (Krause and Weis, 1991). Therefore, fluorescence changes at room temperature reflect the state of PSII and provide a non-intrusive probe to

monitor photosynthetic events *in vivo* (Schreiber et al., 1994). For dark adapted leaves, based on the bipartite model of Butler and Kitajima (1975), minimum fluorescence yield (ΦF_O) occurs when all PSII reaction centers are in the open configuration;

$$[\,Z\ P_{680}\ Pheo\ Q_A\ Q_B\,]$$

and is represented by the following equation;

$$\Phi F_O = k_F / (\,k_F + k_D + k_T + k_P\,)$$

Where k_F, k_D, k_T, and k_P are first order rate constants for fluorescence emission, thermal dissipation, energy transfer to PSI, and photochemistry respectively. ΦF_O represents a small portion (0.6%) of the light absorbed by the pigment bed due to competition by photochemistry (Krause and Weis, 1991). Maximum fluorescence yield (ΦF_M) occurs when all PSII reaction centers are in a closed configuration with the radical pair stabilized and P_{680} oxidized;

$$[\,Z\ P_{680}^{+}\ Pheo\ Q_A^{-}\ Q_B\,]$$

and is represented by the equation below;

$$\Phi F_M = k_F / (\,k_F + k_D + k_T\,)$$

ΦF_M amounts to approximately 3% of light absorbed by the photosynthetic pigments (Krause and Weis, 1991). The yield of PSII photochemistry (Φ_P) can then be expressed as follows;

$$\Phi_P = k_P / (\,k_F + k_D + k_P + k_T\,) = (\Phi F_M - \Phi F_O) / \Phi F_M = F_V / F_M$$

where F_V is the maximum variable fluorescence ($F_V = F_M - F_O$); F_M, maximum fluorescence with all PSII traps closed; and F_O, minimum fluorescence with all

PSII traps open. Therefore, based on the above relationship, the variable to maximal fluorescence ratio (F_V / F_M) is equal to the yield of PSII photochemistry (Φ_P) (Butler, 1978), and can thus be used as an estimate of photosynthetic efficiency. The F_V/F_M ratio has been found to be remarkably constant for a wide variety of species and ecotypes (0.832 ± 0.004) and this ratio is closely correlated with the quantum yield of O_2 evolution (Björkman and Demmig, 1987; Adams et al., 1990). However, this relationship is merely empirical. Cooperativity between reaction centers and experimental evidence indicating two distinct populations of PSII reaction centers ($PSII_\alpha$ and $PSII_\beta$) further demonstrate that no unique relationship exists between F_V/F_M and Φ_P (Krause and Weis, 1991). F_O appears to be fluorescence emission from Chl *a* in the light-harvesting antennae of PSII. Thus, F_O reflects exciton losses during the transfer of excitation energy from the pigment bed to the reaction center, and represents emission from excitons that do not contribute to photochemistry. Fluorescence emission has been shown to increase when antennae Chl cannot transfer their energy to the reaction center thus resulting in an increase in F_V as Q_A is reduced until all PSII reaction centers close and maximum fluorescence or F_M is detected. The source of (F_M or F_V) is controversial, although current evidence points towards fluorescence emission from the Chl *a* antennae (Krause and Weis, 1991; Dau, 1994b).

1.2.2.2 Fluorescence Quenching

Quenching refers to any process which reduces the level of fluorescence below the maximum value (F_M) and may occur during fluorescence induction or under steady-state conditions. Fluorescence emission competes with photochemistry and heat dissipation, thus, two types of fluorescence quenching are evident, photochemical and non-photochemical. It is possible to separate and quantify these quenching mechanisms using the saturating pulse method in combination with a fluorometer base on pulse amplitude modulation (PAM) (Schreiber et al., 1986). The rationale of this technique is that upon a saturating light pulse, Q_A becomes fully reduced and photochemical quenching becomes suppressed. The remaining quenching is therefore non-photochemical (Bradbury and Baker, 1981). After dark adaptation for 1 h which renders all PSII traps in the open configuration (Q_A fully oxidized), a low intensity (0.01 µmol m^{-2} s^{-1}) measuring beam is utilized to measure F_O, without causing PSII trap closure. A subsequent flash with a saturating light (6500 µmol m^{-2} s^{-1}) renders all PSII traps closed (Q_A reduced) resulting in maximum fluorescence yield reaching a maximum (F_M). F_M is rapidly quenched due to the re-oxidation of Q_A by intersystem electron transport and PSI.

An actinic light source is then utilized by which initially, Q_A reduction is greater than Q_A re-oxidation. The resulting fluorescence rise reflects the depletion of the PSII acceptor pool which is slowly quenched to a steady-state level of fluorescence termed F_S. By superimposing saturating flashes in the presence of actinic light, all PSII traps are closed giving rise to F_M', and thus

allowing the determination of photochemical and non-photochemical quenching. F_O' is determined in the presence of FR light to ensure the complete oxidation of all PSII acceptors by preferentially exciting PSI. A typical PAM tracing for leaves of winter rye is presented in Figure 4. The extent of q_P or PSII trap 'openness' is therefore dependant upon the redox state of Q_A, and reflects the balance between reduction of PSII by photochemistry and the oxidation of PSII by intersystem electron transport. Therefore, the re-oxidation of Q_A^- through intersystem electron transport to PSI will quench fluorescence. The quenching coefficients q_P and q_N have been defined for photochemical and non-photochemical quenching respectively (Schreiber et al., 1986; van Kooten and Snel, 1990; Schreiber et al., 1994);

$$q_P = (F_M'-F_S) / (F_M'-F_O') \qquad q_N = 1- ((F_M' - F_O')/ (F_M - F_O))$$

It was originally assumed that only quenching of F_V occurred non-photochemically, It has since been shown that F_O can be quenched by ΔpH-dependent non-photochemical quenching (Bilger and Schreiber, 1986). Thus, knowledge of F_O' is required for the correct calculations of q_P and q_N. However, non-radiative dissipation can also be calculated using the following equation;

$$NPQ = (F_M/F_M') -1$$

which does not require the knowledge of F_O'. Calculations based on this equation, also known as Stern-Volmer NPQ (Bilger and Björkman, 1990) are done with the assumption of the existence of non-photochemical traps such as

Figure 4. Standard nomenclature of characteristic fluorescence levels derived from a PAM fluorometer tracing utilizing the saturating pulse method as described by Schreiber et al. (1994).

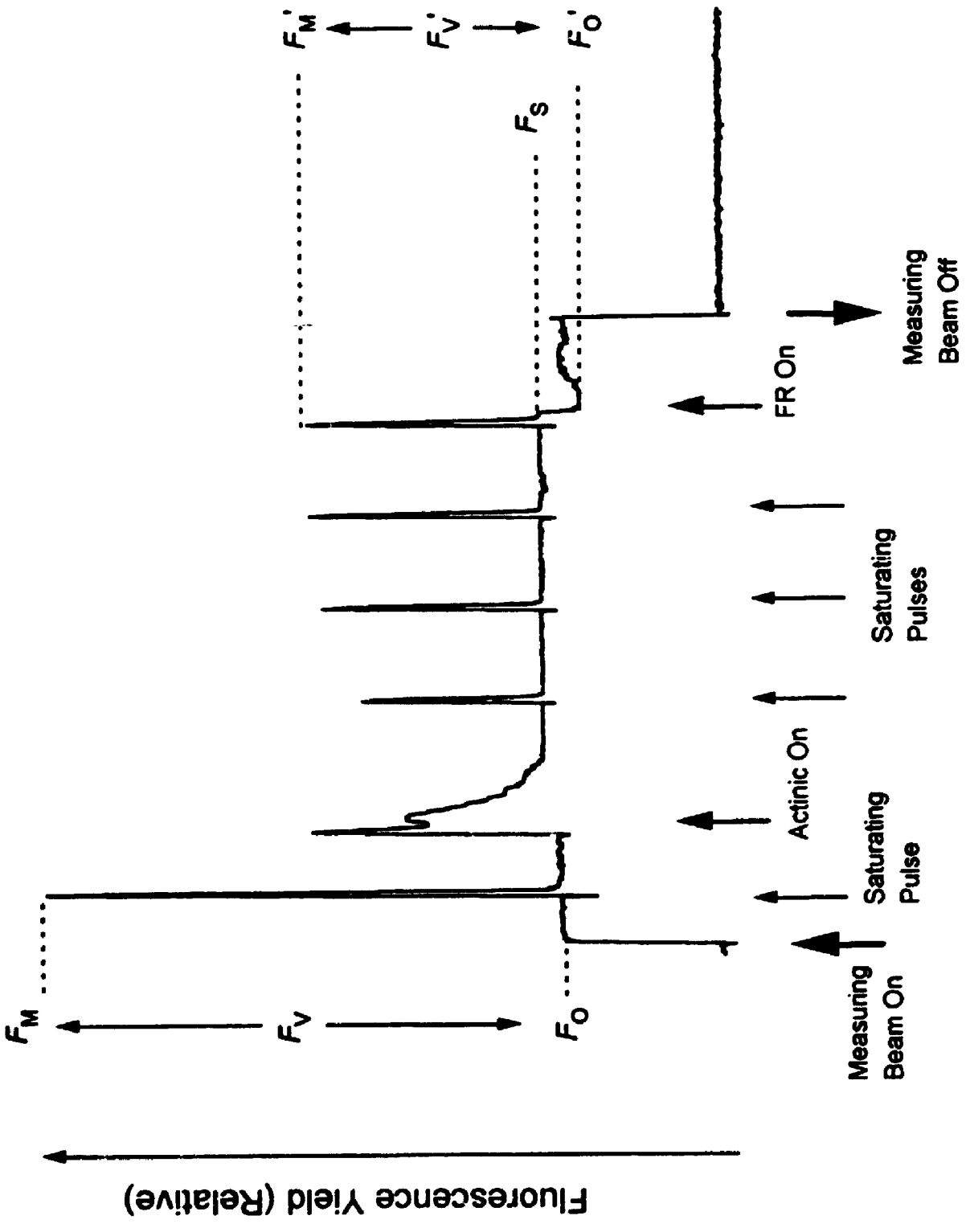
Fluorescence Yield (Relative)
F_M
F_V
F_O
F_M'
F_V'
F_O'
F_S
Measuring Beam On
Saturating Pulse
Actinic On
Saturating Pulses
FR On
Measuring Beam Off

the xanthophylls Zx or Ax. Most studies examining xanthophyll involvement in NPQ processes utilize this equation (Demmig-Adams, 1990).

Non-photochemical quenching of fluorescence occurs by means which are not directly related to the redox state of Q_A (Krause and Weis, 1991). Collectively, these processes are referred to as q_N or NPQ, but they may be further subdivided into three major components, distinguishable by their relaxation kinetics. First, energy dependant quenching (q_E) is related to the *trans*-thylakoid ΔpH during electron transport. The build up of this gradient has been shown to account for up to 90% of all F_V quenching (Krause and Weis, 1991), presumably through increasing the rate constant for thermal dissipation (k_D) (Krause et al., 1983). This is accomplished by increasing non-radiative decay through increased xanthophyll carotenoid levels, Zx and Ax in particular, in the minor Chl *a/b*-binding proteins (Demmig-Adams, 1990; Demmig-Adams and Adams, 1992; Demmig-Adams et al., 1996). Alternatively, a reaction center quenching mechanism has also been suggested which does not require the xanthophylls, only the other carotenoids already present in the reaction center (Schreiber and Neubauer, 1990; Kreiger et al., 1992). Second, quenching related to state I to state II transitions (q_T). State transitions are regulated by LHCII phosphorylation controlled by the redox state of the PQ pool and reflect energy distribution between the photosystems (Fork and Satoh, 1986). A state transition occurs when LHCII becomes physically dissociated from the core

antennae of PSII upon phosphorylation of specific LHCII polypeptides. A state transition from state I (non-phosphorylated) to state II (phosphorylated) reduces the absorptive cross section of PSII relative to PSI, resulting in quenching of F_O and F_V, thus decreasing fluorescence yield associated with PSII (Krause and Weis, 1991). Lastly, photoinhibitory quenching (q_I) which is related to photoinhibition of photosynthesis and represents a light-dependent increase in non-photochemical de-excitation of pigments. However, the mechanisms controlling q_I remain obscure (Krause and Weis, 1991).

1.2.3 Intersystem Electron Pool Size

The redox state of P_{700} can be evaluated by absorbance changes in the cation radical (P_{700}^+) in the near-infrared spectral region around 820 nm (800 to 840 nm) (Harbinson and Woodward, 1987; Schreiber et al., 1988; Harbinson and Hedley, 1989). Figure 5 demonstrates a typical cycle of illumination for the determination of the intersystem electron pool size. Illumination with FR light excites almost exclusively PSI, causing the oxidation of P_{700} to P_{700}^+. When P_{700} is oxidized (P_{700}^+) by continuous illumination with FR light, a saturating ST flash causes a single turnover event of all PSII centers and results in the reduction of P_{700}^+ to P_{700} as shown in Figure 5. However, an initial lag is present (3 ms; not resolvable with this time scale) which represents the electron transfer from PSII to Cyt b_6/f. This is followed by a decay representing the rate limiting step of PQH_2 oxidation at Cyt b_6/f. The FR light driven re-oxidation of P_{700} to P_{700}^+ can

Figure 5. Illustration of the illumination cycle for determination of intersystem electron pool size by monitoring the oxidation and reduction of P_{700} as described by Asada et al. (1992).

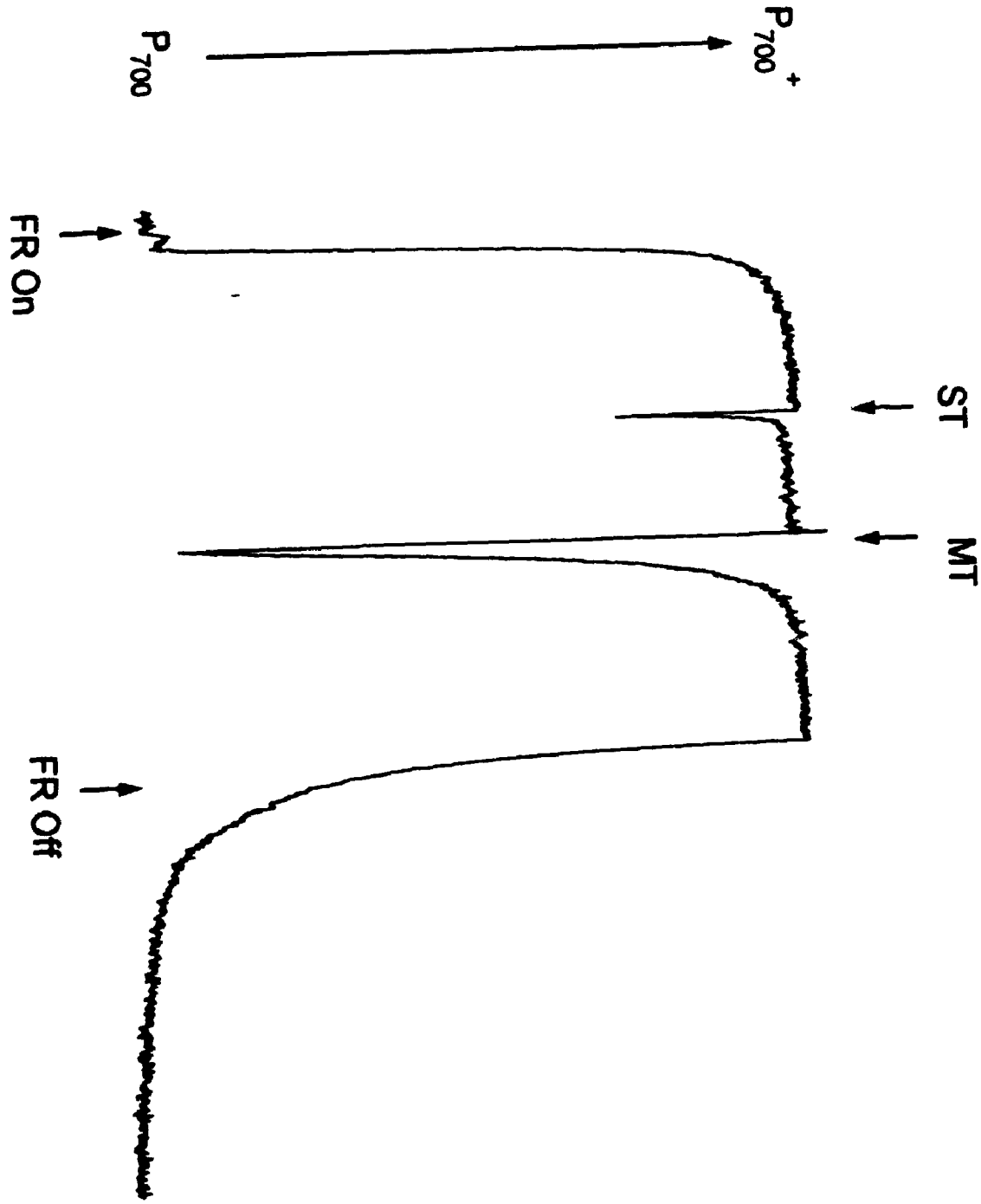
P700
P700+
FR On
ST
MT
FR Off

then be observed (Fig.5). When a MT flash is applied to P_{700}^+, an almost complete reduction of P_{700}^+ is observed due to the saturation of the PQ pool located between PSII and PSI. The electrons from PSII reach P_{700}^+ with a delay imposed by intersystem electron transport. The more electrons stored in the PQ pool, the longer the given FR light requires to re-oxidize P_{700} to P_{700}^+. The complementary area between the oxidation curve of P_{700} after ST or MT excitation and the stationary level of P_{700}^+ under continuous FR light represents the ST- and MT-areas respectively. The ratio of the MT to ST area enables the determination of the functional intersystem electron pool size on a P_{700} reaction center basis (Schreiber et al., 1988; Asada et al., 1992).

1.3 Photoinhibition of Photosynthesis

Photoinhibition has been defined as a light-dependent decrease in photosynthetic efficiency which may or may not be associated with a decrease in PS_{max} as a result of the absorption of excess light energy (Kok, 1956; Powles, 1984; Krause, 1988; Osmond, 1994). Thus, photoinhibition may manifest itself *in vivo* as a decrease in ΦO_2 or ΦCO_2, a reduction in the photochemical efficiency of PSII (F_V/F_M), as well as a reduction in PS_{max} (Krause, 1988; Osmond, 1994) which occurs under field and controlled environment conditions (Long et al., 1994). It is generally agreed that the most sensitive site for photoinhibition is PSII, due to the fact that the oxidation of PSII is rate limiting at the level of the PQ pool (Haehnel, 1984; Mitchell et al., 1990). However, recent studies have

implicated PSI which is usually insensitive to photoinhibition unless under extreme conditions (Jones and Kok, 1966; Sétif and Brettel, 1990; Havaux and Davaud, 1994; Sonoike, 1996). Since PSII appears to be the primary target for photoinhibition, it has been proposed that photoinhibition is the result of an over-reduction of PSII which results in damage to the 32 kD, PSII reaction center D1 polypeptide (Aro et al., 1993a, 1993b; Critchley and Russell, 1994). The primary site of photoinhibitory damage has yet to be conclusively elucidated. However, several studies have shown that the principal site of dysfunction under exposure to photoinhibitory light is the Q_B binding site of the D1 protein (Kyle et al., 1984; Reisman et al., 1986; Kyle, 1987).

Studies with cereals (Lapointe et al., 1991; Hurry and Huner 1992) have demonstrated that decreased photochemical efficiency cannot be attributed to damage at the Q_B site. Furthermore, the rate at which photoinhibition develops is independent of the redox state of Q_B (Cleland and Melis, 1987). However, there is a correlation between the redox state of Q_A and photoinhibition (Öquist et al., 1992b). A loss in Q_A reduction may imply damage in the reaction center complex, possibly impairing charge separation between P_{680} and Pheo This is thought to occur by a configurational change in the reaction center polypeptides which disables electron transfer to Q_A and alters the binding domain of Q_B, thus preventing utilization of trapped energy (Demeter et al., 1987; Ohad et al., 1990).

The OEC has also received attention as a possible site of damage. This is supported by the presence of free Mn associated with a loss of structural

integrity of proteins dissociated from the core complex upon photoinhibition (Hundell et al., 1990). In addition, the OEC has also been shown to be a relatively unstable subunit of PSII (Cleland and Melis, 1987).

Hurry and Huner (1992) have demonstrated that in winter wheat, the fast phase of recovery from photoinhibition occurs at temperatures as low as -3°C without *de novo* protein synthesis. This lack of protein synthesis indicates that in winter wheat, the photoinhibitory response has little to do with damage and is largely regulatory. However, the slower phase does require protein synthesis (Hurry and Huner, 1992; van Wijk and van Hasselt, 1993b). Krause and co-workers have proposed that this regulatory process may be attributed to light induced reversible modifications in PSII structure which enable the reaction centers to act as light traps or quenchers, dissipating excess excitation energy as heat (Krause et al., 1990; Giersch and Krause, 1991). Thus, the observed responses to photoinhibition could be considered regulatory, and not indicative of damage to the photosynthetic apparatus. Instead, this may be a reflection of the ability to balance ATP and NADPH production through photosynthetic electron transport with the requirements of CO_2 fixation under prevailing environmental conditions. Thus, it has been suggested that photoinhibition may be considered a mechanism to protect PSII from over-excitation through the down regulation of PSII photochemistry (Krause, 1988; Hurry et al., 1992; Öquist et al., 1992b; Huner et al., 1993; van Wijk and van Hasselt, 1993a; Krause, 1994a).

It was first proposed by Ögren (1991) and subsequently supported by Öquist et al. (1992a, 1992b) that photoinhibition was related to the redox state of PSII. This relationship was examined for a variety of species from which it was concluded that a fundamental feature of photoinhibition among all taxonomic groups was its dependence upon PSII excitation pressure, measured as $1-q_P$ (Ögren and Rosenqvist, 1992). Thus, susceptibility to photoinhibition has been shown to be correlated to the redox state of PSII, regardless of the environmental constraints on photosynthesis brought about by low temperature or light acclimation (Ögren and Rosenqvist, 1992; Öquist et al., 1992a, 1992b, 1993b; Park et al., 1996a). Further, the adaptive ability of the plant to the environment also reflects, to a degree, the extent of photoinhibitory response. Susceptibility to photoinhibition has been demonstrated to vary depending upon the particular type of carbon fixation pathway utilized (CAM, C_3, or C_4) (Adams et al., 1988; Bolhar-Nordenkampf et al., 1991). In contrast, studies with high- and low-light grown pumpkin have shown that the size of the absorptive cross section of the light-harvesting antenna does not seem to affect the susceptibility to photoinhibition *in vitro* (Tyystjärvi et al., 1991).

Low temperature, in combination with light, increases the susceptibility of photosynthesis to photoinhibition (Powles, 1984; Öquist and Martin, 1986; Öquist et al., 1987; Greer, 1990; Krause, 1994a). This is thought to occur primarily through a temperature suppression of the PSII repair cycle (Greer et al., 1986; Kyle, 1987; Chow et al., 1989; Gong and Nilsen, 1989; Greer et al., 1991; Aro et

al., 1993b). However, it has recently been established that given a certain excitation pressure on PSII, the susceptibility of photosynthesis to photoinhibition occurs independent of temperature between 0 and 25°C (Öquist et al., 1993b). It was concluded that photoinhibition at low temperature is sensitized by a temperature inhibition of photosynthesis and not a low temperature inhibition of the PSII repair cycle (Hurry and Huner, 1992; Huner et al., 1993; Öquist et al., 1993b). The above studies, along with reports for conifers (*Pinus sylvestris*) (Öquist and Martin, 1986) and the chilling sensitive *Zea mays* (Baker et al., 1988) suggest that several mechanisms exist in response to photoinhibition and recovery, dependent upon adaptive strategies and sensitivity to other environmental conditions such as low temperature (Huner et al., 1993).

Winter cultivars of rye (*Secale cereale*), wheat (*Triticum aestivum*) and the herbaceous dicot spinach (*Spinacia oleracea*) grown at low temperature (5°C) and moderate irradiance (250 μmol m^{-2} s^{-1}) exhibit an increased tolerance to photoinhibition as measured by both F_V/F_M and photosynthetic gas exchange (Somersalo and Krause, 1989; Boese and Huner, 1990; Somersalo and Krause, 1990; Hurry and Huner, 1992; Huner et al., 1993; Öquist and Huner, 1993). Growth at low temperature is an absolute requirement for acquisition of this tolerance to photoinhibition (Gray et al., 1994). It has been documented that short-term shifts to low temperature do not induce tolerance to photoinhibition, irrespective of either photoperiod or cold-hardening protocol (Öquist and Huner, 1991; Boese and Huner, 1992; Gray et al., 1994). In addition, the degree of

tolerance to photoinhibition in wheat is cultivar dependent with the winter cultivar, Monopol, exhibiting a greater tolerance to photoinhibition than the spring cultivar, Katepwa, after growth at low temperature. However, cold-grown cultivars are more tolerant to photoinhibition than their warm-grown counterparts (Hurry and Huner, 1992; Hurry et al., 1992). In winter rye, this tolerance is observed at the whole leaf and cellular level, suggesting altered leaf morphology as a result of development at low temperature does not account for the increased tolerance to photoinhibition (Lapointe and Huner, 1993). In contrast, isolated thylakoids do not exhibit the same level of tolerance, suggesting a metabolically competent cell is required for increased tolerance to photoinhibition (Lapointe et al., 1993).

It has been demonstrated previously that the growth of winter cereals at low temperature results in an increased capacity to keep Q_A oxidized under photoinhibitory conditions (Öquist and Huner, 1993; Öquist et al., 1993b). When the reduction state of Q_A is artificially equalized in winter rye, the sensitivity to photoinhibition is the same for 5 and 20°C-grown leaves (Öquist and Huner, 1993; Öquist et al., 1993b). Furthermore, the 5°C leaves require photon fluxes that are 3-fold greater than that of the 20°C leaves to attain the same redox state of Q_A (Öquist and Huner, 1993).

While photoinhibition refers to events involved in the loss of photosynthetic activity, these are readily reversible under low light or in the dark (Krause, 1994a). Photooxidation refers to the extensive non-reversible bleaching caused by the destruction of pigments, proteins, and lipids (Asada,

1994). A common source of photooxidative stress is that of highly reactive oxygen radicals such as superoxide ($O_2^{\cdot-}$) or singlet oxygen ($^1O_2$). $^1O_2$ is produced via intersystem crossing, where a Chl molecule in the excited triplet state ($^3Chl^*$) can react with a triplet oxygen molecule ($^3O_2$) in the ground state, giving rise to $^1O_2$ (Knox and Dodge, 1985; Asada, 1994; McKersie and Leshem, 1994). The oxidation of the PQ by O_2 and psuedo-cyclic electron flow will result in the production of $O_2^{\cdot-}$ which is thought to have an affinity for the Q_B binding site. In this manner, reactive oxygen species have been linked to photoinhibition (Krause, 1994b). In addition, $O_2^{\cdot-}$ can combine with H_2O_2, and in the presence of Fe^{2+} may result in Fenton reactions, giving rise to the highly reactive hydroxyl radical ($OH\cdot$) which may contribute to the damage in the reaction center and antennae complexes (Foyer and Hall, 1980; Asada, 1994; McKersie and Leshem, 1994).

1.4 Cold Acclimation and Photosynthesis at Low Temperature

Responses of plants to changes in the environment can be divided into adaptive and acclimatory responses. Adaptation is a response to long-term change which results in an inheritable change seen over successive generations (Prosser, 1986). Short-term responses may also occur and refer to immediate, direct adaptive changes. In contrast, acclimation is an inducible response which results in a phenotypic alteration over a single generation time. Acclimative responses can be divided in developmental responses and stress responses.

Developmental responses refer to a stable long-term adjustment to environmental change, while stress responses refer to abrupt or short-term changes in the environment. Thus, it is important to distinguish between acclimative responses and transient stress responses when examining environmental physiology.

Low temperature is an important environmental factor which limits plant distribution, survival, and crop yields worldwide (Osmond et al., 1987). Plants may be classified based upon their response to low temperature as either cold-sensitive or cold-tolerant (Levitt, 1980). Cold-tolerant plants, if grown at temperatures greater than 10°C, can survive temperatures as low as -6°C. These same plants, if grown at temperatures less than 10°C, can survive temperatures as low as -30°C, dependent upon plant species and cultivar (Harvey, 1922; Huner et al., 1989). This period of growth at low temperatures is referred to as the cold acclimation period. Exposure to low, non-freezing temperatures induces genetic, morphological, and physiological changes in the plant which result in the development of cold hardiness and the acquisition of freezing tolerance (Vasil'yev, 1961; Levitt, 1980; Guy, 1990; Huner, 1993; Thomashow, 1990, 1993; Hughes and Dunn, 1996). Cold-sensitive plants have little or no capacity to grow at low temperatures and will not be examined here but have been recently reviewed (Baker et al., 1988).

Freezing tolerant plants survive a freezing event by forming ice within their tissues. However, no ice forms intracellularly, as this is thought to be lethal due

to damage at the level of the cellular membranes (Levitt, 1980; Steponkus, 1984). Upon cold acclimation, leaves of winter rye accumulate apoplastic proteins which serve, in part, to nucleated ice formation in xylem vessels and intercellular spaces (Pearce, 1988; Pearce and Ashworth, 1992; Brush et al., 1994; Hon et al., 1995). Cellular contents then dehydrate as water is removed from the cell and added to the growing extracellular ice crystal (Pearce, 1988). The lowest limit for freezing tolerance is determined by the extent to which the cells can survive the desiccation induced by extracellular ice formation (Webb and Steponkus, 1993). In addition, the growth pattern of these ice crystals can be modified by antifreeze proteins, also located in the apoplast, which are thought to play a fundamental role in the mechanism of freezing tolerance by decreasing the rate of ice formation and recrystallization during prolonged freezing (Hon et al, 1995).

Light, through the process of photosynthesis, provides the energy required for cold acclimation which leads to the attainment of freezing tolerance (Dexter, 1933; Tysdall, 1933; Steponkus and Lanphear, 1968; Levitt, 1980; Gusta et al., 1982; Griffith & McIntyre, 1993; Veisz and Tischner, 1995). Huner and co-workers have demonstrated that the freezing tolerance of cereals is not only correlated to the capacity to keep Q_A in the oxidized state, but also to an increased PS_{max} (Huner et al., 1993; Öquist et al., 1993). Therefore, any factor which chronically affects photosynthesis will ultimately influence the induction and maintenance of the cold hardened state.

Increases in PS_{max} as a result of cold acclimation has been shown to be correlated with the accumulation of Suc as well as fructans, whose synthesis are stimulated by the accumulation of Suc in the cytosol (Pollock and Lloyd, 1987; Tognetti et al., 1990; Pollock and Cairns, 1991; Guy et al., 1992; Hurry et al., 1994). The accumulation of these photosynthetic end products have been correlated with increases in Rubisco, SPS and stromal and cytosolic FBPase activities (Guy et al., 1992; Holaday et al., 1992; Hurry et al., 1994, 1995a, 1995b). Although fructans accumulate in the vacuole, Suc , Fru and raffinose accumulate in the cytosol (Koster and Lynch, 1992) where they are proposed to play a cryoprotective role, moderating the dehydration stress caused by water loss during extracellular ice formation by stabilizing membranes as well as substrates for basal metabolism. During freezing, fructans stored in the crown tissue are readily converted to Fru and Suc and accumulate in the cytosol. Upon thawing, these sugars are converted back to fructans (Olien and Clark, 1993). Fructan pools therefore play an active role in alleviating freezing stress and are correlated with freezing tolerance. Thus, increases in amounts and activities of enzymes involved in the PCR cycle and Suc biosynthesis are not simply an adjustment to overcome slower enzyme kinetics at low temperature (Guy et al., 1992). Thus, the physiological state of the plant and the specific environmental conditions to which the plant is exposed are as important as the genetic potential of the plant for the attainment of maximal freezing tolerance (Stushnoff et al., 1984; Gusta and Chen, 1987; Veisz and Tischner, 1995).

Cold acclimation has also been shown to lead to substantial changes in the lipid composition of plant membranes, thought to be the primary lesion of freezing injury (Steponkus, 1984). Freezing injury in non-acclimated leaves is a result of the freeze-induced formation of the H_{II}. In contrast, freezing injury in cold acclimated leaves is associated with the fracture-jump lesion, the threshold temperature of which decreases to lower temperatures with increasing duration of cold acclimation. Changes in the incidence of these freeze-induced lesions are associated with alterations in plasma membrane lipid composition during cold acclimation (Uemura and Steponkus, 1994). In thylakoids, changes in MGDG:DGDG could have significant effects on thylakoid stability and functional integrity as a result of solute accumulation or increases in cellular osmoticum. In contrast to the other lipids which are bilayer forming, MGDG forms a reversed hexagonal phase (H_{II}). The greater amount of MGDG present, the more nonlamellar phase is formed. Thus this ratios may be important in maintaining the correct balance between lamellar and hexagonal lipids (Selstam and Widell Wigge, 1993). Upon exposure to low temperature, many plants demonstrate an increase in the level of fatty acid unsaturation in the major thylakoid lipids. Mutations in chloroplast fatty acid biosynthesis in *Arabidopsis* results in minimal changes in loss of function as a result of a shift to low temperature and appear to play only a minor role in chilling sensitivity (Wu and Browse, 1995). However, it has been suggested that the main effect of these mutations may be at the level of membrane biogenesis and chloroplast ultrastructure during development at

low temperature as well as interfering with thylakoid protein processing and insertion (Somerville, 1995). This may have implications for recovery from photoinhibition at low temperature with respect to the D1 polypeptide repair cycle (Moon et al., 1995). These alterations in MGDG:DGDG and fatty acid unsaturation are species specific, as similar trends have not been observed in cereals such as winter rye (Huner et al., 1987). In contrast, the ability to modulate the *trans*-16:1 content in PG is strongly correlated to the development of freezing tolerance in a variety of species (Huner et al., 1989).

Biochemical and molecular analyses have demonstrated differential gene expression and the accumulation of specific proteins during the induction of freezing tolerance (Guy et al., 1985; Guy, 1990; Thomashow, 1990; Howarth and Ougham, 1993; Lee and Chen, 1993; Thomashow, 1993; Hughes and Dunn, 1996). Cold-induced genes have been isolated and characterized in many species, such as alfalfa, *Arabidopsis thaliana*, barley, *Brassica napus*, and wheat (Houde et al., 1992a; Chauvin et al., 1993; Dhindsa et al., 1993; Chauvin et al., 1994; Danyluk et al., 1994; Lee and Chen, 1993; Thomashow et al., 1993; Weretilnyk et al., 1993; Crosatti et al., 1995; Limin et al., 1995; Pearce et al., 1996). There is an apparent correlation between the expression of some of these genes, which appear to be up-regulated by low temperature, and the development of freezing tolerance (Guy, 1990; Howarth and Ougham, 1993; Lee and Chen, 1993; Thomashow, 1993; Hughes and Dunn, 1996). Since the function of these genes and their encoded polypeptides have not been fully

demonstrated, it is difficult to assess their direct relevance to freezing tolerance. Although this polygenic trait has been investigated for sometime, its regulation by environmental factors has not been elucidated (Guy, 1990; Lee and Chen, 1993; Thomashow, 1993; Pearce et al., 1996). In addition, the mechanism by which low temperature signals are perceived and transduced into specific biochemical responses is largely unknown (Trewavas and Gilroy, 1991; Dhindsa et al., 1993; Bowler and Chua, 1994).

1.5 PSII Excitation Pressure

The rate-limiting step of photosynthetic electron transport is thought to occur at the level of PQ oxidation and reduction (Haehnel, 1984; Mitchell et al., 1990). Thus, the proportion of closed PSII reaction centers, measured as $1\text{-}q_P$, is influenced by the rate of photochemical reduction of Q_A relative to the rate of oxidation of Q_A by intersystem electron transport and subsequent CO_2 assimilation. Therefore, the extent of PSII closure, as estimated by *in vivo* Chl *a* fluorescence parameter $1\text{-}q_P$, reflects the relative reduction state of Q_A, that is $[Q_{A\,red} / (Q_{A\,red} + Q_{A\,ox})]$. PSII closure is the consequence of an imbalance between the energy absorbed through photochemistry and energy either utilized through intersystem electron transport and carbon assimilation, or energy dissipated through non-photochemical processes. It has been suggested that changes in PSII closure and thus changes in the relative reduction state of PSII reflect changes in PSII excitation pressure (Dietz et al., 1985; Ögren, 1991;

Maxwell et al., 1995a, 1995b; Savitch et al., 1996). Although the estimation of the relative reduction state of PSII as 1-q_P may not be linearly related to the absolute reduction state of PSII (Schreiber et al., 1994), this fluorescence parameter provides a useful estimate of relative changes in the PSII reduction state, and thus, relative changes in PSII excitation pressure, for the comparison of plants exposed to changing environmental conditions.

Recently, it has been reported that growth at low temperature mimics high-light acclimation in the green alga *Chlorella vulgaris*. Further studies demonstrated that this green alga adjusts its photosynthetic light-harvesting apparatus in response to PSII excitation pressure rather than to either low temperature or irradiance *per se*. *Chlorella* cells adjust to high PSII excitation pressure created either by growth at low temperature or high irradiance by increasing the capacity for nonradiative dissipation of excess excitation energy through Zx coupled with a lower probability of light absorption due to a decreased abundance of light-harvesting polypeptides (Maxwell et al., 1995a) This occurs without any positive adjustment at the level of enzyme capacity and photosynthetic carbon assimilation (Savitch et al., 1996). Similar trends have been observed in the green alga *Dunaliella salina* and the cyanobacterium, *Plectonema boryanum* (N.P.A. Huner, unpublished). In fact, redox control at the level of gene expression has been demonstrated utilizing the nuclear-encoded Chl *a/b*-binding (*cab*) genes in *Dunaliella* (Escoubas et al., 1995; Maxwell et al., 1995b). Thus, it has been suggested that the redox state of PSII, reflecting the

redox poise of the chloroplast, plays a vital role in sensing environmental changes, which ultimately results in photosynthetic acclimation (Huner et al., 1995, 1996).

1.6 Cereals as a Model System

Rye (*Secale cereale* L.) and wheat (*Triticum aestivum* L.) are overwintering freezing-tolerant annual plants which can survive temperatures below -30°C. Studies of cold acclimation utilize cereals extensively, due largely to their high levels of freezing tolerance and well-established genetics. Responses have been well characterized at the morphological, biochemical, and molecular levels (Vasil'yev, 1961; Fowler et al., 1981; Gusta et al., 1982; Stushnoff et al., 1984; Gusta and Chen, 1987; Tognetti et al., 1990; Pollock and Cairns, 1991; Huner et al., 1993; Lee and Chen, 1993; Olien and Clark, 1993; Limin et al., 1995; Hughes and Dunn, 1996; Pearce et al., 1996). In addition, physiological responses at the level of photosynthesis and photoinhibition have also been extensively studied (Huner et al., 1993). Thus, due to their exhaustive characterization and potential agronomic importance, cereals represent ideal model plants to be utilized in this study.

1.7 Thesis Objectives

While responses to low temperature have been extensively studied, there is a scarcity of information present in the literature with regard to cold acclimation

in response to other environmental factors, such as light. Since both temperature and light can modulate PSII excitation pressure, I have chosen to examine this phenomenon in higher plants. In addition, no experimental data have been obtained with respect to PSII excitation pressure in higher plants. The goals of the present research are:

1. To establish the existence of a response to PSII excitation pressure in higher plants.
2. To characterize the developmental responses as a result of growth at varying PSII excitation pressure.
3. To characterize photosynthetic responses to PSII excitation pressure at the levels of light-harvesting, intersystem electron transport and photosynthetic carbon metabolism.
4. To examine the role of PSII excitation pressure in the acquisition of tolerance to photoinhibition.
5. To separate the roles of temperature, light and PSII excitation pressure during cold acclimation.

CHAPTER 2

GROWTH AND DEVELOPMENT IN RESPONSE TO TEMPERATURE AND LIGHT

2.1 Introduction

Growth kinetic analyses are essential to establish similar physiological ages when examining plants grown under different temperature and/or irradiance regimes. Plants will grow at different rates under different environmental conditions, that is, plants of the same chronological age will not be at the same physiological age (Krol et al., 1984). By ensuring that the plants are at the same physiological age, one minimizes confounding effects that may result due to physiological age differences. This allows for comparison of overall growth and physiological response solely to environmental change such as temperature and/or irradiance.

In this chapter, growth parameters of leaf DW and area are examined and data are presented for winter rye grown under various growth regimes of temperature and irradiance. This allowed for the subsequent design of experiments with plant material of the same physiological age in order to examine the effects of temperature, light and PSII excitation pressure.

PS II excitation pressure is a measure of the reduction state of Q_A, the first, stable quinone electron acceptor of PSII and thus, estimates the relative reduction state of PSII (Dietz et al., 1985; Ögren, 1991; Dau, 1994a). In

addition, PSII excitation pressure may be modulated by growth temperature and growth irradiance. Based on the developmental responses observed in the green alga *Chlorella vulgaris* in response to PSII excitation presssure (Maxwell et al., 1994, 1995a), I hypothesized that higher plants would demonstrate similar responses to PSII excitation pressure. Therefore, data will be presented to characterize the level of PSII excitation pressure as a result of development at the various temperature/irradiance regimes utilized for plant development in this thesis. In addition, pigment contents and distributions, lipid and fatty acid profiles, polypeptide profiles, abundance of the Chl *a/b*-binding proteins and the supramolecular organization of LHCII are characterized for winter rye developed under conditions of high and low PSII excitation pressures.

2.2 Materials and Methods

2.2.1 Plant Material and Growth Conditions

Winter rye (*Secale cereale* L. cv Musketeer), winter wheat (*Triticum aestivum* L. cv Monopol) and spring wheat (*Triticum aestivum* L. cv Katepwa) were germinated from seed in 7 cm plastic pots in coarse vermiculite either at a temperature of 5/5°C or 20/16°C (day/night) with a 16 h photoperiod in controlled environment growth chambers (Conviron, Winnipeg, MB, Canada). Fluorescent tubes (Cool White, 160W, F72T12/CW/VHO; Sylvania, Drummondville, QC, Canada) provided PAR which was adjusted to a PPFD of either 50 or 250 µmol m^{-2} s^{-1} at 5°C (5/50 and 5/250 respectively) and either 50, 250 or 800 µmol m^{-2} s^{-1}

at 20°C (20/50, 20/250 or 20/800 respectively). Supplemental lighting was provided in the 20/800 growth chamber by a metal halide lamp (MS400-HOR, 400W; Venture Lighting International, Cleveland, OH, USA). The PPFD was measured at pot height with a Li-Cor (Lincoln, NE, USA) Quantum/Radiometer/Photometer (model LI-189) equipped with a model LI-190SA quantum sensor (Li-Cor). A modified Hoagland's nutrient solution (No. 1) was supplied to all plants as required which contained: 10 mM KNO_3, 10 mM $Ca(NO_3)_2$, 4 mM KH_2PO_4, 2 mM $MgSO_4$, 0.1 mM H_3BO_3, 18 µM $MnCl_2$, 2 µM $ZnCl_2$, 0.6 µM $CuSO_4$, 0.3 µM Na_2MoO_4 and 18 µM Fe-EDTA (Hoagland and Arnon, 1950; Helson, 1964).

2.2.2 Comparative Growth Kinetics

Growth parameters of leaf DW and leaf area were determined for second leaves of plants grown under all temperature/irradiance conditions. Leaves were harvested at various times after planting, wrapped in aluminium foil and the FW determined immediately. The leaves were dried at 80°C to constant weight and brought to room temperature in a desiccator for the determination of DW and water content. The water content (%) was calculated as;

$$\text{water content} = (FW - DW) / FW \times 100\%$$

Leaf area was measured using a portable leaf area meter (model LI-3000; Li-Cor).

Growth coefficients (k_1') were calculated from the slope of the line from a

plot of ln (growth) versus time (Macdowall, 1972, 1974). Growth was measured as either leaf DW or area.

2.2.3 PSII Excitation Pressure

Chl *a* steady-state fluorescence characteristics were determined *in vivo* under ambient CO_2 conditions using a PAM-101 Chl fluorometer (Heinz Walz, Effeltrich, Germany) equipped with the 101-ED emitter-detector and PAM-103 unit as described by Schreiber et al. (1986). The nomenclature adopted throughout is that defined by van Kooten and Snel (1990). Two Schott flash lamps (model KL1500; Schott Glaswerke, Mainz, Germany) provided saturating flashes (FL103) and a white actinic light source (FL101) following the protocol of Genty et al. (1989). Fluorescence induction was evaluated in a Hansatech leaf-disc cuvette (model LD2; Hansatech Instruments Ltd., King's Lynn, UK) modified to accept the PAM optic fiber. Measurements were made at either 5 or 20°C, maintained by a refrigerated circulating water bath (model LT50-DD; Neslab Instruments Inc., Portsmouth, NH, USA) and recorded on an XY chart recorder (Omnigraphic, model 2000; Houston Instrument, Houston, TX, USA). A humidified stream of ambient air, corresponding to the same temperature as the measuring temperature, was blown over the leaf surface at a rate of 350 mL min^{-1} in order to minimize boundary layer resistance to CO_2 diffusion and to prevent condensation on the cuvette window (Huner et al., 1992). The desired actinic PPFD, as determined at the leaf position with a qu..antum sensor (model

LI-190SA; Li-Cor), was achieved using neutral density filters (Balzers; Fürstentum, Liechtenstein). Actinic PPFDs in the range of 30 to 2000 µmol m^{-2} s^{-1} were utilized for the construction of light response curves. Leaves were sampled 4 h into the photoperiod and dark adapted for 60 min in the electrode chamber prior to the onset of measurement. Minimum fluorescence with all PSII traps open (F_O) was determined by illuminating dark adapted leaves with a photon fluence rate of 0.01 µmol m^{-2} s^{-1} modulated at 1600 Hz. A saturating flash (6500 µmol m^{-2} s^{-1}) of light for 800 ms was used to determine maximal fluorescence (F_M) with all PSII traps closed. Fluorescence induction was superimposed with 800 ms pulses of saturating light (6500 µmol m^{-2} s^{-1}) at 100 s intervals until a stable, steady state level of fluorescence (F_S) was achieved, approximately 30 to 40 min after switching to the next higher light level. Maximum fluorescence in the light adapted state (F_M') was calculated using the extrapolation method of Markgraf and Berry (1990). Three flashes of decreasing photon fluence rate (6500, 3200, and 1700 µmol m^{-2} s^{-1}) were applied for 800 ms each, allowing the fluorescence to relax to the steady state level (F_S) between each flash. Minimum fluorescence in the light adapted state (F_O') was determined immediately after turning off the actinic source in the presence of far-red (>710 nm) background light (Corning 7-69; Corning Glass Works, Corning, NY, USA) to ensure maximal oxidation of PSII electron acceptors (Groom et al., 1993). Variable fluorescence in the dark- (F_V) and light-adapted (F_V') states was calculated as;

$$F_V = F_M - F_O \qquad F_V' = F_M' - F_O'$$

respectively. PSII excitation pressure (1-q_P) was calculated as;

$$1\text{-}q_P = (F_S - F_O') / (F_V')$$

according to Ögren (1991) and expressed as 1-q_P, measured at the growth temperature and growth irradiance of the plants utilized. Excitation pressure represents PSII trap closure and thus, reflects the relative reduction state of Q_A and is an estimate of the redox state of PSII (Dietz et al., 1985). Excitation pressure on PSII was modulated by either decreasing the growth temperature from 20 to 5°C and keeping growth irradiance constant (~50 µmol m^{-2} s^{-1}) or by changing the growth irradiance (50, 250 or 800 µmol m^{-2} s^{-1}) but keeping growth temperature constant.

2.2.4 Pigment Extraction and Determination

Pigments were extracted from leaf samples harvested 4 h into the photoperiod by homogenization with a pre-chilled mortar and pestle in 100% HPLC-grade acetone (OmniSolv; BDH Inc., Toronto, ON, Canada) with 0.3 mg mL^{-1} $CaCO_3$ at 4°C in dim light (< 5 µmol m^{-2} s^{-1}). Following centrifugation at 6,000*g* for 5 min, the supernatant was removed and passed through a 0.22 µm syringe filter (Micron Separations Inc., Westborough, MA, USA) prior to storage under nitrogen at -20°C.

HPLC analysis of leaf acetone extracts was performed using a Beckman System Gold Solvent Module (Beckman Instruments, San Ramon, CA, USA)

equipped with an analytical CSC-Spherisorb ODS-1 reverse phase column (5 µm particle size, 250 mm x 4.6 mm i.d.) and an Upchurch Perisorb A guard column (Chromatographic Specialties Inc., Concord ON, Canada). The protocol of Gilmore and Yamamoto (1991) was utilized with minor modifications. The samples were injected using a Beckman 210A sample-injection valve with a 20 µL sample loop. Pigments were then eluted isocratically for 6 min with a solvent system of 100% of acetonitrile:methanol:0.1 M Tris-HCl (pH 8.0), (74:11:3.5, v/v/v) followed by a 2 min linear gradient to 100% of methanol:ethylacetate (68:32, v/v) which continued isocratically for 4 min. The total run time was 12 min with a flow rate of 2 mL min^{-1}. All solvents were of HPLC-grade (OmniSolv; BDH Inc.).

The A_{440} of the pigments was detected using a diode array detector (System Gold, Beckman Instruments) and peak areas integrated using the System Gold software (Beckman Instruments). Retention times and response factors of β-Car, Lut, Chl *a* and Chl *b* were determined by the injection of known quantities of pure standards (Sigma Chemical Co., St. Louis, MO, USA). The retention times of Neo, Ax, Vx and Zx were determined using pigments isolated from barley by TLC (M. Krol, A.G. Ivanov, D.P. Maxwell and N.P.A. Huner, unpublished results) utilizing the protocol of Diaz et al. (1990). Xanthophyll pool size was calculated as the sum of Vx + Ax + Zx.

To determine leaf absorptance, Chl was extracted in 80% acetone buffered with 25 mM Hepes (pH 7.5) and quantified according to the equations of

Porra et al. (1989) on a recording spectrophotometer (model UV-160; Shimadzu Corp., Kyoto, Japan). Leaf absorptance was estimated as described by Öquist et al. (1992b) as follows;

$$\text{Absorptance} = 0.96X/(X + 0.047)$$

where X corresponds to the Chl concentration expressed in mmol m^{-2}.

2.2.5 Lipid Extraction and Analyses

Lipids were extracted from the uppermost fully expanded leaves harvested 4 h into the photoperiod by homogenization in a pre-chilled mortar and pestle with chloroform:methanol (2:1, v/v) as described in Khan and Williams (1977). All solvents were glass-distilled before use and N_2 was continually added during the extraction procedure to avoid oxidation of highly unsaturated fatty acids. Lipid extracts were filtered through Millipore glass fibre filter paper (934 AH; Millipore, Bedford, MA, USA) under vacuum and washed thoroughly with chloroform:methanol (2:1). Water soluble and non-lipid contaminants were removed by the addition of Sephadex G-25 (Sigma) and eluting total lipids with chloroform as described by Williams and Merrilees (1970). The filtrate was dried down in a rotary evaporator (Büchi Rotavapor, model RE-111/A; Brinkmann Instrements Inc., Mississauga, ON, Canada) and redissolved in a minimal volume of chloroform to give approximately a 1g mL^{-1} tissue:chloroform ratio. Extracts were stored in air-tight glass vials with Teflon-lined caps under nitrogen at -20°C in the dark.

Lipid extracts were streaked onto activated Silica Gel 60 G (E. Merck, Darmstadt, Germany) plates impregnated with 5% (w/v) ammonium sulphate and separated by TLC using a solvent system of acetone:benzene:water (91:30:8, v/v/v) (Pohl et al., 1970; Khan and Williams, 1977). Lipids were identified by using reference compounds and spraying with 0.05% (w/v) 2',7'-dichlorofluorescein dissolved in 100% (v/v) methanol and visualized under UV light. Individual lipids were transesterified with 0.2 N dry methanolic HCl as described by Khan and Williams (1993). The FAME of individual lipids were extracted with hexane and dried down under N_2. The residue was dissolved in 100 µL of hexane and analyzed utilizing a Hewlett-Packard gas-liquid chromatograph (model 5890A; Hewlett-Packard, Mississauga, ON, Canada) equipped with an autosampler (model 7376A; Hewlett-Packard). FAME peaks were separated and quantified in a DB-225 fused silica capillary column (30 m x 0.25 mm i.d.) (J&W Scientific, Folsom, CA, USA). The column oven was programmed from 140 to 210°C at a rate of 3°C min^{-1}. The temperature setting at the injection and detector ports was maintained at 240°C. O_2-free N_2 was used as a carrier gas at a flow rate of 80 mL min^{-1}. An internal standard, methylpentadecanoate (15:0) was used during the transesterification process to identify and quantify FAME peaks based on retention times utilizing a computer acquisition program (HP 3365 Chemstation; Hewlett-Packard). Lipids and fatty acids were expressed as a molar percentage (mol %) of the total.

2.2.6 Isolation and Solubilization of Thylakoid Membranes

Thylakoids were isolated essentially as described by Huner (1985a). Plants were harvested 4 h into the photoperiod and leaf segments macerated by three 4 s bursts of a Waring blender at 4°C in grinding buffer containing 50 mM Tricine-NaOH (pH 7.8), 10 mM NaCl, and 0.4 M sorbitol. The brei was filtered through four layers of cheesecloth and the filtrate centrifuged at 4,000*g* for 3 min at 4°C. The pellet was washed in a buffer containing 50 mM Tricine-NaOH (pH 7.8), 10 mM NaCl, and 5 mM $MgCl_2$. The suspension was centrifuged at 10,000*g* for 5 min at 4°C and the pellet suspended in a buffer consisting of 50 mM Tricine-NaOH (pH 7.8), 10 mM NaCl, 5 mM $MgCl_2$, and 0.1 M sorbitol. Chl concentration of the pellet was determined in 80% acetone according to Arnon (1949).

Isolated thylakoid membranes to be used for polypeptide and immunoblot analyses were solubilized on a Chl basis in a buffer containing 60 mM Tris-HCl (pH 7.8), 12% (w/v) Suc, 2% (w/v) SDS, 1 mM EDTA and 58 mM DTT. Samples were heated in a boiling water bath for 90 s prior to electrophoresis.

For the examination of Chl-protein complexes, isolated thylakoid membranes were washed once in ice cold ddH_2O, once in 1 mM EDTA (pH 8.0) and twice in 50 mM Tricine-NaOH (pH 8.0). The membrane pellets were suspended and solubilized in a buffer containing 0.3 M Tris-HCl (pH 8.8) containing 13% (v/v) glycerol and 1% (w/v) SDS, and then 2% (w/v) DOC in 0.3 M Tris-HCl (pH 8.8) was added immediately to give a final DOC:SDS:Chl ratio of 20:10:1.

Thylakoid protein:Chl ratios were determined by removing a small aliquot of washed thylakoid membranes to which 1 mL of 80% (v/v) acetone was added. This was incubated at -20°C for 15 min and centrifuged at 12,000*g* and the supernatant removed. The Chl concentration of the supernatant was determined according to Arnon (1949). Subsequently, the remaining pellet was air dried and suspended in 100 mM NaOH and 2% (w/v) SDS. Protein concentrations were estimated by the bicinchoninic acid method (Smith et al., 1985) using the BCA reagent (Pierce Chemical Co., Rockford, IL, USA). The manufacturers standard protocol was followed using BSA (fraction V) as a standard.

2.2.7 SDS-PAGE and Immunoblotting

Solubilized membrane polypeptides were separated by SDS-PAGE using a Mini-PROTEAN II apparatus (Bio-Rad Laboratories, Hercules, CA, USA) and the discontinuous buffer system of Laemmli (1970) containing 25 mM Tris-HCl (pH 8.3), 192 mM glycine and 0.1% (w/v) SDS. Electrophoresis was performed using a 5% (w/v) stacking gel and a 15% (w/v) resolving gel prepared according to Piccioni et al. (1982). All samples were loaded on an equal Chl basis (3 µg lane^{-1}) and a constant current of 15 mA was applied for approximately 1.5 h at 20°C. Commercially available pre-stained molecular weight standards (Bio-Rad) were utilized to monitor migration. Polypeptides were either stained with 0.2% (w/v) Coomassie Brilliant Blue R-250 (Bio-Rad) in methanol:acetic acid:water (50:7:43, v/v/v) and destained methanol:acetic acid:water (20:7:73, v/v/v) or

electrophoretically transferred to nitrocellulose membranes for immunoblotting.

Polypeptides were transferred from polyacrylamide gels (Mini-Trans Blot, Bio-Rad) to nitrocellulose membranes (0.2 µm pore size, Bio-Rad) by applying a constant current of 295 mA for 1 h in a transfer buffer containing 25 mM Tris, 192 mM glycine (pH 8.3) and 20% (v/v) methanol as described by Towbin et al. (1979) with 0.0375% (w/v) SDS. The efficiency of protein transfer was determined by Coomassie Blue staining of the gels after transfer and the appearance of the pre-stained standards on the nitrocellulose membrane. After blocking with 4% (w/v) reconstituted milk in TBS [50 mM Tris-HCl (pH 7.6) and 500 mM NaCl] containing 0.5% (v/v) Tween-20 (TBS-T), the membrane was incubated with a 1:5,000 dilution of a rabbit monospecific polyclonal primary antibodies raised against synthetic oligopeptides derived from the consensus sequences of each of the Chl *a/b*-binding proteins associated with PSII (Lhcb1 to Lhcb6) or PSI (Lhca1 to Lhca4) (Jansson, 1994; Jansson et al., 1992; Sigrest and Staehelin, 1992, 1994; Krol et al., 1995). After washing with TBS-T, the polypeptide-primary antibody complexes were incubated with goat anti-rabbit IgG horseradish peroxidase conjugate (Sigma) as a secondary antibody at a 1:20,000 dilution. The complexes were visualized using the ECL chemiluminescent detection system (Amersham Corp., Buckinghamshire, UK) and X-Omat RP film in combination with Kodak GBX developer/replenisher and fixer/replenisher (Eastman-Kodak, Rochester, NY, USA). Polypeptide abundance was determined by densitometric scanning on a computing

densitometer (Molecular Dynamics, Sunnyvale, CA, USA) coupled with ImageQuant software (version 3.22; Molecular Dynamics).

2.2.8 Separation of Chl-Protein Complexes

The solubilized Chl-protein complexes were separated in the dark at 4°C utilizing a buffer system described by Waldron and Anderson (1979). The upper buffer chamber contained 47 mM Tris-boric acid (pH 8.64) buffer with 0.1% (w/v) SDS, while the lower buffer chamber contained a 430 mM Tris-HCl (pH 9.35). A 14 cm home-made gel apparatus was utilized with a 7.5% (w/v) SDS polyacrylamide slab gel and a 4% (w/v) stacking gel. Samples were loaded on an equal Chl basis (40 µg lane^{-1}) and a constant current of 20 mA was applied for approximately 1.5 h. Individual lanes were excised from the gels and scanned at room temperature at 671 nm with a Beckman spectrophotometer (model DU 640; Beckman Instruments Inc., Fullerton, CA, USA) equipped with a gel scanning attachment and software (Beckman). This gel system separates the three main LHCII Chl *a/b* protein subfractions: $LHCII_1$, the major oligomeric form of LHCII, $LHCII_2$ (dimer) and $LHCII_3$ (monomer). The relative Chl contents of the individual pigmented complexes were determined by relative peak areas as;

Chl content = (individual peak area / total area of scan) x 100

This allowed for the determination of LHCII oligomer:monomer ratios (Huner et al., 1987).

2.3 Results

2.3.1 Growth Kinetics

Leaves of winter rye grown at 20/800, 20/250 and 20/50 reached full expansion in the range of 12 to 25 d as shown in Figure 6A and B. Leaves grown at 20/50 exhibited a 1.7-fold greater leaf area and a 1.5-fold reduction in leaf DW in comparison to leaves developed at 20/800 (Fig. 6A and B, respectively). This resulted in the SLW of 20/800 grown leaves being 2.4-fold greater than that of 20/50 grown leaves (Fig. 6C). In addition, the water content of leaves developed at all the 20°C growth regimes ranged from 82 to 93% (results not shown).

The data in Figure 7A and B demonstrate that leaves developed at either 5/250 or 5/50 reached full expansion between 58 and 78 d. Growth at 5/250 resulted in a 2.3-fold greater SLW in comparison to leaves developed at 5/50 (Fig. 7C). This occurred due to a 1.3-fold increase in leaf area and a 44% reduction in leaf DW as a result of development at 5/50. The water content of leaves developed at 5°C ranged from 71 to 82% (results not shown). This is consistent with previous results for plant development at low temperature (Krol et al., 1984).

These results are more clearly demonstrated by examining the growth coefficients based on leaf DW or area (Table I). These data show that whether growth is examined on a leaf DW or leaf area basis, plants developed at the 5°C

Figure 6. Growth parameters for second leaves of winter rye (*S. cereale* L. cv Musketeer) developed at 20°C. Growth irradiance were 800 (♦), 250 (●) or 50 (■) μmol m^{-2} s^{-1}. A, Leaf DW. B, Leaf area. C, SLW. All values represent means ± SE; n = 3 to 5. When not present, error bars are smaller than symbol size.

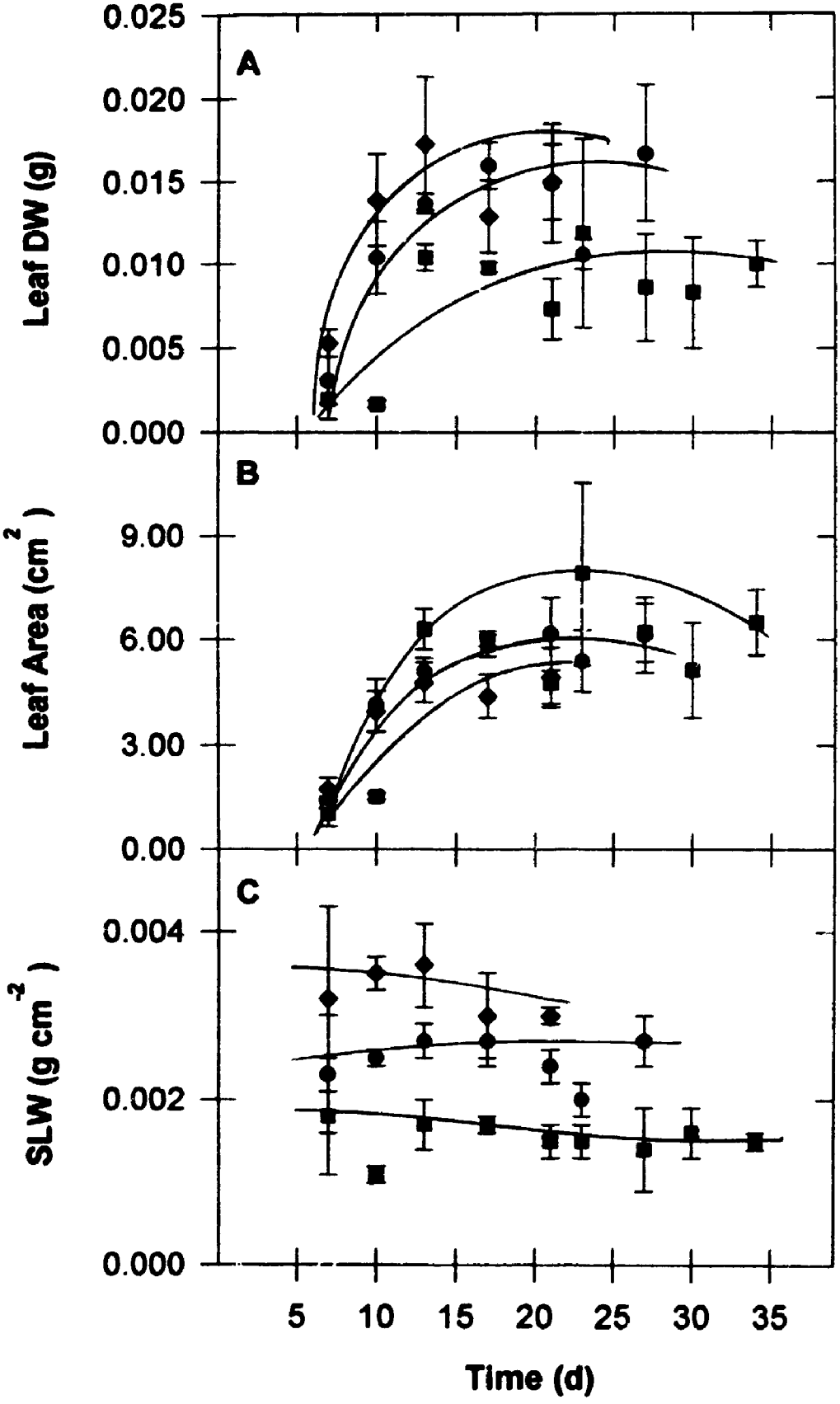
A
B
C
Leaf DW (g)
Leaf Area (cm^2)
SLW (g cm^{-2})
0.025
0.020
0.015
0.010
0.005
0.000
9.00
6.00
3.00
0.00
0.004
0.002
0.000
5
10
15
20
25
30
35
Time (d)

Figure 7. Growth parameters for second leaves of winter rye (*S. cereale* L. cv Musketeer) developed at 5°C. Growth irradiance were 250 (○) or 50 (□) µmol m^{-2} s^{-1}. A, Leaf DW. B, Leaf area. C, SLW. All values represent means ± SE; n = 3 to 5. When not present, error bars are smaller than symbol size.

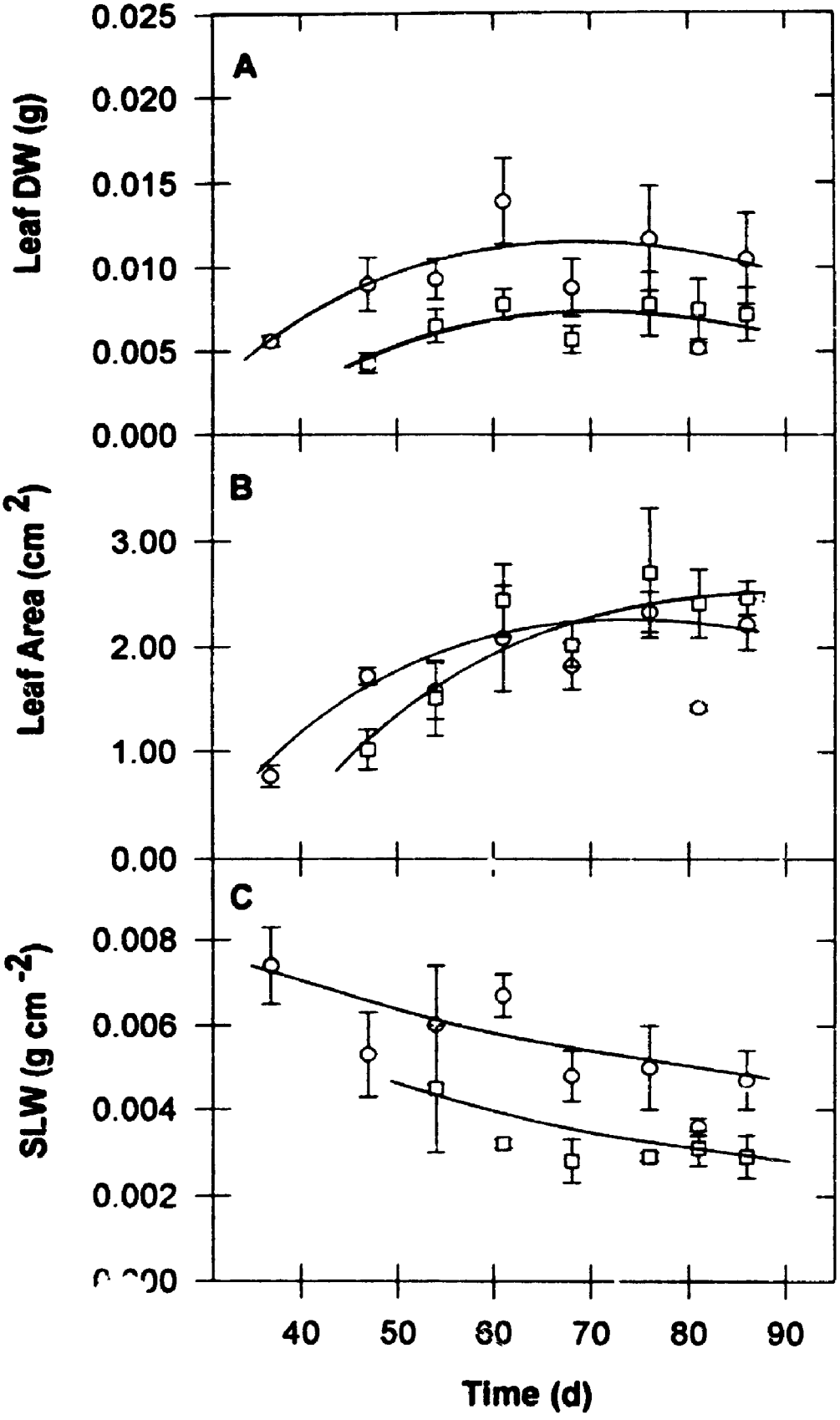
A
B
C
Leaf DW (g)
Leaf Area (cm 2)
SLW (g cm -2)
0.025
0.020
0.015
0.010
0.005
0.000
3.00
2.00
1.00
0.00
0.008
0.006
0.004
0.002
40
50
60
70
80
90
Time (d)

Table I. *Growth coefficients for second leaves of winter rye (S. cereale L. cv Musketeer) developed at various temperature/irradiance regimes.*

Growth coefficients were calculated from plots of ln (growth) versus time, where growth was expressed as either leaf DW or leaf area.

Growth Regime ($°C/\mu mol\ m^{-2}\ s^{-1}$)	Leaf DW k_1 (d^{-1})	Leaf Area k_1 (d^{-1})
20/800	0.20	0.17
20/250	0.15	0.22
20/50	0.10	0.30
5/250	0.035	0.045
5/50	0.043	0.062

growth regimes exhibit exponential growth rates which are 3 to 5-fold lower than those developed at 20°C with the same irradiance. This provides strong evidence for an analysis of growth to ensure plant material is at a similar developmental age, irrespective of the environmental conditions under which they have been exposed, for a useful physiological comparison to occur.

2.3.2 PSII Excitation Pressure, Temperature and Light

The temperature and irradiance dependence of PSII excitation pressure is illustrated in Figure 8 for winter rye grown at typical control conditions of 20/250. When a constant measuring temperature of 20°C is utilized, 1-q_p increases as a function of irradiance, due to increased PSII excitation. If the measuring temperature is lowered to 5°C, 1-q_p is greater at all PPFD, due to the thermodynamic constraints on intersystem electron transport and photosynthetic carbon metabolism (Fig. 8). In contrast, a typical cold-hardened plant grown at 5/250 and measured at 5°C results in lower values of 1-q_p at all PPFD in comparison to the 20/250 grown plant measured at 5°C. The difference between these two curves reflects photosynthetic acclimation or adjustment as a result of growth and development at the cold-hardening temperature of 5°C (Fig. 8).

2.3.3 Growth Regime and PSII Excitation Pressure

The results in Table II and III indicate that at a constant growth temperature of 20°C, increasing growth irradiance from 50 to 800 μmol m^{-2} s^{-1}

Figure 8. Light response curves for PSII excitation pressure (1-q_P) in leaves of winter rye (*S. cereale* L. cv Musketeer). Development occurred at the temperature/irradiance regimes of 20/250 (●) or 5/250 (○) and response was measured at 20 and 5°C respectively. A 5°C measuring temperature for leaves developed at 20/250 (--●--) is also indicated. All values represent means ± SE; n = 3. When not present, error bars are smaller than symbol size.

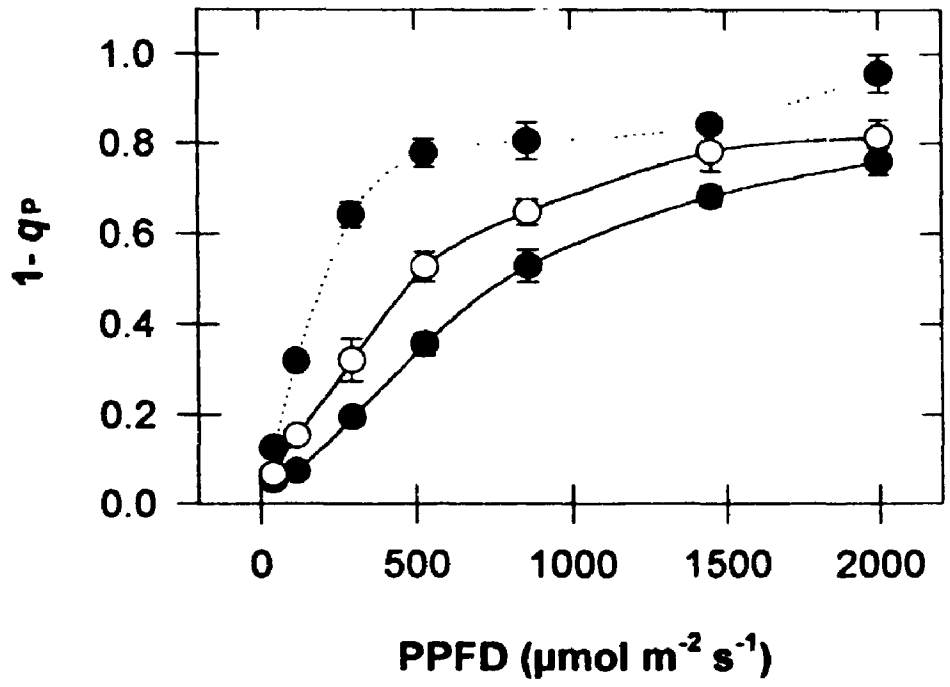
1.0
0.8
0.6
0.4
0.2
0.0
1- qP
0
500
1000
1500
2000
PPFD (µmol m-2 s-1)

Table II. *PSII excitation pressure in leaves of winter rye (S. cereale L. cv Musketeer) developed at various temperature/irradiance regimes.*

PSII excitation pressure is expressed as 1-q_P and was determined at the growth temperature and growth irradiance. All values represent means ± SE; n = 3.

Growth Regime (°C/μmol m^{-2} s^{-1})	PSII Excitation Pressure (1-q_P)
20/800	0.318 ± 0.034
20/250	0.196 ± 0.017
20/50	0.074 ± 0.013
5/250	0.321 ± 0.047
5/50	0.141 ± 0.035

Table III. *PSII excitation pressure in leaves of winter wheat (T. aestivum L. cv Monopol) and spring wheat (T. aestivum L. cv Katepwa) developed at various temperature/irradiance regimes.*

PSII excitation pressure is expressed as 1-q_P and was determined at the growth temperature and growth irradiance. All values represent means ± SE; n = 3.

Growth Regime (°C/µmol m^{-2} s^{-1})	PSII Excitation Pressure (1-q_P)
Monopol	
20/800	0.465 ± 0.031
20/250	0.181 ± 0.006
20/50	0.097 ± 0.003
5/250	0.617 ± 0.051
5/50	0.211 ± 0.023
Katepwa	
20/800	0.476 ± 0.054
20/250	0.205 ± 0.018
20/50	0.087 ± 0.008
5/250	0.625 ± 0.010
5/50	0.410 ± 0.034

resulted in a 4 to 5-fold increase in PSII excitation pressure in both rye and wheat. However, rye and wheat grown at 5/250 exhibited PSII excitation pressures that were 1.6 to 3.5-fold greater, respectively, than plants grown at 20/250 (Table II and III). In fact, rye plants grown at 5/250 exhibited a PSII excitation pressure that was comparable to plants grown at 20°C, but at an irradiance of 800 µmol m^{-2} s^{-1}. Similarly, wheat grown at 5/250 exhibited PSII excitation pressures that were approximately 33% higher than wheat grown at 20/800 (Table II and III). Although plants grown at 20/250 would normally be considered controls for those grown at 5/250, the latter were grown under significantly higher PSII excitation pressures than the former.

2.3.4 Photosynthetic Pigments

The results in Table IV indicate that plants grown at 5/250 presented a 1.5-fold greater Chl leaf $area^{-1}$ compared to plants grown at 20/250 which is consistent with previous results for winter rye (Huner, 1985b; Huner et al., 1993). Although growth temperature and growth irradiance had significant effects on total Chl leaf $area^{-1}$, leaf absorptance changed by less than 10% (Table IV). As expected, the Chl *a/b* ratios of leaves developed at 20°C increased by 10 to 20% upon exposure to increasing growth irradiance from 50 to 800 µmol m^{-2} s^{-1} (Table IV). However, growth temperature had minimal effects on Chl *a/b* (Table IV) which is consistent with previous results (Huner, 1985b; Hurry et al., 1992). Thus, growth of winter rye at high excitation pressure appears to have minimal

Table IV. *Total Chl content, a/b ratios and leaf absorptance in total leaf extracts of winter rye (S. cereale L. cv Musketeer).*

Total Chl content and *a/b* ratios were determined by HPLC. Leaf absorptance was calculated according to Öquist et al. (1992b). All values represent means ± SE; $n = 3$.

Growth Regime (°C/µmol m^{-2} s^{-1})	Total Chl (mg m^{-2})	Chl *a/b*	Leaf Absorptance
20/800	388 ± 6	3.57 ± 0.04	0.85 ± 0.01
20/250	267 ± 14	3.17 ± 0.07	0.84 ± 0.01
20/50	275 ± 18	2.86 ± 0.01	0.82 ± 0.01
5/250	412 ± 51	3.25 ± 0.01	0.86 ± 0.02
5/50	294 ± 6	3.11 ± 0.07	0.79 ± 0.02

effects on Chl *a/b*.

The results in Table V indicate that at 20°C, increasing growth irradiance from 50 to 800 μmol m^{-2} s^{-1} had minimal effects on the content of β-Car, Lut and Neo, but resulted in a 2.8-fold increase in the xanthophyll pool size. A similar trend was observed upon increasing the growth irradiance from 50 to 250 μmol m^{-2} s^{-1} at 5°C except that a 1.3-fold increase in the xanthophyll pool size was observed (Table V). These results are consistent with recent reports of the light and temperature dependence of the xanthophylls (Hurry et al., 1992; Adams and Demmig-Adams, 1995; Adams et al., 1995b).

The thylakoid membrane protein:Chl ratios exhibited minimal differences as a result of varying irradiance at either 20 or 5°C (Table VI), consistent with a previous study (Griffith et al., 1982).

2.3.5 Thylakoid Lipid and Fatty Acid Profiles

The lipid content of the phospholipids, galactolipids, or sulfolipid present in the thylakoid membrane exhibited minimal differences as a result of growth at any of the temperature/irradiance regimes (Table VII). These data are consistent with previous reports for cereals grown at low temperature (Huner et al., 1987). The results presented in Figure 9A demonstrate that as growth irradiance is decreased, the amount of 16:0 in PG increases, irrespective of the growth temperature (20 or 5°C). This increase in 16:0 was accompanied by a concomitant decrease in *trans*-16:1. Absolute amounts of *trans*-16:1 present a

Table V. *Carotenoid content and xanthophyll pool sizes in total leaf extracts of winter rye (S. cereale L. cv Musketeer).*

Pigments were separated and quantified by HPLC and expressed as mmol mol^{-1} Chl *a+b*. nd; none detected. All values represent means ± SE; $n = 3$.

Growth Regime	Carotenoid (mmol mol^{-1} Chl *a+b*)						Pool Size
(°C/µmol m^{-2} s^{-1})	β-Car	Lut	Neo	Ax	Vx	Zx	Ax + Vx + Zx
20/800	102 ± 4	152 ± 4	19 ± 1	2 ± 2	83 ± 1	6 ± 1	91 ± 4
20/250	95 ± 1	130 ± 6	16 ± 2	nd	45 ± 6	4 ± 1	48 ± 7
20/50	87 ± 0	121 ± 0	14 ± 2	nd	31 ± 4	2 ± 1	33 ± 4
5/250	88 ± 2	152 ± 8	19 ± 1	1 ± 1	68 ± 3	7 ± 2	76 ± 2
5/50	82 ± 3	133 ± 5	18 ± 3	nd	54 ± 2	4 ± 0	58 ± 2

Table VI. *Protein:Chl ratios in isolated thylakoid membranes of winter rye (S. cereale L. cv Musketeer).*

Thylakoid protein was determined using the bicinchoninic acid method (Smith et al., 1985). Chl determinations were performed according to Arnon (1949). All values represent means ± SE; $n = 3$.

Growth Regime (°C/μmol m^{-2} s^{-1})	Thylakoid Protein:Chl
20/800	4.10 ± 0.42
20/250	3.35 ± 0.51
20/50	2.82 ± 0.82
5/250	3.65 ± 0.81
5/50	3.36 ± 0.63

Table VII. *Lipid composition in total leaf extracts of winter rye (S. cereale L. cv Musketeer).*

Lipid content was calculated as the molar ratio (mol %) of the total. All values represent means ± SD; $n = 3$.

Growth Regime	Lipid Composition (mol %)					
(°C/µmol m^{-2} s^{-1})	PG	PE	PC	MGDG	DGDG	SQDG
20/800	11 ± 1	5 ± 1	13 ± 3	36 ± 0.5	28 ± 2	7 ± 3
20/250	9 ± 3	5 ± 1	14 ± 1	37 ± 2	27 ± 5	8 ± 2
20/50	9 ± 2	7 ± 1	15 ± 2	37 ± 4	24 ± 2	8 ± 2
5/250	10 ± 1	6 ± 1	14 ± 1	39 ± 3	25 ± 0.5	6 ± 1
5/50	8 ± 2	6 ± 2	15 ± 1	38 ± 15	26 ± 13	7 ± 2

Figure 9. Accumulation of 16:0 and *trans*-16:1 fatty acids in PG in total leaf extracts of winter rye (*S. cereale* L. cv Musketeer) developed at the temperature/irradiance regimes indicated. A, Accumulation of 16:0 () and *trans*-16:1 () fatty acids in PG. B, Ratio of *trans*-16:1 to 16:0 in PG. All values represent means ± SD; $n = 3$. When not present, error bars are smaller than symbol size.

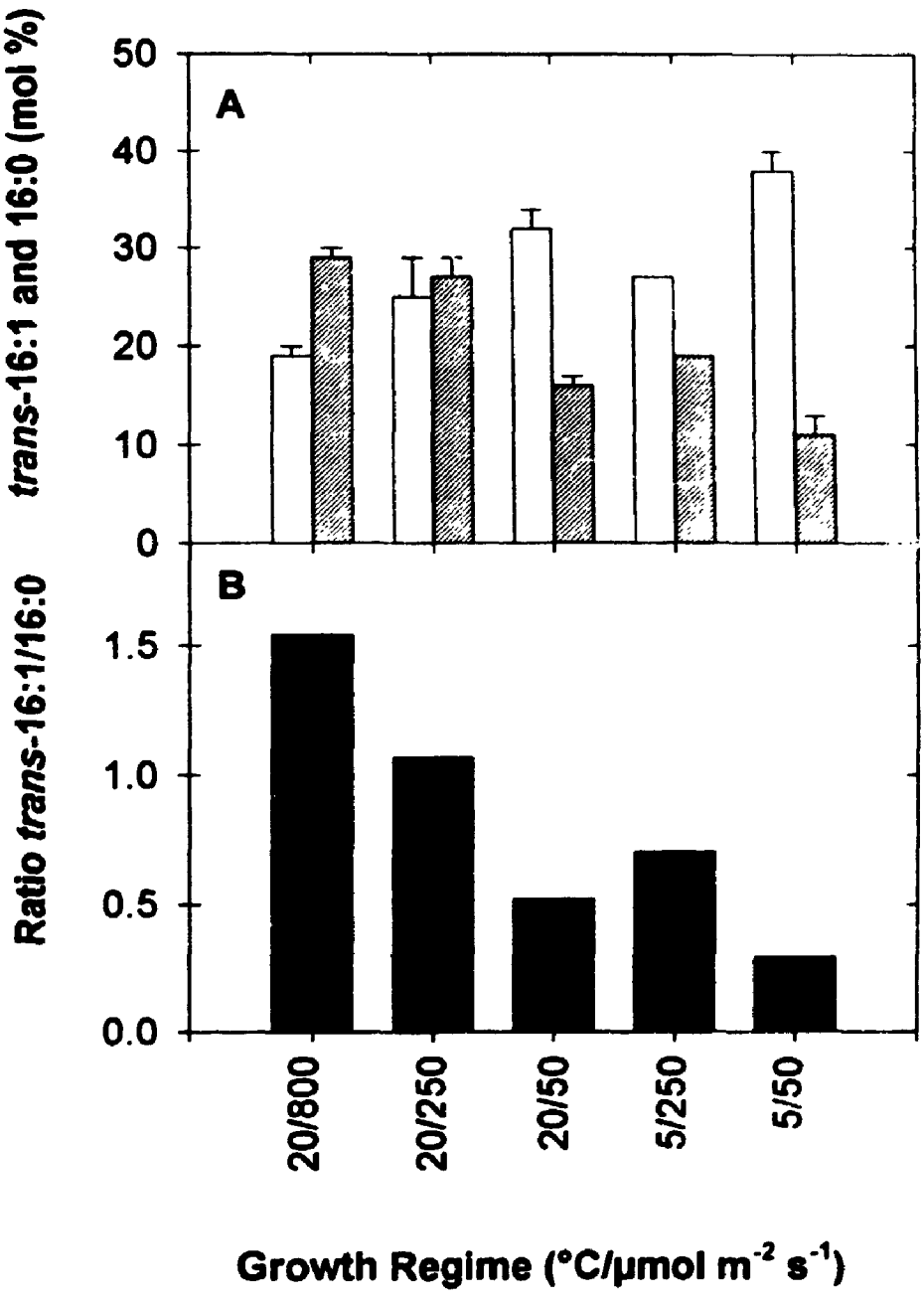
A
B
50
40
30
20
10
0
1.5
1.0
0.5
0.0
trans-16:1 and 16:0 (mol %)
Ratio trans-16:1/16:0
20/800
20/250
20/50
5/250
5/50
Growth Regime (°C/µmol m-2 s-1)

43% decrease upon growth at 20/50 in comparison to the other 20°C growth regimes. Growth at cold-hardening temperatures (5/250) results in a 30% decrease of *trans*-16:1 in PG in comparison to typical non-hardened controls (20/250), confirming previous results (Huner et al., 1987). In addition, growth at 5/50 resulted in a 42% reduction of *trans*-16:1 in comparison to cold-hardened controls (5/250) simply as a result of decreasing the growth irradiance. Decreasing the growth irradiance from 800 to 50 μmol m^{-2} s^{-1} at 20°C resulted in a 3-fold reduction in the *trans*-16:1 to 16:0 ratio (Fig. 9B). Similarly, decreasing growth irradiance at 5°C from 250 to 50 μmol m^{-2} s^{-1} resulted in a 2.3-fold reduction in the *trans*-16:1 to 16:0 ratio. Low temperature growth at 5/250 also resulted in a 36% decrease in this ratio when compared to typical non-hardened controls (20/250), consistent with previous reports (Huner et al., 1987; Krol et al., 1988). Thus, the ratio of *trans*-16:1 to 16:0 present in PG is dependent not only on growth temperature, but also on growth irradiance. This occurs irrespective of the growth temperature, as this light-dependence is observed at 20 and 5°C (Fig. 9B).

The temperature and irradiance effects observed are specific for the 16:0 and *trans*-16:1 fatty acids, as no significant changes were observed in any of the other major fatty acids present in PG (Table VIII). In addition, no major changes were observed in the fatty acid profiles of the other thylakoid phospholipids (PC and PE), galactolipids (MGDG and DGDG), or sulfolipid (SQDG) (Table IX to XIII). This is consistent with previous studies (Huner et al., 1987).

Table VIII. *Fatty acid profile of PG in total leaf extracts of winter rye (S. cereale L. cv Musketeer).*

Fatty acids were calculated as the molar ratio (mol %) of the total. tr; trace amounts (< 0.5%). All values represent means ± SD; $n = 3$.

Growth Regime	Fatty Acid Profile (mol %)					
(°C/µmol m^{-2} s^{-1})	16:0	16:1	18:0	18:1	18:2	18:3
20/800	19 ± 1	29 ± 1	1 ± 0	1 ± 0	9 ± 1	41 ± 1
20/250	25 ± 4	27 ± 2	2 ± 1	2 ± 1	8 ± 1	36 ± 2
20/50	32 ± 2	16 ± 1	1 ± 0	2 ± 0	10 ± 1	39 ± 2
5/250	27 ± 0	19 ± 0	1 ± 0	1 ± 0	7 ± 1	45 ± 0
5/50	38 ± 2	11 ± 2	1 ± 1	1 ± 1	8 ± 0	41 ± 1

Table IX. *Fatty acid profile of PC in total leaf extracts of winter rye (S. cereale L. cv Musketeer).*

Fatty acids were calculated as the molar ratio (mol %) of the total. tr; trace amounts (< 0.5%). All values represent means ± SD; n = 3.

Growth Regime	Fatty Acid Profile (mol %)				
(°C/µmol m^{-2} s^{-1})	16:0	18:0	18:1	18:2	18:3
20/800	33 ± 3	2 ± 0	2 ± 0	30 ± 1	33 ± 3
20/250	29 ± 1	2 ± 0	2 ± 0	35 ± 3	32 ± 2
20/50	31 ± 2	2 ± 0	2 ± 0	34 ± 1	31 ± 1
5/250	24 ± 1	2 ± 0	2 ± 0	42 ± 1	30 ± 1
5/50	28 ± 2	1 ± 0	1 ± 0	28 ± 11	42 ± 9

Table X. *Fatty acid profile of PE in total leaf extracts of winter rye (S. cereale L. cv Musketeer).*

Fatty acids were calculated as the molar ratio (mol %) of the total. tr; trace amounts (< 0.5%). All values represent means ± SD; $n = 3$.

Growth Regime	Fatty Acid Profile (mol %)				
(°C/µmol m^{-2} s^{-1})	16:0	18:0	18:1	18:2	18:3
20/800	35 ± 4	1 ± 0	1 ± 0	34 ± 2	29 ± 2
20/250	36 ± 1	2 ± 0	1 ± 0	34 ± 0	27 ± 1
20/50	38 ± 4	1 ± 0	1 ± 0	34 ± 2	26 ± 2
5/250	30 ± 1	1 ± 0	1 ± 0	37 ± 1	31 ± 0
5/50	36 ± 5	1 ± 0	tr	28 ± 7	35 ± 4

Table XI. *Fatty acid profile of MGDG in total leaf extracts of winter rye (S. cereale L. cv Musketeer).*

Fatty acids were calculated as the molar ratio (mol %) of the total. tr; trace amounts (< 0.5%). All values represent means ± SD; $n = 3$.

Growth Regime	Fatty Acid Profile (mol %)				
(°C/µmol m^{-2} s^{-1})	16:0	18:0	18:1	18:2	18:3
20/800	2 ± 0	tr	tr	3 ± 0	95 ± 3
20/250	2 ± 0	tr	tr	3 ± 0	95 ± 1
20/50	2 ± 0	tr	1 ± 0	4 ± 0	93 ± 0
5/250	1 ± 0	tr	tr	2 ± 0	97 ± 0
5/50	1 ± 1	tr	tr	2 ± 1	97 ± 2

Table XII. *Fatty acid profile of DGDG in total leaf extracts of winter rye (S. cereale L. cv Musketeer).*

Fatty acids were calculated as the molar ratio (mol %) of the total. tr; trace amounts (< 0.5%). All values represent means ± SD; $n = 3$.

Growth Regime	Fatty Acid Profile (mol %)				
(°C/µmol m^{-2} s^{-1})	16:0	18:0	18:1	18:2	18:3
20/800	9 ± 0	1 ± 0	1 ± 0	2 ± 0	87 ± 0
20/250	10 ± 2	1 ± 0	1 ± 0	3 ± 0	85 ± 3
20/50	13 ± 1	1 ± 0	1 ± 0	4 ± 0	81 ± 3
5/250	6 ± 1	1 ± 0	tr	1 ± 0	92 ± 1
5/50	10 ± 3	1 ± 0	tr	2 ± 0	87 ± 3

Table XIII. *Fatty acid profile of SQDG in total leaf extracts of winter rye (S. cereale L. cv Musketeer).*

Fatty acids were calculated as the molar ratio (mol %) of the total. tr; trace amounts (< 0.5%). All values represent means ± SD; $n = 3$.

Growth Regime	Fatty Acid Profile (mol %)				
(°C/µmol m^{-2} s^{-1})	16:0	18:0	18:1	18:2	18:3
20/800	35 ± 5	1 ± 0	tr	5 ± 1	59 ± 5
20/250	32 ± 1	2 ± 0	tr	8 ± 5	58 ± 6
20/50	31 ± 4	2 ± 0	tr	8 ± 1	59 ± 4
5/250	24 ± 2	1 ± 0	tr	4 ± 0	71 ± 2
5/50	30 ± 5	1 ± 1	tr	10 ± 4	59 ± 1

2.3.6 Chl-Protein Complexes

Separation of the Chl-protein complexes indicated a 18% decrease in the ratio of oligomeric:monomeric LHCII with a decrease in irradiance from 800 to 50 µmol m^{-2} s^{-1} at 20°C (Table XIV). This was even more pronounced at 5°C with a 39% decrease in the oligomeric:monomeric ratio when growth irradiance was decreased from 250 to 50 µmol m^{-2} s^{-1} (Table XIV).

2.3.7 Chl *a/b*-Binding Proteins

The results for SDS-PAGE and immunoblotting (Fig. 10 and 11) indicated only small changes (20 to 35%) in the Chl *a/b*-binding proteins associated with PSII as a function of growth irradiance, with similar trends evident for growth temperature, which is consistent with the data for Chl *a/b* (Table IV). However, the Lhcb6 polypeptide demonstrated a 60 and 40% decrease as a result of growth at 5/250 and 5/50 respectively.

The organizational change in oligomer to monomer ratios observed in the Chl-protein complexes of LHCII (Table XIV) occurs with only slight changes to the absolute amount of LHCII when examined through immunoblotting (Fig. 11). The Lhcb1 and Lhcb2 polypeptides, thought to compose the LHCII trimer (Jansson, 1994), show minimal change (15 to 20%) as a result of growth under any of the temperature/irradiance regimes examined (Fig. 11).

In contrast, the majority of the Chl *a/b*-binding proteins associated with PSI exhibit a 20 to 30% decrease in abundance upon growth at 5°C, the effects

Table XIV. *Oligomer:monomer ratios of LHCII (Lhcb1/Lhcb2) in isolated thylakoid membranes of winter rye (S. cereale L. cv Musketeer).*

Chl contents of oligomeric and monomeric LHCII complexes isolated from mildly denaturing SDS-PAGE were calculated from peak area as a percentage of the total area from gel scans (Huner et al., 1987). All values represent means ± SD; n = 2 to 4.

Growth Regime (°C/µmol m^{-2} s^{-1})	LHCII Oligomer:Monomer
20/800	1.49 ± 0.06
20/250	1.36 ± 0.18
20/50	1.23 ± 0.01
5/250	1.08 ± 0.22
5/50	0.79 ± 0.29

Figure 10. Polypeptide profile in isolated thylakoid membranes of winter rye (*S. cereale* L. cv Musketeer) developed at the temperature/irradiance regimes indicated. Molecular mass markers in kD are indicated at the right. Regions of the Lhca and Lhcb Chl *a/b*-binding proteins are indicated to the left.

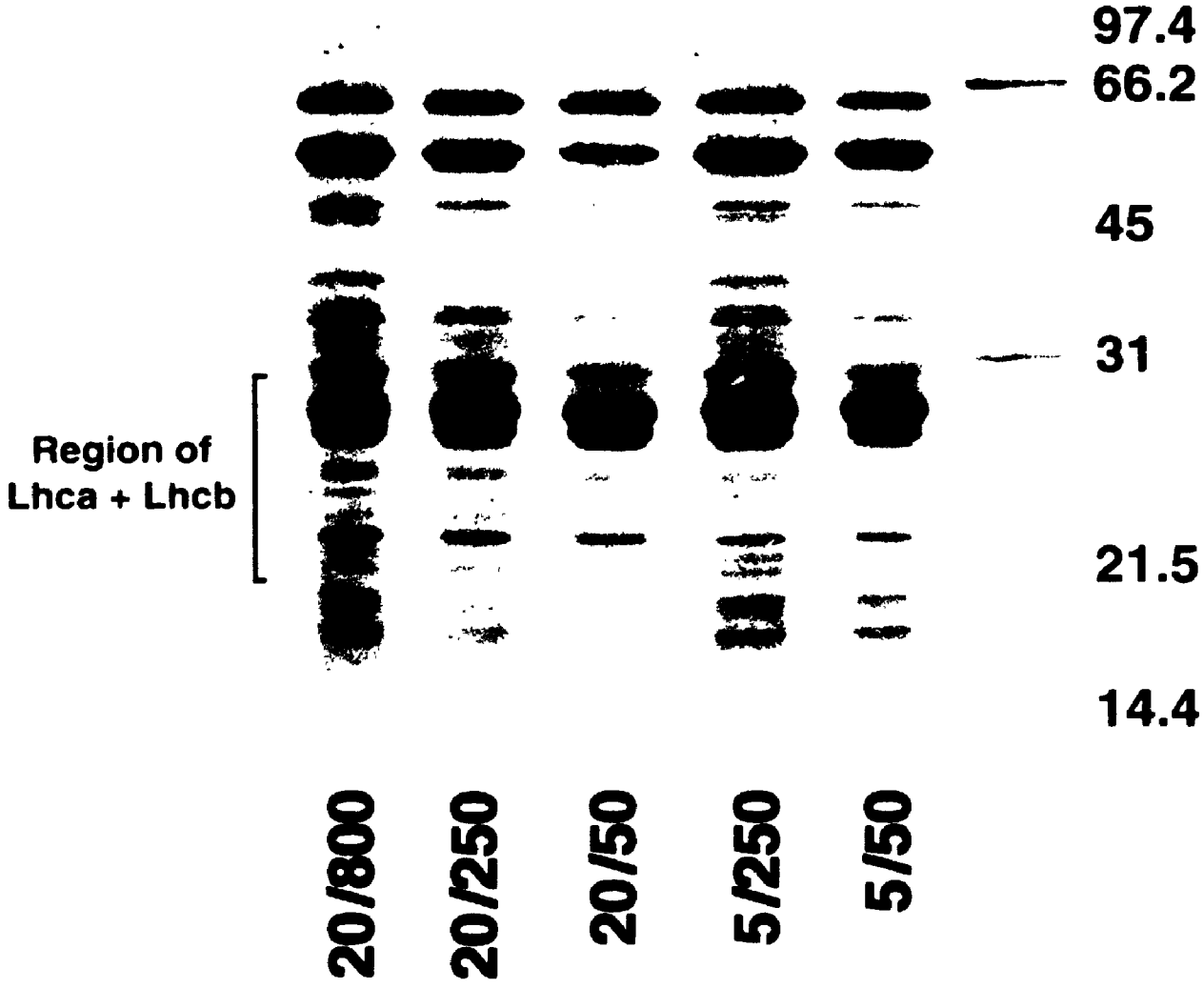
97.4
66.2
45
31
21.5
14.4
Region of
Lhca + Lhcb
20/800
20/250
20/50
5/250
5/50

Figure 11. Immunological detection of the Chl *a/b*-binding proteins associated with PSII in isolated thylakoid membranes of winter rye (*S. cereale* L. cv Musketeer) developed at the temperature/irradiance regimes indicated. Blots were performed at least twice and similar results obtained with each experiment. A, Lhcb1. B, Lhcb2. C, Lhcb3. D, Lhcb4. E, Lhcb5. F, Lhcb6.

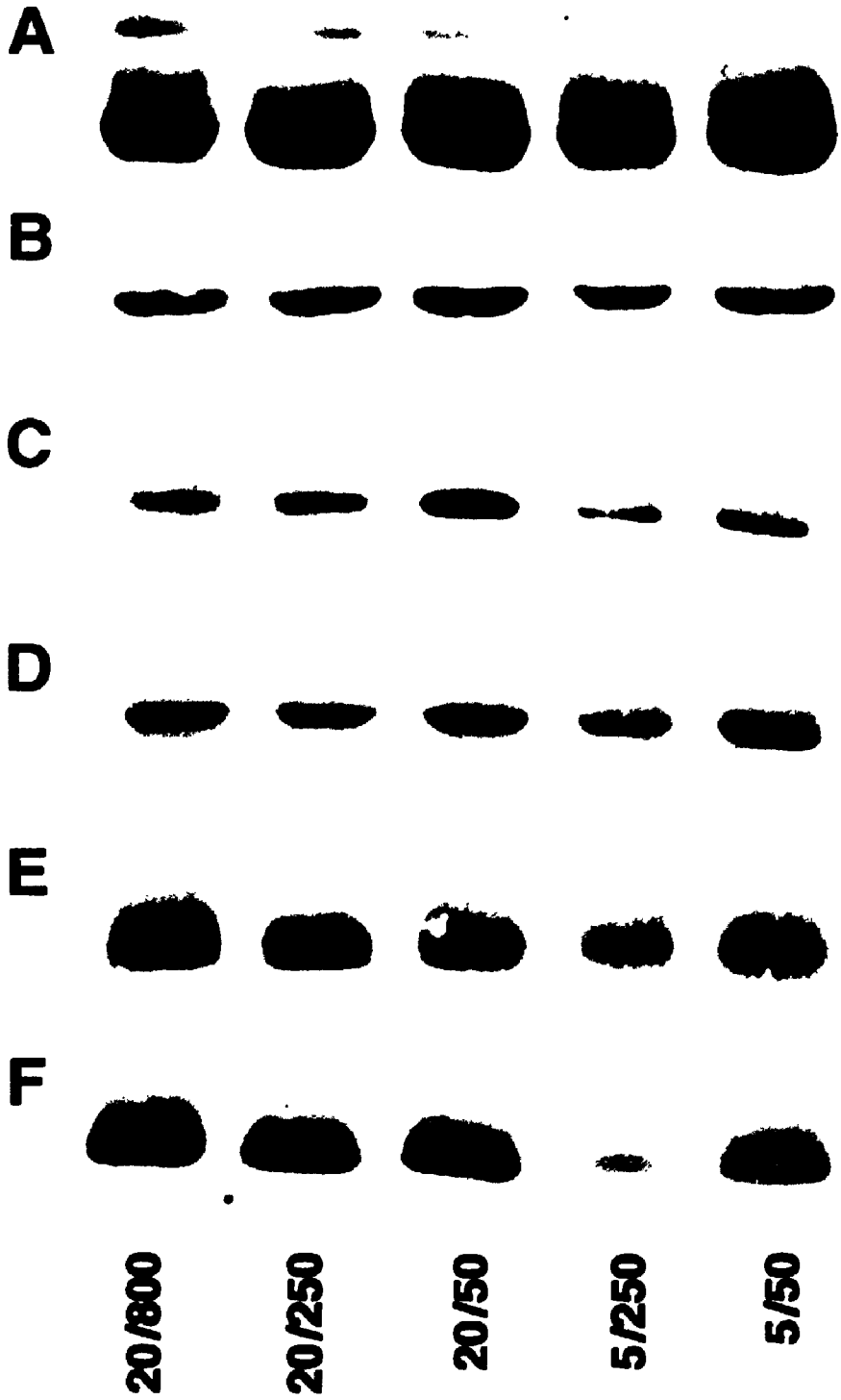
A
B
C
D
E
F
20/800
20/250
20/50
5/250
5/50

being most pronounced at the 5/250 growth regime (Fig. 12). Minimal effects (11 to 15%) were observed at any irradiance of the 20°C growth regimes (Fig. 12).

2.4 Discussion

Based on growth kinetics, all plants were compared in the vegetative state when maximum leaf area and DW had been attained irrespective of developmental temperature or irradiance conditions (Krol et al., 1984).

The relative reduction state of PSII can be estimated from parameters of steady-state Chl *a* fluorescence and expressed as $1-q_P$ which is determined at the growth temperature and growth irradiance. This is what will be referred to in the context of this thesis as PSII excitation pressure (Dietz et al., 1985; Ögren, 1991; Dau, 1994a). However, this estimation of the reduction state of Q_A is not linearly related to the actual reduction state of PSII, presumably due to cooperativity and exciton transfer between PSII units at the antenna level (Joliot and Joliot, 1964; Schreiber et al., 1994). Thus, this parameter provides only a relative estimate of the PSII reduction state for the growth regimes utilized in this thesis.

PSII excitation pressure ($1-q_P$) estimates PSII trap closure, that is, the relative reduction state of PSII (Dietz et al., 1985; Ögren, 1991; Dau, 1994a, 1994b). The relative reduction of PSII reflects the balance between light energy absorbed through the temperature-independent photochemical reactions of PSII

Figure 12. Immunological detection of the Chl *a/b*-binding proteins associated with PSI in isolated thylakoid membranes of winter rye (*S. cereale* L. cv Musketeer) developed at the temperature/irradiance regimes indicated. Blots were performed at least twice and similar results obtained with each experiment. A, Lhca1. B, Lhca2. C, Lhca3. D, Lhca4.

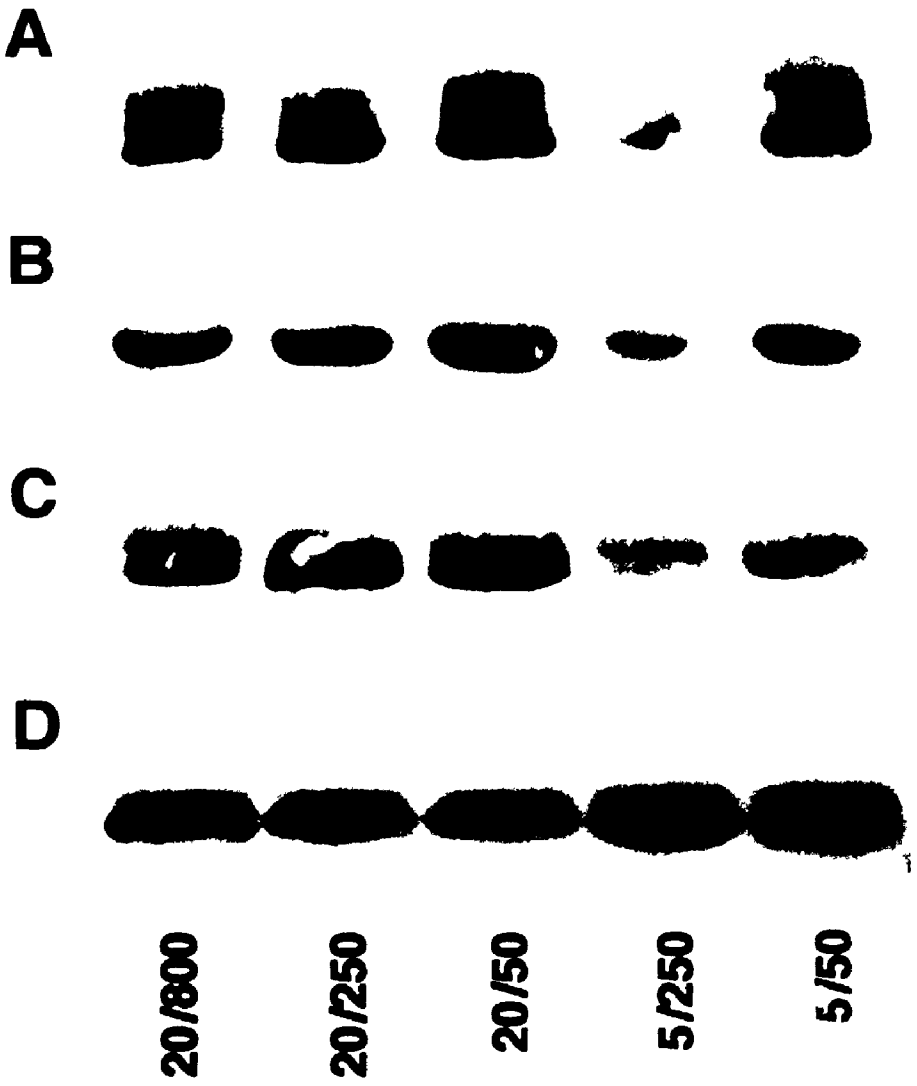
A
B
C
D
20/800
20/250
20/50
5/250
5/50

and the energy utilized through the temperature-dependent reactions of intersystem electron transport and CO_2 assimilation at physiological relevant temperatures (Huner et al., 1996). While variations in 1-q_P estimates changes in the relative reduction state of PSII, it has also been suggested that this parameter may reflect changes in the overall redox poise of the chloroplast (Huner et al.. 1995, 1996).

The modulation of PSII excitation pressure may occur either by increasing irradiance at constant temperature or by decreasing temperature at constant irradiance. This is demonstrated by the data presented in Figure 8 and Table II and III. Growth of rye and wheat at 20/800 or 5/250 resulted in comparably high PSII excitation pressure whereas growth at either 20/250 or 5/50 resulted in comparably low PSII excitation pressure. PSII excitation pressure, therefore, reflects the integration of the environmental factors of temperature and light (Fig. 8; Table II and III).

In experiments designed to elucidate the effects of environmental stresses, such as low temperature, one typically compares plants grown at 5°C with control plants grown at 20°C with irradiance held constant. The assumption is that any changes observed must be due to a growth temperature effect. While one would normally compare plants grown at 5/250 with those grown at 20/250 based on growth temperature alone, I suggest that a more appropriate comparison would be plants grown at 5/250 with those grown at 20/800 based on high PSII excitation pressure (Table II and III). Thus, cold tolerant plants

grown at low temperature and moderate irradiance (5/250) should be physiologically comparable to the same plants grown at high temperature and high light (20/800). The results presented in this chapter for rye and wheat provide the basis for the comparisons that follow in this thesis.

The major Chl *a/b*-binding protein associated with PSII, LHCII, is thought to be a trimer composed of Lhcb1 and Lhcb2 polypeptides which is stabilized by PG (Dubacq and Trémolières, 1983; Krupa et al., 1987, 1992) and plays a fundamental role in photosynthetic light-harvesting (Jansson, 1994). In addition, PG is the major phospholipid present in thylakoid membranes and characterized by the presence of a novel fatty acid, *trans*-16:1 (Dubacq and Trémolières, 1983). The results for Chl *a/b* and immunoblotting for PSII Chl *a/b*-binding proteins are consistent and demonstrate minimal adjustment of the Chl and polypeptide compositions of the photochemical apparatus (Fig. 10 and 11; Table IV). Thus, growth at high PSII excitation pressures appears to have minimal effects on Chl *a/b* and the abundance of the proteins associated with PSII light-harvesting.

However, mild SDS-PAGE indicates an adjustment in the supramolecular organization of LHCII with the oligomer being more prominent at high light and the monomer at low light (Table XIV). In addition, low temperature also promotes the monomeric form (Huner et al., 1987). Growth at cold-hardening temperatures modulates LHCII organization such that the oligomeric form ($LHCII_1$) predominates at 20°C and monomeric ($LHCII_3$) and/or intermediate

forms ($LHCII_2$) predominate at 5°C. However, low temperature also results in a specific decrease in *trans*-16:1 content associated with PG, both *in vivo* and *in situ*, with minimal changes in lipid and pigment profiles (Huner, 1988). The results presented here indicate that the organization of LHCII is dependent upon both temperature and light, in a synergistic manner. This is consistent with the lipid and fatty acid data which demonstrates a light- and temperature-dependent decrease in the amount of *trans*-16:1 associated with the thylakoid phospholipid PG, concomitant with an increase in 16:0 (Fig. 9 and Table VIII).

The role of thylakoid lipids in the stabilization of LHCII remains controversial, although several reports have implicated a functional association between PG and the stabilization of oligomeric LHCII (Dubacq and Trémolières, 1983; Browse et al., 1985; McCourt et al., 1985; Plumley and Schmidt, 1987; Garnier et al., 1990; Krupa et al., 1992). Dubacq and Trémolières (1983) were the first to present evidence that *trans*-16:1 in PG is correlated to LHCII stabilization. This was verified by Huner and co-workers who demonstrated that it is the capacity to change the *trans*-16:1 content of PG that is correlated with the capacity to change the supramolecular organization of LHCII (Huner et al., 1987; Krupa et al., 1987, 1992). Thus, I have confirmed previous results that the reduction in the levels of *trans*-16:1 is temperature-dependent. However, I have also demonstrated for the first time, a light-dependence for the *trans*-16:1 content of PG at both 5 and 20°C, which cannot be rationalized on the basis of PSII excitation pressure (Fig. 9 and Table VIII). Upon decreasing irradiance at

20 or 5°C a concomitant decrease in the *trans*-16:1 to 16:0 ratio is observed (Fig. 9). In addition, if one examines plants grown under typical cold-hardening (5/250) and non-hardening (20/250) conditions a temperature-dependent decrease in the *trans*-16:1 to 16:0 ratio is observed in response to growth at 5°C (Fig. 9). While growth at 20/800 and 5/250 results in comparable levels of high PSII excitation pressure (Table II), these plants do not exhibit the same *trans*-16:1 to 16:0 ratios (Fig. 9). Similarly, plants grown at comparable low PSII excitation pressure (20/250 or 5/50; Table II) also do not demonstrate similar *trans*-16:1 to 16:0 ratios. Thus, this phenomenon cannot be attributed to PSII excitation pressure. However, it is clear that the changes in the *trans*-16:1 to 16:0 ratio of PG is both temperature- and light-dependent (Fig. 9 and Table VIII). The capacity to modulate *trans*-16:1 and hence LHCII organization may reflect an acclimatory mechanism for the regulation of energy distribution in the photosynthetic apparatus to allow for photosynthesis to occur efficiently under conditions of varying temperature and irradiance.

The temperature-dependent decreases observed in the Chl *a/b*-binding proteins associated with PSI are aiso of interest as this may represent a regulatory mechanism to control energy balance at the level of PSI as a result of cold-hardening. However, the physiological significance of these changes has yet to be fully elucidated.

In contrast to green algae, minimal adjustment of the photochemical apparatus occurs in winter rye in response to high PSII excitation pressure.

Chlorella vulgaris responds to growth at high PSII excitation pressure by decreasing its capacity to absorb incident radiation through a reduction in LHCII content and Chl cell^{-1}, accompanied by vast increases in the xanthophyll Zx (Maxwell et al., 1994, 1995a). However, growth of winter rye at high PSII excitation pressure results in an increase in Chl content with minimal changes in LHCII abundance and Zx accumulation (Fig. 10 and 11; Table V). These data support the thesis that cereals exhibit a different mechanism of adjustment to high PSII excitation pressure than green algae.

CHAPTER 3

PHOTOSYNTHETIC ADJUSTMENT IN RESPONSE TO PSII EXCITATION PRESSURE

3.1 Introduction

Photosynthetic acclimation to temperature usually refers to the process of shifting the temperature optimum for net photosynthesis closer to that of the environmental temperature range to which the species has adapted (Berry and Björkman, 1980; Öquist, 1983; Huner et al., 1993). Photosynthesis provides the energy required for growth and development, irrespective of environmental conditions to which the plant is subjected. Thus, the mechanisms by which plants maintain optimal photosynthetic capacity under different growth conditions are of fundamental importance.

It has been demonstrated previously that the growth of winter cereals at low temperature (5°C) results in an increased capacity to keep Q_A oxidized under given temperature and irradiance conditions (Öquist and Huner, 1993; Öquist et al., 1993b). Furthermore, the leaves developed at 5°C require photon fluxes that are 3-fold greater than that of the 20°C leaves to attain the same redox state of Q_A (Öquist and Huner, 1993). In addition, winter cereals grown at 5°C modulate their rates of photosynthesis so as to increase PS_{max} O_2 with no change in ΦO_2 (Huner et al., 1993). This increase in PS_{max} O_2 in cold-grown plants is associated with increased Pi availability, which may allow these plants to maintain a larger

pool of Q_A in the oxidized state (Huner et al., 1993; Hurry et al., 1993). Thus, low temperature growth results in the alteration of the proportion of open PSII reaction centers, concomitant with an increase in photosynthetic capacity. However, low temperature typically induces Pi limitations due to decreased triose-P utilization (Sage and Sharkey, 1987; Labate and Leegood, 1988; Labate et al., 1990). Since these low temperature grown plants exhibit an increased capacity for photosynthesis, it has been suggested that they have in some way overcome the Pi limitation which typically results at low temperature (Huner et al., 1993; Hurry et al., 1993, 1995a). However, the physiological role of this photosynthetic modulation and the mechanism by which Q_A is kept in the oxidized state remain to be elucidated.

Since the growth of wheat and rye at 5/250 or 20/800 results in higher PSII excitation pressure in comparison to that of plants grown at 20/250, I hypothesized that cold tolerant plants grown at low temperature and moderate irradiance (5/250) should be photosynthetically comparable to the same plants grown at high temperature and high light (20/800). Thus, the modulation of photosynthesis observed upon growth at low temperature may not be a growth temperature effect *per se*, but rather, reflects photosynthetic adjustment or acclimation to high PSII excitation pressure. In this chapter, I test this hypothesis.

3.2 Materials and Methods

3.2.1 Plant Material and Growth Conditions

Winter rye (*S. cereale* L. cv Musketeer), winter wheat (*T. aestivum* L. cv Monopol) and spring wheat (*T. aestivum* L. cv Katepwa) were germinated from seed as described in section 2.2.1.

3.2.2 PSII Excitation Pressure

Photosystem II excitation pressure ($1-q_P$) was calculated from Chl *a* steady-state fluorescence parameters at the growth temperature and irradiance as described in section 2.2.3.

3.2.3 Chl *a* Fluorescence

Room temperature Chl *a* fluorescence at 695 nm was measured *in vivo* using a PSM fluorometer (Biomonitor S.C.I. AB, Umeå, Sweden) as described by Öquist and Wass (1988). Exposure of the dark adapted leaf surface for 2 s to an actinic light with a photon flux of 400 μmol m^{-2} s^{-1} and a peak wavelength of 500 nm resulted in the instantaneous measurement of F_O, F_M, F_V, and the F_V / F_M ratio. The F_V / F_M ratio was used to determine the maximal photochemical efficiency or optimal quantum yield of PSII (Schreiber et al., 1994) as a result of growth at the various temperature/irradiance regimes. Leaves were sampled 4 h into the photoperiod and dark adapted at room temperature for 1 h prior to measurement of F_V / F_M.

Steady-state Chl *a* fluorescence parameters were determined as

described in section 2.2.3. The photochemical efficiency or yield of open PSII reaction centers (F_V'/F_M') was determined as described by Genty et al. (1989). The coefficient of photochemical quenching (q_P) and the effective quantum yield of PSII electron transport (Φ_{PSII}) were calculated as:

$$q_P = (F_M'-F_S) / (F_V') \qquad \Phi_{PSII} = (F_M'-F_S) / (F_M')$$

according to Schreiber et al. (1994) and Genty et al. (1989) respectively. The PSII RET rate was calculated as:

$$\text{PSII RET} = \Phi_{PSII} \times \text{PPFD}$$

as described by Schreiber et al. (1994).

3.2.4 Photosynthetic Oxygen Evolution

CO_2-saturated O_2 evolution of 10-cm^2 discs, composed of segments cut from the middle of several leaves, was measured in the gas phase at 5 or 20°C with a Hansatech oxygen electrode (model LD2; Hansatech Instruments Ltd.). Leaves were sampled 4 h into the photoperiod. An array of photodiodes (model LH 36-109 Ultra-Bright, λ_{max} 660 nm; Hansatech), connected to a Hansatech LS3 light source control box provided PPFD values from 0 to 800 µmol m^{-2} s^{-1}. The photodiodes were calibrated using Simpson's three-eigths rule as described previously (Boese and Huner, 1990). Measuring temperature was maintained by the use of a Neslab refrigerated circulating water bath (model LT50-DD; Neslab Instruments Inc.). Leaf discs were dark-adapted for 5 min in a gas mixture of 5% CO_2, 5% O_2 and 90% N_2 and then pre-illuminated at 50% of their respective

growth irradiance for 10 min to ensure maximal photosynthetic rates. The light source was shut off and dark respiration was allowed to stabilize for 10 min before engaging a computerized acquisition program. Rates of O_2 evolution were calculated using the Hansatech A/D interface board (model IF/1) and associated software (Leaf Disc, version 1.31; Hansatech) installed in an IBM-compatible personal computer. Additional CO_2 was provided from capillary matting saturated with a 1.0 M sodium carbonate/bicarbonate buffer (pH 7.9) in equilbrium with ambient air. Irradiance response curves were obtained by using 13 irradiance values over the range of 0 to 800 µmol m^{-2} s^{-1} PPFD and were corrected for the levels of dark respiration. The ΦO_2 was calculated by regression analyses (SigmaPlot®, version 1.02; Jandel Scientific,Corte Madera, CA, USA) of points in the linear, light-limiting range of the irradiance response curves (0 to 50 µmol m^{-2} s^{-1} PPFD) and corrected for leaf absorptance as described by Öquist et al. (1992b). Values of PS_{max} O_2 were obtained essentially as described above except that saturating white light (3000 µmol m^{-2} s^{-1} PPFD) was supplied from a Hansatech light source (model LS2H) controlled by a light source control box (model LS2; Hansatech).

3.2.5 Isolation and Solubilization of Thylakoid Membranes

Thylakoid membranes for immunological detection of intersystem electron transport components, with the exception of plastocyanin, were isolated as described in section 2.2.6. Thylakoids for plastocyanin immunodetection were

isolated essentially as outlined in section 2.2.6 with minor modifications as described by Burkey (1993). After maceration in grinding buffer, filtration, and centrifugation, the pellet was suspended in grinding buffer and immediately frozen in liquid N_2. Prior to use, frozen thylakoids were thawed and solubilized without additional washing steps to prevent the loss of plastocyanin (Burkey, 1993). After Chl determination, the thylakoids were precipitated with 80% (v/v) acetone at -20°C and subsequently suspended in solubilzation buffer. Solubilization for all isolated thylakoids was performed as indicated in section 2.2.6.

3.2.6 SDS-PAGE and Immunoblotting

SDS-PAGE and immunoblotting occurred essentially as described in section 2.2.7. Primary monospecific polyclonal antibodies raised in rabbits against; amino acids 232-242 located in the DE-loop of the D1 polypeptide of *Synechocystis* PCC 6803 (32 kD), recombinant protein of Cyt *f* (34 kD), purified plastocyanin from barley (8 kD) and the PSI reaction center heterodimer (*psaA/psaB* gene) were utilized (Burkey, 1993; Ghosh et al., 1994; Kim et al., 1993). In addition, monoclonal antibodies raised in rats against the β-subunit of the *Escherichia coli* F_1-ATPase was also employed (Dunn et al., 1985). This cross-reacted with the β-subunit (56 kD) of the chloroplast coupling factor CF_1-ATPase (Dunn et al., 1985). Concentrations of the antibodies varied from 1:500 to 1:10,000 depending on their titer. All gels were loaded on an equal Chl basis

(3 µg lane^{-1}) with the exception of gels for the immunodetection of plastocyanin in which the Chl content was increased to 10 µg lane^{-1}.

3.2.7 Redox State of P_{700}

The redox state of P_{700} was determined *in vivo* under ambient CO_2 conditions using a PAM-101 Chl fluorometer (Heinz Walz) equipped with the ED-800T emitter-detector and PAM-102 unit as described by Schreiber et al. (1988). A Schott flash lamp (model KL1500; Schott Glaswerke) provided a white actinic light source (FL-101) of appropriate PPFD in combination with neutral density filters (Balzers) as determined at the leaf position with a quantum sensor (model LI-190SA; Li-Cor). FR light (λ_{max} 735 nm) at an intensity of approximately 15 W m^{-2} was provided by the 102-FR LED light source (Heinz Walz) in combination with the PAM-102 unit. FR and actinic light was applied to the leaf surface via a multibranched fiberoptic system that was attached to the emitter-detector following the protocol of Asada et al. (1992).

A XF-103 xenon discharge flash lamp (Heinz Walz) provided saturating flashes of blue light with an intensity of 1,500 W m^{-2}, obtained using a blue-green filter (Schott BG18). MT (50 ms) saturating flashes and ST (half peak width 14 µs) saturating flashes were applied with the XMT-103 and XST-103 power/control units (Heinz Walz) respectively.

The redox state of P_{700} was evaluated as the absorbance change due to the cation radical (P_{700}^{+}) in the near-infrared spectral region around 820 nm (800

to 840 nm) in a custom designed cuvette modified to accept the PAM fiber optic. The fiberoptic system connected to the emitter-detector was attached to the adaxial side of the leaf and measurements were made at 20°C, maintained by a Neslab refrigerated circulating water bath (model LT50-DD; Neslab Instruments Inc.) and recorded on an Omnigraphic XY chart recorder (model 2000; Houston Instrument). A humidified stream of ambient air corresponding to the measuring temperature was blown over the leaf surface to assist in maintaining the leaf temperature which was monitored using a constantan-copper (Type T) thermocouple in conjunction with a temperature logger (model MDSS41-TC:G1; Omega Engineering Inc., Stamford, CT, USA). The signals were also recorded using an oscilloscope card (PC-SCOPE T6420, version 2.43x; Intelligente Meßtechnik GmbH, Backnang, Germany) installed in an IBM-compatible personal computer with a sampling frequency of 156 Hz. The traces consisted of 16,280 data points recorded for a period of 104 seconds. Data files were exported to a graphing program for smoothing by the Savitzky-Golay method and integration of areas under the curves (MicoCal Origin version 3.01; MicroCal Software Inc., Northampton, MA, USA).

The functional pool size of electrons in the intersystem chain was determined as described by Asada et al. (1992). Leaves were sampled 4 h into the photoperiod and utilized immediately upon removal from the growth chamber. A stable P_{700} signal was first established by illuminating leaves with a photon fluence rate of 0.01 μmol m^{-2} s^{-1} modulated at 100 kHz. Under

continuous background FR light, a stable P_{700}^+ signal was obtained and a ST flash was given for a single excitation, resulting in the reduction of P_{700}^+ to P_{700} which was re-oxidized to P_{700}^+ by background FR light to a level prior to the ST application. When a stable P_{700}^+ signal was obtained again, a 50 ms MT flash was applied. This resulted in the reduction of P_{700}^+ and which was also re-oxidized back to a level prior to MT excitation. The complementary area between the oxidation curve of P_{700} after ST or MT excitation and the stationary level of P_{700}^+ under FR represent the ST- and MT-areas respectively and were used for calculations of the functional pool size of intersystem electrons on a P_{700} reaction center basis which was determined as;

$$e^- / P_{700} = \text{ST-area/MT-area}$$

according to Asada et al. (1992). A similar control experiment was performed in leaves exposed to DCMU, an inhibitor of electron transport. Leaves were harvested as described above and placed in a small glass vial which contained a solution of 1 mM DCMU in H_2O. This was prepared from a 10 mM DCMU stock in 100% (v/v) ethanol. The DCMU solution was introduced to the leaves via the transpiration stream at room temperature with a PPFD of 5 μmol m^{-2} s^{-1} for 2 h prior to the measurements.

3.2.8 PQ Analyses

Oxidized PQA was extracted under nitrogen and quantified according to Lichtenthaler (1968). Whole leaves were harvested 4 h into the photoperiod

and homogenized in a pre-chilled motar and pestle with 100% (v/v) acetone. The acetone extract was transferred to a separatory funnel and combined with 100% (v/v) petroleum ether (b.p. 35 to 60°C) (Caledon Laboratories, Georgetown, ON, Canada). The ether phase was removed and dried in a rotary evaporator (Büchi Rotavapor, model RE-120, Brinkmann). The extract was suspended in a minimum volume of 100% (v/v) petroleum ether and stored in air-tight glass vials with Teflon-lined caps under nitrogen at -20°C in the dark. The extracts were streaked onto Silica Gel 60 G TLC plates (Merck) and separated using a solvent system consisting of petroleum ether:ethyl ether (10:1, v/v) as described by (Lichtenthaler, 1969). The band corresponding to PQA was identified by spraying the plates with 1mM methylene blue acidified with 2 to 3 drops of sulphuric acid. The PQA band was recovered from the plate and dissolved in 1 mL 100% (v/v) ethanol. PQA was quantified spectrophotometrically (model UV-160; Shimadzu Corp.) at A_{225} by the difference in extinction between the oxidized ($E^{1\%}_{1cm}$ 198) and reduced ($E^{1\%}_{1cm}$ 225) forms which was determined using sodium borohydride as a reducing agent (Lichtenthaler, 1968).

3.3 Results

3.3.1 Photosynthetic Efficiency and Capacity

Development of winter rye at 20°C and a growth irradiance of 50, 250 or 800 µmol m^{-2} s^{-1} resulted in minimal changes in F_V / F_M (Table XV). Similar

Table XV. *Photosynthetic characteristics in leaves of winter rye (S. cereale L. cv Musketeer).*

The ΦO_2 was determined from light response curves measured at 20°C and corrected for leaf absorptance and dark respiration. F_V / F_M ratios were determined at 20°C after dark adaptation using the PSM. Measurements of PS_{max} O_2 occurred with a saturating PPFD of 3000 µmol m^{-2} s^{-1} at 20 or 5°C. All values represent means ± SE; $n = 3$.

Growth Regime (°C/µmol m^{-2} s^{-1})	F_V / F_M	ΦO_2 (µmol O_2 µmol photons^{-1})	PS_{max} O_2 (µmol O_2 m^{-2} s^{-1})	
			20°C	5°C
20/800	0.74 ± 0.02	0.097 ± 0.002	35.6 ± 0.9	11.7 ± 0.6
20/250	0.75 ± 0.01	0.088 ± 0.004	22.0 ± 0.6	6.0 ± 0.1
20/50	0.74 ± 0.01	0.092 ± 0.001	10.4 ± 0.3	2.7 ± 0.1
5/250	0.71 ± 0.01	0.092 ± 0.003	45.1 ± 1.0	11.3 ± 0.5
5/50	0.73 ± 0.01	0.098 ± 0.004	23.0 ± 1.4	3.5 ± 0.1

results were obtained with winter and spring wheat (Table XVI). In rye, this was consistent with measurements of ΦO_2 which varied by less than 10% as a result of growth at the different temperature/irradiance regimes (Fig. 13A; Table XV). However, the increase in growth irradiance from 50 to 800 μmol m^{-2} s^{-1} did result in a 3-fold increase in PS_{max} O_2 measured at 20°C in all cultivars examined (Table XV and XVI). This occurred independent of measuring temperature since this same trend was observed in winter rye measured at 5°C (Fig 13C; Table XV).

Rye and wheat leaves developed at 5/250 exhibited a 5 to 10% lower F_V / F_M ratio in comparison to those developed at 20/250 (Table XV and XVI). Furthermore, the difference in the ΦO_2 between rye plants grown at 5/250 and 20/250 was less than 5% (Fig. 13A and B; Table XV). These results are consistent with a previous report (Öquist and Huner, 1993). However, both winter rye and wheat grown at 5/250 exhibited a PS_{max} O_2 that was 2.1 and 1.2-fold higher respectively than plants grown at 20/250 (Table XV and XVI). This same trend was observed in rye whether PS_{max} O_2 was measured at 20 or 5°C (Fig. 13C and D; Table XV). In contrast, Katepwa spring wheat grown at 5/250 exhibited a 10% lower PS_{max} O_2 than spring wheat grown at 20/250 (Table XVI).

3.3.2 Fluorescence Quenching and PSII RET

When the quenching parameters of steady-state Chl *a* fluorescence were examined for growth at different PSII excitation pressures, mimimal differences

Table XVI. *Photosynthetic characteristics in leaves of winter wheat (T. aestivum L. cv Monopol) and spring wheat (T. aestivum L. cv Katepwa).*

Measurements of PS_{max} O_2 occurred at 20°C with a saturating PPFD of 3000 µmol m^{-2} s^{-1}. F_V / F_M ratios were determined at 20°C after dark adaptation using the PSM. All values represent means ± SE; $n = 3$.

Growth Regime (°C/µmol m^{-2} s^{-1})	PS_{max} O_2 (µmol m^{-2} s^{-1})	F_V / F_M
	Monopol	
20/800	31.5 ± 2.0	0.76 ± 0.01
20/250	22.3 ± 0.7	0.79 ± 0.01
20/50	9.8 ± 0.2	0.76 ± 0.03
5/250	27.2 ± 0.6	0.71 ± 0.01
5/50	31.2 ± 1.0	0.75 ± 0.01
	Katepwa	
20/800	27.1 ± 2.0	0.76 ± 0.02
20/250	18.8 ± 0.7	0.78 ± 0.01
20/50	9.7 ± 0.1	0.78 ± 0.01
5/250	16.9 ± 0.4	0.70 ± 0.02
5/50	17.3 ± 0.6	0.75 ± 0.01

Figure 13. Light response curves for CO_2-saturated O_2 evolution in leaves of winter rye (*S. cereale* L. cv Musketeer). Development occurred at a temperature of 20°C (closed symbols) or 5°C (open symbols) with an irradiance of 800 (♦), 250 (●, ○) or 50 (■, □) µmol m^{-2} s^{-1}. Response was measured at 20°C (A and B) and 5°C (C and D). All values represent means ± SE; $n = 3$. When not present, error bars are smaller than symbol size.

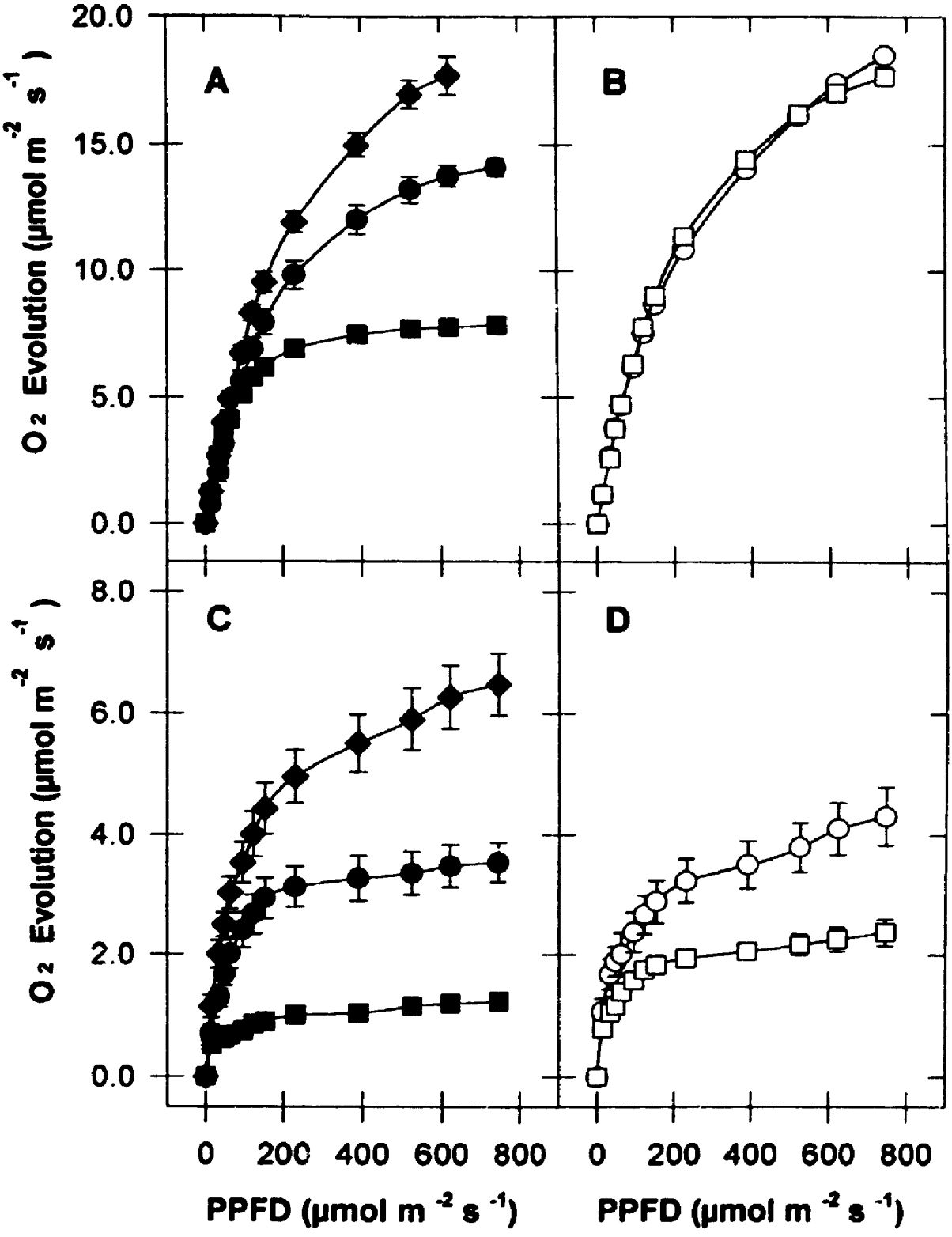
A
B
C
D
O2 Evolution (µmol m-2 s-1)
O2 Evolution (µmol m-2 s-1)
20.0
15.0
10.0
5.0
0.0
8.0
6.0
4.0
2.0
0.0
0
200
400
600
800
PPFD (µmol m-2 s-1)
PPFD (µmol m-2 s-1)

(± 15%) were observed in the photochemical yield of open PSII reaction centers (F_V'/F_M'), regardless of measuring temperature at saturating irradiance (Fig. 14A to D). Furthermore, increasing growth irradiance from 50 to 800 µmol m^{-2} s^{-1} at 20°C resulted in an increased capacity (2.9 to 3.1-fold) to keep Q_A oxidized (q_P) regardless of measuring irradiance or measuring temperature (Fig. 15A and C). Increasing growth irradiance at 5°C from 50 to 250 µmol m^{-2} s^{-1} also resulted in higher q_P values (1.4 to 2.0-fold) at all measuring irradiance and temperatures (Fig. 15B and D). In addition, values of q_P for rye grown at 5/250 closely matched that of plants grown at 20/800 regardless of measuring temperature and irradiance (Fig. 15A to D). PSII RET rates were also affected by increasing the growth irradiance from 50 to 800 µmol m^{-2} s^{-1} at 20°C when measured at 20°C. A 3.3-fold increase was observed in plants grown at 20/800 in comparison to those grown at 20/50 (Fig. 16A). At a measuring temperature of 20°C, a 1.7-fold increase in PSII RET rate was observed upon increasing growth irradiance at 5°C from 50 to 250 µmol m^{-2} s^{-1} (Fig. 16B). A similar trend in PSII RET was displayed for plants grown under all temperature/irradiance regimes when the measuring temperature was lowered to 5°C (Fig. 16C and D).

3.3.3 Intersystem Electron Pool Size

Figure 17A demonstrates a typical cycle of illumination for the determination of the intersystem electron pool size. When a leaf is illuminated with FR light it causes the oxidation of P_{700} to P_{700}^+. The ST flash causes a single

Figure 14. Light response curves for F_V' / F_M' in leaves of winter rye (*S. cereale* L. cv Musketeer). Development occurred at a temperature of 20°C (closed symbols) or 5°C (open symbols) with an irradiance of 800 (♦), 250 (●, ○) or 50 (■, □) µmol m^{-2} s^{-1}. Response was measured at 20°C (A and B) and 5°C (C and D). All values represent means ± SE; $n = 3$. When not present, error bars are smaller than symbol size.

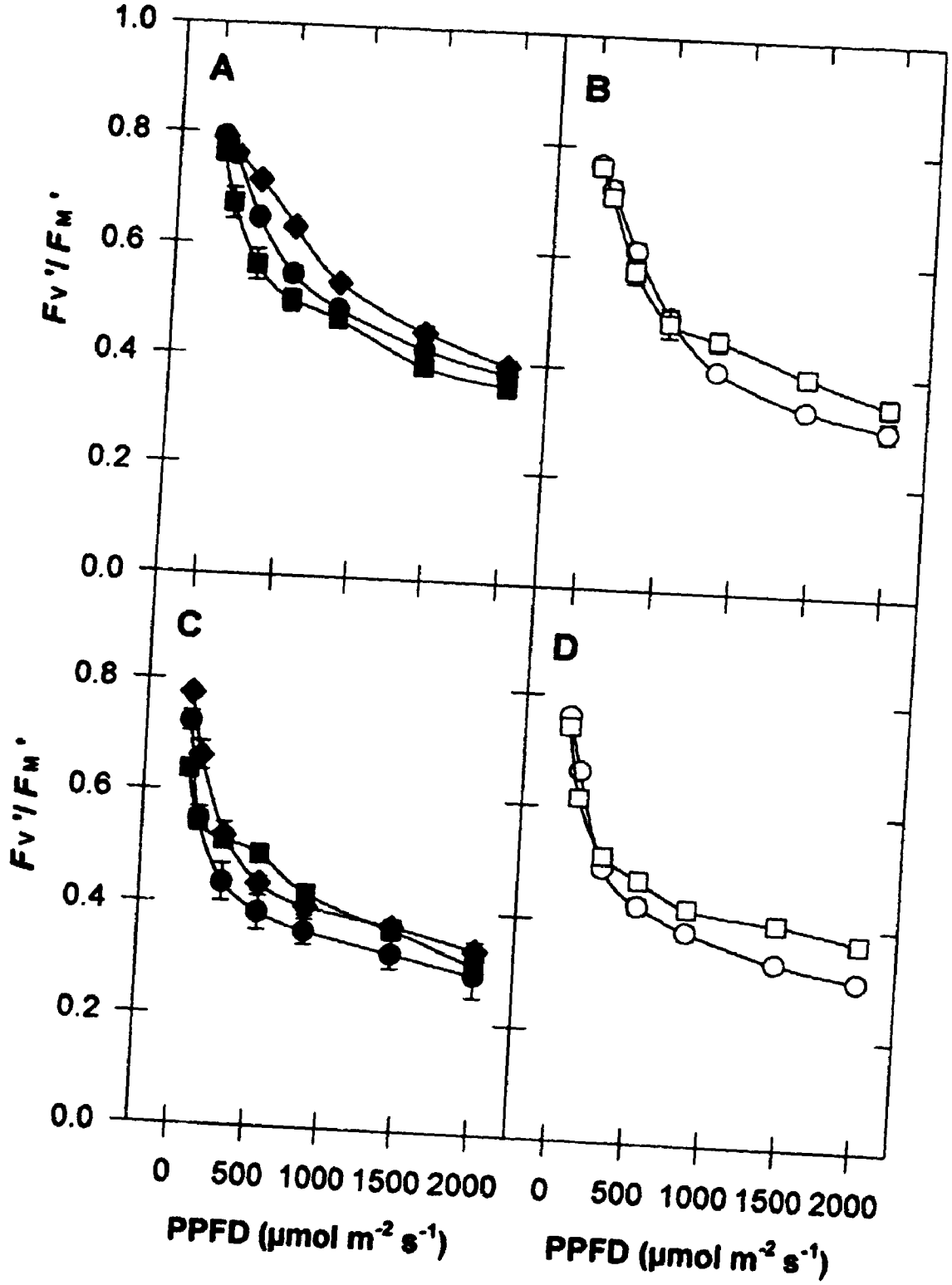
A
B
C
D
1.0
0.8
0.6
0.4
0.2
0.0
Fv'/Fm'
0
500
1000
1500
2000
PPFD (µmol m-2 s-1)

Figure 15. Light response curves for q_P in leaves of winter rye (*S. cereale* L. cv Musketeer). Development occurred at a temperature of 20°C (closed symbols) or 5°C (open symbols) with an irradiance of 800 (♦), 250 (●, ○) or 50 (■, □) µmol m^{-2} s^{-1}. Response was measured at 20°C (A and B) and 5°C (C and D). All values represent means ± SE; $n = 3$. When not present, error bars are smaller than symbol size.

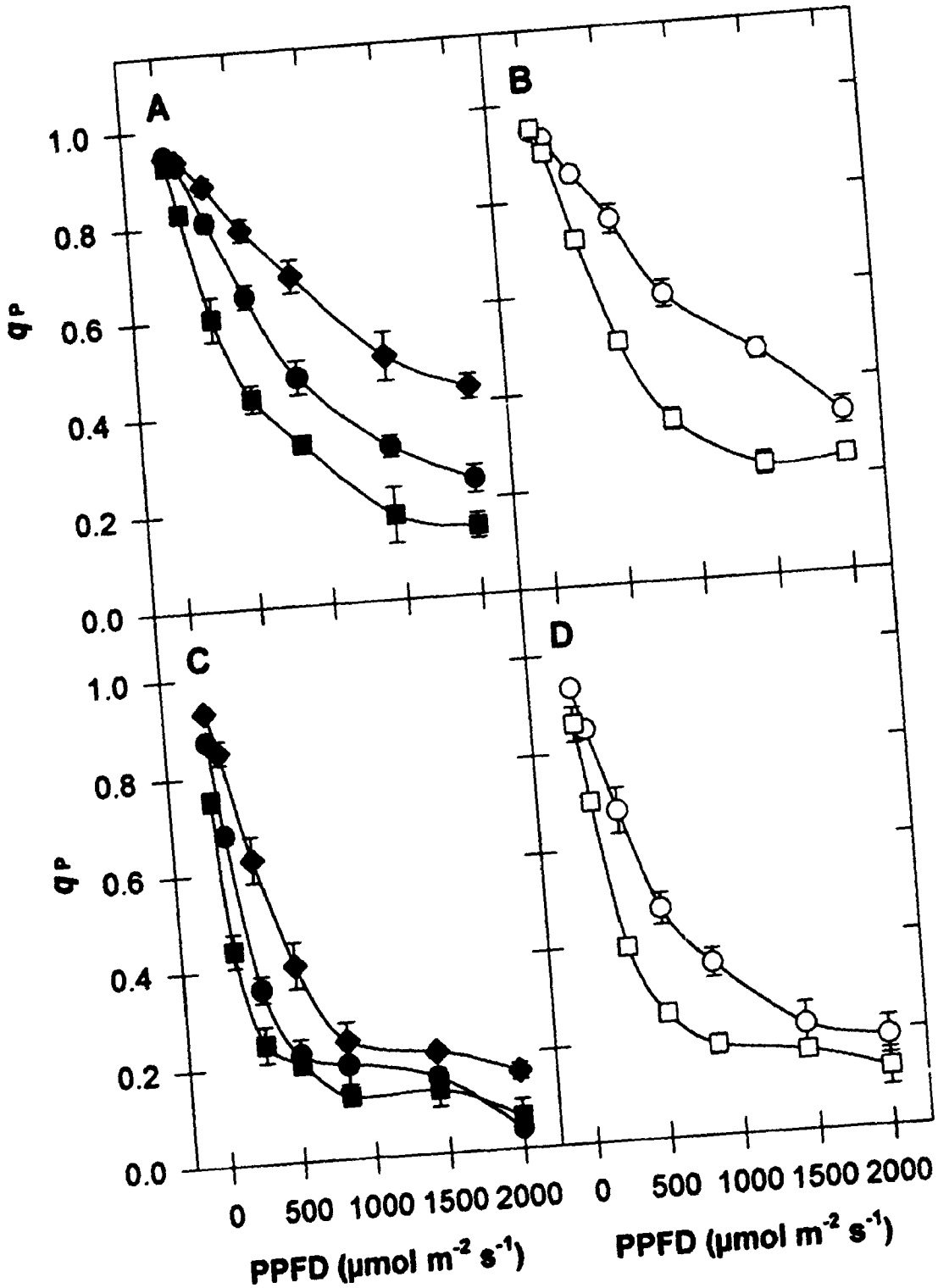
A
B
C
D
1.0
0.8
0.6
0.4
0.2
0.0
q_P
0
500
1000
1500
2000
PPFD (µmol m^{-2} s^{-1})

Figure 16. Light response curves for PSII RET rates in leaves of winter rye (*S. cereale* L. cv Musketeer). Development occurred at a temperature of 20°C (closed symbols) or 5°C (open symbols) with an irradiance of 800 (♦), 250 (●, ○) or 50 (■, □) μmol m^{-2} s^{-1}. Response was measured at 20°C (A and B) and 5°C (C and D). All values represent means ± SE; n = 3. When not present, error bars are smaller than symbol size.

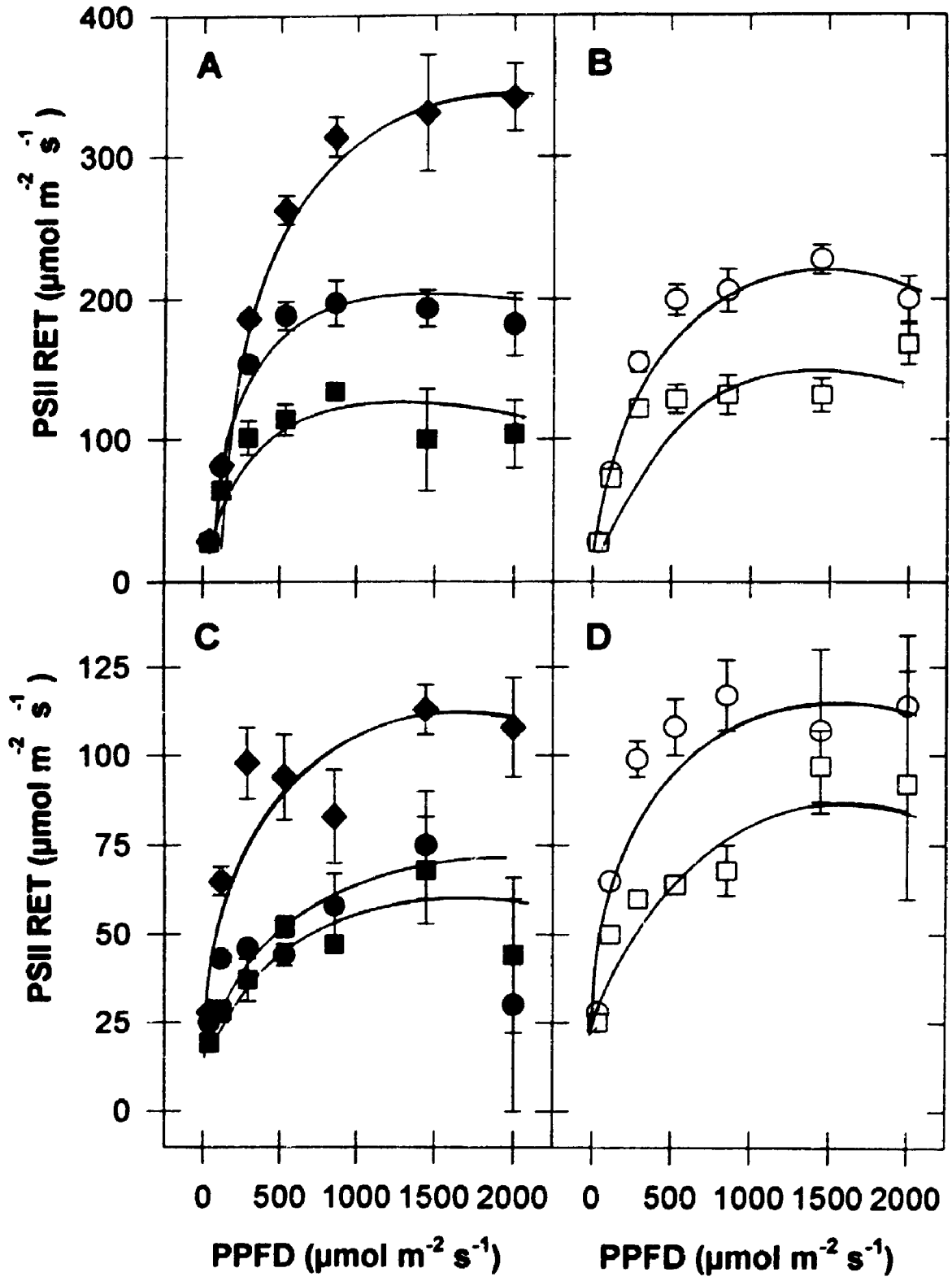
A
B
C
D
PSII RET (µmol m-2 s-1)
PSII RET (µmol m-2 s-1)
400
300
200
100
0
125
100
75
50
25
0
0 500 1000 1500 2000
0 500 1000 1500 2000
PPFD (µmol m-2 s-1)
PPFD (µmol m-2 s-1)

Figure 17. Measurements of intersystem electron pool size in leaves of winter rye (*S. cereale* L. cv Musketeer). A, Representative determination in leaves developed at the 20/800 growth regime. B, Similar determination in the presence of 1 mM DCMU. DCMU was introduced th.ough the transpiration stream at room temperature for 2 h with a PPFD of 5 µmol m^{-2} s^{-1}.

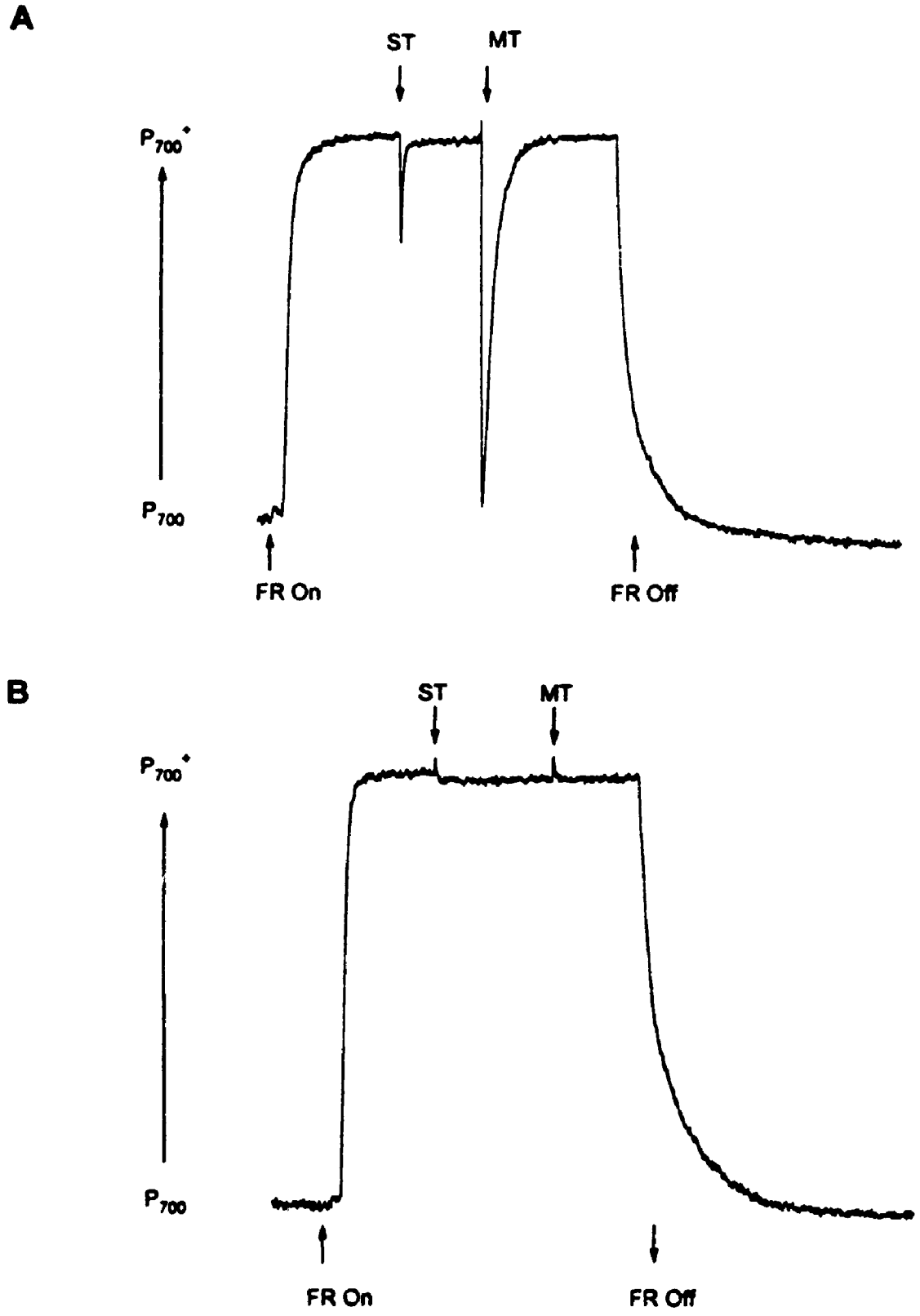
A
ST
MT
P_{700}^+
P_{700}
FR On
FR Off
B
ST
MT
P_{700}^+
P_{700}
FR On
FR Off

turnover of all PSII reaction centers while the MT flash saturates the PQ pool located between PSII and PSI. The electrons from PSII reach P_{700}^+ with a delay imposed by intersystem electron transport. The more electrons stored in the PQ pool, the longer the given FR light requires to re-oxidize P_{700} to P_{700}^+. However, in the presence of DCMU, an inhibitor of electron transport to PQ, both the ST and MT flashes do not cause a reduction of P_{700}^+ (Fig. 17B). DCMU binds to the Q_B site and inhibits electron transfer to the PQ pool, thus preventing electrons from reaching P_{700}^+. Therefore, the re-oxidation of P_{700} to P_{700}^+ observed in untreated leaves in the presence of FR light does indeed reflect the intersystem electron transport between PSII and PSI (Fig. 17A).

The data in Figure 18 indicate that plants grown at 20°C exhibit a 2.5-fold higher intersystem electron pool size with increasing growth irradiance from 50 to 800 μmol m^{-2} s^{-1}. Plants grown at 5°C also show this same trend upon increasing growth irradiance from 50 to 250 μmol m^{-2} s^{-1}, exhibiting a 2.2-fold increase in intersystem electron pool size. In addition, there is a high correlation ($r^2 = 0.83$) between intersystem electron pool size and $1\text{-}q_P$ (Fig. 19). Thus, on a P_{700} reaction center basis, plants grown at high PSII excitation pressure exhibit greater pools of intersystem electrons in comparison to plants grown at low excitation pressure.

3.3.4 Components of the Intersystem Electron Transport Chain

Immunological detection of specific polypeptides associated with the

Figure 18. Intersystem electron pool size in leaves of winter rye (*S. cereale* L. cv Musketeer) developed at the temperature/irradiance regimes indicated. Measurement occurred at 20°C. All values represent means ± SD; n = 3 to 6. When not present, error bars are smaller than symbol size.

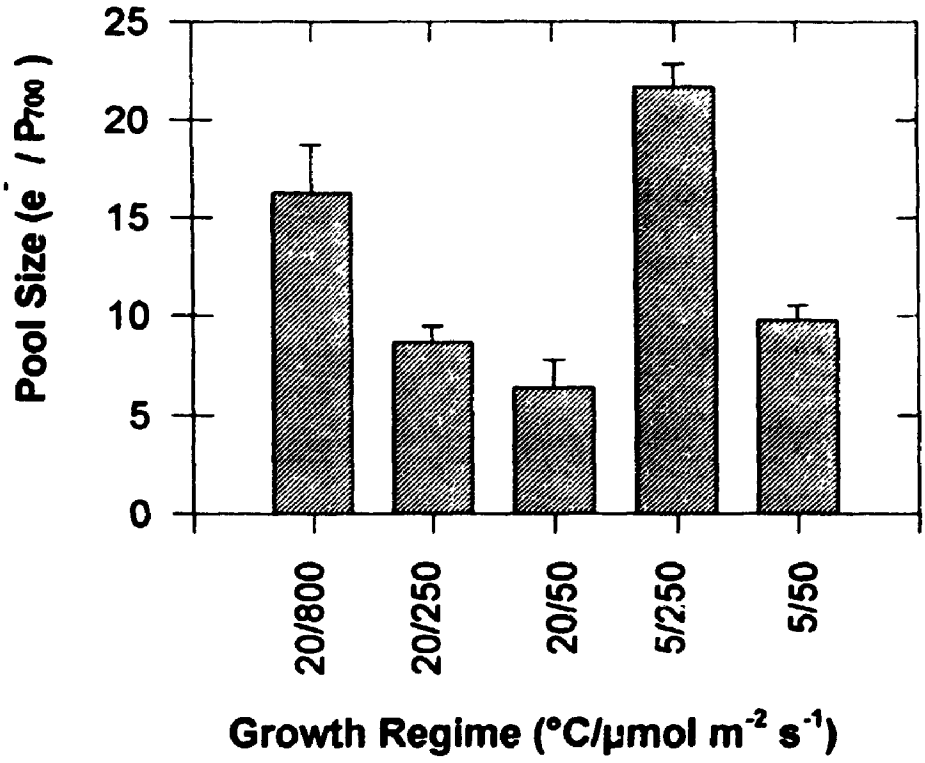
25
20
15
10
5
0
Pool Size (e^- / P_{700})
20/800
20/250
20/50
5/250
5/50
Growth Regime (°C/µmol m^{-2} s^{-1})

Figure 19. Correlation between intersystem electron pool size and 1-q_P in leaves of winter rye (*S. cereale* L. cv Musketeer). Development occurred at a temperature of 20°C (closed symbols) or 5°C (open symbols) with an irradiance of 800 (♦), 250 (●, ○) or 50 (■, □) µmol m^{-2} s^{-1}. 1-q_P was measured at the growth temperature and growth irradiance. All values represent means ± SE or SD; n = 3 to 6. When not present, error bars are smaller than symbol size. Regression analysis was performed in SigmaPlot® version 1.02 (Jandel Scientific, Corte Madera, CA USA).

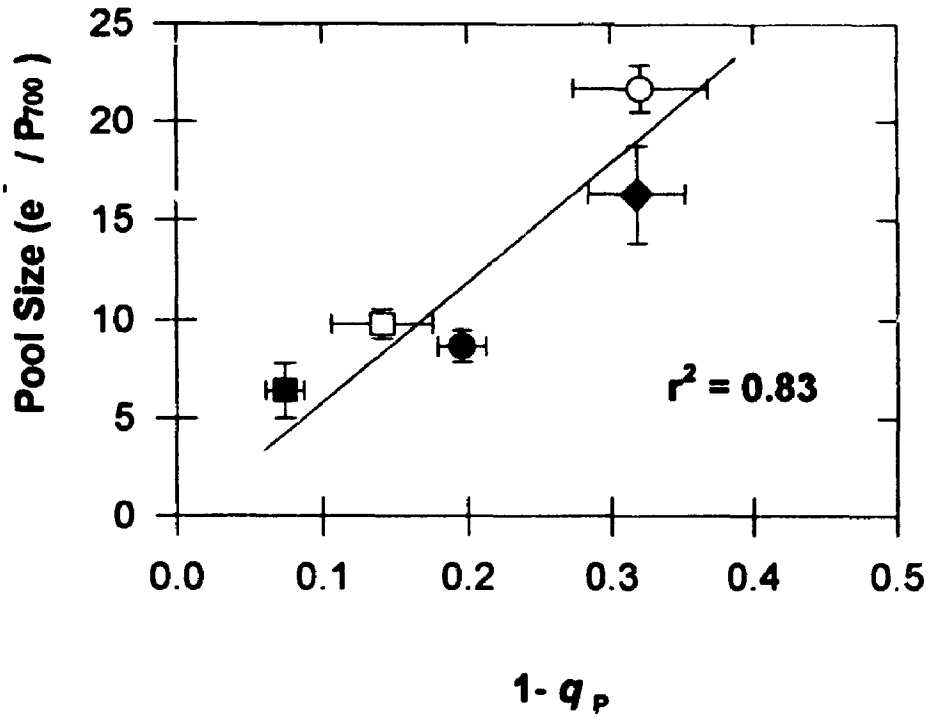
Pool Size (e^- / P_{700})
25
20
15
10
5
0
0.0
0.1
0.2
0.3
0.4
0.5
r^2 = 0.83
1- q_P

thylakoid membrane provides an estimate of the abundance of these components and the supramolecular complexes in which they are contained. The PSII reaction center D1 polypeptide, Cyt *f*, PSI reaction center heterodimer, plastocyanin and the β-subunit of the CF_1-ATPase complex were examined. The abundance of all of these polypeptides varied by less than 25% as determined by densitiometric scanning, irrespective of growth temperature or irradiance (Fig. 20). In contrast, PQA exhibited a 1.8 and 1.5-fold increase in leaves from plants grown at high PSII excitation pressure (20/800 or 5/250 respectively) in comparison to plants grown at low excitation pressure (20/250 and 5/50) (Table XVII).

3.4 Discussion

Growth of rye and wheat at 5/250 or 20/800 results in higher PSII excitation pressure in comparison to that of plants grown at 20/250. Thus, cold tolerant plants grown at low temperature and moderate irradiance (5/250) should be photosynthetically comparable to the same plants grown at high temperature and high light (20/800). The results for winter rye and winter wheat are consistent with this hypothesis. First, both winter cultivars, Musketeer and Monopol, grown at 5/250 or 20/800 exhibited comparable $PS_{max}O_2$ (Table XV and XVI). Second, winter rye grown at 5/250 was comparable to plants grown at 20/800 with respect to its capacity to keep Q_A oxidized as a function of irradiance when measured at either 20 or 5°C (Fig. 15). Third, the pool size of intersystem

Figure 20. Immunological detection of intersystem electron transport components in isolated thylakoid membranes of winter rye (*S. cereale* L. cv Musketeer) developed at the temperature/irradiance regimes indicated. Blots were performed at least twice and similar results obtained with each experiment. A, D1 polypeptide. B, Cyt *f*. C, PSI reaction center heterodimer. D, plastocyanin. E, β-subunit of the CF_1 ATP synthase.

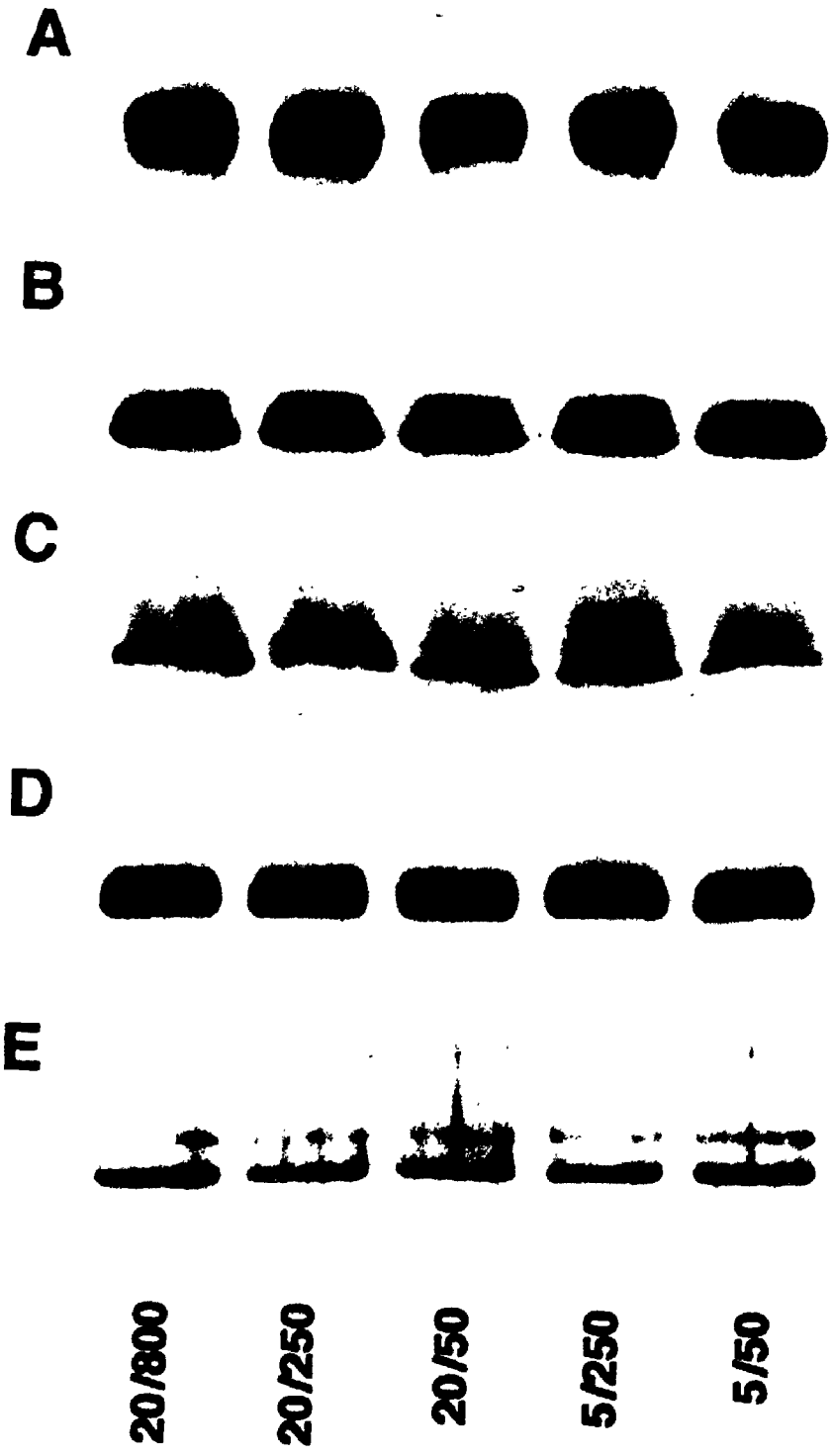
A
B
C
D
E
20/800
20/250
20/50
5/250
5/50

Table XVII. *PQA content in total leaf extracts of winter rye (S. cereale L. cv Musketeer).*

PQA was extracted, isolated by TLC and quantified spectrophotometrically according to Lichtenthaler (1969). Data are expressed on a leaf FW basis. All values represent means ± SD; $n = 3$.

Growth Regime (°C/µmol m^{-2} s^{-1})	PQA (µg g^{-1} FW)
20/800	60.5 ± 7.3
20/250	33.8 ± 7.0
20/50	37.5 ± 6.7
5/250	50.8 ± 3.8
5/50	31.8 ± 3.5

electrons on a P_{700} reaction center basis is similar in plants grown at 20/800 or 5/250 (Fig. 18). Fourth, the stoichiometry of the intersystem electron transport components is altered due to increases in PQA content in plants grown at high PSII excitation pressure (Fig. 20 and Table XVII).

Thus, the data presented in this chapter indicate that growth of winter rye and wheat at 5/250 or 20/800 appears to stimulate PS_{max} O_2 with a concomitant higher capacity to keep Q_A oxidized and modulate intersystem electron transport relative to plants grown at 20/250. However, this was correlated with the fact that winter rye and wheat grown at 5/250 were exposed to a high PSII excitation pressure, comparable to that of plants grown at 20/800. In contrast, Katepwa spring wheat decreases its PS_{max} upon growth at low temperature (5/250), but increases this same parameter under growth conditions of 20/800 in comparison to control plants grown at 20/250 (Table XVI). This occurs with minimal adjustment in photochemical efficiency as measured by F_V/F_M (Table XVI). However, it is not possible from the data presented to determine if increased excitation pressure as a result of low temperature (5/250) elicits the same response as increased excitation pressure due to increased irradiance (20/800) or whether this simply reflects a cultivar difference. Similar results have been reported for differential photosynthetic adjustment of CO_2 exchange involving spring and winter cultivars of wheat grown at low temperature (Hurry and Huner, 1991). The authors concluded that the site of low temperature inhibition of CO_2 exchange was not associated with PSII or the thylakoid membrane, and most

likely occurred at the level of photosynthetic carbon metabolism (Hurry and Huner, 1991).

Immunological examination of the membrane bound components of the intersystem chain indicate that absolute amounts of these polypeptides were not altered significantly as a result of growth at any of the temperature/irradiance regimes (Fig. 20). In addition, the abundance of the β-subunit of CF_1, used as a marker for the ATPase complex, and the mobile electron carrier plastocyanin also remain relatively constant regardless of growth temperature or irradiance (Fig. 20). However, this does not exclude changes in the functional properties of these components. In contrast, the lipophilic electron carrier PQA demonstrates a 1.5 to 1.8-fold increase in leaves from plants grown at high PSII excitation pressure (Table XVII) in comparison to plants grown at low PSII excitation pressure. This is the only component of the photosynthetic electron transport chain examined which presents significant changes. Thus, growth at high PSII excitation presssure (20/800 or 5/250) results in an altered stoichiometry of the components in the intersystem electron transport chain.

The stoichiometry of the intersystem carriers relative to P_{700} have been determined in spinach thylakoids to be six PQ, one Fe-S in the Cyt b_6/f complex, one Cyt *f* and two plastocyanin. This results in the maximum potential to store 16 electrons in the intersystem elecron transport chain (Grann and Ort, 1984; Whitmarsh and Ort, 1984). However, the determinations of intersystem electron pool size presented in this chapter in leaves of plants grown at both the high

excitation pressure regimes (20/800 or 5/250) result in values greater than this theoretical maximum (Fig. 18). This may be rationalized by examining the PQA data. If each PQ equates to two electrons, a two-fold increase in PQA would more than account for the observed increases in intersystem pool size. A 1.5 to 1.8-fold increase in PQA in leaves from plants grown at high PSII excitation pressure has been observed in this study (Table XVII) which is consistent with previous reports (Griffith et al., 1984; Krol and Huner, 1985). Thus, the increase in PQA content observed as a result of growth at high PSII excitation pressure most likely accounts for the increased intersystem electron pool size also observed upon growth at high PSII excitation pressure.

The mechanism by which Q_A is kept in the oxidized state at high PSII excitation pressure is still unclear. In part, increased PQA pool size resulting in greater intersystem electron pool size and overall greater rates of PS_{max} may be responsible. Alternatively, non-photocnemical mechanisms could play a role. The photosynthetic data presented in this chapter point towards a mechanism of regulation beyond PSII.

CHAPTER 4

PHOTOSYNTHETIC CARBON METABOLISM IN RESPONSE TO LOW TEMPERATURE

4.1 Introduction

Low temperature stress has been shown to inhibit starch and Suc biosynthesis differentially, resulting in the accumulation of soluble carbohydrates such as Fru, Glc, Suc and fructans (Steponkus and Lanphear, 1968; Pollock and Lloyd, 1987; Tognetti et al., 1990; Guy et al., 1992). In addition, the inhibition of Suc biosynthesis leads to restrictions in phosphate recycling and photophosphorylation (Sage and Sharkey, 1987; Labate and Leegood, 1988; Labate et al., 1990). This restriction in triose-P utilization may trigger feedback mechanisms that reduce rates of photosynthetic electron transport and limit ATP supply, resulting in reduced rates of CO_2 assimilation (Sharkey, 1990; Pammenter et al., 1993). In contrast, cold acclimation results in increased rates of CO_2 assimilation which have been associated with increases in activities of the enzymes of carbon metabolism (Guy et al., 1992; Holaday et al., 1992; Hurry et al., 1994, 1995a, 1995b). However, this adjustment in CO_2 assimilation is cultivar and species dependent (Tognetti et al., 1990; Holaday et al., 1992). It has been established that cold acclimated winter, but not spring cultivars, are able to adjust CO_2 assimilation to rates equal to or greater than control rates (Huner et al., 1986; Huner et al., 1993; Hurry et al., 1994, 1995a, 1995b). Huner

et al. (1993) suggested that this occurs due to the ability of the winter cultivar to overcome the potential restrictions of triose-P utilization imposed by growth at low temperature. A simplified scheme of carbon metabolism is presented in Figure 21.

The results in the previous chapter indicated that the photosynthetic capacity of Katepwa spring wheat was depressed upon growth at low temperature compared to Monopol winter wheat. Based on these data, I hypothesized that the winter cultivar should exhibit no restrictions in photosynthesis, while the spring cultivar should demonstrate reduced rates of CO_2 assimilation and electron transport due to restrictions in triose-P utilization. However, low temperature stressed winter and spring cultivars, imposed by a shift to low temperature, should both exhibit limitations in photosynthesis. To test this hypothesis, I have examined CO_2 assimilation, electron transport, carbohydrate accumulation, metabolite pool sizes, and four important regulatory enzymes of carbon metabolism in both winter and spring cultivars of wheat grown at low temperature (5/250) and shifted to low temperature (20/250 → 5/250). In addition, I have also examined the effects of PSII excitation pressure by examining plants grown at non-hardening temperatures and high light (20/800).

4.2 Materials and Methods

4.2.1 Plant Material and Growth Conditions

Figure 21. Simplified scheme of carbon flux in the chloroplast and cytosol. Photosynthetic enzymes examined in this thesis are italicized.

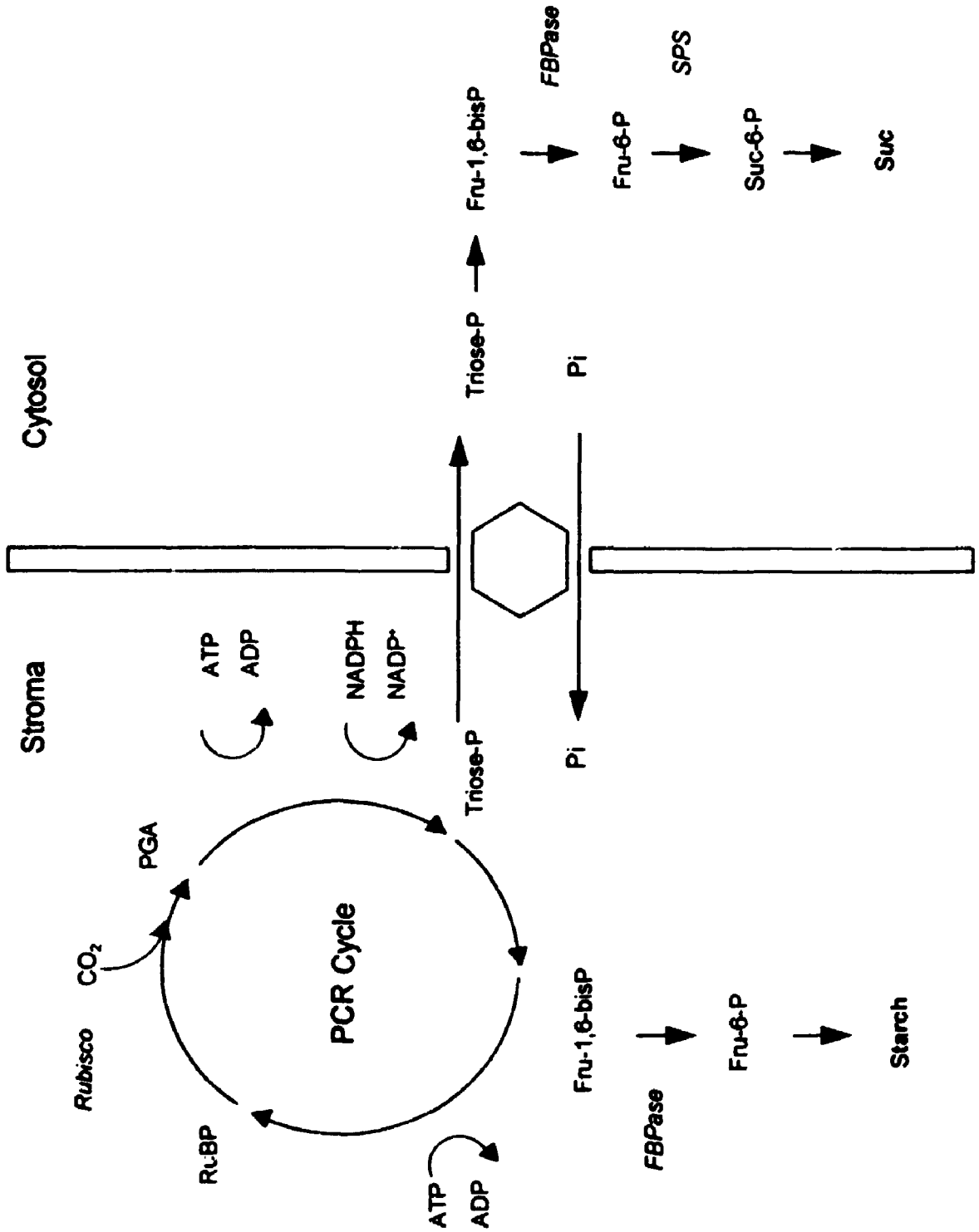
Cytosol
Stroma
Triose-P
Pi
Fru-1,6-bisP
FBPase
Fru-6-P
SPS
Suc-6-P
Suc
ATP
ADP
NADPH
NADP+
Triose-P
Pi
PGA
CO2
Rubisco
PCR Cycle
RuBP
ATP
ADP
Fru-1,6-bisP
FBPase
Fru-6-P
Starch

Winter wheat (*T. aestivum* L. cv Monopol) and spring wheat (*T. aestivum* L. cv Katepwa) were germinated from seed in coarse vermiculite in 7 cm plastic pots at a temperature of 20/16°C (day/night) with a 16 h photoperiod and a PPFD of 250 µmol $m^{-2} s^{-1}$ (20/250) essentially as described in section 2.2.1. After 7 d, when the primary leaf had fully expanded, some of the winter and spring wheat seedlings were shifted to growth conditions of 20°C with a PPFD of 800 µmol $m^{-2} s^{-1}$ (20/800), whereas other seedlings were transferred to temperature regime of 5/5°C (day/night) with a PPFD of 250 µmol $m^{-2} s^{-1}$ (5/250) for cold acclimation. The photoperiod was unchanged and control plants remained at the 20/250 growth regime. When the third and fourth leaves were fully expanded, some 20/250 control plants were transferred for 12 h to the 5/250 growth regime and designated as low temperature stressed plants (20/250 → 5/250). All measurements were made on fully expanded fourth leaves of 75 d old cold acclimated and 25 d old control plants. At these stages, seedlings were considered to be of similar developmental age based on previous growth kinetic analyses (Hurry and Huner, 1991).

4.2.2 PSII Excitation Pressure

Photosystem II excitation pressure ($1-q_P$) was calculated from Chl *a* steady-state fluorescence parameters at the growth temperature and irradiance as described in section 2.2.3.

4.2.3 PSII RET

Steady-state Chl *a* fluorescence parameters were determined as described in section 2.2.3. PSII RET rates were calculated as described in section 3.2.3.

4.2.4 Gas Exchange Measurements

Photosynthetic CO_2 assimilation rates were measured on attached leaves using an open gas exchange system using a IR CO_2/H_2O analyzer (model 6262; Li-Cor). The relative humidity of the air stream was maintained at 50% and gas mixtures were created by mixing N_2, O_2 and 5% CO_2 using flow controllers (Omega Engineering Inc.). CO_2 exchange rates were measured at a $p(CO_2)$ of 35 Pa and a $p(O_2)$ of 20 kPa. The temperature of the aluminum chamber was maintain at either 20 or 5°C by the use of a Neslab refrigerated circulating water bath (model LT50-DD; Neslab Instruments Inc.) and a Hansatech light source (model LS2H) controlled by a light source control box (model LS2; Hansatech) provided a PPFD of PPFD of 250 µmol $m^{-2} s^{-1}$. Shifted plants which were grown at 20°C but measured at 5°C were equilibrated at the measurement temperature during the regular 8 h dark period prior to measurement of CO_2 exchange to ensure that the entire plant was equilibrated to the measurement temperature. In addition, gas exchange measurements were made 4 h after the beginning of the photoperiod. Thus, temperature shifted plants were equilibrated at the measurement temperature for a total 12 h prior to measurement of CO_2

exchange. Calculations of gas-exchange parameters were made using the equations of von Caemmerer and Farquhar (1981). Rates of carboxylation (v_C) and oxygenation (v_O) were calculated according to Di Marco et al. (1994) by combining the following equations;

$$P_N + R_D = v_C - 0.5v_O \qquad J_t = 4v_C + 6v_O$$

Where P_N is the rate of CO_2 assimilation, R_D is the rate of mitochondrial respiration and J_t is the PSII RET calculated from Chl *a* fluorescence parameters (Schreiber et al., 1994). For this calculation it is assumed that alternative reductions are negligible and that 4 and 6 electrons are needed for the reduction of one molecule of CO_2 and O_2 respectively (DiMarco et al., 1994).

4.2.5 Carbohydrate Determinations

Starch, Glc, Fru and Suc contents were measured according to Rufty and Huber (1983). Leaves were harvested 4 h into the photoperiod and extracted in hot 80% (v/v) ethanol until the tissue was pigment-free. The sample was ground with a mortar and pestle and particulates, including starch, were pelleted by centrifugation at 16,000*g* for 2 min at 5°C. The pellet was washed twice with ddH_2O, suspended in 1 mL of 0.2 N KOH and incubated in a boiling water bath for 30 min. After cooling, the pH of the mixture was adjusted to pH 5.5 by adding 200 µL of 1 N acetic acid. For starch digestion, 1 mL of dialysed amyloglucosidase solution (35 units mL^{-1} in 50 mM sodium acetate buffer (pH 4.5) from *Aspergillus niger*, Sigma) was added and the sample incubated at

55°C for 30 min. The samples were then incubated in a boiling water for 1 min and centrifuged at 16,000*g* for 2 min at 5°C. Glc in the supernatant was analyzed enzymically as described below. The water phase was dried at 30°C and the residue suspended in 400 µL ddH_2O. An aliquot of this fraction was used for the determination of Glc, Fru and Suc in an assay buffer containing 360 mM Tris-HCl (pH 6.9), 0.4 mM NADP, 1 mM ATP, 5 mM $MgCl_2$, 1 mM DTT and 0.02% (w/v) BSA. In addition, the reaction mixture contained for the Glc assay, 1 unit hexokinase; for the Fru assay, 1 unit hexokinase and 5 units PGI; for the Suc assay, 80 units invertase in addition to the Fru reaction mixture. The reaction was started by adding 2 units of Glc-6-PDH. The reduction of NADP was monitored at A_{340}. Starch, Fru and Suc were measured in Glc equivalents.

4.2.6 Metabolite Determinations

For all determinations, the mid-portion of fully expanded third and fourth leaves were harvested 4 h into the photoperiod in the growth chamber at the prevailing growth conditions and immediately frozen in liquid N_2 for subsequent analyses. Prior to performing assays, frozen leaf tissue was ground in a pre-chilled mortar and pestle with the addition of 1 mL 3.5% (v/v) $HClO_4$ during grinding. After thawing and centrifugation at 16,000*g* for 2 min at 5°C, the supernatant was neutralized using 2 N KOH with 0.15 M Hepes and 10 mM KCl. This solution was centrifuged again and the precipitate was discarded. The supernatant was used for an enzyme-linked spectrophotometric assay of

metabolites (Lowry and Possonneau, 1976) as described by Loreto and Sharkey (1993). For all assays the oxidation of NADH or reduction of NADP was monitored as the difference between A_{334} and A_{405} or A_{340} respectively.

4.2.6.1 Glc-6-P, Fru-6-P and Adenylates

Glc-6-P, Fru-6-P and ATP levels were determined using a buffer of 100 mM Tris (pH 8.1), 5 mM $MgCl_2$, 1 mM EDTA, 0.4 mM NADP and 1 mM Glc. The reaction was started by adding 1 unit of Glc-6-PDH to measure Glc-6-P. When the reaction was complete, the amount of Fru-6-P was measured by adding 2.5 units of PGI. After the changes in absorbance were negligible, 1.5 units of hexokinase were added to measure ATP content.

ADP content was determined in a buffer consisting of 50 mM Hepes (pH 7.0), 4 mM $MgCl_2$, 150 mM KCl, 0.1 mM NADH and 0.3 mM phosphoenolpyruvate. The reaction was started by adding 2 units of pyruvate kinase and 2 units of lactic dehydrogenase.

4.2.6.2 Fru-1,6-bisP and Triose-P

Triose-P and Fru-1,6-bisP were measured in a buffer containing 50 mM Hepes (pH 7.1), 20 mM NaCl, 2 mM $MgCl_2$, 0.12 mM NADH, 7 mM ATP. To start the reaction for triose-P, 2 units of glycerophosphate dehydrogenase and 5 units of triose-P isomerase were added. At the end of this reaction, 2 units of aldolase was added to measure the amount of Fru-1,6-bisP.

4.2.7 Enzyme Extractions and Assays

For all assays, the mid-portion of fully expanded third and fourth leaves were harvested 4 h into the photoperiod in the growth chamber at the prevailing growth conditions and immediately frozen in liquid N_2 for subsequent analyses. Prior to performing assays, leaf tissue was ground in a Ten-Broeck glass homogenizer with the appropriate extraction buffer. Spectrophotometric enzyme assays were conducted at 25°C using a Shimadzu recording spectrophotometer (model UV-160).

4.2.7.1 Rubisco

Rubisco activity was determined according to Sharkey et al. (1991a) in 2 mL of an extraction buffer containing 100 mM Bicine (pH 7.8), 5 mM $MgCl_2$, 1mM EDTA, 5 mM DTT, 1.5% (w/v) PVPP and 0.02% (w/v) BSA. The extract was centrifuged at 16,000*g* for 2 min at 5°C and 5 µL of the supernatant was immediately used to determine initial Rubisco activity. The total Rubisco activity was determined after the preincubation of 1 mL of extract for 10 min with 20 mM $MgCl_2$ and 10 mM $NaHCO_3$ (final concentration). The carbamylation ratio of Rubisco was calculated as initial Rubisco activity/total Rubisco activity. Rubisco activity was determined in an assay buffer containing 50 mM Bicine (pH 8.0), 15 mM $MgCl_2$, 1 mM EDTA, 10 mM NaCl, 5 mM DTT, 10 mM $NaHCO_3$, 5 mM phosphocreatine and 5 mM ATP in a final volume of 750 µL. The following were

also added; 10 µL of 20 mM RuBP, 10 µL of 10 mM NADH, 10 units of GAPDH/3-PGK and 2 units of creatine phosphokinase. The reaction was initiated by the addition of 5 µL of appropriate extract and the oxidation of NADH monitored as the difference between A_{334} and A_{405}.

Total Rubisco protein was determined by using CABP to inhibit partially Rubisco activity in the leaf extract. A 100 µL aliquot of the extract, preincubated with CO_2 and Mg^{2+} was mixed with 2 to 10 µL of 27 mM CABP and the solution incubated on ice for 5 min. A 5 µL aliquot of this solution was used to determine Rubisco activity. Rubisco activity was plotted against CABP concentration to determine the concentration of CABP corresponding to zero activity. This extrapolation gives the total number of Rubisco sites to which CABP was bound. This is divided by eight (eight sites per Rubisco enzyme) to give the total amount of Rubisco protein.

4.2.7.2 SPS

SPS was assayed according to Vassey and Sharkey (1989). Leaf tissue was homogenized in 1.5 mL of an extraction buffer containing 50 mM Hepes-NaOH (pH 7.5), 5 mM $MgCl_2$, 1 mM EDTA, 2.5 mM of freshly added DTT and 0.1% (v/v) Triton X-100. The extract was centrifuged at 16,000*g* for 2 min at 5°C and the supernatant desalted by centrifugal filtration on a cold Sephadex G-25 (Sigma) column equilibrated with extraction buffer minus the Triton X-100. SPS activity was assayed under saturating substrate concentrations in the

absence of Pi (V_{max} assay) as the time dependent formation of Suc plus Suc-P from UDP-Glc and Fru-6-P. In the V_{max} assay, 45 µL of tissue extract was incubated at room temperature with 10 mM UDP-Glc, 10 mM Fru-6-P, 40 mM Glc-6-P, 50 mM Hepes-NaOH (pH 7.5), 15 mM $MgCl_2$ and 2.5 mM DTT in a total volume of 70 µL. Reactions were terminated at 1 and 11 min by adding 70 µL of 30% (w/v) KOH and the tubes were placed in a boiling water bath for 10 min. After cooling to room temperature, 1 mL of 0.14% (w/v) anthrone in 13.8 N H_2SO_4 was added, and the tubes incubated at 40°C for 20 min prior to measuring A_{620} as described by Huber et al. (1991). These values were then interpolated from a Suc standard curve and SPS activity determined.

4.2.7.3 FBPase

FBPase was assayed according to the procedure of Sharkey et al. (1991b) using 1.5 mL of an extraction buffer containing 20 mM Hepes-NaOH (pH 7.5), 125 mM NaCl, 0.5 mM EDTA, 0.02% (w/v) BSA and 2% (w/v) PVPP. The extract was centrifuged at 16,000*g* for 2 min at 5°C an the supernatant used for the determination of stromal and cytosolic FBPase activity. Cytosolic FBPase activity was determined in an assay buffer containing 100 mM Hepes-NaOH (pH 7.5), 100 mM KCl, 4 mM $MgCl_2$, 0.5 mM EDTA, 0.5 mM NADP, 2 units of PGI and 1 unit of G-6-PDH. The reaction was initiated by the addition of 50 µM Fru-1,6-bisP. Stromal FBPase activity was measured in an assay buffer containing 100 mM Bicine (pH 8.8), 0.5 mM EDTA, 50 mM DTT, 0.5 mM NADP, 2 units of

PGI and 1 unit of G-6-PDH. The reaction was initiated by the addition of 0.4 mM Fru-1,6-bisP and 10 mM $MgCi_2$. The reduction of NADP was monitored at A_{340} and the FBPase rates were determined 5 min after the start of the reaction.

4.3 Results

4.3.1 CO_2 Assimilation Rate and Rubisco

Growth at 20/800 (high PSII excitation pressure) resulted in 1.4 and 1.3-fold increases in CO_2 assimilation, concomitant with a 1.7 and 2-fold increase in electron transport compared to the 20/250 controls in both the winter and spring cultivars respectively (Table XVIII). In contrast, growth at low temperature (5/250), also high PSII excitation pressure, in the spring cultivar resulted in 31 and 67% decreases in CO_2 assimilation and electron transport rates respectively (Table XVIII). However, while electron transport decreased by 69% in the winter cultivar upon growth at 5/250, minimal changes were observed in the CO_2 assimilation rate in comparison to growth at 20/250 (Table XVIII). Both the winter and spring wheat cultivars decreased their rates of CO_2 assimilation and electron transport by 21 and 36% and 78 and 75% respectively upon a temperature shift (20/250 → 5/250) (Table XVIII).

Spring wheat, as a result of growth at 20/800, did not change Rubisco parameters relative to the 20/250 plants (Table XIX). In contrast, winter wheat exhibited a 20% decrease in total amount and total activity of Rubisco and a 50% decrease in the Rubisco carbamylation ratio (Table XIX). Upon growth at

Table XVIII. *Photosynthetic CO_2 assimilation and PSII RET rates in leaves of winter wheat (T. aestivum L. cv Monopol) and spring wheat (T. aestivum L. cv Katepwa).*

CO_2 assimilation and PSII RET rates were determined at the growth temperature and growth irradiance. The arrow (→) represents a shift to the growth regime indicated for a 12 h period prior to measurement. Values represent means ± SE; *n* = 3 to 6.

Growth Regime (°C/μmol m^{-2} s^{-1})	CO_2 Assimilation (μmol m^{-2} s^{-1})	PSII RET
	Monopol	
20/800	15.7 ± 0.6	247.2 ± 35.3
20/250	11.6 ± 1.0	149.1 ± 0.1
5/250	12.5 ± 0.7	46.2 ± 0.3
20/250 → 5/250	9.2 ± 0.5	32.9 ± 2.66
	Katepwa	
20/800	16.6 ± 1.0	273.7 ± 33.8
20/250	12.8 ± 0.9	140.9 ± 9.6
5/250	8.8 ± 0.5	46.5 ± 2.9
20/250 → 5/250	8.2 ± 0.2	35.60 ± 8.4

Table XIX. *Temperature and irradiance responses of Rubisco in total leaf extracts of winter wheat (T. aestivum L. cv Monopol) and spring wheat (T. aestivum L. cv Katepwa).*

Velocities of Rubisco oxygenation to carboxylation (v_O / v_C) were calculated from gas exchange data measured at the growth temperature and growth irradiance (DiMarco et al., 1994). All other data were obtained spectrophotometrically at 25°C (Sharkey et al., 1991b). Where indicated, values represent means ± SE; n = 3 to 6.

Growth Regime (°C/µmol m^{-2} s^{-1})	Total Activity (µmol m^{-2} s^{-1})	Total Amount (µmol m^{-2})	Carbamylation Ratio (%)	v_O / v_C (µmol m^{-2} s^{-1})
		Monopol		
20/800	52.5 ± 2.2	2.6 ± 0.2	32	0.90
20/250	65.8 ± 4.8	3.2 ± 0.3	61	0.78
5/250	74.7 ± 7.2	4.3 ± 0.2	75	0.34
		Katepwa		
20/800	60.7 ± 4.1	2.8 ± 0.3	51	1.02
20/250	62.8 ± 3.7	3.2 ± 0.3	55	0.63
5/250	72.5 ± 4.4	4.6 ± 0.5	83	0.57

5/250, both wheat cultivars demonstrated a 15% increase in total Rubisco activity, a 30 to 40% increase in total amount of Rubisco protein, and a 20 to 50% increase in carbamylation ratio of Rubisco when compared to the same plants grown at 20/250 (Table XIX). However, growth at 20/800 resulted in 1.2 and 1.6-fold increases in the ratio of v_O/v_C in the winter and spring cultivars respectively. In addition, the winter cultivar exhibited a 56% decrease in the ratio of v_O/v_C in comparison to only a 10% decrease observed in the spring cultivar under 5/250 growth conditions (Table XIX). Thus, winter wheat appears to have a reduced capacity for photorespiration based upon rates of oxygenation and carboxylation as a result of growth at low temperature in comparison to the spring cultivar.

4.3.2 Enzyme Activities and Metabolite Pool Sizes

Suc:starch ratios increased 3 to 5-fold and 15 to 17-fold as a result of growth at high PSII excitation pressure in the winter and spring cultivars respectively (Table XX). In addition, growth at 5/250 resulted in a 3-fold increase in SPS activity in the winter cultivar, Monopol, but did not affect the SPS activity in the spring cultivar, Katepwa (Table XXI). Growth at 20/800 resulted in 1.3-fold increases in SPS activity in comparison to the 20/250 control plants (Table XXI). Thus, winter wheat appears to exhibit a specific, differential stimulation of SPS activity in response to growth at 5/250.

Glu-6-P:Fru-6-P ratios decreased by 38% upon growth at high PSII

Table XX. *Soluble and insoluble carbohydrates and photosynthetic metabolites in total leaf extracts of winter wheat (T. aestivum L. cv Monopol) and spring wheat (T. aestivum L. cv Katepwa).*

Data were obtained spectrophotometrically (Rufty and Huber, 1983; Loretto and Sharkey, 1993) and reflect total pool sizes. Where indicated, values represent means ± SE; n = 3 to 6.

Growth Regime (°C/µmol m^{-2} s^{-1})	Suc:Starch (w/w)	Glc-6-P:Fru-6-P (mol/mol)	Fru-1,6-bisP:Fru-6-P (mol/mol)	Triose-P (µmol m^{-2} s^{-1})	ATP:ADP (mol/mol)
			Monopol		
20/800	2.2	0.8	0.38	20.0 ± 2.0	1.6
20/250	0.6	1.3	0.30	12.0 ± 3.0	2.9
5/250	3.0	0.8	0.41	25.0 ± 3.0	1.4
			Katepwa		
20/800	3.0	0.8	0.55	18.0 ± 2.0	1.8
20/250	0.2	1.3	0.28	10.0 ± 1.0	3.5
5/250	3.3	0.7	0.37	17.0 ± 3.0	1.5

Table XXI. *Temperature and irradiance responses of SPS in total leaf extracts of winter wheat (T. aestivum L. cv Monopol) and spring wheat (T. aestivum L. cv Katepwa).*

SPS activity was determined spectrophotometrically using the V_{max} assay performed at 25°C (Vassey and Sharkey, 1989; Huber et al., 1991). All values represent means ± SE; n = 3 to 6.

Growth Regime (°C/µmol m^{-2} s^{-1})	Activation State (%)	Activity (µmol m^{-2} s^{-1})
	Monopol	
20/800	36	2.0 ± 0.2
20/250	22	1.6 ± 0.1
5/250	66	5.0 ± 1.0
	Katepwa	
20/800	27	2.0 ± 0.1
20/250	25	1.6 ± 0.2
5/250	55	1.6 ± 0.1

excitation pressure (20/800 or 5/250), indicating a restriction in the conversion of Fru-6-P to Glu 6-P (Table XX). However, this restriction was similar in both cultivars. In contrast, Fru-1,6-bisP:Fru-6-P ratios in winter and spring cultivars exhibited 1.3 to 2-fold increases as a result of growth at either 20/800 or 5/250 (Table XX). In addition, growth of both Monopol and Katepwa at 5/250 resulted in stromal and cytosolic FBPase activities which increased 1.3 and 1.4 to 1.7-fold respectively, in comparison to the same plants grown at 20/250 (Table XXII). Growth at 20/800 also resulted in stromal and cytosolic FBPase activities which demonstrated a 1.1 to 1.5 and 1.2 to 2.3-fold increase in comparison to growth at 20/250 in the winter and spring cultivars respectively (Table XXII). Triose-P pools in the winter and spring cultivars exhibited 1.7 to 2.1-fold increases due to growth at high PSII excitation pressure, indicative of decreased triose-P utilization (Table XX). This presumably induced feedback mechanisms on photosynthesis and subsequently resulted in a 45 to 57% decrease in ATP:ADP ratios for both winter and spring cultivars (Table XX).

4.4 Discussion

Exposure to low temperatures results in a feedback limited restriction of photosynthesis due to a decrease in triose-P utilization and limited Pi availability (Sage and Sharkey, 1987; Labate and Leegood, 1988). However, it has been suggested that growth of winter cultivars at low temperatures alleviates the effects of feedback limited photosynthesis, resulting in increased photosynthetic

Table XXII. *Temperature and irradiance responses of FBPase in total leaf extracts of winter wheat (T. aestivum L. cv Monopol) and spring wheat (T. aestivum L. cv Katepwa).*

FBPase activity was determined spectrophotometrically at 25°C (Sharkey et al., 1991b). All values represent means ± SE; n = 3 to 6.

Growth Regime (°C/µmol m^{-2} s^{-1})	FBPase Stromal	FBPase Cytosolic
	Activity (µmol m^{-2} s^{-1})	
	Monopol	
20/800	10.4 ± 0.3	2.2 ± 0.1
20/250	9.1 ± 0.8	1.5 ± 0.1
5/250	11.6 ± 0.6	1.9 ± 0.1
	Katepwa	
20/800	11.4 ± 0.7	3.0 ± 0.3
20/250	9.3 ± 0.9	1.3 ± 0.2
5/250	12.8 ± 0.7	2.2 ± 0.2

capacity (Huner et al., 1993). The data presented in this chapter indicate that growth at 5/250 for spring wheat results in an inhibition of CO_2 assimilation, while growth under the same conditions in the winter cultivar results in CO_2 assimilation rates comparable to that of 20/250 grown controls (Table XVIII). These observations are consistent with previous reports (Hurry and Huner, 1991; Hurry et al., 1994, 1995a, 1995b). Furthermore, this appears to be strictly a low temperature phenomenon, as the same response was absent in winter and spring cultivars grown at high excitation pressure created by growth at high light (20/800). In addition, low temperature stress, created by a shift from 20/250 to 5/250 resulted in a similar decrease in CO_2 assimilation and electron transport for both winter and spring wheat cultivars (Table XVIII). It has been suggested previously that the site of this low temperature inhibition of CO_2 exchange in spring cultivars is at the level of photosynthetic carbon metabolism (Hurry and Huner, 1991; Hurry et al., 1995a). However, the only differences observed based on the data presented in this chapter that could account for the increased CO_2 assimilation in the winter cultivar are a decrease in the ratio of v_O/v_C, reflecting reduced photorespiration and an increase in SPS activity, reflecting stimulation of Suc biosynthesis (Table XIX and XXI). Despite the fact that high CO_2 assimilation rates were maintained in winter cultivars grown at 5/250, concomitant with a stimulation of the Suc biosynthetic pathway and reduced photorespiratory capacity, these plants still exhibit a restriction at the level of triose-P utilization as demonstrated by the decreased Glu-6-P:Fru-6-P and

ATP:ADP ratios, increased Fru-1,6-bisP:Fru-6-P ratio and the accumulation of triose-P (Table XX). Thus, decreases in capacity for photorespiration as determined from the ratio of v_O/v_C and stimulation of Suc biosynthesis in the winter cultivar cannot alleviate the restrictions at the level of triose-P utilization. Furthermore, both cultivars exhibited comparable decreases in electron transport while presenting a differential response in rates of CO_2 assimilation (Table XVIII). Thus, growth at 5/250 stimulates feedback limited photosynthesis in both spring and winter cultivars of wheat at the level of electron transport which is not evident at the level of CO_2 assimilation. The means by which winter cultivars maintain high CO_2 assimilation rates under conditions where photosynthetic electron transport is limited remains to be fully elucidated. However, the decreases in capacity for photorespiration and stimulation of Suc biosynthesis in the winter cultivar will increase the flux of carbon through the PCR cycle which may play a role in maintaining high CO_2 assimilation.

CHAPTER 5

PHOTOINHIBITORY RESPONSES IN RELATION TO PSII EXCITATION PRESSURE

5.1 Introduction

Photoinhibition has been typically defined as a light-dependent decrease in photosynthetic efficiency (F_V/F_M, ΦO_2 or ΦCO_2) which may or may not be associated with a decrease in PS_{max} as a result of the absorption light energy in excess of that required for CO_2 assimilation (Powles, 1984; Krause, 1988; Chow, 1994; Krause, 1994a; Osmond, 1994). It was first proposed by Ögren (1991) and subsequently supported by Öquist et al. (1992a, 1992b) that photoinhibition was related to the redox state of PSII. Further, susceptibility to photoinhibition has also been shown to be correlated to the redox state of PSII, regardless of the environmental constraints on photosynthesis brought about by low temperature or light acclimation (Öquist et al., 1992a, 1992b, 1993b; Park et al., 1996b).

NPQ is thought to play an important role in susceptibility to photoinhibition by dissipating excess excitation energy as heat (Krause and Weis, 1991; Gilmore et al., 1995; Ruban and Horton, 1995; Demmig-Adams et al., 1996; Park et al., 1996b). In addition, the development of NPQ is thought to be mediated by the xanthophyll carotenoids Zx and Ax (Demmig-Adams, 1990; Gilmore and Yamamoto, 1993; Pfündel and Bilger, 1994; Demmig-Adams and Adams, 1996).

Tolerance to photoinhibition is usually associated with the pre-exposure of plants or algae to high (>700 µmol m^{-2} s^{-1}) irradiance (Powles, 1984; Anderson and Osmond, 1987; Öquist et al., 1992a; Aro et al., 1993a; Osmond, 1994; Baroli and Melis, 1996; Park et al., 1996a, 1996b). However, winter cultivars of rye (*S. cereale*), wheat (*T. aestivum*), the herbaceous dicot spinach (*Spinacia oleracea*) and the green alga *Chlorella vulgaris* grown at low temperature also exhibit an increased tolerance to photoinhibition (Somersalo and Krause, 1989; Öquist and Huner, 1991; Boese and Huner, 1992; Hurry and Huner, 1992; Maxwell et al., 1995a). The latter situation is unique in that plants grown at low temperature are exposed to only moderate irradiance (250 µmol m^{-2} s^{-1}) but exhibit tolerance to light stress 5 to 7 times higher than the growth irradiance (Huner et al., 1993).

It has been demonstrated previously that the growth of winter cereals at low temperature results in an increased capacity to keep Q_A oxidized under photoinhibitory conditions (Öquist and Huner, 1993; Öquist et al., 1993b). In addition, winter cereals grown at 5°C modulate their rates of photosynthesis so as to increase $PS_{max}O_2$ (Huner et al., 1993). This in turn, is thought to account, in part, for the differential tolerance to photoinhibition observed between 5 and 20°C grown plants (Öquist and Huner, 1993; Öquist et al., 1993b).

In this chapter I test the hypothesis that tolerance to photoinhibition is a result of photosynthetic adjustment to high PSII excitation pressure and not due to low temperature growth *per se*.

5.2 Materials and Methods

5.2.1 Plant Material and Growth Conditions

Winter rye (*S. cereale* L. cv Musketeer), winter wheat (*T. aestivum* L. cv Monopol) and spring wheat (*T. aestivum* L. cv Katepwa) were germinated from seed as described in section 2.2.1.

5.2.2 PSII Excitation Pressure

Photosystem II excitation pressure ($1\text{-}q_P$) was calculated from Chl *a* steady-state fluorescence parameters at the growth temperature and irradiance as described in section 2.2.3.

5.2.3 Chl *a* Fluorescence

For all photoinhibition experiments, room temperature fluorescence was measured *in vivo* using a PSM fluorometer (Bicmonitor S.C.I. AB, Umeå, Sweden) as described in section 3.2.3. Changes in F_V/F_M were used to quantify susceptibility to photoinhibition.

Steady-state Chl *a* fluorescence parameters were determined as described in section 2.2.3. Stern-Volmer NPQ and $1\text{-}q_O$ were calculated as;

$$NPQ = (F_M/F_M') - 1 \qquad 1\text{-}q_O = F_O' / F_O$$

according to Bilger and Björkman (1990) and Bilger and Schreiber (1986) respectively.

5.2.4 Photoinhibitory Treatments

Photoinhibition of photosynthesis was induced at 5°C under ambient air conditions. Leaf segments (4 to 8 cm long) were placed side by side on moist filter paper adaxial side face-up in aluminum trays. The cut ends of the leaves were anchored using glass microscope slides and the filter paper was kept moist with distilled water throughout the experiment to prevent desiccation (Öquist and Huner, 1993). Susceptibility to photoinhibition was quantified by monitoring changes in F_V/F_M as a function of exposure time to a PPFD of 1600 µmol m^{-2} s^{-1} measured at the leaf surface from a bank of three high-pressure sodium pressure lamps (CGE Lucalox, LU-400, Canadian General Electric, Toronto, ON, Canada). A 10 cm deep plexiglass heat filter containing a continuous flow of cold water was placed between the lamps and samples. In addition, a 15 cm oscillating fan provided continuous air circulation over the samples. This apparatus was maintained in a cold room set for an air temperature of 5°C. Temperature at the leaf surface was monitored using a constantan-copper (Type T) thermocouple in conjunction with a temperature logger (model MDSS41-TC:G1; Omega Engineering Inc.) and did not exceed 6°C (results not shown).

5.2.5 Pigment Extraction and Determination

Pigments were extracted from leaf samples and determined by HPLC as described in section 2.2.4.

The EPS of the samples was estimated according to Thayer and Björkman (1990) using the following equations;

$$EPS = (Vx + 0.5Ax)/(Vx + Ax + Zx)$$

Xanthophyll pool size was calculated as the sum of Vx + Ax + Zx.

5.3 Results

5.3.1 Tolerance to Photoinhibition

Regardless of the growth irradiance or temperature, the F_V/F_M of winter rye leaves decreased with time during exposure to a photoinhibitory irradiance of 1600 µmol m^{-2} s^{-1} at 5°C (Fig. 22A and B). However, increasing the growth irradiance from 50 to 800 µmol m^{-2} s^{-1} at 20°C increased the tolerance to photoinhibition at 5°C by 47% (Fig. 22A). Increasing the growth irradiance from 50 to 250 at 5°C resulted in a 1.5-fold increase in tolerance to photoinhibition (Fig. 22B). Furthermore, winter rye grown at 5/250 exhibited a similar tolerance to photoinhibition as plants grown at 20/800 (Fig. 22A and B). The results presented in Figure 23 clearly demonstrate that tolerance to photoinhibiton, as reflected by the F_V/F_M ratio, is strongly correlated ($r^2 = 0.96$) to the level of excitation pressure on PSII (Fig. 23). Winter and spring wheat demonstrate similar trends with respect to tolerance to photoinhibition as that observed for winter rye (Fig. 24).

In addition, initial F_O values of leaves of winter rye increased by 66% as a result of decreasing the growth irradiance from 800 to 50 at 20°C (Fig. 22C).

Figure 22. Photoinhibitory response curves for leaves of winter rye (*S. cereale* L. cv Musketeer). Development occurred at a temperature of 20°C (closed symbols) or 5°C (open symbols) with an irradiance of 800 (♦), 250 (●, ○) or 50 (■, □) µmol m^{-2} s^{-1}. A and B, F_V / F_M. C and D, F_O. Photoinhibition occurred at 5°C with a PPFD of 1600 µmol m^{-2} s^{-1}. Initial F_V / F_M values are indicated in Table XV. All values represent means ± SE; $n = 3$. When not present, error bars are smaller than symbol size.

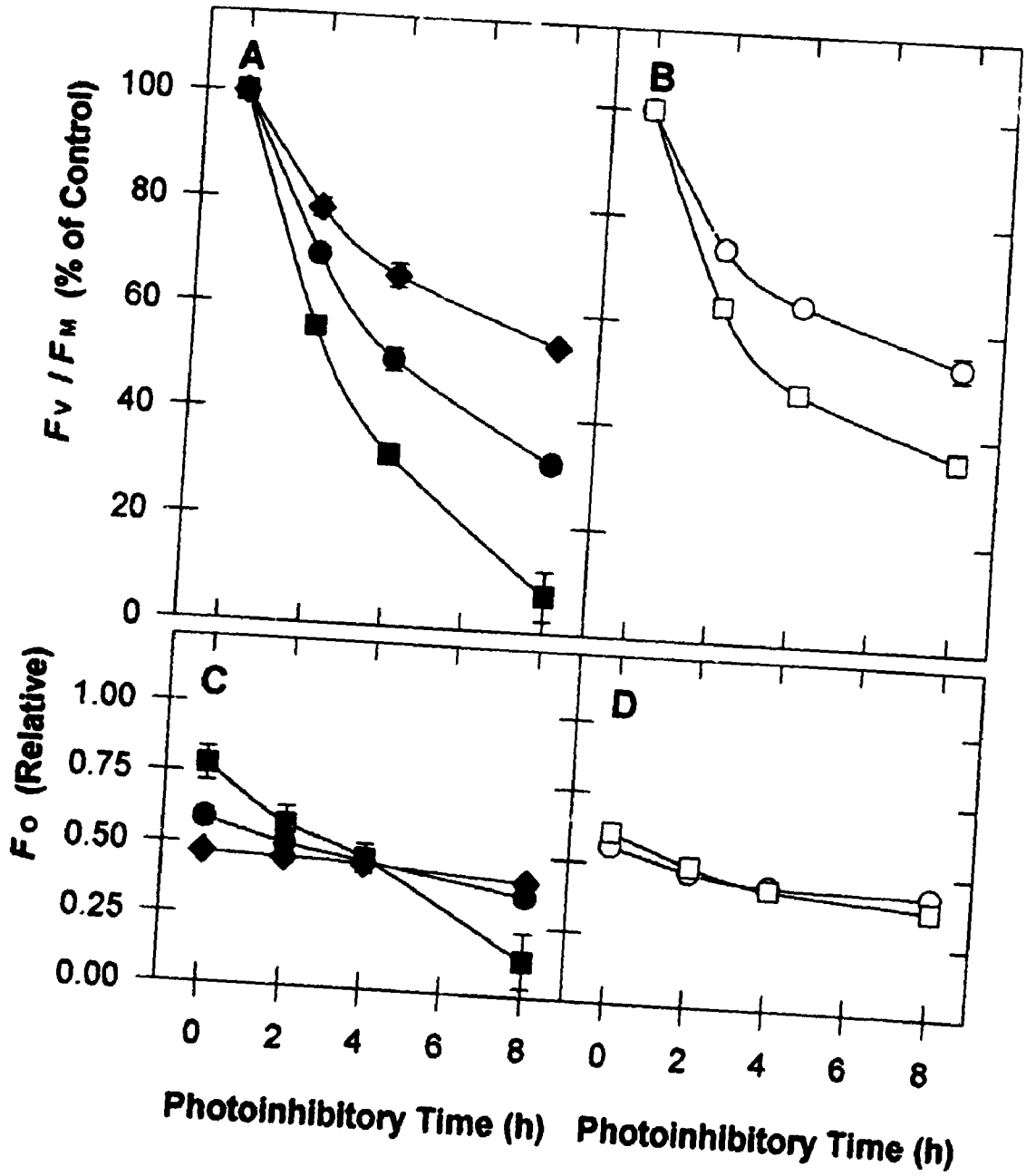
A
B
C
D
100
80
60
40
20
0
1.00
0.75
0.50
0.25
0.00
F_V / F_M (% of Control)
F_O (Relative)
0
2
4
6
8
Photoinhibitory Time (h)
Photoinhibitory Time (h)

Figure 23. Correlation between photoinhibitory response and 1-q_P in leaves of winter rye (*S. cereale* L. cv Musketeer). Development occurred at a temperature of 20°C (closed symbols) or 5°C (open symbols) with an irradiance of 800 (♦), 250 (●, ○) or 50 (■, □) µmol m^{-2} s^{-1}. Photoinhibition occurred at 5°C with a PPFD of 1600 µmol m^{-2} s^{-1}. Values for the 4 h time point in the photoinhibitory treatment are shown. 1-q_P was measured at the growth temperature and growth irradiance. All values represent means ± SE; n = 3. When not present, error bars are smaller than symbol size. Regression analysis was performed in SigmaPlot® version 1.02 (Jandel Scientific, Corte Madera, CA USA).

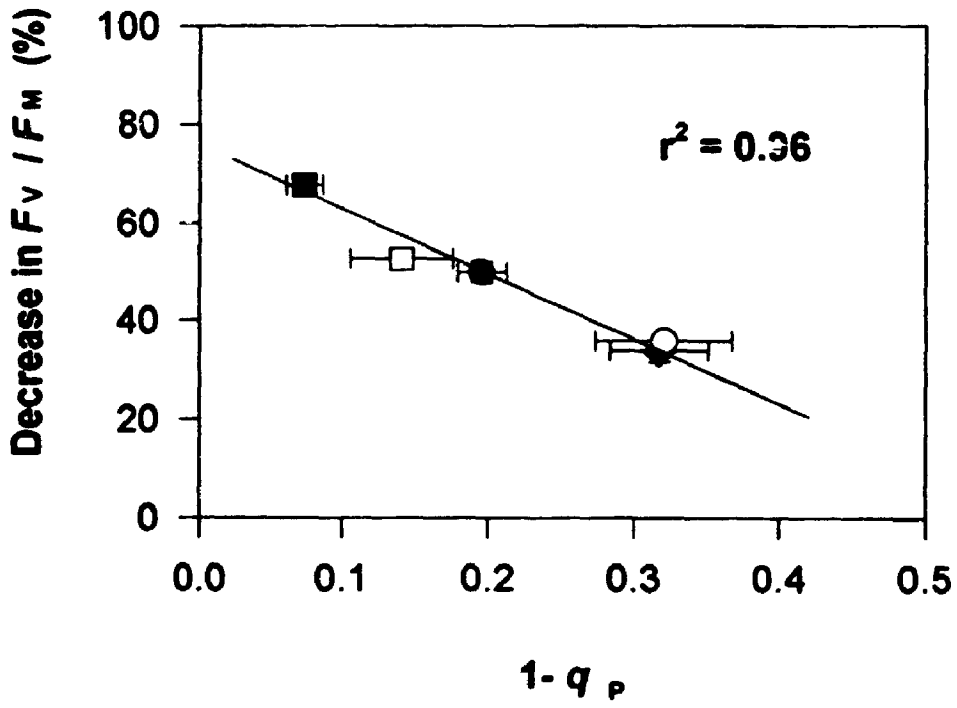
Decrease in F_V / F_M (%)
100
80
60
40
20
0
0.0
0.1
0.2
0.3
0.4
0.5
r^2 = 0.96
1- q_P

Figure 24. Photoinhibitory response curves for leaves of winter wheat (*T. aestivum* L. cv Monopol) and spring wheat (*T. aestivum* L. cv Katepwa). Development occurred at a temperature of 20°C (closed symbols) or 5°C (open symbols) with an irradiance of 800 (♦), 250 (●, ○) or 50 (■, □) µmol m^{-2} s^{-1}. A and B, cv Monopol. C and D, cv Katepwa. Photoinhibition occurred at 5°C with a PPFD of 1600 µmol m^{-2} s^{-1}. Initial F_V / F_M values are indicated in Table XVI. All values represent means ± SE; $n = 3$. When not present, error bars are smaller than symbol size.

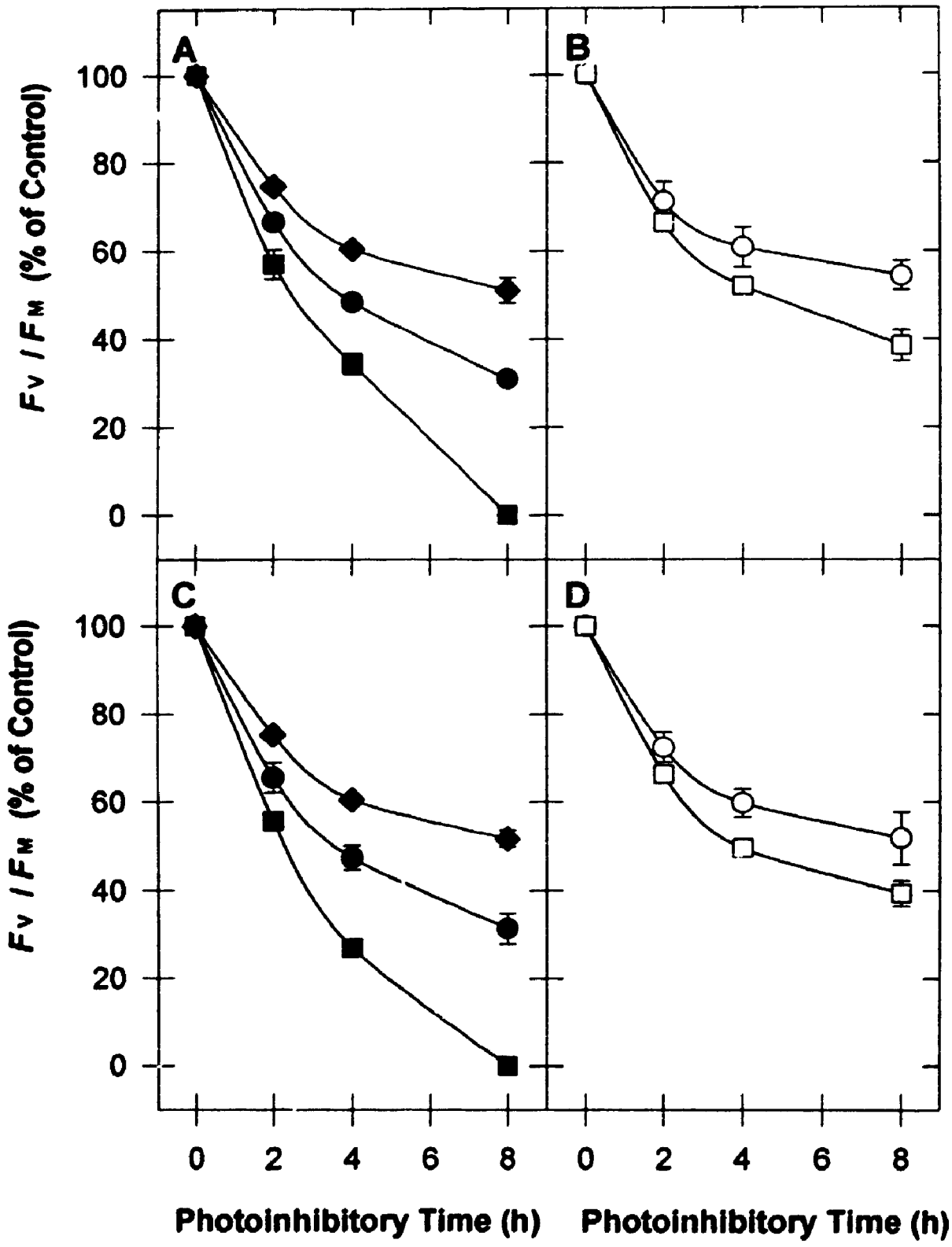
A
B
C
D
100
80
60
40
20
0
F_V / F_M (% of Control)
0
2
4
6
8
Photoinhibitory Time (h)
Photoinhibitory Time (h)

However, growth irradiance had minimal effects on initial F_o values at 5°C (Fig. 22D). Plants grown at 20/250, 5/250, or 5/50 exhibited 39, 23, and 38% decreases respectively over the 8 h course of the photoinhibitory treatment (Fig. 22C and D). However, F_o values for 20/800 leaves did not significantly change as a result of photoinhibiton (Fig. 22C). In contrast, the leaves of 20/50 grown plants demonstrated a 6-fold reduction in F_o values over the same time period (Fig. 22C). Similar data were obtained for winter and spring wheat (results not shown).

5.3.2 NPQ and the Xanthophyll Cycle

Upon comparing the results presented in Table XXIII with those of Table V (See also section 2.3.4; Table V), it is clear that exposure to a photoinhibitory PPFD at 5°C resulted in minimal differences in all carotenoid pigments and xanthophyll pool size as a result of growth at the various temperature/irradiance regimes (Fig. 25A; Table V and XXIII). However, photoinhibitory light treatments stimulated the conversion of Vx to Zx which resulted in a significant reduction in the EPS from approximately 0.9 to 0.3 (Fig. 25B). Similar trends with respect to the effects of growth regime and photoinhibition on carotenoid pigments were observed for winter and spring wheat (results not shown), which is consistent with a previous report (Hurry et al., 1992).

Growth at 20/800 resulted in a maximal 1.9-fold decrease in NPQ at a PPFD of 500 μmol m^{-2} s^{-1} in comparison to 20/50 and 20/250 leaves when

Figure 25. Xanthophyll characteristics in total leaf extracts of winter rye (*S. cereale* L. cv Musketeer) developed at the temperature/irradiance regimes indicated. A, Xanthophyll pool size pre- (□) and post (▨) photoinhibition. B, Xanthophyll EPS pre- (□) and post (▨) photoinhibition. Photoinhibition occurred at 5°C for 3 h with a PPFD of 1600 μmol m^{-2} s^{-1}. All values represent means ± SE; n = 3. When not present, error bars are smaller than symbol size.

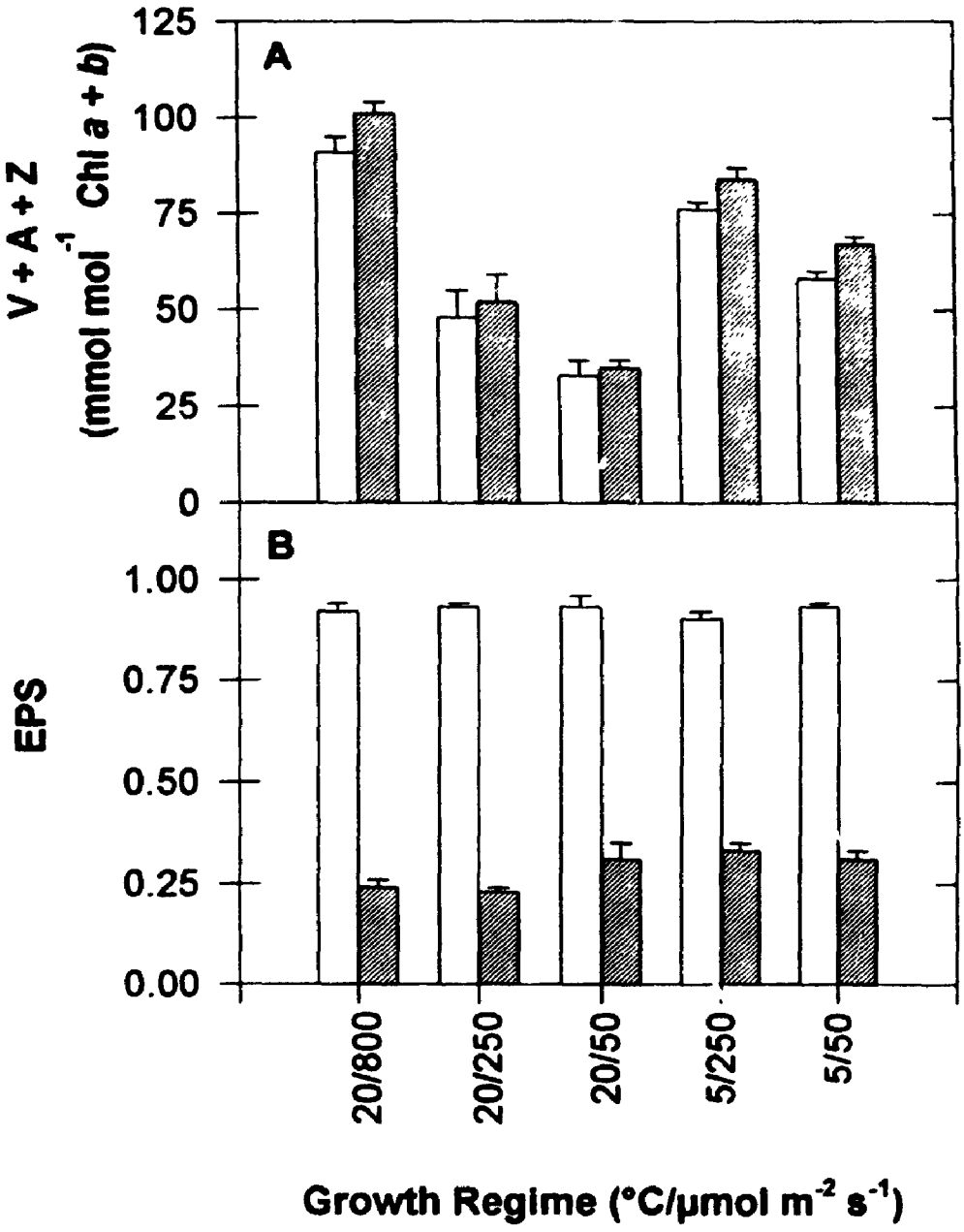
A
B
V + A + Z
(mmol mol-1 Chl a + b)
EPS
125
100
75
50
25
0
1.00
0.75
0.50
0.25
0.00
20/800
20/250
20/50
5/250
5/50
Growth Regime (°C/µmol m-2 s-1)

Table XXIII. *Post-photoinhibition carotenoid content and xanthophyll pool sizes in total leaf extracts of winter rye (S. cereale L. cv Musketeer).*

Pigments were separated and quantified by HPLC after a photoinhibitory treatment of 1600 µmol m^{-2} s^{-1} for 3 h at 5°C. Data are expressed as mmol mol^{-1} Chl *a+b*. All values represent means ± SE; *n* = 3.

Growth Regime	Carotenoid (mmol mol^{-1} Chl *a+b*)						Pool Size
(°C/µmol m^{-2} s^{-1})	β-Car	Lut	Neo	Ax	Vx	Zx	Ax + Vx + Zx
20/800	108 ± 4	160 ± 4	19 ± 2	20 ± 3	14 ± 1	67 ± 2	101 ± 3
20/250	88 ± 2	146 ± 8	15 ± 1	4 ± 3	10 ± 0	38 ± 3	52 ± 7
20/50	75 ± 0	130 ± 3	15 ± 3	nd	10 ± 1	24 ± 3	35 ± 2
5/250	91 ± 2	158 ± 9	22 ± 3	21 ± 5	17 ± 1	45 ± 2	84 ± 3
5/50	76 ± 2	146 ± 4	21 ± 4	12 ± 0	15 ± 1	40 ± 2	67 ± 2

measured at 20°C (Fig. 26A). However, when the measuring temperature was lowered to 5°C, the 20/50 leaves demonstrated a 1.2-fold lower capacity for NPQ in comparison to the 20/800 and 20/250 leaves at saturating PPFD (> 500 µmol m^{-2} s^{-1}) (Fig. 26C). Increasing the growth irradiance at 5°C from 50 to 250 µmol m^{-2} s^{-1} resulted in 1.2-fold greater values of NPQ at saturating irradiance (> 500 µmol m^{-2} s^{-1}) when measured at 20°C (Fig. 26B). A similar increase was observed at the 5°C measuring temperature (Fig. 26D). In addition, minimal changes were observed in steady-state F_o quenching (1-q_o) as a result of growth under the different temperature/irradiance regimes, irrespective of measuring temperature (Fig. 27).

5.4 Discussion

In all of the experiments previously reported regarding low temperature-induced tolerance to photoinhibition, plants grown at 5/250 are compared with control plants grown at 20/250. Since the only difference in growth condition is the growth temperature, the assumption is that any difference in photosynthetic response must represent a growth temperature response. Thus, the development of low temperature-induced tolerance to photoinhibition has been interpreted as a low temperature growth response (Huner et al., 1993). However, the results in this chapter clearly demonstrate that cold tolerant cereals grown at similar high PSII excitation pressures (20/800 or 5/250) also exhibited a similar tolerance to photoinhibition at low temperature (Fig. 22 and 24). I

Figure 26. Light response curves for NPQ in leaves of winter rye (*S. cereale* L. cv Musketeer). Development occurred at a temperature of 20°C (closed symbols) or 5°C (open symbols) with an irradiance of 800 (♦), 250 (●, ○) or 50 (■, □) μmol m^{-2} s^{-1}. Response was measured at 20°C (A and B) and 5°C (C and D). All values represent means ± SE; $n = 3$. When not present, error bars are smaller than symbol size.

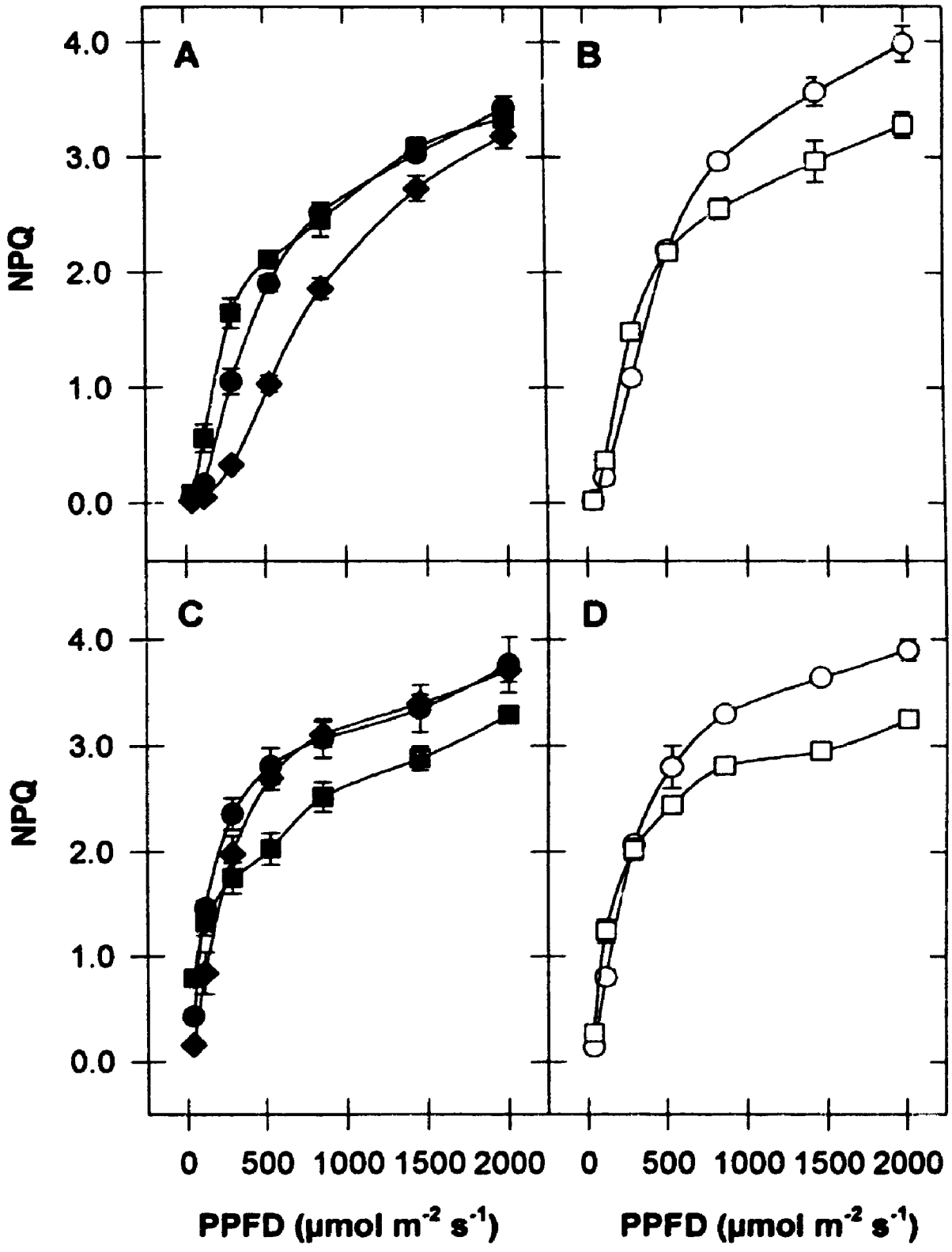
A
B
C
D
NPQ
NPQ
4.0
3.0
2.0
1.0
0.0
0
500
1000
1500
2000
PPFD (µmol m-2 s-1)
PPFD (µmol m-2 s-1)

Figure 27. Light response curves for 1-q_O in leaves of winter rye (*S. cereale* L. cv Musketeer). Development occurred at a temperature of 20°C (closed symbols) or 5°C (open symbols) with an irradiance of 800 (♦), 250 (●, ○) or 50 (■, □) µmol m^{-2} s^{-1}. Response was measured at 20°C (A and B) and 5°C (C and D). All values represent means ± SE; n = 3. When not present, error bars are smaller than symbol size.

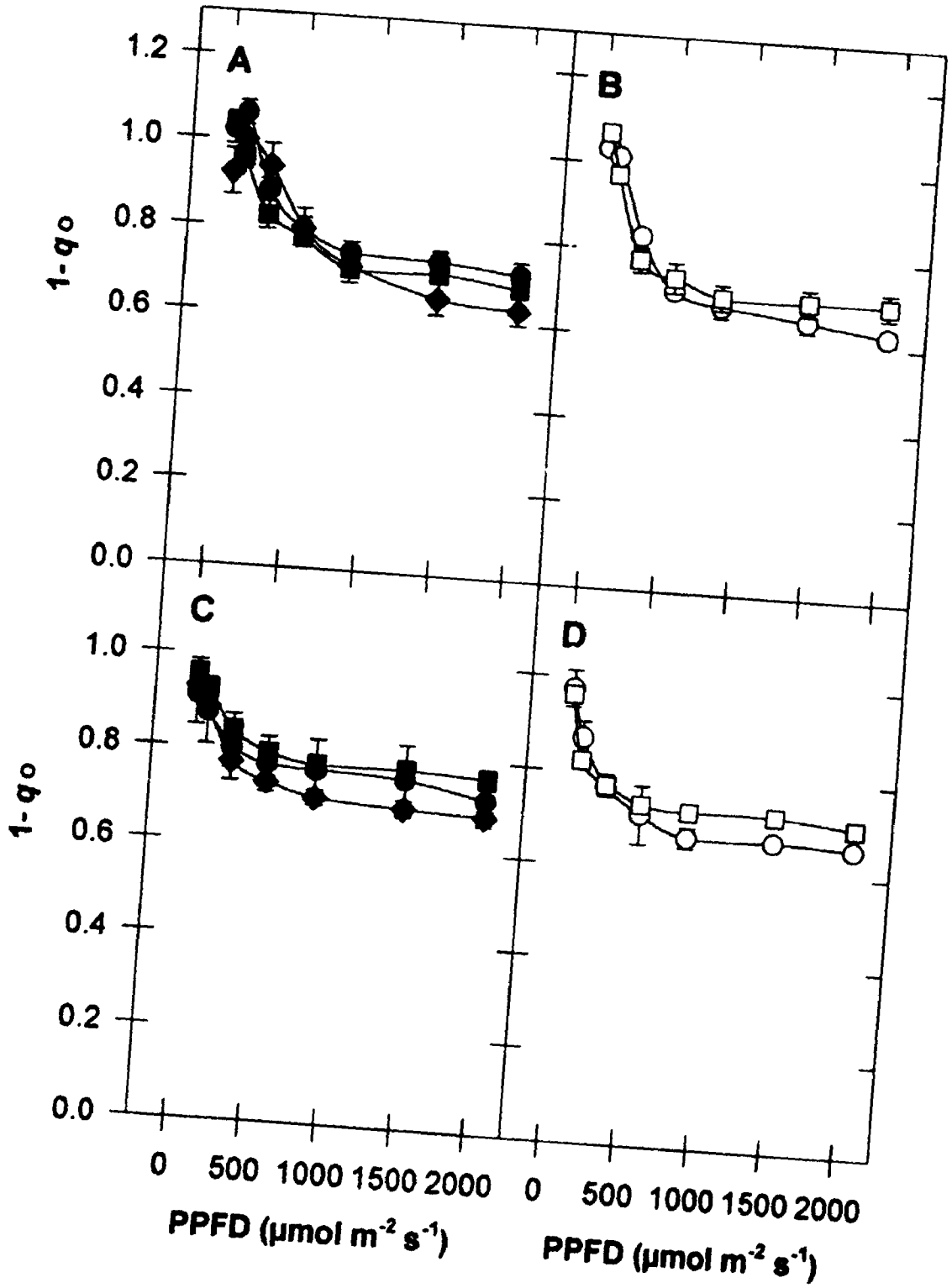
A
B
C
D
1-qo
1-qo
1.2
1.0
0.8
0.6
0.4
0.2
0.0
0
500
1000
1500
2000
PPFD (µmol m-2 s-1)
PPFD (µmol m-2 s-1)

suggest that the development of increased tolerance to photoinhibition upon growth of cold tolerant herbaceous plants at low temperature can be explained on the basis of growth under high PSII excitation pressure. Therefore, it appears that the increased tolerance to photoinhibition observed in plants grown at 5/250 reflects photosynthetic adjustment to growth under high PSII excitation pressure rather than photosynthetic adjustment to growth temperature as previously assumed. These data, coupled with the data previously presented indicating growth at high PSII excitation pressure resulted in an increased PS_{max} O_2 (Table V and VI) and an increased capacity to keep Q_A oxidized as a function of irradiar. , (Fig. 15) are consistent with this notion. Thus, I conclude that cold tolerant, herbaceous plants grown at 5/250 exhibit a greater tolerance to photoinhibition than plants grown at 20/250 not because of low growth temperature *per se*, but rather, as a consequence of growth under high PSII excitation pressure.

Excess excitation energy can be quenched in the Chl *a* light-harvesting antenna and is typically monitored by F_o quenching (Horton and Ruban, 1993; Horton et al., 1994). Since F_o fluorescence is thought to emanate from Chl *a* antennae, quenching of F_o is also thought to occur in the Chl *a* antennae (Krause and Weis, 1991). Presumably, this mechanism results in the protection of PSII by altering the excitation energy reaching the reaction center. There were no differential changes observed in F_o quenching as a result of photoinhibitory treatment or steady-state F_o quenching that could account for the

tolerance to photoinhibition observed (Fig. 22 and 27). The xanthophylls have also been implicated in F_o quenching and photoprotection of PSII (Demmig-Adams, 1990; Demmig-Adams et al., 1995). Although the xanthophyll pool size was greater in those plants most tolerant to photoinhibition, this did not result in any significant level of F_o quenching (Fig. 22, 25 and 27).

Since the xanthophyll cycle has been linked to NPQ formation, the contribution of NPQ tc increased tolerance to photoinhibition was also examined. Light-driven electron transport or chloroplast ATPase activity results in an acidification of the thylakoid lumen which activates Vx de-epoxidase and thus promoting conversion from Vx to Zx via Ax in the minor Chl *a/b*-binding proteins. These xanthophylls are somehow thought to mediate the formation of NPQ. In addition, the minor Chl *a/b*-binding proteins also become protonated, resulting in a structural modiication of these pigment-protein complexes (Gilmore and Yamamoto, 1992; Crofts and Yerkes, 1994; Gilmore et al., 1995; Demmig-Adams et al., 1996). While xanthophyll pool sizes may reflect the degree of tolerance to photoinhibition, if they are associated with NPQ one would expect to see greater NPQ in those leaves with the greatest xanthophyll pool sizes. However, values of NPQ are not greatest in those leaves most tolerant to photoinhibition, irrespective of the xanthophyll content (Fig. 25 and 26). Therefore, NPQ cannot account for the differential tolerance to photoinhibition observed as a result of growth at the various temperature/irradiance regimes. Thus, while significant evidence exists to support a role for the xanthophylls in

the development of NPQ, their precise contribution to increased tolerance to photoinhibition remains controversial (Pfundel and Bilger, 1994; Thiele and Krause, 1994; Adams et al., 1995a; Adams et al., 1995b; Koroleva et al., 1995; Demmig-Adams and Adams, 1996; Thiele et al., 1996).

Therefore, it appears that neither NPQ nor F_O quenching can account for the differential tolerance exhibited towards photoinhibition and that it is best rationalized on the basis of photosynthetic adjustment to high PSII excitation pressure. However, it remains unclear as to the mechanism by which Q_A is kept in the oxidized state.

CHAPTER 6

COLD ACCLIMATORY PROCESSES IN RESPONSE TO LOW TEMPERATURE, LIGHT AND THE REDOX STATE OF PSII

6.1 Introduction

Exposure to low, non-freezing temperatures induces molecular, morphological, and physiological changes in the plant which result in the development of cold hardiness and the acquisition of freezing tolerance (Vasil'yev, 1961; Levitt, 1980; Guy, 1990; Thomashow, 1993; Hughes and Dunn, 1996).

Morphologically, the development of a prostrate or rosette growth habit is assumed to be a consequence of development at low temperature (Vasil'yev, 1961; Roberts, 1984). In addition, it has been shown that the rosette growth habit is correlated with freezing tolerance and has been used as a selection criterion in breeding for cold hardiness (Fowler et al., 1981; Roberts, 1984; Stushnoff et al., 1984; Blum, 1988).

In wheat, cold acclimation rapidly induces a specific set of *W*heat-*c*old-*s*timulated genes (*Wcs* genes) which subsequently disappear upon deacclimation. *Wcs* genes are up-regulated by low temperature at the transcriptional level and winter wheat cultivars exhibit higher levels of expression than spring cultivars (Houde et al., 1992a; Chauvin et al., 1993; Ouellet et al., 1993; Danyluk et al., 1994; Limin et al., 1995). Thus, it is assumed

that there is a high correlation between the expression of these genes and the development of freezing tolerance. *Wcs120* is a nuclear-encoded gene induced by low temperature and encodes a major protein with an apparent molecular mass of 50 kD (Houde et al., 1992a). Studies utilizing the anti-WCS120 antibody have identified a wheat protein family sharing a common antigenicity. All members of this protein family are up-regulated by low temperature and associated with freezing tolerance (Houde et al., 1992b; Ouellet et al., 1993; Chauvin et al., 1994). Immunolocalization studies have demonstrated a differential tissue expression, with high levels of all members of this protein family present in the vascular tissue transition zone (Houde et al., 1995). These proteins are thought to provide a specific micro-environment necessary for cell survival during freezing stress (Houde et al., 1995). *Wcs19* is another nuclear-encoded gene specifically regulated by low temperature, but also requiring light for maximal induction (Chauvin et al., 1993). Recently, WCS19 has been localized in the chloroplast stroma (T. Krause, M. Houde and F. Sarhan, unpublished results).

It is possible that the effects of PSII excitation pressure extend to processes other than photosynthesis. Since low temperature modulates both PSII excitation pressure and genes associated with cold tolerance, I hypothesized that the reduction state of PSII would influence the molecular responses associated with cold acclimation and the subsequent acquisition of freezing tolerance. For these studies, the expression of two low temperature-

responsive genes, *Wcs120* (low temperature-specific) and *Wcs19*, (low temperature-specific and light-dependent) were examined under growth conditions of varying PSII excitation pressure. In addition, growth habit as it relates to cold acclimation and freezing tolerance in winter rye and the cold tolerant herbaceous dicot, spinach, are also examined.

6.2 Materials and Methods

6.2.1 Plant Material and Growth Conditions

Winter rye (*S. cereale* L. cv Musketeer) and spinach (*Spinacia oleracea* L. cv Savoy) were germinated from seed in coarse vermiculite as described in section 2.2.1. Spinach plants were thinned to a density of three per pot at 1 and 3 weeks after germination at 20 and 5°C respectively as previously described (Gray et al., 1994).

6.2.2 PSII Excitation Pressure

Photosystem II excitation pressure ($1-q_P$) was calculated from Chl *a* steady-state fluorescence parameters at the growth temperature and irradiance as described in section 2.2.3.

6.2.3 Growth Habit

Plants were photographed at similar developmental ages, irrespective of growth temperature or irradiance, as determined by growth kinetic analyses

described in section 2.2.2.

6.2.4 Spectral Distributions

The spectral photon distribution in all growth chambers was measured at pot height using a spectroradiometer consisting of a Instaspec II™ photodiode array detector (model 77112), Multispec™ spectrograph/monochromator (model 77400) and an integrating sphere (model 70451; Oriel Corp., Stratford, CT, USA). The contribution of FR (725 to 735 nm), R (655 to 665 nm), and B (400 to 480 nm) light, as well as UV-A (320 to 400 nm) and UV-B (290 to 320 nm) were calculated as a percentage of PAR (400 to 700 nm) from the photon distribution. In addition, the light quality ratios for R:FR and R:B were also determined.

6.2.5 RNA Isolation

Uppermost fully expanded leaves were harvested 4 h into the photoperiod, frozen in liquid N_2 and stored at -80°C until use. Total RNA was extracted essentially as described by Danyluk and Sarhan (1990). Leaf tissue (1 g) was ground to a fine powder in dry ice using a mortar and pestle. The powder was mixed with equal volumes (2.5 mL) of extraction buffer [100 mM Tris-HCl (pH 8.8), 100 mM NaCl, 5 mM EDTA, 1% (w/v) SDS, heparin (40 units mL^{-1})] and phenol saturated with 100 mM Tris-HCl (pH 8.8), containing 0.5% (w/v) 8-hydroxyquinoline at 60°C. The homogenate was allowed to cool to room temperature and an equal volume of chloroform-isoamyl alcohol (24:1, v/v) was

added. Following centrifugation at 6,000*g* for 10 min, the aqueous phase was removed and the organic phase washed again with extraction buffer. The aqueous phases were combined and re-extracted once with an equal volume of phenol-chloroform-isoamyl alcohol (25:24:1, v/v/v) and once with chloroform-isoamyl alcohol (24:1, v/v). Total nucleic acids were precipitated overnight with 2.5 volumes of cold 100% (v/v) ethanol and 0.1 volume of 3.0 M sodium acetate (pH 5.5) with 5 mM EDTA at -20°C. Nucleic acids were collected by centrifugation at 6,000*g* for 20 min and then washed in an equal volume (5 mL) of 3.0 M sodium acetate (pH 5.5) with 5mM EDTA for 1 h with constant agitation. The suspension was frozen at -80°C for 30 min and allowed to thaw at room temperature, followed by centrifugation at 6,000*g* for 20 min. This was repeated and the subsequent RNA pellet was washed once with cold 70% (v/v) ethanol, dried under vacuum and suspended in DEPC-treated water. RNA was quantified spectrophotometrically by A_{260} (model UV-160; Shimadzu).

6.2.6 DNA Probe Labelling

Double stranded DNA probes (20 ng) containing the inserts *Wcs19* (*pWcs19*; Chauvin et al., 1993) or *Wcs120* (*pWcs120*; Houde et al., 1992a) were denatured by boiling for 5 min and rapidly cooled on ice. DNA fragments were labelled by random priming using a mix of hexanucleotides as primers with the large fragment of *Escherichia coli* DNA polymerase (Klenow fragment) as described by Feinberg and Vogelstein (1983, 1984). To the denatured probes,

10 µL of OLB buffer [OLB: (1 mL of 1.25 M Tris-HCl (pH 8.0) and 0.125 M $MgCl_2$, 18 µL β-mercaptoethanol, 5 µL 0.1 M dATP in TE (3 mM Tris-HCl (pH 7.0), 0.2 mM EDTA) and 5 µL 0.1 M dGTP in TE) with 2 M Hepes (pH 6.6), 90 OD units of hexanucleotides mL^{-1} TE (100:250:150, v/v/v)], 2 µL BSA (10 mg mL^{-1}, nucleic acid enzyme grade; Boehringer Mannheim, Laval QC, Canada), 20 µCi each of [α-^{32}P] dTTP and [α-^{32}P] dCTP (specific activity ≥3000 Ci/mmol; ICN, Costa Mesa, CA, USA) and 2 units of Klenow (Pharmacia, Uppsala, Sweden) in a final volume of 50 µL were added to direct the synthesis of the labelled fragment. Following a 60 min labelling reaction at 37°C, the mixture was combined with 5 µL each of 0.5 M EDTA (pH 8.0), 3 M sodium acetate (pH 5.5) and tRNA (5 mg mL^{-1}). Unincorporated radionucleotides were removed by precipitating the probe at -80°C with 2.5 volumes of 100% (v/v) ethanol. After centrifugation at 12,000*g* for 5 min, the pellet was solubilized in 50 µL of 0.1 N NaOH prior to immediate use in hybridization experiments.

6.2.7 RNA Gel Blot Hybridization

Samples (10 µg total RNA) were denatured in 14 µL of formamide-formaldehyde (1:0.4, v/v) and mixed with 1 µL ethidium bromide (5 mg mL^{-1}) and 2.5 µL of 10x Mops buffer [200 mM Mops (pH 7.0), 50 mM sodium acetate, 10 mM EDTA]. The ethidium bromide allowed for visual evaluation of RNA quality and equal loading on the gel (Rosen and Villa-Komaroff, 1990). The mixture was heated at 65°C for 15 min and rapidly cooled on ice for 2 min at which time 4 µL

of loading buffer [(0.25% (w/v) BPB, 5% (v/v) glycerol, 150 mM EDTA (pH 8.0)] was added prior to loading on 1.5% (w/v) formaldehyde-agarose gels. Gels were electrophoresed on a DNA Sub Cell apparatus (Bio-Rad) for 5 h at 80 V (constant voltage) using 1x Mops (pH 7.0) as a running buffer. Gels were then photographed on a UV-transilluminator (model UVB-40E; Ultra Lum Inc., Carson, CA, USA) with a Polaroid MP-4 Land camera and type 57 black-and-white Land film (Polaroid Corp. Cambridge, MA, USA) in combination with a Wratten No. 22 filter (Eastman-Kodak). RNA was transferred to supported nitrocellulose membranes (Hybond-C Extra, 0.2 µm pore size; Amersham Corp.) in 20x SSC overnight [1x SSC: 0.15 M NaCl and 0.015 M sodium citrate (pH 7.0)]. The membranes were air-dried and then baked at 80°C for 1 h. The membranes were transferred to a 0.1x SSC solution at 50°C for 10 min and then to a 5x SSC at room temperature for 5 min prior to hybridization. The membranes were placed in glass hybridization tubes and pre-hybridized in a solution containing 2.5 mL of 20x SSC, 1 mL of 0.5 M sodium phosphate buffer (pH 6.5), 1 mL of 100x Denhardt's's reagent [2% (w/v) Ficoll 400 (Sigma), 2% (w/v) PVPP, 2% (w/v) BSA], 200 µL of denatured herring sperm DNA (5 mg mL^{-1}) and 300 µL of ddH_2O mixed at a 1:1 ratio with deionized formamide in a hybridization oven (Bachofer, Reutlingen, Germany) for 2 h at 42°C. The membranes were then subjected to hybridization in a solution containing 2.5 mL of 20x SSC, 1 mL of 0.5 M sodium phosphate buffer (pH 6.5), 100 µL of 100x Denhardt's's reagent, 300 µL of denatured herring sperm DNA (5 mg mL^{-1}), 63 µL poly rA (4 mg mL^{-1}),

50 µL poly rC (4 mg mL^{-1}), 50 µL yeast tRNA (10 mg mL^{-1}) and 1 g dextran sulfate (Pharmacia) mixed at a 1:1 ratio with deionized formamide solution to which the ^{32}P labelled *Wcs19* or *Wcs120* probe was added, and incubated at 42°C for 12 h. Following hybridization, the membranes were subjected to several buffer changes of decreasing SSC concentrations (5 to 0.1x). Washing of the membranes was completed in 0.1x SSC with 0.1% (w/v) SDS at 65°C at which time they were autoradiographed on X-Omat AR film (Eastman-Kodak) at -80°C with intensifying screens (Cronex Lightning Plus; DuPont, Mississauga, ON, Canada). Development occured with GBX developer/replenisher and fixer/replenisher (Eastman-Kodak). Transcript abundance was determined by densitometric scanning on a computing densitometer (Molecular Dynamics) coupled with ImageQuant software (version 3.22; Molecular Dynamics).

6.2.8 Soluble Protein Extraction

Polypeptides of the soluble fraction were extracted as described by Houde et al., (1992b) with minor modifications. Leaf tissue was harvested 4 h into the photoperiod and homogenized with a pre-chilled mortar and pestle in a grinding buffer containing 100 mM Tris-HCl (pH 8.0) and 1 mM PMSF with a 0.3 g mL^{-1} tissue-to-buffer ratio. The homogenate was centrifuged at 12,000*g* for 5 min at 4°C. The supernatant was removed and solubilized in an equal volume of 2x electrophoresis sample buffer [62.5 mM Tris-HCl (pH 6.8), 2% (w/v) SDS, 10% (w/v) glycerol, 5% (w/v) β-mercaptoethanol, 0.001% (w/v) BPB] as described by

Laemmli (1970). Protein concentrations were estimated after acetone precipitation at -20°C and suspension of the pellet in 100 mM NaOH by the bicinchoninic acid method (Smith et al., 1985) using the BCA reagent (Pierce Chemical Co.). The manufacturers standard protocol was followed using BSA (fraction V) as a standard.

6.2.9 SDS-PAGE and Immunoblotting

Proteins were separated by SDS-PAGE using a Mini-PROTEAN II apparatus (Bio-Rad) utilizing a 4% (w/v) stacking gel and 10% (w/v) resolving gel with a buffer system containing 25 mM Tris-HCl (pH 8.3), 192 mM glycine and 0.1% (w/v) SDS as described by Laemmli (1970). All samples were loaded on an equal protein basis (5 µg lane^{-1}) and a constant current of 15 mA was applied for 1.5 h at room temperature. Separated polypeptides were electrophoretically transferred (Mini-Trans Blot; Bio-Rad) to supported nitrocellulose membranes (Hybond-C Extra, 0.2 µm pore size; Amersham) by applying a constant current of 295 mA for 1 h in a transfer buffer containing [25 mM Tris, 192 mM glycine (pH 8.3) and 20% (v/v) methanol as described by Towbin et al. (1979). Equal protein loading was confirmed by Coomassie Brilliant Blue R-250 (Bio-Rad) staining of gels run in parallel with the same samples.

After blocking in a 4% (w/v) solution of reconstituted milk powder prepared in PBS [80mM Na_2HPO_4, 20mM NaH_2PO_4 (pH 7.5), 100mM NaCl] containing 0.2% (v/v) Tween-20 (PBS-T), the membranes were probed with an antibody

raised against the 50 kD cold-induced protein from winter wheat (WCS120) at a 1:10,000 dilution (Houde et al., 1992b). After washing with PBS-T, the proteins recognized by the primary antibody were identified with anti-goat IgG horseradish peroxidase conjugate (Sigma) as a secondary antibody at a 1:25,000 dilution. The complex was visualized using the chemiluminescent detection system (ECL; Amersham) and X-Omat RP film in combination with GBX developer/replenisher and fixer/replenisher (Eastman-Kodak) following the manufacturers suggested protocol. Protein abundance was determined by densitometric scanning on a computing densitometer (Molecular Dynamics) coupled with ImageQuant software (version 3.22; Molecular Dynamics).

6.2.10 Freezing Tolerance

The ability of leaves to tolerate freezing was determined by changes in electrical conductivity (Dexter et al., 1932). Three leaf sections, approximately 15 mm in length, were wrapped in wet cheesecloth and placed in test tubes in a Neslab refrigerated circulating freezing bath (model LT-50DD, Neslab Instruments Inc.) Each tube was seeded with an ice chip and equilibrated at -1 °C for 1 h to initiate freezing, and then cooled at a rate of 2 °C h^{-1}. Tubes were removed at 5°C intervals and allowed to thaw at 7°C overnight. Samples were then equilibrated in deionized water for 24 h at 7°C under constant agitation. Electrical conductivity of the leachate (C_L) was measured with a Radiometer conductivity meter (model CDM3; Copenhagen, Denmark) at room temperature.

The tubes were then boiled in a water bath and the total conductivity (C_T) in the leachate determined. Relative conductance (%) was calculated as;

$$RC = C_L / C_T \times 100\%$$

The temperature at which 50% of the total conductivity was measured in the leachate was defined as the LT_{50}, or lethal temperature at which freezing injury occurred (Griffith and McIntyre, 1993). This was determined from plots of relative conductivity versus freezing temperature (Krol et al., 1984).

6.2.11 Cellular Osmolality

Osmolality of cell contents was determined as described by Huner et al. (1981). Leaves were harvested 4 h into the photoperiod and quickly frozen in liquid N_2, followed by grinding with a pre-chilled mortar and pestle. The homogenate was centrifuged at 30,000*g* for 15 min at 4°C to pellet particulate matter. The osmolality of the supernatant was determined using a vapour pressure osmometer (model 5100C; Wescor, Logan, UT, USA) calibrated using sorbitol as a standard.

6.3 Results

6.3.1 Spectral Distributions

The data in Figure 28 and Table XXIV indicate that minimal differences in light quality were observed for FR, R and B light expressed as a percentage of PAR. However, UV-A was 3.9-fold greater in the metal halide supplemented

Figure 28. Spectral photon distributions for light sources in Conviron growth chambers. A, High-output (160W) cool white fluorescent lamps. B, High-output (160W) cool white fluorescent lamps supplemented with a metal halide lamp (400W).

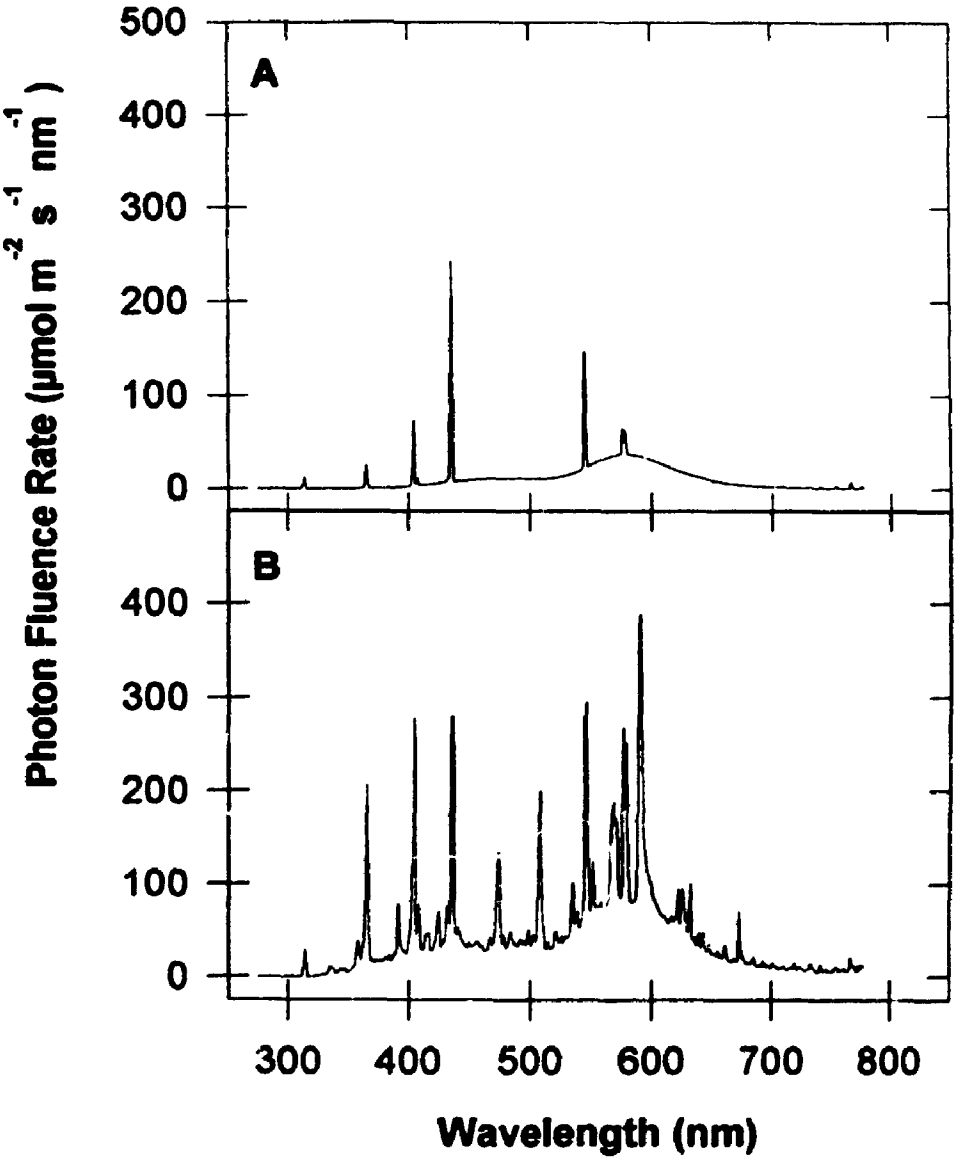
A
B
500
400
300
200
100
0
400
300
200
100
0
300
400
500
600
700
800
Photon Fluence Rate (µmol m-2 s-1 nm-1)
Wavelength (nm)

Table XXIV. *Spectral photon distributions and light quality ratios of light sources utilized for developmental studies.*

Photon distributions are expressed as a percentage of PAR for high-output cool white fluorescent lamps and the identical source supplemented with a metal halide lamp. Measurements were determined with a calibrated spectroradiometer (Oriel Corp.).

Spectral Region	Photon Distribution (% of PAR)	
	Fluorescent	Metal Halide
FR	0.004	0.007
R	0.02	0.02
B	16.30	18.60
UV-A	1.50	5.80
UV-B	0.30	0.20
	Light Quality Ratios	
R:FR	4.3	2.20
R:B	0.10	0.09

chamber. The R:B ratio exhibited no change, while the R:FR ratio demonstrated a 49% decrease in the metal halide supplemented chamber.

6.3.2 Plant Growth Habit and Osmolality

Figure 29A demonstrates that growth of winter rye at typical non-hardening conditions (20/250), that is low PSII excitation pressure, resulted in an elongated growth habit in contrast to the short, compact growth habit associated with growth at cold-hardening temperatures (5/250), that is high PSII excitation pressure (Fig. 29A). However, growth at 20/800 also resulted in a growth habit comparable to that of plants grown at 5/250 (Fig. 29A). Thus, growth at high PSII excitation pressure appears to induce the compact growth habit whereas growth at low PSII excitation pressure (either 20/250 or 5/50) induces an elongated growth habit (Fig. 29A). Although both 20/800 and 5/250 grown plants exhibited a compact growth habit, the crown of the 5/250 plants (Fig. 29B, arrow) was considerably larger in comparison to that of 20/800 plants (Fig. 29B). In addition, the plants grown at 5/50 exhibited greater stem elongation compared to those grown at 20/250 (Fig. 29B and C). Similar trends in growth habits were observed for the herbaceous cold tolerant dicot, spinach (Fig. 29C) as well as winter wheat (results not shown). Thus, changes in plant growth habit also appear to be sensitive to the reduction state of PSII as estimated by $1\text{-}q_P$.

The results presented in Table XXV indicate a 1.5-fold increase in cellular osmolality in 5/250 control plants in comparison to 20/250 grown plants. A

Figure 29. Growth habits for plants of winter rye (*S. cereale* L. cv Musketeer) and spinach (*S. oleracea* L. cv Savoy) developed at the temperature/irradiance regimes indicated. A, Potted winter rye. B, Individual plants of winter rye. C, Potted spinach. The arrow indicates the crown tissue. All plants were photographed at similar developmental ages.

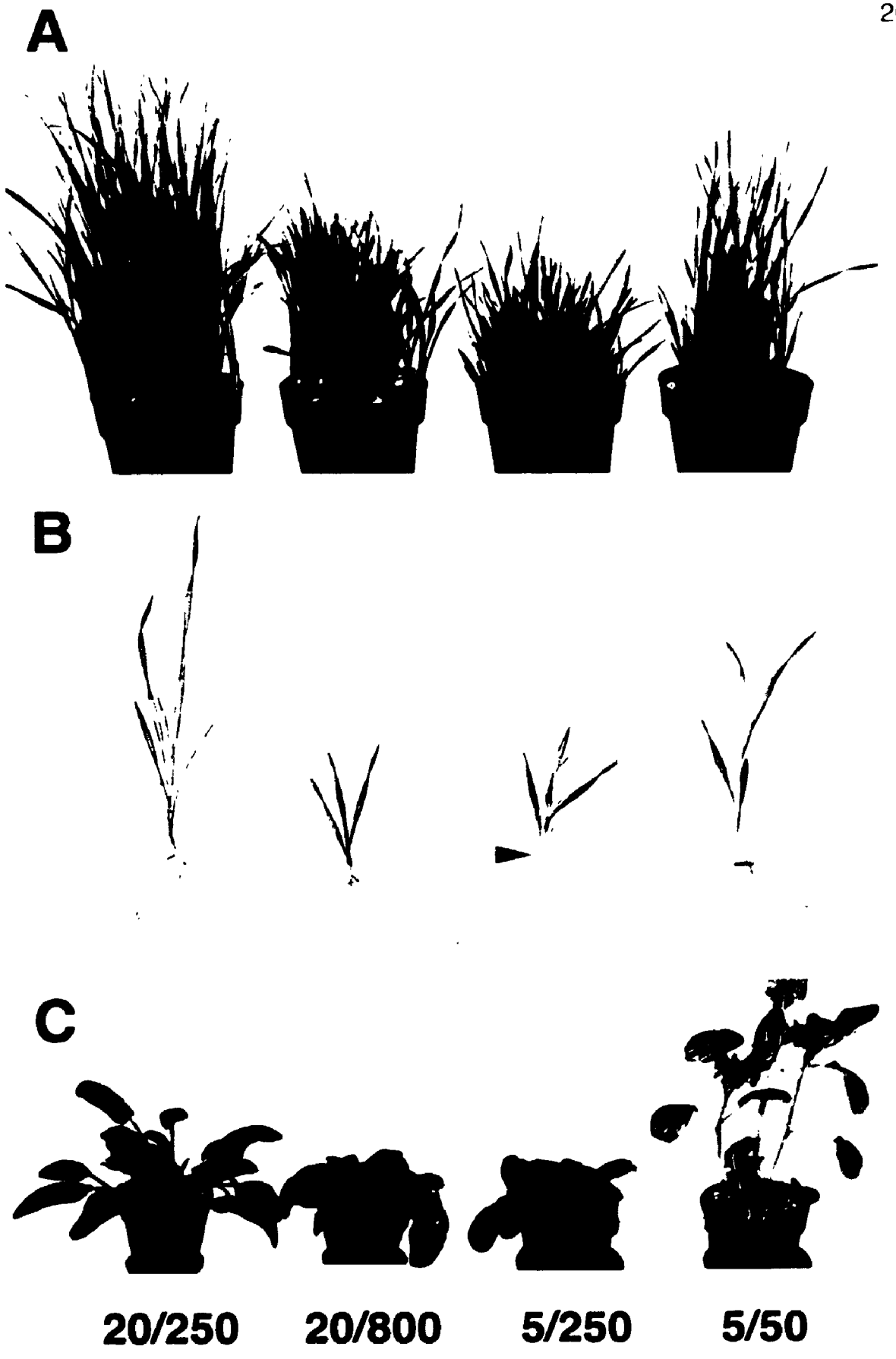
A
B
C
20/250
20/800
5/250
5/50

Table XXV. *Cellular osmolality in total leaf extracts of winter rye (S. cereale L. cv Musketeer).*

Measurements were made with a vapour pressure osmometer using sorbitol as a standard (Huner et al., 1981). All values represent means ± SE; $n = 3$.

Growth Regime (°C/µmol m^{-2} s^{-1})	Cellular Osmolality (mosmol)
20/800	575 ± 6
20/250	442 ± 3
20/50	451 ± 3
5/250	678 ± 12
5/50	579 ± 43

minimal difference was exhibited upon decreasing in the growth irradiance from 250 to 50 µmol m^{-2} s^{-1} at 5°C (Table XXV). However, increasing the growth irradiance from 50 to 800 µmol m^{-2} s^{-1} at 20°C resulted in a 1.3-fold increase in osmolality (Table XXV).

6.3.3 *Wcs19* mRNA Accumulation

RNA gel blot hybridization indicated that *Wcs19* mRNA levels were 37% higher in rye plants grown at 5/250 than those grown at 20/250 as shown in Figure 30A. Furthermore, the light-dependence of *Wcs19* accumulation was demonstrated by 49 and 25% decreases in mRNA levels with decreasing irradiance at either 20 or 5°C respectively (Fig. 30A). These data are consistent with previously published results (Chauvin et al., 1993). However, the level of *Wcs19* mRNA in 20/800 plants was similar (±10%) to that of the 5/250 cold-hardened plants, despite the fact that the former had not been exposed to low temperature. In addition, the accumulation of *Wcs19* mRNA for plants grown at 5/50 was similar (± 2%) to that of plants grown at 20/250 (Fig. 30A). Since the level of *Wcs19* mRNA accumulation is directly correlated ($r^2 = 0.91$) with $1\text{-}q_P$ (Fig. 31), the accumulation of *Wcs19* mRNA in rye appears to respond to PSII excitation pressure, rather than to either temperature or light *per se*.

6.3.4 *Wcs120* mRNA Accumulation

Accumulation of *Wcs120* mRNA for winter rye is indicated in Figure 32A.

Figure 30. *Wcs19* mRNA accumulation in total leaf extracts of winter rye (*S. cereale* L. cv Musketeer) developed at the temperature/irradiance regimes indicated. A molecular size marker in kb is indicated at the right. A, RNA gel blot. B, Ethidium bromide-stained gel. Blots were performed at least twice and similar results obtained with each experiment.

A

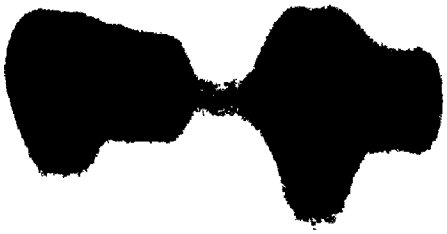

◂1.0

B

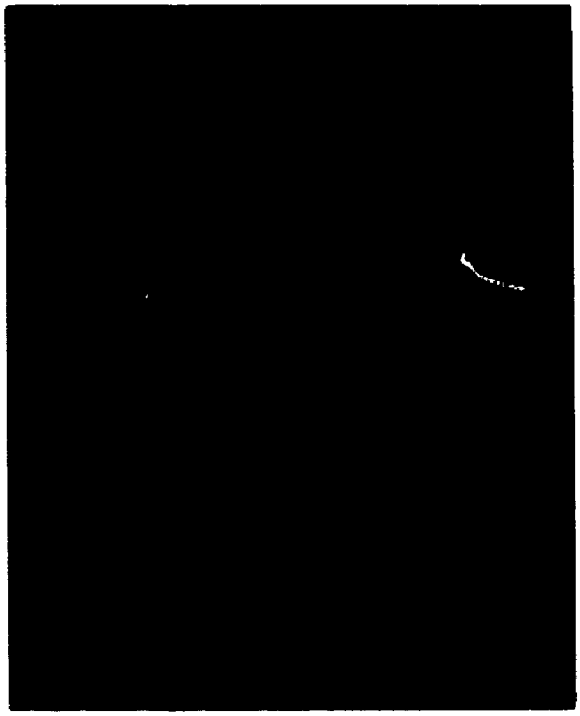

20/600 20/250 20/50 5/250 5/50

Figure 31. Correlation between *Wcs19* mRNA accumulation and 1-q_P in leaves of winter rye (*S. cereale* L. cv Musketeer). Development occurred at a temperature of 20°C (closed symbols) or 5°C (open symbols) with an irradiance of 800 (♦), 250 (●, ○) or 50 (■, □) µmol m^{-2} s^{-1} mRNA accumulation was quantified by densitometric scanning standardized to the 20/250 growth regime of blots with a shorter exposure time. 1-q_P was measured at the growth temperature and growth irradiance. Where indicated, values represent means ± SE; n = 3. When not present, error bars are smaller than symbol size. Regression analysis was performed in SigmaPlot® version 1.02 (Jandel Scientific, Corte Madera, CA USA).

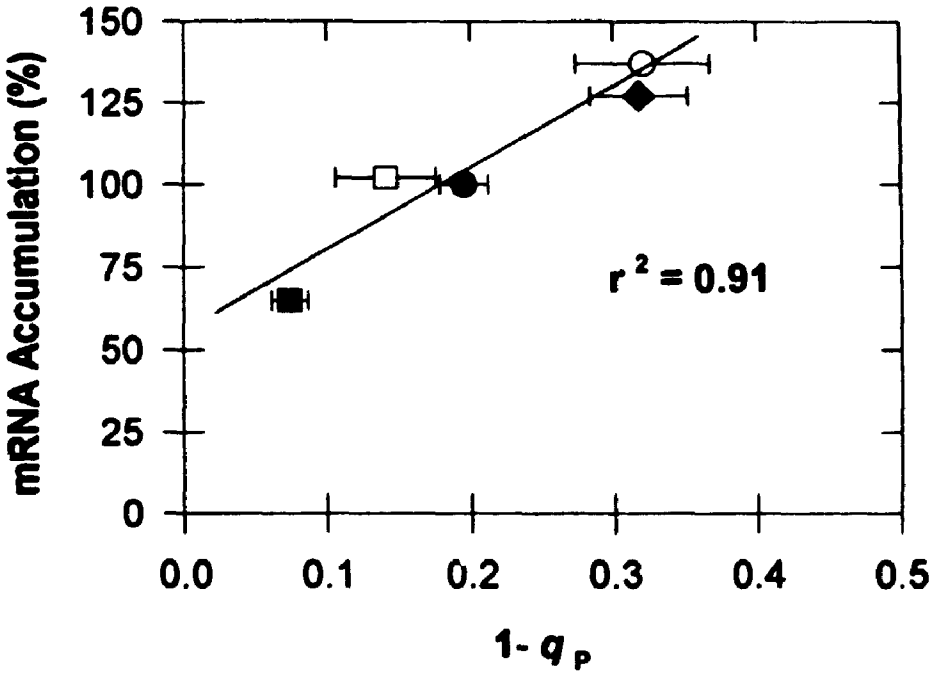
150
125
100
75
50
25
0
mRNA Accumulation (%)
0.0
0.1
0.2
0.3
0.4
0.5
1- q_P
$r^2 = 0.91$

Figure 32. *Wcs120* mRNA accumulation in total leaf extracts winter rye (*S. cereale* L. cv Musketeer) developed at the temperature/irradiance regimes indicated. Molecular size markers in kb are indicated at the right. A, RNA gel blot. B, Ethidium bromide-stained gel. Blots were performed at least twice and similar results obtained with each experiment. Blots were standardized to the 5/250 growth regime for quantification by densitometric scanning of blots with a shorter exposure time.

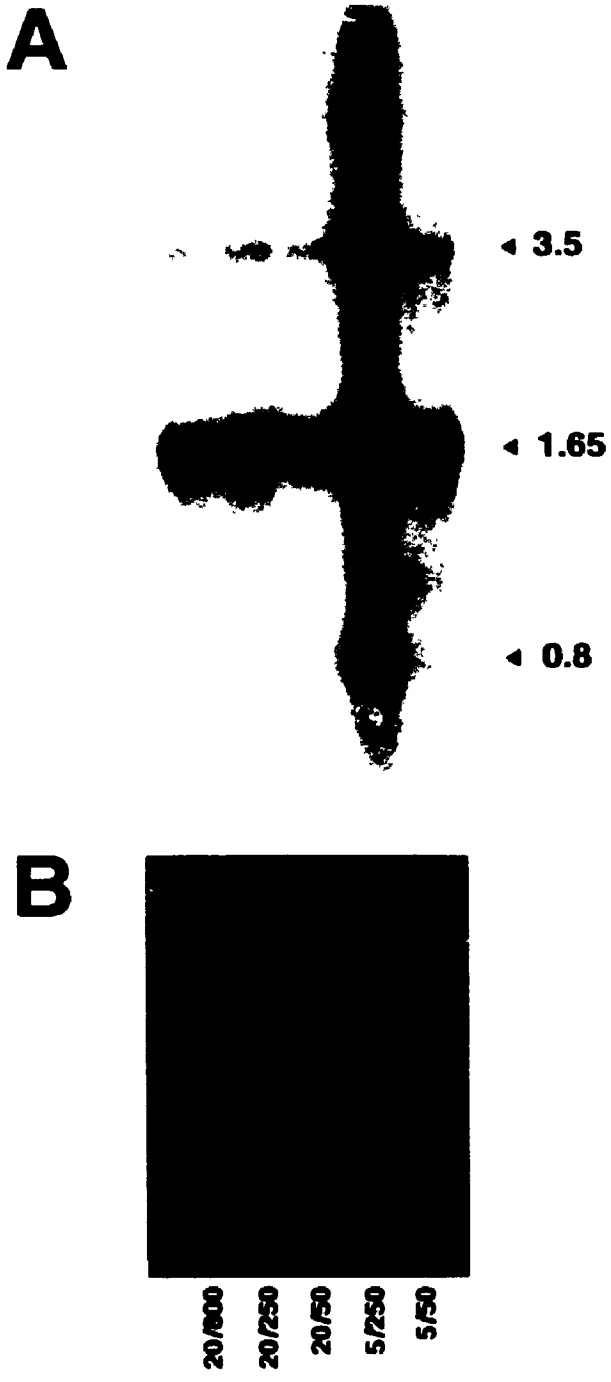
A
3.5
1.65
0.8
B
20/600
20/250
20/50
5/250
5/50

In contrast to *Wcs19*, the mRNA accumulation of *Wcs120* is greatest at 5/250. However, low levels (7 to 15%) can be observed at all the 20°C and the 5/50 growth regimes (Fig. 32A).

6.3.5 Abundance of the WCS120 Protein Family

The accumulation of the WCS120 protein family was also examined as a function of growth temperature and growth irradiance by immunoblot analysis with the anti-WCS120 antibody. Figure 33 indicates that high levels of the WCS120 family of polypeptides were detected upon growth solely at low temperature. However, growth at 5/50 resulted in a 80% decrease in the WCS120 protein family abundance in comparison to growth at 5/250 (Fig. 33). This is consistent with the mRNA accumulation presented in Figure 32A for the 5°C growth regimes. Thus, the WCS120 protein family in winter rye appears to be regulated by temperature alone.

6.3.6 Freezing Tolerance

As indicated in Figure 34, cold-hardened rye plants (5/250) exhibited a 2.6-fold greater freezing tolerance in comparison to non-hardened controls (20/250). However, at 5°C, decreasing growth irradiance from 250 to 50 µmol m^{-2} s^{-1} resulted in a 52% decrease in freezing tolerance (Fig. 34). In addition, the LT_{50} of plants grown at 20°C increased by 41% as a function of varying growth irradiance from 50 to 800 µmol m^{-2} s^{-1} (LT_{50} = -4.3 and -7.3°C respectively; Fig.

Figure 33. Immunological detection of the WCS120 protein family in total leaf extracts of winter rye (*S. cereale* L. cv Musketeer) developed at the temperature/irradiance regimes indicated. Molecular mass markers in kD are indicated at the right. Blots were performed at least twice and similar results obtained with each experiment. Blots were standardized to the 5/250 growth regime for quantification by densitometric scanning of blots with a shorter exposure time.

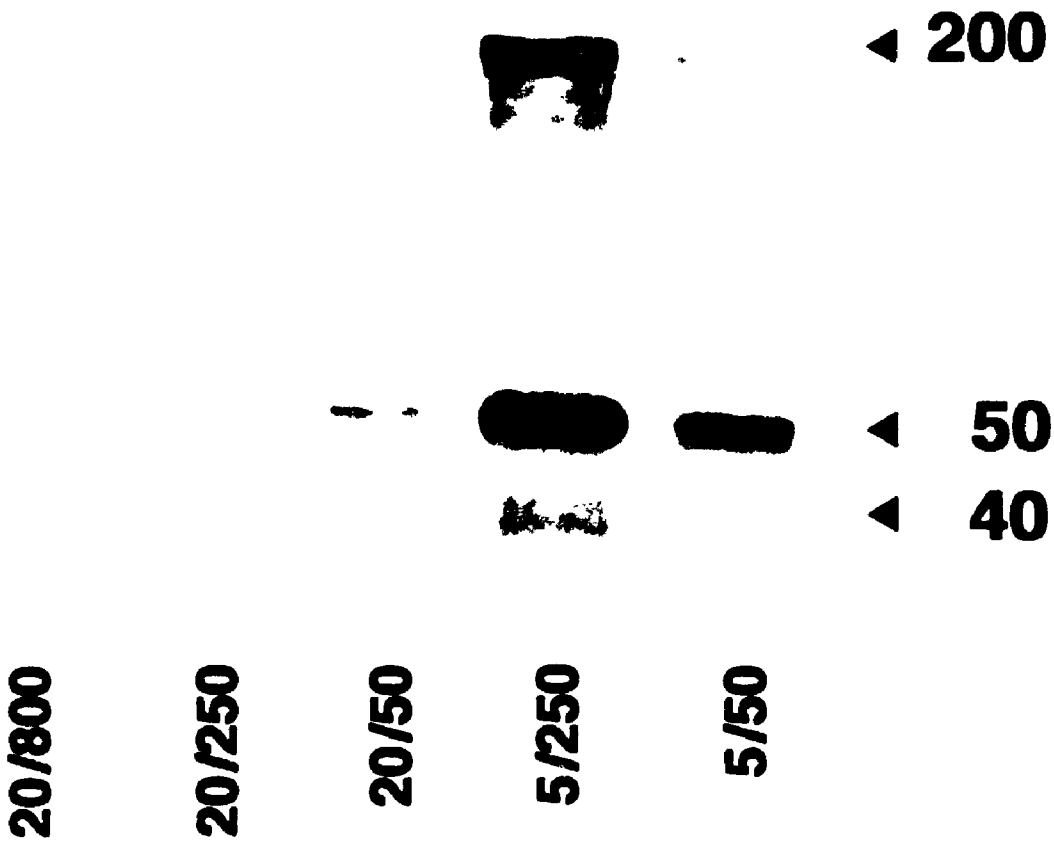
200
50
40
20/800
20/250
20/50
5/250
5/50

Figure 34. Freezing tolerance in leaves of winter rye (*S. cereale* L. cv Musketeer) developed at the temperature/irradiance regimes indicated. All values represent means ± SE; $n = 3$. When not present, error bars are smaller than symbol size.

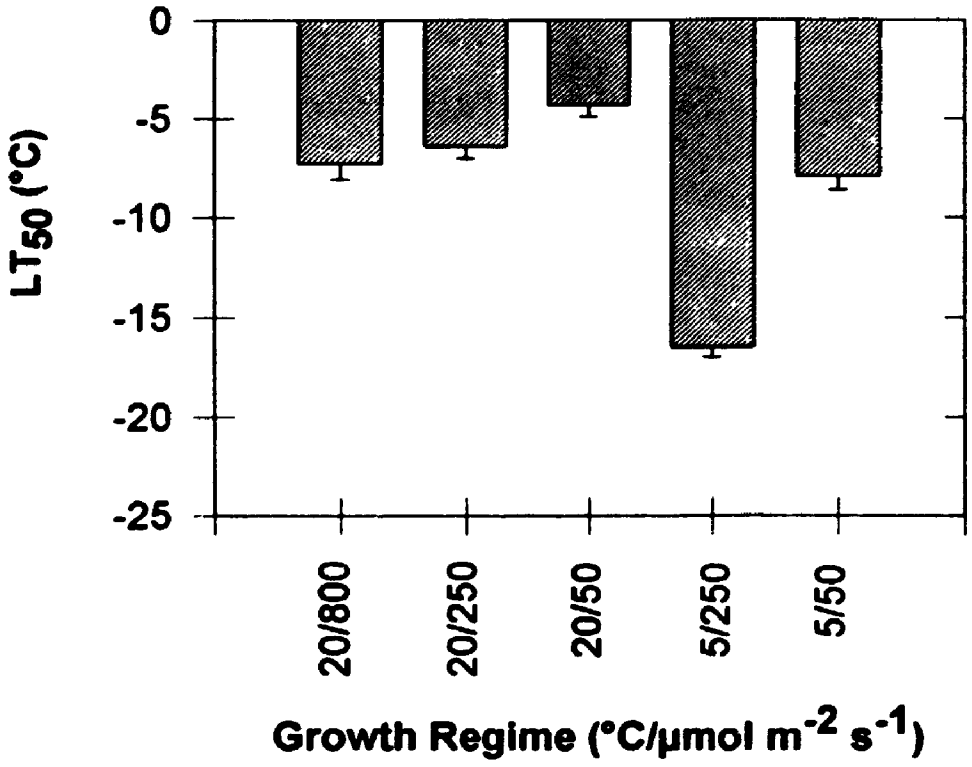
0
-5
-10
-15
-20
-25
LT50 (°C)
20/800
20/250
20/50
5/250
5/50
Growth Regime (°C/µmol m-2 s-1)

34). Although plants grown at 5/250 exhibited a similar PSII excitation pressure compared to those grown at 20/800, their LT_{50} were significantly different (Fig. 34). Thus, freezing tolerance does not appear to be regulated by PSII excitation pressure. Although the induction of freezing tolerance is dependent upon exposure to low temperature, the attainment of maximal freezing tolerance is clearly light-dependent. This is consistent with recent results of Griffith and McIntyre (1993).

6.4 Discussion

The data presented in previous chapters indicates that photosynthetic adjustment can be rationalized in terms of a response to PSII excitation pressure. I demonstrate with the results presented in this chapter that the reduction state of PSII, and thus PSII excitation pressure, also has a significant impact on plant growth habit. The sensing of light and signalling events in photomorphogenic development are typically associated with photoreceptors, such as phytochrome, as well as the B and UV photoreceptors (McNellis and Deng, 1995). However, the results I obtained with respect to the compact growth habit cannot be due to phytochrome for the following reasons. First, the compact growth habit was observed with no change in photoperiod or light quality (Fig. 28; Table XXIV). Second, the compact growth habit was induced in both monocotyledonous and dicotyledonous plants by simply decreasing the growth temperature from 20 to 5°C at constant irradiance.

While the control of growth habit can be explained as a response to PSII excitation pressure, it cannot explain the acquisition of freezing tolerance. Based on the classic morphological selection criterion of short, compact growth habit (Fowler et al., 1981; Roberts, 1984; Stushnoff et al., 1984; Blum, 1988), one would expect 20/800 plants to be as freezing tolerant as the 5/250 cold-hardened plants (Fig. 29A). However, the former were much less freezing tolerant than the latter (Fig. 34). This is consistent with the observation of increased crown size in the 5/250 grown plants in comparison to the 20/800 grown plants, despite the similarity in growth habit (Figure 29B). Thus, I have shown that the correlation between growth habit and freezing tolerance in herbaceous plants is serendipitous, and thus, should not be considered a reliable selection criterion by itself in breeding programmes for freezing tolerance.

Although freezing tolerance is clearly temperature-dependent, the attainment of maximal LT_{50} is light-dependent. Since plants grown at 20/800 and 5/250 exhibited similar PSII excitation pressures but quite different LT_{50}, I suggest that LT_{50} cannot be regulated by PSII excitation pressure. Instead, it appears to be regulated independently by both temperature and by light, but in an additive manner. These changes in LT_{50} are also parallelled by changes in cellular osmotic potential (Table XXV). Osmolality measurements reflect overall solute accumulation and demonstrate an independent temperature and light effect. In addition, these changes are observed regardless of the genetic

potential of the plant for the acquisition of freezing tolerance, as winter rye has the ability to develop a LT_{50} of -28°C. Since maximal LT_{50} is dependent upon both temperature and light (Fig. 34), I suggest that the physiology of the plant supercedes the genetic potential of the same plant in the ultimate expression of maximal freezing tolerance. I believe that this has very important implications for breeding programmes as well as research into the genetic engineering of freezing tolerant plants with respect to markers for selection purposes.

I have shown that rye grown at comparably high PSII excitation pressures (either 20/800 or 5/250) exhibited comparable levels of *Wcs19* mRNA accumulation. Similarly, rye grown at comparably low PSII excitation pressures (either 20/250 or 5/50) also exhibited comparable levels of *Wcs19* mRNA accumulation (Fig. 30A). These results cannot be explained on the basis of either growth temperature or growth irradiance alone. Alternatively, these results can be rationalized on the basis of PSII excitation pressure which integrates the combined effects of temperature and irradiance. Thus, rye plants which exhibit similar PSII excitation pressures also exhibit comparable levels of *Wcs19* mRNA accumulation (Fig. 30A). Therefore, I suggest that in rye, *Wcs19* is under PSII redox control rather than temperature or light *per se.*

Overall, these data indicate that the regulation of maximal freezing tolerance in herbaceous plants may be even more complicated than previously assumed. This process appears to result from the interactions of low temperature, light and redox dependent signals. In order to elucidate this

complex phenomenon, I believe that the contribution(s) of all three potential signals must be taken into consideration.

CHAPTER 7

SUMMARY

The proportion of closed PSII reaction centers, measured as $1\text{-}q_P$, is influenced by the rate of photochemical reduction of Q_A relative to the rate of oxidation of Q_A by intersystem electron transport and subsequent CO_2 assimilation. Therefore, the extent of PSII closure reflects the relative reduction state of Q_A, that is $[Q_{A\,red} / (Q_{A\,red} + Q_{A\,ox})]$. PSII closure is the consequence of an imbalance between the energy absorbed through photochemistry and energy either utilized through intersystem electron transport and carbon assimilation, or energy dissipated through non-photochemical processes (Dietz et al., 1985; Ögren, 1991; Dau, 1994a, 1994b; Huner et al., 1995; Maxwell et al., 1995a; 1995b; Huner et al., 1996; Savitch et al., 1996). Photoautotrophic organisms must constantly achieve this balance of overall energy supply and energy consumption through intersystem electron transport and cellular metabolism. Since the oxidation of PSII represents the rate-limiting step in the conversion of light energy to ATP and NADPH, any imbalance can be sensed through the modulation of the redox state of PSII (Huner et al., 1996).

The results presented in this thesis demonstrate that higher plants respond to PSII excitation pressure ($1\text{-}q_P$), as do green algae and cyanobacteria, but in a significantly different manner. The green alga *Chlorella vulgaris* adjusts to high PSII excitation pressure created either by growth at low temperature or at high irradiance by increasing the capacity for non-radiative dissipation of excess

excitation energy through Zx and lowering the probability of light absorption due to a decreased abundance of light-harvesting polypeptides (Maxwell et al.,1995a; 1995b). This occurs without any positive adjustment at the level of enzyme capacity and photosynthetic carbon assimilation (Savitch et al., 1996). In contrast, growth of winter cereals at high PSII excitation pressure results in an increase in Chl content and minimal changes in photosynthetic light-harvesting, with no significant changes in xanthophyll profiles. Furthermore, winter cereals appear to exhibit an enhanced PS_{max}, in part, as a consequence of increased SPS activity whereas *Chlorella* is unable to adjust at the level of the Suc biosynthetic pathway (Savitch et al., 1996).

The data presented demonstrate that the typical experimental design used to elucidate cold acclimation by comparing 20/250 and 5/250 plants is seriously flawed from a mechanistic point of view. Typically, the assumption which is made is that any differences observed in these cold-hardened plants compared to the non-hardened control plants are due to growth temperature effects. However, the previous reports for green algae (Maxwell et al., 1995a, 1995b), as well as the data presented in this thesis show that this assumption is invalid. I suggest that only by comparing physiological and molecular responses as a function of growth at high (5/250; 20/800) and low (5/50; 20/250) PSII excitation pressures can one separate the effects of temperature, light, and redox control.

This is particularly evident if one examines the photosynthetic data

presented in this thesis. In contrast to previous reports, I conclude that cold tolerant, herbaceous plants grown at 5/250 exhibit a greater tolerance to photoinhibition than plants grown at 20/250 not because of low growth temperature *per se*, but rather, as a consequence of growth under high PSII excitation pressure, and the subsequent photosynthetic adjustment which occurs. In addition, it has been reported that the ability of cereals to increase PS_{max} as a consequence of low growth temperature was correlated to their freezing tolerance, with spring cereals being less able to adjust PS_{max} than winter cereals (Öquist et al., 1993a). The results in this thesis are consistent with this report. However, I also demonstrate that SPS activity is sensitive to growth irradiance as well as growth temperature. These data indicate that spring and winter wheat exhibit a differential capacity to adjust photosynthetic carbon metabolism to growth irradiance, as well as growth temperature.

I believe that the experimental design presented in this thesis is valid for any environmental stress condition and should not be confined to low temperature responses. Light, the ultimate source of energy for all processes in photoautotrophs, enters the biological system through the chloroplast. Although light is essential, excessive excitation is detrimental to all photoautotrophs. Therefore, photosynthetic organisms must constantly balance energy absorbed through the photosynthetic apparatus with energy utilized through metabolism. All environmental stresses have the potential to upset this balance and alter redox poise (Huner et al., 1995; 1996). Therefore, it has been suggested that

the redox state of PSII, measured as $1\text{-}q_P$ reflects overall chloroplastic redox poise (Huner et al., 1996). Based on this assumption, I suggest that a photosynthetically generated redox signal may be the first component in a redox sensing/signalling pathway, synergistic to other signal transduction pathways which may trigger an integrated stress response. Thus, the photosynthetic apparatus is not only involved in energy transduction, but should also be considered an important sensor, capable of detecting alterations in the environment through changes in chloroplastic redox poise as illustrated in Figure 35.

The green alga *Dunaliella salina* responds at the level of gene expression to PSII excitation pressure with respect to *cab* mRNA abundance which is a product of nuclear-encoded genes (Escoubas et al., 1995; Maxwell et al. 1995b). The data presented in this thesis also provides evidence that this redox signal affects nuclear gene expression. By examining two genes associated with cold acclimation, I have demonstrated that one (*Wcs19*) is responsive to PSII excitation pressure and not low temperature *per se*. This provides further evidence for the experimental design adopted in this thesis. Further, it calls to question the actual relevance of these genes to the process of cold acclimation and their precise role in freezing tolerance. In addition, overall plant growth habit is affected by PSII excitation pressure and chloroplastic redox poise. Clearly, a developmental response such as this would require the temporal and spatial expression of a large number of genes. Thus, I believe chloroplastic redox

Figure 35. Proposed sequence of events in chloroplastic redox signal transduction associated with environmental stress responses.

In photoautotrophic organisms, light energy is absorbed by the photosynthetic apparatus and transduced through a series of thylakoid membrane redox reactions to produce chemical energy (ATP) and reducing equivalents (NADPH). PSII excitation pressure is a measure of the redox state of Q_A and is equal to $Q_{A\,red} / (Q_{A\,red} + Q_{A\,ox})$. This reflects the redox poise of intersystem electron transport and photosynthetic carbon metabolism. Environmental stress of any type is sensed by the plant through an imbalance in chloroplastic redox poise which is induced by a decreased ability to utilize absorbed energy through metabolism. Chloroplastic redox poise has been shown to regulate chloroplastic gene expression (Allen et al., 1995a; Danon and Mayfield, 1994). In addition, a photosynthetically generated redox signal is transduced to the nucleus which results in altered expression of nuclear genes such as *Wcs19* in winter rye and *cab* in green algae (Escoubas et al., 1995; Maxwell et al., 1995b). Regulation by chloroplastic redox poise as reflected by changes in PSII excitation pressure extends beyond photosynthetic acclimation and influences the growth habit of cold tolerant, herbaceous plants.

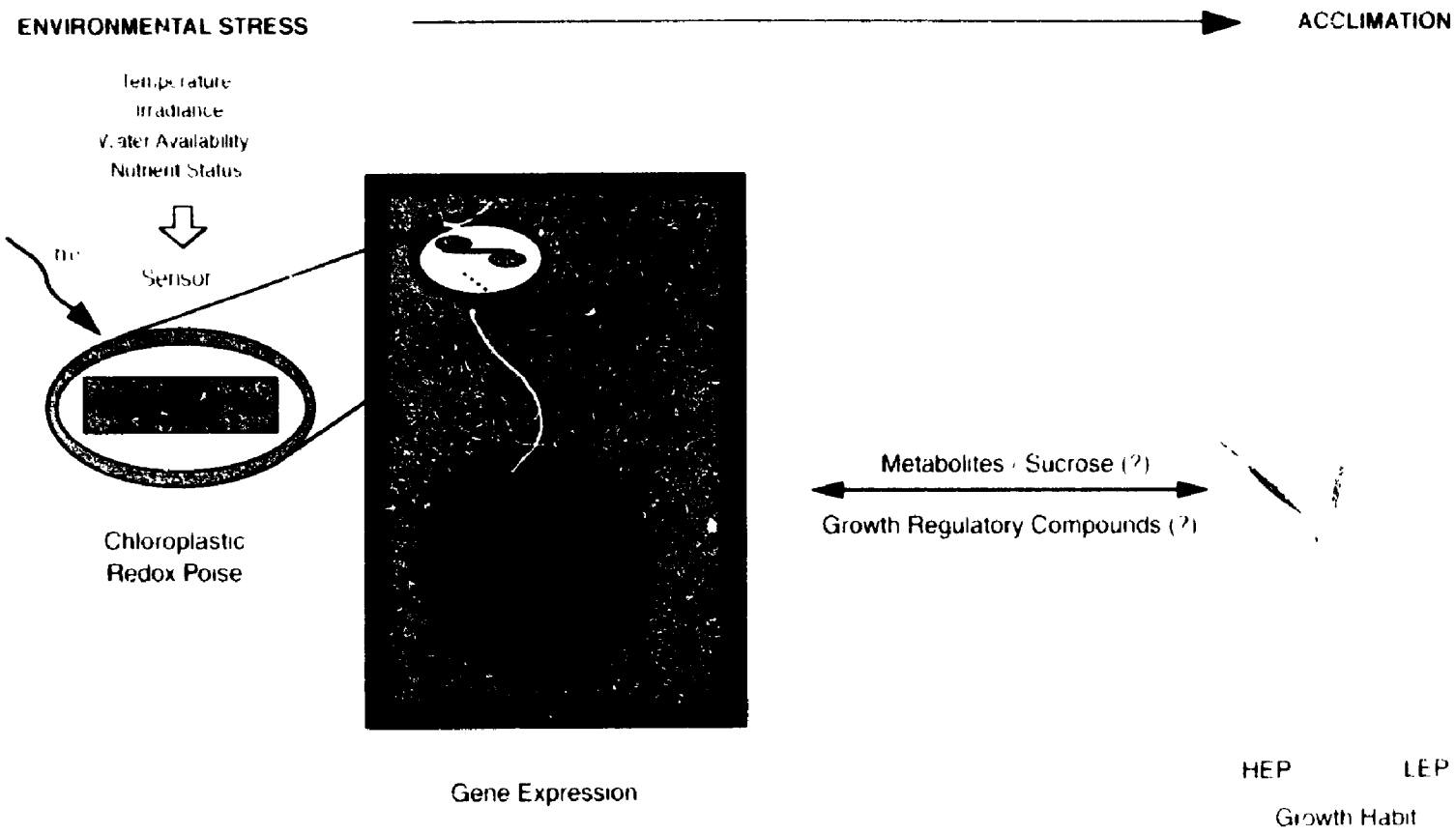
ENVIRONMENTAL STRESS
ACCLIMATION
Temperature
Irradiance
Water Availability
Nutrient Status
Sensor
Chloroplastic
Redox Poise
Metabolites - Sucrose (?)
Growth Regulatory Compounds (?)
Gene Expression
HEP
LEP
Growth Habit

control may play a significant role in development, providing the appropriate cues, sensed from the prevailing environment (Anderson et al., 1995).

However, relatively little is known with respect to the complex mechanisms involved in plant signal transduction in comparison to other well studied systems (Trewavas and Gilroy, 1991; Verhey and Lomax, 1993; Bowler and Chua, 1994). Recent studies involving low-temperature signal transduction in alfalfa have demonstrated the induction of *c*old-*a*cclimation-*s*pecific (*cas*) genes at 25°C by simply providing a transitory influx of extracellular calcium, confirming its role in the transduction pathway (Monroy and Dhindsa, 1995). Redox regulation as a mechanism of translational control has been implicated in components of photosynthetic and mitochondrial electron transport chains (Kim et al., 1993; Allen et al., 1995a, 1995b; Levings and Siedow, 1995; Vanlerberghe et al., 1995) and PSII core polypeptides (Danon and Mayfield, 1994). Furthermore, two-component redox sensing/signalling mechanisms previously assumed to be prokaryotic specific (Bourret et al., 1991; Iuchi and Lin, 1993; Parkinson, 1993) have been reported in eukaryotes such as yeast and higher plants (Chang et al., 1993; Ota and Varshavsky, 1993; Alex and Simon, 1994; Hughes, 1994; Maeda et al., 1994; Braun and Walker, 1996; Chang, 1996).

In this thesis I show that cold acclimation is a complex process, influenced not only by temperature, but also by light and chloroplastic redox poise. In addition, regulation by chloroplastic redox poise extends beyond photosynthetic acclimation and influences plant growth habit and the expression of a gene

thought to be involved in the cold acclimation process. Therefore, I suggest that acclimation of photoautotrophs to temperature, light, or any environmental stress, share a common redox sensing/signalling mechanism which may be integrated with other signal transduction pathways to elicit the appropriate physiological and molecular responses to the environment. Clearly, any attempts to increase levels of freezing tolerance or the tolerance to any abiotic stress must take into account the complexity of the interaction between abiotic stresses such as temperature, nutrient status, water availability and the fundamental energy source for all photoautotrophs, light.

LITERATURE CITED

Adams WW III, Demmig-Adams B (1995) The xanthophyll cycle and sustained thermal energy dissipation activity in *Vinca minor* and *Euonymus kiautschovicus* in winter. Plant Cell Environ **18:** 117-127

Adams WW III, Demmig-Adams B, Verhoeven AS, Barker DH (1995a) 'Photoinhibition' during winter stress: Involvement of sustained xanthophyll cycle-dependent energy dissipation. Aust J Plant Physiol **22:** 261-276

Adams WW III, Demmig-Adams B, Winter K, Schreiber U (1990) The ratio of variable to maximal fluorescence from photosystem II, measured in leaves at ambient temperature and at 77K, as an indicator of the photon yield of photosynthesis. Planta **180:** 166-174

Adams WW III, Hoehn A, Demmig-Adams B (1995b) Chilling temperatures and the xanthophyll cycle. A comparison of warm-grown and overwintering spinach. Aust J Plant Physiol **22:** 75-85

Adams WW III, Terashima I, Brugnoli E, Demmig B (1988) Comparisons of photosynthesis and photoinhibition in the CAM vine *Hoya australis* and several C_3 vines growing on the coast of eastern Australia. Plant Cell Environ **11:** 173-181

Alex LA, Simon MI (1994) Protein histidine kinases and signal transduction in prokaryotes and eukaryotes. Trends Genet **10:** 133-138

Allen JF (1995a) Thylakoid protein phosphorylation, state 1-state 2 transitions, and photosystem stoichiometry adjustment: redox control at multiple levels of gene expression. Physiol Plant **93:** 196-205

Allen JF, Alexciev K, Håkansson G (1995b) Regulation by redox signalling. Curr Biol **5:** 869-872

Anderson JM (1986) Photoregulation of the composition, function, and structure of thylakoid membranes. Annu Rev Plant Physiol **37:** 93-136

Anderson JM, Chow WS, Park Y-I (1995) The grand design of photosynthesis: Acclimation of the photosynthetic apparatus to environmental cues. Photosynth Res **46:** 129-139

Andersson B, Barber J (1994) Composition, organization, and dynamics of thylakoid membranes. *In* EE Bittar, J Barber, eds, Advances in Molecular and

Cell Biology, Molecular Processes of Photosynthesis, Vol 10. JAI Press Inc., London, pp 1-53

Andersson B, Styring S (1991) Photosystem II: Molecular organization, function and acclimation. In Krogmann, ed, Current Topics in Bioenergetics, Vol 16. Academic Press, New York, pp 1-81

Andréasson L-E, Vänngård T (1988) Electron transport in photosystem I and II. Ann Rev Plant Physiol Plant Mol Biol **39:**379-411

Arnon DI (1949) Copper enzymes in isolated chloroplasts: Polyphenoloxidase in *Beta vulgaris*. Plant Physiol **24:**1-15

Arnon DI, Tsujimoto HY, Tang GM-S (1981) Proton transport in photooxidation of water: A new perspective on photosynthesis. Proc Natl Acad Sci USA **78:** 2942-2946

Aro E-M, McCaffery S, Anderson JM (1993a) Photoinhibition and D1 degradation in peas acclimated to different growth irradiances. Plant Physiol **103:** 835-843

Aro E-M, Virgin I, Andersson B (1993b) Photoinhibition of photosystem II. Inactivation, protein damage and turnover. Biochim Biophys Acta **1143:** 113-134

Asada K (1994) Production and action of active oxygen species in photosynthetic tissues. *In* CH Foyer, PM Mullineaux, eds, Causes of Photooxidative Stress and Amelioration of Defense Systems in Plants. CRC Press, Boca Raton, pp 77-104

Asada K, Heber U, Schreiber U (1992) Pool size of electrons that can be donated to $P700^+$, as determined in intact leaves: Donation to $P700^+$ from stromal components via the intersystem chain. Plant Cell Physiol **33:** 927-932

Baker NR, Long SP, Ort DR (1988) Photosynthesis and temperature with particular reference to the effects of quantum yield. *In* SP Long, FI Woodward, eds, Plants and Temperature. Cambridge University Press, Cambridge, pp 347-375

Barber J, De Las Rivas J (1993) A functional model for the role of cytochrome b_{559} in the protection against doner and acceptor side photoinhibition. Proc Natl Acad Sci USA **90:** 10942-10946

Baroli I, Melis A (1996) Photoinhibition and repair in *Dunaliella salina*

acclimated to different growth irradiances. Planta **198:** 640-646

Bassi R, Rigoni F, Giacometti GM (1990) Chlorophyll binding proteins with antenna function in higher plants and green algae. Photochem Photobiol **52:**1187-1206

Berry J, Björkman O (1980) Photosynthetic response and adaptation to temperature in higher plants. Ann Rev Plant Physiol **31:** 491-453

Bilger W, Björkman O (1990) Role of the xanthophyll cycle in photoprotection elucidated by measurements of light-induced absorbance changes, fluorescence and photosynthesis in leaves of *Hedera canariensis*. Photosynth Res **25:** 173-185

Bilger W, Schreiber U (1986) Energy-dependent quenching of dark-level chlorophyll fluorescence in intact leaves. Photosynth Res **10:** 303-308

Björkman O, Demmig B (1987) Photon yield of O_2 evolution and chlorophyll fluorescence characteristics at 77K among vascular plants of diverse origins. Planta **170:** 489-504

Blum. A (1988) Plant Breeding for Stress Environments. CRC Press, Boca Raton

Boekema EJ, Hankamer B, Bald D, Kruip J, Nield J, Boonstra AF, Barber J, Rögner M (1995) Supramolecular structure of the photosystem II complex from green plants and cyanobacteria. Proc Natl Acad Sci USA **92:** 175-179

Boese SR, Huner NPA (1990) Effect of growth temperature and temperature shifts on spinach leaf morphology and photosynthesis. Plant Physiol **94:** 1830-1836

Boese SR, Huner NPA (1992) Developmental history affects the susceptibility of spinach leaves to *in vivo* low temperature photoinhibition. Plant Physiol **99:** 1141-1145

Bolhar-Nordenkampf HR, Hofler M, Lechner EG (1991) Analysis of light-induced reduction of photochemical capacity in field-grown plants. Evidence for photoinhibition? Photosynth Res **27:** 31-39

Bourret RB, Borkovich KA, Simon MI (1991) Signal transduction pathways involving protein phosphorylation in prokaryotes. Annu Rev Biochem **60:** 401-441

Bowler C, Chua N-H (1994) Emerging themes of plant signal transduction. Plant Cell **6:** 1529-1541

Bradbury M, Baker NR (1981) Analysis of the slow phases of the in vivo chlorophyll fluorescence induction curve. Changes in the redox state of photosystem II electron acceptors and fluorescence emission from photosystem I and II. Biochim Biophys Acta **63:** 542-551

Braun DM, Walker JC (1996) Plant transmembrane receptors: new pieces in the signaling puzzle. Trends Biochem Sci **21:** 70-73

Browse J, McCourt P, Somerville CR (1985) A mutant of Arabidopsis lacking a chloroplast-specific lipid. Science **227:** 763-765

Brush RA, Griffith M, Mlynarz A (1994) Characterization and quantification of intrinsic ice nucleators in winter rye (*Secale cereale*) leaves. Plant Physiol **104:** 725-735

Burkey KO (1993) Effect of growth irradiance on plastocyanin levels in barley. Photosynth Res **36:** 103-110

Butler WL (1978) Energy distribution in the photochemical apparatus of photosynthesis. Ann Rev Plant Physiol **29:** 345-378

Butler WL, Kitajima M (1975) Fluorescence quenching of photosystem II of chloroplasts. Biochim Biophys Acta **376:** 116-125

Chang C (1996) The ethylene signal transduction pathway in *Arabidopsis*: an emerging paradigm? Trends Biochem Sci **21:** 129-133

Chang C, Kwok SF, Bleecker AB, Meyerowitz EM (1993) *Arabidopsis* ethylene-response gene *ETR1*: Similarity of product to two-component regulators. Science **262:** 539-544

Chauvin LP, Houde M, Sarhan F (1993) A leaf-specific gene stimulated by light during wheat acclimation to low temperature. Plant Mol Biol **23:** 255-265

Chauvin LP, Houde M, Sarhan F (1994) Nucleotide sequence of a new member of the freezing tolerance-associated protein family in wheat. Plant Physiol **105:** 1017-1018

Chitnis PR (1996) Photosystem I. Plant Physiol **111:** 661-669

Chow WS (1994) Photoprotection and photoinhibitory damage. *In* EE Bittar, J Barber, eds, Advances in Molecular and Cell Biology, Molecular Processes of Photosynthesis, Vol 10. JAI Press Inc., London, pp 151-196

Chow WS, Osmond CB, Huang LK (1989) Photosystem II function and herbicide binding sites during photoinhibition of spinach chloroplasts *in vivo* and *in vitro*. Photosynth Res **21:** 17-26

Cleland RE, Melis A (1987) Probing the events of photoinhibition by altering electron-transport activity and light harvesting capacity in chloroplast thylakoids. Plant Cell Environ **10:** 747-752

Correia MJ, Chaves MMC, Pereira JS (1990) Afternoon depression in photosynthesis in grapevine leaves - Evidence for a high light stress effect. J Exp Bot **255:** 417-426

Critchley C, Russell AW (1994) Photoinhibition of photosynthesis in vivo: The role of protein turnover in photosystem II. Physiol Plant **92:** 188-196

Crofts AR, Yerkes CT (1994) A molecular mechanism for q_E-quenching. FEBS Lett **352:** 265-270

Crosatti C, Soncini C, Stanca AM, Cattivelli L (1995) The accumulation of a cold-regulated chloroplastic protein is light-dependent. Planta **196:** 458-463

Danon A, Mayfield SP (1994) Light-regulated translation of chloroplast messenger RNAs through redox potential. Science **266:** 1717-1719

Danyluk J, Houde M, Rassart É, Sarhan F (1994) Differential expression of a gene encoding an acidic dehydrin in chilling sensitive and freezing tolerant gramineae species. FEBS Lett **344:** 20-24

Danyluk J, Sarhan F (1990) Differential mRNA transcription during the induction of freezing tolerance in spring and winter wheat. Plant Cell Physiol **31:** 609-619

Dau H (1994a) Short-term adapatation of plants to changing light intensities and its relation to photosystem II photochemistry and fluorescence emission. J Photochem Photobiol B: Biol **26:** 3-27

Dau H (1994b) Molecular mechanisms and quantitative models of variable photosystem II fluorescence. J Photochem Photobiol **60:** 1-23

Delieu T, Walker DA (1981) Polarographic measurement of photosynthetic

oxygen evolution by leaf discs. New Phytol **89:** 165-178

Demeter S, Neale PJ, Melis A (1987) Photoinhibition: Impairment of the primary charge separation between P_{680} and pheophytin in photosystem II of Chloroplasts. FEBS Lett **214:** 370-374

Demmig-Adams B (1990) Carotenoids and photoprotection in plants: A role for the xanthophyll zeaxanthin. Biochim Biophys Acta **1020:**1-24

Demmig-Adams B, Adams WW III (1992) Photoprotection and other responses of plants to high light stress. Annu Rev Plant Physiol Plant Mol Biol **43:** 599-626

Demmig-Adams B, Adams WW III (1996) The role of xanthophyll cycle carotenoids in the protection of photosynthesis. Trends Plant Sci **1:** 21-26

Demmig-Adams B, Adams WW III, Logan BA, Verhoeven AS (1995) Xanthophyll cycle-dependent energy dissipation and flexible photosystem II efficiency in plants acclimated to light stress. Aust J Plant Physiol **22:** 249-260

Demmig-Adams B, Gilmore AM, Adams WW III (1996) In vivo functions of carotenoids in higher plants. FASEB J **10:** 403-412

Dexter ST (1933) Effects of several environmental factors on the hardening of plants. Plant Physiol **8:**123-139

Dexter ST, Tottingham LF, Graber LF (1932) Investigations of hardiness of plants by measurement of electrical conductivity. Plant Physiol **7:** 63-78

Dhindsa RS, Monory AF, Wolfraim LA, Dong G (1993) Signal transduction and gene expression during cold acclimation of alfalfa. *In* PH Lee, L Christersson eds, Advances in Plant Cold Hardiness. CRC Press, Boca Raton, pp 57-71

Di Marco G, Iannelli MA, Loreto F (1994) Relationship between photosynthesis and photorespiration in field-grown wheat leaves. Photosynthetica **30:** 45-51

Diaz M, Ball E, Lüttge U (1990) Stress-induced accumulation of the xanthophyll rhodoxanthin in leaves of *Aloe vera*. Plant Physiol Biochem **28:** 679-682

Dietz K-J, Schreiber U, Heber U (1985) The relationship between the redox state of Q_A and photosynthesis in leaves at various carbon-dioxide, oxygen and light regimes. Planta **166:** 219-226

Dilley RA, Theg SM, Beard WA (1987) Membrane-proton interactions in chloroplast bioenergetics: Localized proton domains. Ann Rev Plant Physiol **38**:347-389

Dubacq JP, Trémolières A (1983) Occurance and function of phosphatidylglycerol containing 3-trans-hexadecenoic acid in photosynthetic lamellae. Physiol Veg **21:** 293-312

Dujardyn M, Foyer CH (1989) Limitation of CO_2 assimilation and regulation of Benson-Calvin cycle activity in barley leaves in response to changes in irradiance, photoinhibition, and recovery. Plant Physiol **91:** 1562-1568

Dunn SD, Tozer RG, Antczak DF, Heppel LA (1985) Monoclonal antibodies to *Escherichia coli* F_1-ATPase. Correlation of binding site location with interspecies cross-reactivity and effects on enzyme activity. J Biol Chem **260:** 10418-10425

Escoubas J-M, Lomas M, LaRoche J, Falkowski PG (1995) Light intensity regulation of *cab* gene transcription is signalled by the redox state of the plastoquinone pool. Proc Natl Acad Sci USA **92:** 10237-10241

Faibel TG, Staehelin LA (1992) Species-related differences in the electrophoretic behaviour of CP29 and CP26: an immunochemical analysis. Photosynth Res **34:** 249-262

Feinberg AP, Vogelstein B (1983) A technique for radiolabeling DNA restriction endonuclease fragments to high specific activity. Anal Biochem **132:** 6-13

Feinberg AP, Vogelstein B (1984) Addendum "A technique for radiolabeling DNA restriction endonuclease fragments to high specific activity". Anal Biochem **137:** 266-267

Fork DC, Herbert SK (1993) Electron transport and photophosphorylation by photosystem I in vivo in plants and cyanobacteria. Photosynth Res **36:** 149-168

Fork DC, Satoh K (1986) The control by state transitions of the distribution of excitation energy in photosynthesis. Ann Rev Plant Physiol **37:** 335-361

Fowler DB, Gusta LV, Tyler NJ (1981) Selection for winter hardiness in wheat. III. Screening methods. Crop Sci **21:** 896-901

Foyer C, Furbank R, Harbinson J, Horton P (1990) The mechanisms contributing to photosynthetic control of electron transport by carbon assimilation in leaves. Photosynth Res **25:** 83-100

Foyer CH, Hall DO (1980) Oxygen metabolism in the active chloroplast. Trends Biochem Sci **5**:188-191

Frank HA, Cua A, Chynwat V, Young A, Gosztola D, Wasielewski MR (1994) Photophysics of the carotenoids associated with the xanthophyll cycle in photosynthesis. Photosynth Res **41:** 389-395

Garnier J, Wu B, Maroc J, Guyon D, Trémolières A (1990) Regulation of both an oligomeric form of the light-harvesting antenna CPII and a fluorescence state II - state I transition by ^{3}-trans-hexadecenoic acid containing pnosphatidylglycerol, in cells of a mutant of *Chlamydomonas reinhardtii*. Biochim Biophys Acta **1020:** 153-162

Genty B, Briantais J-M, Baker NR (1989) The relationship between the quantum yield of photosynthetic electron transport and quenching of chlorophyll fluorescence. Biochim Biophys Acta **990:** 87-92

Ghanotakis DF, Yocum CF (1990) Photosystem II and the oxygen-evolving complex. Ann Rev Plant Physiol Plant Mol Biol **41:** 255-276

Ghosh S, Hudak KA, Dumbroff EB, Thompson JE (1994) Release of photosynthetic protein catabolites by blebbing from thylakoids. Plant Physiol **106:** 1547-1553

Giersch C, Krause GH (1991) A simple model relating photoinhibitory fluorescence quenching in chloroplasts to a population of altered photosystem II reaction centers. Photosynth Res **30:** 115-121

Gilmore AM, Hazlett TL, Govindjee (1995) Xanthophyll cycle-dependent quenching of photosystem II chlorophyll *a* fluorescence: Formation of a quenching complex with a short fluorescence lifetime. Proc Natl Acad Sci USA **92:** 2273-2277

Gilmore AM, Yamamoto HY (1991) Resolution of lutein and zeaxanthin using a non-endcapped, lightly carbon-coated C_{18} high-performance liquid chromatographic column. J Chromatogr **543:** 137-145

Gilmore AM, Yamamoto HY (1992) Dark induction of zeaxanthin-dependent nonphotochemical fluorescence quenching mediated by ATP. Proc Natl Acad Sci USA **89:** 1899-1903

Gilmore AM, Yamamoto HY (1993) Linear models relating xanthophylls and lumen acidity to non-photochemical fluorescence quenching. Evidence that

antheraxanthin explains zeaxanthin-independent quenching. Photosynth Res **35:** 67-78

Golbeck JH (1992) Structure and function of photosystem I. Annu Rev Plant Physiol Plant Mol Biol **43:** 293-324

Gong H, Nilsen S (1989) Effect of temperature on photoinhibition of photosynthesis, recovery, and turnover of the 32 kD chloroplast protein in *Lemna gibba*. J Plant Physiol **135:** 9-14

Graan T, Ort DR (1984) Quantitation of the rapid electron donors to P_{700}, the functional plastoquinone pool, and the ratio of the photosystems in spinach chloroplasts. J Biol Chem **259:** 14003-14010

Gray GR, Boese SR, Huner NPA (1994) A comparison of low temperature growth vs low temperature shifts to induce resistance to photoinhibition in spinach (*Spinacia oleracea*). Physiol Plant **90:** 560-566

Greenberg BM (1991) Photosynthesis. *In* Encyclopedia of Food Science and Technology. John Wiley & Sons Inc., New York, pp 2065-2073

Greer DH (1990) The combined effects of chilling and light stress on photoinhibition of photosynthesis and its subsequent recovery. Plant Physiol Biochem **28:** 447-455

Greer DH, Berry JA, Björkman O (1986) Photoinhibition of photosynthesis in intact bean leaves: Role of light and temperature and requirement of chloroplast-protein synthesis during recovery. Planta **168:** 253-260

Greer DH, Öttander C, Öquist G (1991) Photoinhibition and recovery of photosynthesis in intact barley leaves at 5 and 20°C. Physiol Plant **81:** 203-210

Griffith M, Brown GN, Huner NPA (1982) Structural changes in thylakoid proteins during cold acclimation and freezing of winter rye (*Secale cereale* L. cv. Puma). Plant Physiol **70:** 418-423

Griffith M, Elfman B, Camm EL (1984) Accumulation of plastoquinone A during low temperature growth of winter rye. Plant Physiol **74:** 727-729

Griffith M, McIntyre HCH (1993) The interrelationship of growth and frost tolerance in winter rye. Physiol Plant **87:** 335-344

Groom QJ, Kramer DM, Crofts AR, Ort DR (1993) The non-photochemical

reduction of plastoquinone in leaves. Photosynth Res **36:** 205-215

Gusta LV, Chen THH (1987) The physiology of water and temperature stress. *In* EG Heyne, ed, Wheat and Wheat Improvement, Ed 2. ASA, CSSA, SSSA Inc., pp 115-150

Gusta LV, Fowler DB, Tyler NJ (1982) Factors influencing hardening and survival in winter wheat. *In* PH Li, A Sakai, eds, Plant Cold Hardiness and Freezing Stress. Mechanisms and Crop Implications, Vol 2. Academic Press, New York, pp 23-40

Guy CL (1990) Cold acclimation and freezing stress tolerance: Role of protein metabolism. Annu Rev Plant Physiol Plant Mol Biol **41:** 187-223

Guy CL, Huber JLA, Huber SC (1992) Sucrose phosphate synthase and sucrose accumulation at low temperature. Plant Physiol **100:** 502-508

Guy CL, Nieme KJ, Brambl J (1985) Altered gene expression during cold acclimation of spinach. Proc Natl Acad Sci USA **82:** 3673-3677

Haehnel W (1984) Photosynthetic electron transport in higher plants. Annu Rev Plant Physiol **35:** 659-693

Hansson Ö, Wydrzynski T (1990) Current perceptions of photosystem II. Photosynth Res **23:** 131-162

Harbinson J, Genty B, Baker NR (1990) The relationship between CO_2 assimilation and electron transport in leaves. Photosynth Res **25:** 213-224

Harbinson J, Hedley CL (1989) The kinetics of P-700$^+$ reduction in leaves: a novel *in situ* probe of thylakoid functioning. Plant Cell Environ **12:** 357-369

Harbinson J, Woodward FI (1987) The use of light-induced absorbance changes at 820 nm to monitor the oxidation state of P-700 in leaves. Plant Cell Environ **10:** 131-140

Harvey RB (1922) Varietal differences in the resistance of cabbage and lettuce to low temperatures. Ecol **3:** 134-139

Havaux M, Davaud A (1994) Photoinhibition of photosynthesis in chilled potato leaves is not correlated with a loss of photosystem II activity. Preferential inactivation of photosystem I. Photosynth Res **40:** 75-92

Heber U, Walker D (1992) Concerning a dual function of coupled cyclic electron transport in leaves. Plant Physiol **100:** 1621-1626

Helson VA (1964) Greenhouse-Garden-Grass, Vol 4. Agriculture Canada, Ottawa, pp 22-37

Hill R, Bendall F (1960) Function of the two cytochrome components in chloroplasts: A working hypothesis. Nature **186:**136-137

Hoagland DR, Arnon DI (1950) The water culture method for growing plants without soil. Calif Agric Exp Sta Bull No. 347

Holaday AS, Martindale W, Alred R, Brooks AL, Leegood RC (1992) Changes in activities of enzymes of carbon metabolism in leaves during exposure of plants to low temperature. Plant Physiol **98:** 1105-1114

Hon W-C, Griffith M, Mlynarz A, Kwok YC, Yang DSC (1995) Antifreeze proteins in winter rye are similar to pathogenesis-related proteins. Plant Physiol **109:** 879-889

Horton P, Ruban AV (1993) ΔpH-dependent quenching of the F_o level of chlorophll fluorescence in spinach leaves. Biochim Biophys Acta **1142:** 203-206

Horton P, Ruban AV, Walters RG (1994) Regulation of light-harvesting in green plants. Induction by nonphotochemical quenching of chlorophyll fluorescence. Plant Physiol **106:** 415-420

Houde M, Daniel C, Lachapelle M, Allard F, Laliberté S, Sarhan F (1995) Immunolocalization of freezing-tolerance-associated proteins in the cytoplasm and nucleoplasm of wheat crown tissues. Plant J **8:** 583-593

Houde M, Danyluk J, Laliberté JF, Rassart E, Dhindsa RS, Sarhan F (1992a) Cloning, characterization, and expression of a cDNA encoding a 50-kilodalton protein specifically induced by cold acclimation in wheat. Plant Physiol **99:** 1381-1387

Houde M, Dhindsa RS, Sarhan F (1992b) A molecular marker to select for freezing tolerance in Gramineae. Mol Gen Genet **234:** 43-48

Howarth CJ, Ougham HJ (1993) Gene expression under temperature stress. New Phytol **125:** 1-26

Huber JL, Hite DRC, Outlaw WH Jr, Huber SC (1991) Inactivation of highly activated spinach leaf sucrose-phosphate synthase by dephosphorylation. Plant Physiol **95:** 291-297

Hughes DA (1994) Histidine kinases hog the limelight. Nature **369:** 187-188

Hughes MA, Dunn MA (1996) The molecular biology of plant acclimation to low temperature. J Exp Bot **47:** 291-305

Hundell T, Virgin I, Styring S, Andersson B (1990) Changes in the organization of photosystem II following light induced D1 protein degradation. Biochim Biophys Acta **1017:** 235-241

Huner NPA (1985a) Acclimation of winter rye to cold-hardening temperatures results in an increased capacity for photosynthetic electron transport. Can J Bot **63:** 506-511

Huner NPA (1985b) Morphological, anatomical, and molecular consequences of growth and development at low temperature in *Secale cereale* L. cv Puma. Am J Bot **72:** 1290-1306

Huner NPA (1988) Low-temperature induced alterations in phot nthetic membranes. CRC Crit Rev Plant Sci **7:** 257-278

Huner NPA, Krol M, Williams JP, Maissan E, Low PS, Roberts D, Thompson JE (1987) Low temperature development induces a specific decrease in *trans*-Δ^3-hexdecenoic acid content which influences LHCII organization. Plant Physiol **84:** 12-18

Huner NPA, Maxwell DP, Gray GR, Savitch LV, Krol M, Ivanov AG, Falk S (1996) Sensing environmental temperature change through imbalances between energy supply and energy consumption: redox state of photosystem II. Physiol Plant - in press

Huner NPA, Maxwell DP, Gray GR, Savitch LV, Laudenbach DE, Falk S (1995) Photosynthetic response to light and temperature: PSII excitation pressure and redox signalling. Acta Physiol Plant **17:** 167-176

Huner NPA, Migus W, Tollenaar M (1986) Leaf CO_2 exchange rates in winter rye grown at a cold-hardening and non-hardening temperatures. Can J Plant Sci **66:** 443-445

Huner NPA, Öquist G, Hurry VM, Krol M, Falk S, Griffith M (1993) Photosynthesis, photoinhibition and low temperature acclimation in cold tolerant plants. Photosynth Res **37:** 19-39

Huner NPA, Öquist G, Sundblad L-G (1992) Low measuring temperature induced artifactual increase in chlorophyll a fluorescence. Plant Physiol **98:** 749-752

Huner NPA, Palta JP, Li PH, Carter JV (1981) Anatomical changes in leaves of Puma rye in response to growth at cold-hardening temperatures. Bot Gaz **142:** 55-62

Huner NPA, Williams JP, Krol M, Boese SR, Hurry VM, Lapointe L, Reynolds TL (1989) Photosynthesis, low temperature development and freezing tolerance. Curr Topics in Plant Biochem **8:** 6-20

Huner NPA, Williams JP, Maissan E, Myscich EG, Krol M, Laroche A, Singh J (1989) Low temperature-induced decrease in *trans*-Δ^3-hexdecenoic acid is correlated with freezing tolerance in cereals. Plant Physiol **89:** 144-150

Hurry VM, Gardeström P, Öquist G (1993) Reduced sensitivity to photoinhibition following frost-hardening of winter rye is due to increased phosphate availability. Planta **190:** 484-490

Hurry VM, Huner NPA (1991) Low growth temperature effects a differential inhibition of photosynthesis in spring and winter wheat. Plant Physiol **96:** 491-497

Hurry VM, Huner NPA (1992) Effect of cold hardening on sensitivity of winter and spring wheat leaves to short-term photoinhibition and recovery of photosynthesis. Plant Physiol **100:** 1283-1290

Hurry VM, Keerberg O, Pärnik T, Gardeström P, Öquist G (1995a) Cold-hardening results in increased activity of enzymes involved in carbon metabolism in leaves of winter rye (*Secale cereale* L). Planta **195:** 554-562

Hurry VM, Krol M, Öquist G, Huner NPA (1992) Effect of long-term photoinhibition on growth and photosynthesis of cold-hardened spring and winter wheat. Planta **188:** 369-375

Hurry VM, Malmberg G, Gardeström P, Öquist G (1994) Effects of a short-term shift to low temperature and of long-term cold hardening on

photosynthesis and ribulose-1,5-bisphosphate carboxylase/oxygenase and sucrose phosphate synthase activity in leaves of winter rye (*Secale cereale* L.). Plant Physiol **106:** 983-990

Hurry VM, Strand Å, Tobiæson M, Gardeström P, Öquist G (1995b) Cold hardening of spring and winter wheat and rape results in differential effects on growth, carbon metabolism and carbohydrate content. Plant Physiol **109:** 697-706

Iuchi S, Lin ECC (1993) Adaptation of *Escherichia coli* to redox environments by gene expression. Mol Microbiol **9:** 9-15

Jansson S (1994) The light-harvesting chlorophll *a/b*-binding proteins. Biochim Biophys Acta **1184:** 1-19

Joliot A, Joliot P (1964) Etude cinétique de la reaction photochimique libérant l'oxygène au cours de la photosynthèse. CR Acad Sci Paris **258:** 4622-4625

Jones LW, Kok B (1966) Photoinhibition of chloroplast reactions. I. Kinetics and action spectra. Plant Physiol **11:** 1037-1043

Keegstra K, Bruce B, Hurley M, Li H, Perry S (1995) Targeting of proteins into chloroplasts. Physiol Plant **93:** 157-162

Khan MU, Williams JP (1977) Improved thin-layer chromatographic method for the separation of major phospholipids and glycolipids from plant lipid extracts and phosphatidylglycerol and bis(monoacylglyceryl) phosphate from animal and lipid extracts. J Chromatogr **140:** 179-185

Khan MU, Williams JP (1993) Microwave-mediated methanolysis of lipids and activation of thin-layer chromatographic plates. Lipids **28:** 953-955

Kim JH, Glick RE, Melis A (1993) Dynamics of photosystem stoichiometry adjustment by light quality in chloroplasts. Plant Physiol **102:** 181-190

Knox JP, Dodge AD (1985) Singlet oxygen and plants. Phytochem **24:** 889-896

Kok B (1956) On the inhibition of photosynthesis by intense light. Biochim Biophys Acta **21:** 234-244

Koroleva OY, Thiele A, Krause GH (1995) Increased xanthophyll cycle activity as an important factor in acclimation of the photosynthetic apparatus to high-light stress at low temperatures. *In* P Mathis, ed, Photosynthesis: from Light to

Biosphere, Vol. IV. Kluwer Academic Publishers, Dordrecht, pp 425-428

Koster KL, Lynch DV (1992) Solute accumulation and compartmentation in during the cold acclimation of Puma rye. Plant Physiol **98:** 108-113

Koyama Y (1991) Structures and functions of carotenoids in photosynthetic systems. J Photochem Photobiol B: Biol **9:** 265-280

Krause GH (1988) Photoinhibition of photosynthesis. An evaluation of damaging and protective mechanisms. Physiol Plant **74:** 566-574

Krause GH (1994a) Photoinhibition induced by low temperatures. *In* NR Baker, JR Bowyer, eds, Photoinhibition of Photosynthesis: from molecular mechanisms to the field. βios Scientific Publishers, Oxford, pp 331-348

Krause GH (1994b) The role of oxygen in photoinhibition of photosynthesis. *In* CH Foyer, PM Mullineaux, eds, Causes of Photooxidative Stress and Amelioration of Defense Systems in Plants. CRC Press, Boca Raton, pp 43-76

Krause GH, Briantais J-M, Vernotte C (1983) Characterization of chlorophyll fluorescence quenching in chloroplasts by fluorescence spectroscopy at 77K. I. pH dependent quenching. Biochim Biophys Acta **723:** 169-175

Krause GH, Somersalo S, Zumbusch E, Weyers B, Laasch A (1990) On the mechanism of photoinhibition in chloroplasts. Relationship between changes in fluorescence and activity of photosystem II. J Plant Physiol **136:** 472-479

Krause GH, Weis E (1991) Chlorophyll fluorescence and photosynthesis: The basics. Ann Rev Plant Physiol Plant Mol Biol **42:** 313-349

Krieger A, Moya I, Weis E (1992) Energy-dependent quenching of chlorophyll *a* fluorescence: effect of pH on stationary fluorescence and picosecond-relaxation kinetics in thylakoid membranes and photosystem II preparations. Biochim Biophys Acta **1102:** 167-176

Krol M, Griffith M, Huner NPA (1984) An appropriate physiological control for environmental temperature studies: comparative growth kinetics of winter rye. Can J Bot **62:** 1062-1068

Krol M, Huner NPA (1985) Growth and development at cold-hardening temperatures. Pigment and benzoquinone accumulation in winter rye. Can J Bot **63:** 716-721

Krol M, Huner NPA, Williams JP, Maissan EE (1988) Chloroplast biogenesis at cold-hardening temperatures. Kinetics of *trans*-Δ^3-hexdecenoic acid accumulation and the asembly of LHCII. Photosynth Res **15:** 115-132

Krol M, Spangfort MD, Huner NPA, Öquist G, Gustafsson P, Jansson S (1995) Chlorophyll *a/b*-binding proteins, pigment conversions, and early light-induced proteins in a chlorophyll *b*-less barley mutant. Plant Physiol **107:** 873-883

Krupa Z, Huner NPA, Williams JP, Maissan E, James DR (1987) Development at cold-hardening temperatures. The structure and composition of purified rye light harvesting complex II. Plant Physiol **84:** 19-24

Krupa Z, Williams JP, Khan MU, Huner NPA (1992) The role of acyl lipids in reconstitution of lipid-depleted light-harvsting complex II from cold-hardened and nonhardened rye. Plant Physiol **100:** 931-938

Kühlbrandt W (1994) Structure and function of the plant light-harvesting complex, LHC-II. Curr Opin Struct Biol **4:** 519-528

Kühlbrandt W, Wang DN, Fujiyoshi Y (1994) Atomic model of plant light-harvesting complex by electron crystallography. Nature **367:** 614-621

Kyle DJ (1987) The biochemical basis for photoinhibition of photosystem II. *In* DJ Kyle, CB Osmond, CJ Arntzen, eds, Photoinhibition, Topics in Photosynthesis, Vol 9. Elsevier Science Publishers BV (Biomedical Division), Amsterdam, pp 197-226

Kyle DJ, Ohad I, Arntzen CJ (1984) Membrane protein damage and repair: Selective loss of a quinone-protein function in chloroplast membranes. Proc Natl Acad Sci USA **81:** 4070-4074

Labate CA, Adcock MD, Leegood RC (1990) Effects of temperature on the regulation of photosynthetic carbon accimilation in leaves of maize and barley. Planta **181:** 547-554

Labate CA, Leegood RC (1988) Limitation of photosynthesis by changes in temperature. Planta **173:** 519-527

Laemmli UK (1970) Cleavage of structural proteins during the assembly of the head of bacteriophage T4. Nature **227:** 680-685

Lapointe L, Huner NPA (1993) Photoinhibition of isolated mesophyll cells from cold-hardened and non-hardened winter rye. Plant Cell Environ **16:** 249-258

Lapointe L, Huner NPA, Carpentier R, Ottander C (1991) Resistance to low temperature photoinhibition is not associated with thylakoid membranes in winter rye. Plant Physiol **97:** 804-810

Lee SP, Chen THH (1993) Molecular biology of plant cold hardiness development. In PH Lee, L Christersson, eds, Advances in Plant Cold Hardiness. CRC Presss, Boca Raton, pp 1-29

Leegood RC, Walker DA, Foyer CH (1985) Regulation of the Benson-Calvin cycle. *In* J Barber, NR Baker, eds, Photosynthetic Mechanisms and the Environment, Topics in Photosynthesis, Vol 6. Elsevier Science Publishers BV (Biomedical Division), Amsterdam, pp 189-258

Levings CS III, Siedow JN (1995) Regulation by redox poise in chloroplasts. Science **268:** 695-696

Levitt J (1980) Responses of Plants to Environmental Stresses. Chilling, Freezing, and High Temperature Stresses, Ed 2, Vol I. Academic Press, New York

Lichtenthaler HK (1968) Verbeitung des lipophilen plastidenchinone im nicht-grunen pflazengewebe. Z Pflanzenphysiol **59:** 195-210

Lichtenthaler HK (1969) Zur synthese der lipophilen plastidenchinone und sekundarkarotenoide wahrend der chromoplastenentwicklung. Ber DTSCH Bot Ges **82:** 483-497

Limin AE, Houde M, Chauvin LP, Fowler DB, Sarhan F (1995) Expression of the cold-induced wheat gene *Wcs120* and its homologs in related species and interspecific combinations. Genome **38:** 1023-1031

Long SP, Humphries S, Falkowski PG (1994) Photoinhibition of photosynthesis in nature. Annu Rev Plant Physiol Plant Mol Biol **45:** 633-662

Loreto F, Sharkey TD (1993) On the relationship between isoprene emission and photosynthetic metabolites under different environmental conditions. Planta **189:** 420-424

Lorimer GH (1981) The carboxylation and oxygenation of ribulose-1,5-bisphosphate: The primary events in photosynthesis and photorespiration. Ann

Rev Plant Physiol **32:** 349-383

Lowry OH, Passonneau JV (1972) A flexible system of enzymatic analysis. Academic Press, Orlando

Macdowall FDH (1972) Growth kinetics of Marquis wheat. I. Light dependence. Can J Bot **50:** 89-99

Macdowall FDH (1974) Growth kinetics of Marquis wheat. VI. Genetic dependence and winter hardening. Can J Bot **52:** 151-157

Maeda T, Wurgler-Murphy SM, Saito H (1994) A two-component system that regulates an osmosensing MAP kinase cascade in yeast. Nature **369:** 242-245

Markgraf T, Berry J (1990) Measurement of photochemical and non-photochemical quenching: correction for turnover of PSII during steady state photosynthesis. *In* M Baltscheffsky, ed, Current Research in Photosynthesis, Vol IV. Kluwer, Dordrecht pp 279-282

Mattoo AK, Marder, JB, Edelman M (1989) Dynamics of the photosystem II reaction center. Cell **56:** 241-246

Maxwell DP, Falk S, Huner NPA (1995a) Photosystem II excitation pressure and development of resistance to photoinhibition I. Light-harvesting complex II abundance and zeaxanthin content in *Chlorella vulgaris*. Plant Physiol **107:** 687-694

Maxwell DP, Falk S, Trick CG, Huner NPA (1994) Growth at low temperature mimics high-light acclimation in *Chlorella vulgaris*. Plant Physiol **105:** 535-543

Maxwell DP, Laudenbach DE, Huner NPA (1995b) Redox regulation of light-harvesting complex II and *cab* mRNA abundance in *Dunaliella salina*. Plant Physiol **109:** 787-795

McCourt P, Browse J, Watson J, Arntzen CJ, Somerville CR (1985) Analysis of the photosynthetoic antenna function in a mutant of *Arabidopsis thaliana* lacking trans-hexadecenoic acid. Plant Physiol **78:** 853-858

McKersie BD, Leshem YY (1994) Stress and Stress Coping in Cultivated Plants. Kluwer Academic Publishers, Dordrecht

McNellis TW, Deng X-W (1995) Light control of seedling morphogenetic pattern. Plant Cell **7:** 1749-1761

Mehler AH (1951) Studies of reactivities on illuminated chloroplasts. I. Mechanism of the reduction of oxygen and other Hill reagents. Arch Biochem Biophys **33:** 65-77

Mitchell F, Spillmann A, Haehnel W (1990) Plastoquinol diffusion in linear photosynthetic electron transport. Biophys J **58:** 1011-1024

Mitchell P (1961) Coupling of phosphorylation to electron and hydrogen transfer by a chemi-osmotic type of mechanism. Nature **191:** 144-148

Mitchell P (1975) The proton motive Q cycle: A general formulation. FEBS Lett **59:** 137-139

Monroy AF, Dhindsa RS (1995) Low-temperature signal transduction: Induction of cold acclimation-specific genes of alfalfa by calcium at 25°C. Plant Cell **7:** 321-331

Moon BY, Higashi SI, Gombos Z, Murata N (1995) Unsaturation of the membrane lipids of chloroplasts stabilizes the photosynthetic machinery against low-temperature photoinhibition in transgenic tobacco plants. Proc Natl Acad Sci USA **92:** 6219-6223

Nanba O, Satoh K (1987) Isolation of a photosystem II reaction center consisting of D1 and D2 polypeptides and cytochrome b_{559}. Proc Natl Acad Sci USA **84:** 109-112

Ögren E (1991) Prediction of photoinhibition of photosynthesis from measurements of fluorescence quenching components. Planta **184:** 538-544

Ögren E, Rosenqvist E (1992) On the significance of photoinhibition of photosynthesis in the field and its generality among species. Photosynth Res **33:** 63-71

Ogren WL (1984) Photorespiration: Pathways, regulation, and modification. Ann Rev Plant Physiol **35:** 415-442

Ohad I, Adir N, Koike H, Kyle DJ, Inoue Y (1990) Mechanism of photoinhibition *in vivo*. A reversible light-induced conformational change of reaction center II is related to an irreversible modification of the D1 protein. J Biol Chem **265:** 1972-1979

Olien CR, Clark JL (1993) Changes in soluble carbohydrate composition of barley, wheat, and rye during winter. Crop Sci **85:** 21-29

Öquist G (1983) Effects of low temperature on photosynthesis. Plant Cell Environ **6:** 281-300

Öquist G, Anderson JM, McCaffery S, Chow WS (1992a) Mechanistic differences in photoinhibition of sun and shade plants. Planta **188:** 422-431

Öquist G, Chow WS, Anderson JM (1992b) Photoinhibition of photosynthesis represents a mechanism for long-term regulation of photosystem II. Planta **186:** 450-460

Öquist G, Greer DH, Ögren E (1987) Light stress at low temperature. *In* DJ Kyle, CB Osmond, CJ Arntzen, eds, Photoinhibition, Topics in Photosynthesis, Vol 9. Elsevier Science Publishers BV (Biomedical Division), Amsterdam pp 67-88

Öquist G, Huner NPA (1991) Effects of cold acclimation on the susceptibility of photosynthesis to photoinhibition in Scots pine and in winter and spring cereals: a fluorescence analysis. Func Ecol **5:** 91-100

Öquist G, Huner NPA (1993) Cold-hardening induced resistance to photoinhibition in winter rye is dependent upon an increased capacity for photosynthesis. Planta **189:** 150-156

Öquist G, Hurry VM, Huner NPA (1993a) Low-temperature effects on photosynthesis and correlation with freezing tolerance in spring and winter cultivars of wheat and rye. Plant Physiol **101:** 245-250

Öquist G, Hurry VM, Huner NPA (1993b) The temperature dependence of the redox state of Q_A and the susceptibility of photosynthesis to photoinhibition. Plant Physiol Biochem **31:** 683-691

Öquist G, Martin B (1986) Cold Climates. *In* NR Baker, SP Long, eds, Photosynthesis in Contrasting Environments, Topics in Photosynthesis, Vol 7. Elsevier Science Publishers BV (Biomedical Division), Amsterdam, pp 237-293

Öquist G, Wass R (1988) A portable, microprocessor operated instrument for measuring chlorophyll fluorescence kinetics in stress physiology. Physiol Plant **73:** 211-217

Osmond CB (1994) What is photoinhibition? Some insights from comparison of shade and sun plants. *In* NR Baker, JR Bowyer, eds, Photoinhibition of Photosynthesis: from molecular mechanisms to the field. βios Scientific Publishers, Oxford, pp 1-24

Osmond CB, Austin MP, Berry JA, Billings WD, Boyer JS, Dacey JWH, Nobel PS, Smith SD, Winner WE (1987) Stress physiology and the distribution of plants. BioSci **37:** 38-48

Ota IM, Varshavsky A (1993) A yeast protein similar to bacterial two-component regulators. Science **262:** 566-568

Ouellet F, Houde M, Sarhan F (1993) Purification, characterization and cDNA cloning of the 200 kDa protein induced by cold acclimation in wheat. Plant Cell Physiol **34:** 59-65

Pammenter NW, Loreto F, Sharkey TD (1993) End product feedback effects on photosynthetic electron transport. Photosynth Res **35:** 5-14

Park Y-I, Anderson JM, Chow WS (1996a) Photoinactivation of functional photosystem II and D1 protein synthesis in vivo are independent of the modulation of the photosynthetic apparatus by growth irradiance. Planta **198:** 300-309

Park Y-I, Chow WS, Anderson JM, Hurry VM (1996b) Differential susceptibility of photosystem II to light stress in light-acclimated pea leaves depends upon the capacity for photochemical and non-radiative dissipation of light. Plant Sci **115:** 137-149

Parkinson JS (1993) Signal transduction schemes of bacteria. Cell **73:** 857-871

Pearce RS (1988) Extracellular ice and cell shape in frost-stressed cereal leaves: a low-temperature scanning-electron-microscopy study. Planta **175:** 313-324

Pearce RS, Ashworth EN (1992) Cell shape and localization of ice in leaves of overwintering wheat during frost stress in the field. Planta **188:** 324-331

Pearce RS, Dunn MA, Rixon JE, Harrison P, Hughes MA (1996) Expression of cold-inducible genes and frost hardiness in the crown meristem of young barley (*Hordeum vulgare* L. cv. Igri) plants grown in different environments. Plant Cell Environ **19:** 275-290

Pfündel E, Bilger W (1994) Regulation and possible function of the violaxanthin cycle. Photosynth Res **42:** 89-109

Piccioni R, Bellemare G, Chua N-H (1982) Methods of polyacrylamide gel electrophoresis in the analysis and preparation of plant polypeptides. *In* M Edelmann, RB Hallick, N-H Chua, eds, Methods in Chloroplast Molecular Biology. Elsevier Biomedical Press, Amsterdam, pp 985-1014

Plumley FG, Schmidt GW (1987) Reconstitution of chlorophyll a/b light harvesting complexes: xanthophyll-dependent assembly and energy transfer. Proc Natl Acad

Sci USA **84:** 146-150

Pohl P, Glasl H, Wagner H (1970) Zur analytik pflanzlicher glyko- und phospholipoide und ihrer fettsauren. I. Eine neue dünnschichtchromatographische methode zur trennung pflanzlicher lipoide und quantitativen bestimmung ihrer fettsäure-zusammensetzung. J Chromatogr **49:** 488-492

Pollock CJ, Cairns AJ (1991) Fructan metabolism in grasses and cereals. Annu Rev Plant Physiol Plant Mol Biol **42:** 77-101

Pollock CJ, Lloyd EJ (1987) The effect of low growth temperature upon starch, sucrose and fructan synthesis in leaves. Ann Bot **60:** 231-235

Porra RJ, Thompson WA, Kriedemann PE (1989) Determination of accurate extinction coefficients and simultaneous equations for assaying chlorophylls *a* and *b* extracted with different solvents: verification of the concentration of chlorophyll standards by atomic absorption spectroscopy. Biochim Biophys Acta **975:** 384-394

Powles SB (1984) Photoinhibition of photosynthesis induced by visible light. Annu Rev Plant Physiol **35:** 15-44

Prince RC (1996) Photosynthesis: the Z-scheme revised. Trends Biochem Sci **21:** 121-122

Prosser CL (1986) Adaptational Biology. Molecules to organisms. John Wiley & Sons, New York

Quinn PJ, Williams WP (1985) Environmentally induced changes in chloroplast membranes and their effects on photosynthetic function. *In* J Barber, NR Baker, eds, Photosynthetic Mechanisms and the Environment, Topics in Photosynthesis, Vol 6. Elsevier Science Publishers BV (Biomedical Division), Amsterdam, pp 1-48

Reisman S, Michaels A, Ohad I (1986) Lack of recovery from photoinhibition in a temperature-sensitive *Chlamydomonas reinhardtii* mutant T_{44} unable to synthesize and/or integrate the Q_B protein of photosystem II at 37°C. Biochim Biophys Acta **849:** 41-50

Roberts DWA (1984) The effect of ligh[illegible] velopment of the rosette growth habit of winter wheat. Can J Bot **62:** 818-822

Rosen KM, Villa-Komaroff L (1990) An alternative method for the visualization of RNA in formaldehyde agarose gels. Focus **12:** 23-24

Ruban AV, Horton P (1995) Regulation of non-photochemical quenching of chlorophyll fluorescence in plants. Aust J Plant Physiol **22:** 221-230

Rufty TW Jr, Huber SC (1983) Changes in starch formation and activities of sucrose phosphate synthase and cytoplasmic fructose-1,6-bisphosphatase in response to source-sink alterations. Plant Physiol **72:** 474-480

Sage RF, Sharkey TD (1987) The effect of temperature on the occurrence of O_2 and CO_2 insensitive photosynthesis in field grown plants. Plant Physiol **84:** 658-664

Santini C, Tidu V, Tognon G, Magaldi AG, Bassi R (1994) Three-dimensional structure of the higher-plant photosystem II reaction center and evidence for its dimeric organization *in vivo*. Eur J Biochem **221:** 307-315

Savitch LV, Maxwell DP, Huner NPA (1996) Photosystem II excitation pressure and photosynthetic carbon metabolism in *Chlorella vulgaris*. Plant Physiol **111:** 127-136

Schatz G, Brock H, Holzwarth AR (1988) Kinetic and energetic model for the primary processes in photosystem II. Biophys J **54:** 397-405

Schreiber U, Bilger W, Neubauer C (1994) Chlorophyll fluorescence as a nonintrusive indicator for rapid assessment of *in vivo* photosynthesis. *In* E-D Shulze, MM Caldwell, eds, Ecophysiology of photosynthesis. Springer-Verlag, Berlin, pp 49-70

Schreiber U, Klughammer C, Neubauer C (1988) Measuring P700 absorbance changes around 830 nm with a new type of pulse modulation system. Z Naturforsch **43c:** 686-698

Schreiber U, Neubauer C (1990) O_2-depende . electron flow, membrane organization and the mechanism of non-photochemical quenching of chlorophyll fluorescence. Photosynth Res **25:** 279-293

Schreiber U, Schwiiwa U, Bilger W (1986) Continuous recording of photochemical and non-photochemical chlorophyll fluorescence quenching with a new type of modulation fluorometer. Photosynth Res **10:** 51-62

Selstam E, Widell Wigge A (1993) Chloroplast lipids and the assembly of membranes. *In* C Sundqvist, M Ryberg, eds, Pigment-Protein Complexes in Plastids: Synthesis and Assembly. Academic Press Inc., San Diego, pp 241-277

Sétif P, Brettel K (1990) Photosystem I photochemistry under highly reducing

conditions: study of the P_{700} triplet state formation from the second radical pair (P_{700}^{+}-A_1^{-}). Biochim Biophys Acta **1020:** 232-238

Sharkey TD (1990) Feedback limitation of photosynthesis and the physiological role of ribulose bisphosphate carboxylase carbamylation. Bot Mag **2:** 87-105

Sharkey TD, Savitch LV, Butz ND (1991a) Photometric method for routine determination of k_{cat} and carbamylation of rubisco. Photosynth Res **28:** 41-48

Sharkey TD, Stitt M, Heineke D, Gerhardt R, Raschke K, Heldt HW (1986) Limitation of photosynthesis by carbon metabolism. II. O_2 insensitive CO_2 assimilation results from triose phosphate utilisation limitations. Plant Physiol **81:** 1123-1129

Sharkey TD, Vassey TL, Vanderveer PJ, Vierstra RD (1991b) Carbon metabolism enzymes and photosynthesis in transgenic tobacco (*Nicotiana tabacum* L.) having excess phytochrome. Planta **185:** 287-296

Shipman LL (1982) Electronic Structure and Function of Chlorophylls and their Pheophytins. *In* Govindgee, ed, Photosynthesis, Vol I. Academic Press, New York, pp 276-291

Sigrist M, Staehelin LA (1992) Identification of type 1 and type 2 light-harvesting chlorophyll *a/b*-binding proteins using monospecific antibodies. Biochim Biophys Acta **1098:** 191-200

Sigrist M, Staehelin LA (1994) Appearance of type 1, 2, and 3 light-harvesting complex II and light-harvesting complex I proteins during light-induced greening of barley (*Hordeum vulgare*) etioplasts. Plant Physiol **104:** 135-145

Smith PK, Krohn RI, Hermanson GT, Mallia AK, Gartner FH, Provenzano MD, Fujimoto EK, Goeke NM, Olson BJ, Klenk DC (1985) Measurement of protein using bicinchoninic acid. Anal Biochem **150:** 76-85

Somersalo S, Krause GH (1989) Photoinhibition at chilling temperature. Fluorescence characteristics of unhardened and cold-acclimated spinach leaves. Planta **177:** 409-416

Somersalo S, Krause GH (1990) Reversible photoinhibition of unhardened and cold-acclimated spinach leaves at chilling temperatures. Planta **180:** 181-187

Sommerville C (1995) Direct tests of the role of membrane lipid composition in low-temperature-induced photoinhibition and chilling sensitivity in plants and bacteria.

Proc Natl Acad Sci USA **92:** 6215-6218

Sonoike K (1996) Photoinhibition of photosystem I: Its physiological significance in the chilling sensitivity of plants. Plant Cell Physiol **37:** 239-247

Steponkus PL (1984) Role of the plasma membrane in freezing injury and cold acclimation. Ann Rev Plant Physiol **35:** 543-584

Steponkus PL, Lanphear FO (1968) The role of light in cold acclimation of Hedera helix L. var. Thorndale. Plant Physiol **43:** 151-156

Stushnoff C, Fowler DB, Brûelé-Babel A (1984) Breeding and selection for resistance to low temperature. *In* PE Vose, SG Blixt, eds, Crop Breeding. A Contemporary Basis. Pergamon Press, New York, pp 115-136

Thayer SS, Björkman O (1990) Leaf xanthophyll content and composition in the sun and shade determined by HPLC. Photosynth Res **23:** 331-343

Thiele A, Krause GH (1994) Xanthophyll cycle and thermal energy dissipation in photosystem II: Relationship between zeaxanthin formation, energy-dependent fluorescence quenching and photoinhibition. J Plant Physiol **144:** 324-332

Thiele A, Schirwitz K, Winter K, Krause GH (1996) Increased xanthophyll cycle activity and reduced D1 protein inactivation related to photoinhibition in two plant systems acclimated to excess light. Plant Sci **115:** 237-250

Thomashow MF (1990) Molecular genetics of cold acclimation in higher plants. *In* JG Scandalios, ed, Advances in Genetics, Genomic Responses to Environmental Stress, Vol 28. Academic Press, New York, pp 99-131

Thomashow MF (1993) Genes induced during cold acclimation in higher plants. *In* PL Steponkus, ed, Advances Low-Temperature Biology, Vol 2. JAI Press, London, pp 183-210

Thomashow MF, Gilmour SJ, Lin C (1993) Cold-regulated genes of *Arabidopsis thaliana*. In PH Lee, L Christersson, eds, Advances in Plant Cold Hardiness. CRC Press, Boca Raton, pp 31-44

Tognetti JA, Salerno GL, Crespi MD, Pontis HG (1990) Sucrose and fructan metabolism of different wheat cultivars at chilling temperatures. Physiol Plant **78:** 554-559

Towbin H, Staehelin T, Gordon J (1979) Electrophoretic transfer of proteins from

polyacrylamide gels to nitrocellulose sheets: Procedure and some applications. Proc Natl Acad Sci USA **76:** 4350-4354

Trewavas A, Gilroy S (1991) Signal transduction in plant cells. Trends Genet. **7:** 356-361

Tysdal HM (1933) Influence of light, temperature, and soil moisture on the hardening process in alfalfa. J Agr Res **46:** 483-515

Tyystjärvi E, Koivuniemi A, Kettunen R, Aro E-M (1991) Small light-harvesting antenna does not protect from photoinhibition. Plant Physiol **97:** 477-483

Uemura M, Steponkus PL (1994) A contrast of the plasma membrane lipid composition of oat and rye leaves in relation to freezing tolerance. Plant Physiol **104:** 479-496

van Kooten O, Snel JFH (1990) The use of chlorophyll fluorescence nomenclature in plant stress physiology. Photosynth Res **25:** 147-150

van Wijk KJ, van Hasselt PR (1993a) Photoinhibition of photosystem II *in vivo* is preceded by down-regulation through light-induced acidification of the lumen: Consequences for the mechanism of photoinhibition *in vivo*. Planta **189:** 359-368

van Wijk KJ, van Hasselt PR (1993b) Kinetic resolution of different recovery phases of photoinhibited photosystem II in cold-acclimated and non-acclimated spinach leaves. Physiol Plant **87:** 187-198

Vanlerberghe GC, Day DA, Wiskich JT, Vanlerberghe AE, McIntosh L (1995) Alternative oxidase activity in tobacco leaf mitochondria. Dependence on tricarboxylic acid cycle-mediated redox regulation and pyruvate activation. Plant Physiol **109:** 353-631

Vasil'yev IM (1961) Wintering of Plants. American Institute of Biological Sciences, Washington DC

Vassey TL, Sharkey TD (1989) Mild water stress of *Phaseolus vulgaris* plants leads to reduced starch synthesis and extractable sucrose phosphate synthase activity. Plant Physiol **89:** 1066-1070

Veisz O, Tischner T (1995) Hardiness of winter wheat varieties as a function of changes in certain environmental factors. Biotronics **24:** 73-83

Verhey SD, Lomax TL (1993) Signal transduction in vascular plants. J Plant

Growth Regul **12:** 179-195

von Caemmerer S, Farquhar GD (1981) Some relationships between the biochemistry of photosynthesis and the gas exchange of leaves. Planta **153:** 376-387

Waldron JC, Anderson JM (1979) Chlorophyll-protein complexes from thylakoids of a mutant barley lacking chlorophyll *b*. Eur J Biochem **102:** 357-362

Walker D (1990) The use of the oxygen electrode and fluorescence probes in simple measurements of photosynthesis. Oxgraphics, Sheffield

Webb MS, Steponkus PL (1993) Freeze-induced membrane ultrastructural alterations in rye (*Secale cereale*) leaves. Plant Physiol **101:** 955-963

Weretilnyk E, Winson O, White TC, Iu B, Singh J (1993) Characterization of three related low-temperature-regulated cDNAs from winter *Brassica napus*. Plant Physiol **101:** 171-177

Whitmarsh J, Ort DR (1984) Stoichiometries of electron transport complexes in spinach chloroplasts. Arch Biochem Biophys **231:** 378-389

Williams JP, Merrilees PA (1970) The removal of water and nonlipid contaminents from lipid extracts. Lipids **5:** 367-370

Williams WP (1994) The role of lipids in the structure and function of photosynthetic membranes. Prog Lipid Res **33:** 119-127

Woodrow IE, Berry JA (1988) Enzymatic regulation of photosynthetic CO_2 fixation in C_3 plants. Ann Rev Plant Physiol Plant Mol Biol **39:** 533-594

Wu J, Browse J (1995) Elevated levels of high-melting-point phosphatidylglycerols do not induce chilling sensitivity in an Arabidopsis mutant. Plant Cell **7:** 17-27

Young AJ (1991) The photoprotective role of carotenoids in higher plants. Physiol Plant **83:** 702-708